# VISUAL PROCESSING IN THE HUMAN BRAIN

## Investigating Deviance Detection from a Predictive Coding Perspective

Alie Gabriella Male

Bachelor of Psychology with Honours and Criminology

This thesis is presented for the degree of Doctor of Philosophy

Discipline of Psychology

College of Science, Health, Engineering, and Education

Murdoch University

June 2019

# TABLE OF CONTENTS

# LIST OF TABLES

## Chapter 2

**Chapter 3**



**Chapter 4**



**Chapter 5**

**Chapter 6**



**Appendix**

# LIST OF FIGURES

## Chapter 2



## Chapter 3

**Chapter 4**



**Chapter 5**



**Chapter 6**

**Appendix**

# GENERAL DECLARATION


*I declare that this thesis is my own account of my research and contains as its main content work that has not previously been submitted for a degree at any tertiary institution.*

.....

Alie Gabriella Male

# COPYRIGHT NOTICE

# STATEMENT OF CONTRIBUTION OF CANDIDATE AND OTHERS

The work involved in designing and conducting the studies described in this thesis was my responsibility. I developed and planned the thesis, its outline, and experimental design of all studies in consultation with Prof. Robert P. O'Shea and Dr. Urte Roeber. Mr. Andreas Widmann, Prof. Erich Schröger, and Dr. Dagmar Müller contributed to the development of the study I conducted at Leipzig University, Germany.

I was responsible for all data collection, data analysis, and original drafting of all chapters contained within this thesis, as well as all publications arising from this thesis. The supervisors provided feedback on all chapters contained within this thesis. Chapters prepared as publications received feedback from all authors and all authors have given permission for work listed in *Publications Arising from this Thesis* to be included in this thesis.

Alie G. Male (Candidate) .....

Prof Robert P. O'Shea (Principal External Supervisor and Co-author)

Dr Urte Roeber (Co-Supervisor and Co-author) .....

Mr Andreas Widmann (Co-author) .....

Dr Dagmar Müller (Co-author) .....

Prof Erich Schröger (Co-author) .....

# PUBLICATIONS ARISING FROM THIS THESIS

## Submitted manuscript

Male, A. G., O'Shea, R. P., Schröger, E., Müller, D., Roeber, U., & Widmann, A. (2019, submitted). The quest for the visual mismatch negativity (vMMN): Event-related potential indications of deviance detection for low-level visual features. *Psychophysiology*.

## Manuscripts in Preparation

Male, A. G., Roeber, U., & O'Shea, R. P. (2019). Does brain processing of unpredicted visual changes increase with the size of the change? A visual mismatch negativity (vMMN) study.

Male, A. G., Roeber, U., & O'Shea, R. P. (2019). Precision of visual predictions: A study of deviant-related negativity (DRN) for unpredicted orientation changes.

Male, A. G., Roeber, U., & O'Shea, R. P. (2019). Does the brain process unexpected changes in orientation and contrast differently?

## Conference Proceedings

Male, A., Müller, D., Roeber, U., O'Shea, R. P., Schröger, E., & Widmann, A. (2018). *No visual mismatch negativity to well-controlled orientation deviants*. Paper presented at the MMN2018: 8th Mismatch Negativity conference "MMN from basic science to clinical applications", Helsinki.

Male, A., O'Shea, R. P., & Roeber, U. (2017). *Brain responses to unpredicted changes in the structure and clarity of unpredicted visual input: Visual mismatch negativity to orientation and contrast changes in upper and lower visual fields*. Paper presented at the 40th European Conference on Visual Perception (ECVP 2017), Berlin.

Male, A., Roeber, U., & O'Shea, R. (2016). An ERP study investigating memory-theory and predictive-coding of visual mismatch negativity (vMMN). Paper presented at the 2016 Australasian Cognitive Neuroscience Society (ACNS) Conference, Shoal Bay, NSW. Abstract published in F. Karayanidis, & J. Todd (Eds.), *2016 Australasian Cognitive Neuroscience Society (ACNS) Conference* (pp. 42). Shoal Bay, NSW: University of Newcastle.

# NOTE ON THESIS FORMATTING, STYLE, AND INCLUSION

This PhD thesis contains one manuscript submitted for publication and three manuscripts in preparation for publication. These formatted documents are incorporated into this thesis. For this reason, some information is repeated across chapters. Some information appears in footnotes, for example, details of methodology.

Each study within this thesis includes a preface that is not included in the original manuscript, describing how the study relates to the thesis and previous findings.

Research findings published after February 2019 are not included in the initial (unpublished) chapters.

# FUNDING

I am grateful to the Australian Government Research Training Program Scholarship and to the BioCog laboratory in Leipzig, directed by Erich Schröger, for funding different parts of the research within this thesis. I am also grateful to the Deutscher Akademischer Austausch Dienst (DAAD) for supporting my visit to University of Leipzig under the Short-Term Grant number 91651341.

# ACKNOWLEDGEMENTS

I would like to acknowledge the time and effort of the student volunteers and students who helped to collect data as part of their fourth-year or honours projects. They were diligent and enthusiastic in the lab, making it a pleasure for me to get to know them. It has been especially rewarding for me to see some of those students, Evie especially, continue down the academic path. I look forward to working with you in the future.

Thank you to the BioCog lab members in Leipzig for being so welcoming of me during my time there, Erich Schröger, Dagmar Müller, and Andreas Widmann, in particular. Erich, thank you for your gracious invitation and for hosting me. The skills I developed at the institute has ultimately enhanced the quality of the work within this thesis. For this, I thank you. Andreas, this thesis would not be what it is without your tutelage. Thank you for continuing to guide me in all research related matters.

An enormous thank you goes to my external supervisors, Robert O'Shea and Urte Roeber, for their contributions to the studies within this thesis and their enduring guidance, kindness, and support over the years. I am especially grateful that they continued to supervise me despite the distance between us. I would not be the researcher I am today without your mentorship and for this I will forever be grateful to you both. Thank you.

I am also enormously grateful to my internal supervisor, Peter Drummond. Peter was always there with his calm demeanour, his experience, and his knack of

dealing with obstacles efficiently. If not for Peter's support and feedback on the work within this thesis, the last stage of my candidature would have been especially difficult, thank you Peter.

I would also like to acknowledge my research committee chair, Alasdair Dempsey. Alasdair was always available for advice. Thank you for your support, ensuring my progress, and propelling me, as a researcher, forward.

To the friends and colleagues in my office, I can wholeheartedly say that the hardest part of leaving will be leaving behind this office and the people in it. Trish, having known you since honours, it has been truly satisfying to share in your successes. I am so fortunate to have worked alongside such a supportive group of people, thank you all.

To the friends beyond these walls, many of whom volunteered their time as participants, thank you for being there and for accepting my extended absences with grace and humility. Kara-Jane, my most loyal participant, your emotional support throughout this entire undergraduate and postgraduate experience has been invaluable. Sincerely, I thank you.

I thank my mother for her love and encouragement. You still may not fully appreciate my research, but you care enough to ask me about it and smile encouragingly as I ramble on. Thank you.

# VISUAL PROCESSING IN THE HUMAN BRAIN
## Investigating Deviance Detection from a Predictive Coding Perspective

Alie Gabriella Male

Murdoch University

PERTH, WESTERN AUSTRALIA

## THESIS ABSTRACT

According to predictive coding, the brain gives extra processing to unpredicted events that disrupt anticipated patterns. To adapt to these events, the brain continually extracts statistical regularities about sensory input from past input. When something unpredicted occurs, it produces an error. In vision, this can be shown by the visual mismatch negativity (vMMN) in event-related potentials (ERPs). The vMMN reaches its maximum amplitude between 150 and 300 ms after the onset of an irregular, *deviant* event in a sequence of otherwise regular, *standard* events and it is usually measured from areas on the scalp closest to the visual cortices (e.g., parieto-occipital areas). Attention toward a deviant is not necessary to generate the vMMN, suggesting that regularities and irregularities are pre-attentively encoded and detected, respectively.

Although vMMN research continues to grow, there are still unanswered questions about it. This thesis focuses on clarifying some of these issues, asking

whether the type or size of the difference between predicted and unpredicted visual input (i.e., the magnitude of deviance) or visual field in which deviance occurs can affect the vMMN. To remedy this, I manipulated these facets across four studies. My thesis was that local aspects of change detection, such as the magnitude of deviance, affect the brain's error response to unpredicted input, evidenced by the vMMN.

A conclusion regarding the effect of magnitude of deviance, the type of change, or visual field on the vMMN was not possible given that (1) ERPs to rule-based deviants and standards did not differ where participants found it difficult to detect irregularities in visual input, and (2) changes in basic properties of well-controlled visual stimuli do not evoke the vMMN. Subsequently, my thesis became that isolated changes in basic properties of visual input do not evoke the vMMN, perhaps because these changes are detected and resolved prior to the vMMN.

Instead, this thesis provides evidence for an earlier deviant-related positivity for changes in low-level features of visual input. This is the first report of a possible pre-vMMN positive prediction error and represents a significant and original contribution to the wider field.

# CHAPTER 1

## GENERAL INTRODUCTION

# 1. GENERAL INTRODUCTION

## 1.1 Overview

Our senses are flooded by information. For example, Attneave (1954) calculated that the four million cones of the human retina could encode a staggering $10^{1,200,000}$ bits of information at any instant, even if their responses to light were binary, which they are not. Still, we do not experience a flood of information—only a stream—to which we pay attention or of which we become conscious (James, 1890). Attneave explained that what we see does not require such an impossible burden of encoding, because it is highly redundant, instead allowing prediction of the state of one cone at any instant from its state the instant before and from the state of its neighbours. This seminal idea has developed into predictive coding theory, first of the retina (Srinivasan, Laughlin, & Dubs, 1982) and then of the brain's hierarchical sensory systems (Friston, 2003, 2005, 2010; Rao & Ballard, 1999).

Predictive coding theory is the leading theory of how the brain deals with sensory input (e.g., Clarke, 2013; Huang, & Rao, 2011; Rao, 1999; Rao & Ballard, 1997, 1999; Spratling, 2017; Stefanics, Astikainen, & Czigler, 2015; Stefanics, Kremláček, & Czigler, 2014). It is also the theory that I endorse.

According to Friston (2003), the brain incorporates information about statistical regularities and causal inferences into internal models of sensory input so that such models can accurately represent, and make predictions about, the state of the world. Models of increasing abstraction are constructed at each

higher level of the nervous system and models at higher positions in the hierarchy propagate predictions (or predictive constraints) about upcoming stimuli to lower levels in the hierarchy (Friston, 2003, 2005). These internal/predictive models can easily represent abstract regularities or relationships between stimuli as well as simplistic representations (Todd & Cornwell, 2018). This allows estimations about change, as well as constancy. For example, my brain will have encoded the clockwise direction in which the blades of my desk fan are rotating—change (i.e., an abstract representation/regularity)—in addition to the visual field my desk fan occupies—a constant (i.e., a simple representation/regularity).

Perhaps the most important tenet of predictive coding theory is that predicted sensory input requires less dedicated processing than unexpected (i.e., unpredicted) sensory input. This is exemplified by changes in neural responsivity to predicted vs. unpredicted input following changes at low and high levels of the processing hierarchy. For example, at lower levels of the hierarchy, repetition leads to reduced responsivity to a stimulus (e.g., stimulus specific adaptation, Ulanovsky, Las, & Nelken, 2003). Simultaneously, higher levels attenuate responsiveness to regularly occurring input (Garrido et al., 2009). This interaction between bottom-up sensory input and top-down predictive processes determines the response to any given stimulus (Friston, 2003).

Notably, the extent of attenuation or suppression is not universal for all predicted input. This is because a model's precision and, therefore, reliability of

model-based predictions, will determine the extent of suppression to regularly occurring input and, by corollary, the magnitude of the cortical response to a deviation from the predicted input (Friston, 2005, 2010; Friston et al., 2009; Winkler, 2007). Accordingly, increased model precision coincides with larger differences in the neural responsivity to predicted vs. unpredicted input. However, various aspects can affect model precision. These include the probability of an irregularity occurring (Garrido et al., 2009), how unstable or volatile the environment is (Frost, Winkler, Provost, Todd, 2016; Todd, Provost, Cooper, 2011; Lieder, Stephan, Daunizeau, Garrido, & Friston, 2013), or how attention is being focused (Clark, 2013; Hohwy, 2012, 2013; Schröger, Marzecová, & SanMiguel, 2015). The scientific study of these effects is largely enabled by electrophysiological measures of prediction error in the brain.The mismatch negativity (MMN, Näätänen, Gaillard, & Mäntysalo, 1978) is an electrophysiological index of extra brain processing for unexpected changes in auditory input. Initially, Näätänen (1992) conceptualised the MMN as mismatch signal, occurring because of a physical mismatch between the memory trace of a repeated stimulus and a current stimulus—hence the *mismatch* in MMN. Now, the MMN is regarded as a neural correlate of prediction error (Clark, 2013; Garrido et al., 2008, 2009) within predictive coding theory.

The MMN is a ubiquitous phenomenon. For example, it occurs in sleeping infants (Ruusuvirta, Huotilainen, Fellman, & Näätänen, 2009), in comatose patients (Fischer et al., 1999; Fischer, Morlet, & Giard, 2000), and in animals, such as cats (Csépe, Karmos, & Molnár, 1987) and mice (Umbricht, Vyssotki,

Latanov, Nitsc, & Lipp, 2005). Researchers have since explored analogues of the MMN in other sensory modalities, including olfaction (Krauel, Schott, Sojka, Pause, & Ferstl, 1999), touch (Kekoni et al., 1997), and vision (Cammann, 1990). This thesis is concerned with visual MMN (i.e., vMMN).

Various changes in visual input can evoke the vMMN and although added constraints in vision research prevent one from investigating the vMMN in some settings, the consensus is that the vMMN also occurs for all unexpected changes outside of attention—it is pre-attentive (Kujala, Tervaniemi, & Schröger, 2007). However, there are still some unanswered questions about the vMMN. For example, it is unclear whether local context of an unexpected change (e.g., the size of difference between the predicted and unpredicted input) affect the brain's processing of the change. This motivated the current thesis.

However, in the course of investigating whether the vMMN differs depending on whether the change is large versus small (i.e., the magnitude of deviance) or whether the type of change or visual field in which it occurs affects the vMMN, I learned that changes in basic properties of visual input do not evoke the vMMN. These include orientation, contrast, phase, and spatial frequency, and are basic properties because they are among the key dimensions used to describe visual input (Daugman, 1984, 1985). This caused me to re-evaluate my thesis to show: that isolated changes in basic properties of visual input do not evoke the vMMN, perhaps because these changes are detected and resolved prior to the vMMN.

## 1.2 The vMMN (and MMN)

Since the initial discovery of the MMN to unexpected changes in tone frequency (Näätänen et al., 1978), many kinds of unanticipated changes in auditory input have been shown to evoke the MMN, such as shifts in tone intensity, speech sounds, and even omissions (Näätänen et al., 2012). Collectively, these are auditory irregularities.

Abstract irregularities are a subset of auditory regularities. These are irregularities that violate a category or rule established by regularly occurring stimuli. For example, irregular tonal repetitions heard in sequences of rising or falling tones will evoke the MMN (Tervaniemi, Maury, & Näätänen, 1994). Similarly, if a rule dictates one pairing of acoustic features (e.g., the higher the frequency, the louder the intensity), a tone that does not adhere to the rule (e.g., a higher frequency and quieter tone) will evoke the MMN (Paavilainen, Simola, Jaramillo, Näätänen, & Winkler, 2001). Evidently, the auditory system encodes abstract regularities as well as simple auditory regularities because both types of irregularity evoke the MMN.

Although the body of research is comparatively smaller, evidence suggests that the visual system similarly encodes feature-specific and abstract regularities. I discuss vMMN research in more detail in Chapter 2 but, in short, others have found that changes in stimulus features evoke the vMMN, including orientation (e.g., Kimura, Katayama, Ohira, & Schröger, 2009; Kimura & Takeda, 2013, 2014, 2015), luminance (e.g., Stagg, Hindley, Tales, & Butler, 2004), contrast

(Wei, Chan, & Luo, 2002, but see also Nyman et al., 1990), spatial frequency (e.g., Heslenfeld, 2003; Maekawa et al., 2005), colour (e.g., Athanasopoulos, Dering, Wiggett, Kuipers, & Thierry, 2010), and shape or size (e.g., Alho, Woods, Algazi, & Näätänen, 1992).

The vMMN also occurs for various abstract irregularities. These include categorical irregularities in facial expressions (Astikainen & Hietanen, 2009; Chang, Xu, Shi, Zhang, & Zhao, 2010; Csukly et al., 2013; Fujimura & Okanoya, 2013; Kovarski et al., 2017; Kreegipuu et al., 2013; Stefanics, Csukly, Komlosi, Czobor, & Czigler, 2012; Zhao & Li, 2006) and hand laterality (Stefanics & Czigler, 2012). For example, Stefanics and Czigler (2012) showed participants images of hands oriented at different angles. Hands were either dextral or sinistral. When hand laterality changed unexpectedly, the vMMN occurred.

Other abstract irregularities include asymmetries (Kecskés-Kovács, Sulykos, & Czigler, 2013a), object-based irregularities (Müller, Widmann, & Schröger, 2013; Müller et al., 2010), numeric irregularities (i.e., number of items expected to appear, Hesse, Schmitt, Klingenoefer, & Bremmer, 2017), and even semantic irregularities (Wei & Gillion-Downens, 2018). This is not an exhaustive list of all the studies investigating vMMN, but it does illustrate that the visual system can readily encode higher-order regularities as well as feature-specific regularities such that their corresponding irregularity can evoke a vMMN.

## 1.3 Measuring the vMMN

To measure the vMMN, one typically uses electroencephalography (EEG). EEG reveals real-time changes in the brain's electrical activity, in the order of milliseconds (ms). One separates event-specific brain activity from exogenous and unrelated endogenous activity by averaging segments of an EEG in response to the same stimulus or event to produce an event-related potential (ERP). In the ERP, the vMMN emerges as enhanced negativity—hence the *negativity* in MMN—to an unexpected, rare, *deviant* image relative to an expected *standard* image. This method of interspersing deviants in an otherwise regular sequence is the oddball paradigm (Squires, Squires, & Hillyard, 1975) and is the preferred experimental paradigm for vMMN research.

The primary method for showing the vMMN is to subtract the standard ERP from the deviant ERP to produce a difference wave. By doing so, we find that vMMN is usually largest between 150 and 300 ms after stimulus onset in the modality-specific visual cortices (i.e., parieto-occipital scalp regions).

In visual ERPs, there are canonical visual ERP components—peaks and troughs named for whether they are positive (P) or negative (N) and the time they occur relative to the onset of the event (e.g., a stimulus). O'Shea, Roeber, and Bach (2010) described the major components in an ERP to visual input: the P1 (peak at 80–140 ms in the parieto-occipital scalp regions), N1 (trough at 140–200 ms in the parieto-occipital scalp regions), P2 (peak at 200–300 ms in the parieto-occipital scalp regions), and N2 (trough at 200–300 ms in the parieto-

occipital scalp regions). The underlying assumption is that each ERP component (or subcomponent) reflects different processes. To illustrate, the N1 is associated with early sensory processing and variance in N1 amplitudes is now widely regarded as resulting from a difference in adaptation whereas at least one subcomponent of the posterior N2 is associated with categorizing stimuli (Luck, 2005).

## 1.4 Adaptation

Adaptation-related differences arise because neurons respond less vigorously for a repeated stimulus—ERP negativities are less negative and positivities are less positive—whereas neurons responding to a novel stimulus respond vigorously for the first time. Together, increased negativity in the difference waveform owing to adaptation-related differences (e.g., N1 difference) and increased negativity owing to prediction error (e.g., the vMMN) form deviant-related negativity (DRN, Alho et al., 1992; Clifford, Holmes, Davies, & Franklin, 2010; Kimura, Ohira, & Schröger, 2010; Kimura & Takeda, 2013; Lorenzo-López, Amenedo, Pazo-Alvarez, & Cadaveira, 2004; Pazo-Álvarez, Amenedo, & Cadaveira, 2004b; Pazo-Álvarez, Amenedo, Lorenzo-López, & Cadaveira, 2004a; Wei et al., 2002).

Two controls allow one to quantify the size of the adaptation-related differences in ERP components and in doing so distinguish genuine (v)MMN from adaptation in DRN. These are the equiprobable control (Schröger & Wolff, 1996) and cascadic control (Ruhnau, Herrmann, & Schröger, 2012). I describe

these in further detail in the following chapter. For now, suffice is to say that such controls have allowed researchers to discount adaptation as a viable explanation for the (v)MMN (May & Tiitinen, 2009). Doing so has helped to shape the existing conceptualisation of the (v)MMN as a neural correlate of prediction error within predictive coding theory.

## 1.5 Thesis Structure

This thesis consists of seven Chapters. I have defined terminology, methodology, and the framework of visual processing I work within in the general introduction (Ch. 1). I do not revisit these aspects in as much detail until the concluding chapter (Ch. 7). The next chapter (Ch. 2) is a review of vMMN literature illuminating my thesis. Chapters 3 to 6 are prepared as self-contained manuscripts describing studies in which I tested my original and then revised thesis. I conclude with a general discussion of these findings and their implications.

My research agenda originally comprised three experiments addressing my original thesis: that local context and the type of unexpected change affect the vMMN. Study 1 (Ch. 3), Study 2 (Ch. 4), and Study 3 (Ch. 5) took place as planned. In Study 1, I tested whether there is a monotonic relationship between the magnitude of deviance and the size of the vMMN to changes in orientation, a basic property of visual input—an example of low-level deviance. In Study 2, I tested whether the magnitude of deviance affects the vMMN to violation in an abstract, rule-based regularity—an example of high-level deviance. In Study 3,

I tested whether changes in orientation and contrast produced distinct vMMNs (after equating for physical differences).

Conclusions were not possible. This was, in part, due to having found that changes in basic properties of visual input do not evoke the vMMN. I revised my thesis and conducted Study 4 (Ch. 6). This confirmed that isolated changes in basic properties of visual input that I tested do not evoke the vMMN, perhaps because low-level deviance is resolved in an earlier process revealed by deviant-related positivity.

# CHAPTER 2

## LITERATURE REVIEW

# 2. LITERATURE REVIEW

## 2.1 Overview

In this Chapter, I consider the evidence for aspects known (and perhaps unknown) for affecting the known neural correlate of prediction error in vision—the vMMN. I had intended to show that the local context of a change, such as the size of the difference between the anticipated and actual input (i.e., the magnitude of deviance), affects the vMMN. Only a few studies have examined the relationship between magnitude of deviance and the vMMN despite the potential for gaining further insights into the purpose of prediction error. For example, if the sole purpose of the prediction error is to update the predictive model, then a monotonic relationship between the magnitude of deviance and the vMMN is unnecessary (Horváth et al., 2008). Alternatively, if larger magnitudes of deviance produce larger vMMNs, then perhaps this is because larger vMMNs also predict later processes, such as attention switch—a redirection of attentional resources towards the changing input (Näätänen, 1990). In fact, this was one of the originally proposed reasons for the auditory MMN (Näätänen, 1990; Schröger, 1996). The assumption was indeed supported by evidence of a monotonic relationship between amplitudes of the MMN and P3a—a known neural correlate of attention switch (Friedman, Cycowicz, & Gaeta, 2001; Kimura, Katayama, & Murohashi, 2008).

However, while reviewing the vMMN literature, it became clear that there were some inconsistencies in studies testing changes in properties or features of

visual input—this is low-level deviance research. I describe these changes as feature deviants. To accommodate this, I adopted a systematic approach to summarising the existing low-level deviance research. This allowed me to capture the existing approach to investigating low-level deviance detection and identify areas in which further research is essential, in addition to exploring those aspects that do, or might, affect the vMMN.

## 2.2 Magnitude of Deviance and the vMMN

The relationship between the magnitude of deviance and the vMMN is still unknown for three reasons:

1. Conclusions about the relationship between the magnitude of deviance and the vMMN are mostly based on findings from MMN research. This research shows that larger magnitudes of deviance yield larger and earlier MMNs (Amenedo & Escera, 2000; Berti et al., 2004; Baldeweg, Richardson, Watkins, Foale, & Gruzelier, 1999; Daikhin & Ahissar, 2012; Näätänen, 1992; Novitski, Tervaniemi, Huotilainen, & Näätänen, 2004; Opitz, Rinne, Mecklinger, von Cramon, & Schröger, 2002; Pakarinen, Takegata, Rinne, Huotilainen, & Näätänen, 2007; Sams, Paavilainen, Alho, & Näätänen, 1985; Schröger, 1996; Tervaniemi et al. 1994; Tiitinen, May, Reinikainen, & Näätänen, 1994). If neural correlates of prediction error behaved similarly in different sensory modalities, one could easily generalise MMN findings (including the

relationship between magnitude of deviance and the MMN) to the vMMN. However, some experimental manipulations affect the vMMN, but not the MMN, such as attention (Alho et al., 1992). Therefore, one needs to be cautious when generalising MMN findings to the vMMN.

2. Findings concerning magnitude of deviance and the vMMN are limited and contradictory (Czigler et al., 2002; Czigler & Csibra, 1990; Czigler & Sulykos, 2010; Flynn et al., 2009; Maekawa et al., 2005; Takacs et al., 2013). For example, Czigler et al. (2002) found that small colour deviants did not yield a vMMN whereas large colour deviants did. Although this could represent a magnitude of deviance effect, a higher deviance threshold for colour deviants could explain it. Furthermore, in two different stimulus orientation studies, one found no magnitude of deviance effect whatsoever (Czigler & Sulykos, 2010) whereas another found an effect on vMMN amplitude, but not on vMMN latency (Takács, Sulykos, Czigler, Barkaszi, & Balázs, 2013). Adding to the complexity, Maekawa et al. (2005) tested spatial-frequency deviants and found that the magnitude of deviance affected vMMN latency, but not amplitude.
3. The relationship between magnitude of deviance and the vMMN is unclear because most of the research investigating the relationship between the magnitude of deviance and (v)MMN did not employ a control for adaptation. This is especially problematic because larger

differences between adapted and unadapted stimuli yield larger ERP differences, causing what appears to be a magnitude of deviance effect. For example, the larger the difference between the frequencies of standard and deviant tones, the larger the adaptation-related difference is (e.g., Daikhin & Ahissar, 2012).

## 2.3 Adaptation

Adaptation-related differences occur because the ERP for repeated stimuli is attenuated (neurons respond less vigorously or fewer neurons respond) compared to the ERP to novel stimuli (neurons respond vigorously for the first time). In an oddball sequence (Squires et al., 1975), a rare, novel stimulus—known as the *deviant*—interrupts a series of regular events—known as the *standards*. Traditionally, all stimuli appear for a specified amount of time—this is the stimulus duration—and an inter-stimulus-interval (ISI)—in which no stimulus occurs—separates all stimuli. The standards occur more frequently than the deviant (***italicized in boldface***). Therefore, the standards establish regularity and a deviant violates it (e.g., S... S... ***D***... S...; "..." denotes the ISI). This is the most popular paradigm used for showing the (v)MMN (Kujula et al., 2007) and because standards occur more frequently (e.g., between 80% and 90% of trials are standards), they are more adapted than the deviant, producing an adaptation-related difference that must be controlled for.

There are two methods for controlling for adaptation. These are the equiprobable control (Schröger & Wolff, 1996) and the cascadic control

(Ruhnau et al., 2012). In the equiprobable control, equally probable random stimuli replace standards. The stimulus in the control sequence that is physically identical to the deviant in the oddball sequence is the so-called control. The number of other stimuli in control sequences usually depends on the frequency with which the deviant occurs in the oddball sequence. For example, if an oddball sequence contains 20% controls, an equiprobable control sequence also contains 20% deviants, along with four other kinds of stimuli of equal probability, including the standards. All stimuli in the control sequences appear with the same frequency so that no regularity is established. This eliminates all probability-related differences. The deviant and control are different from the preceding stimulus and they are both infrequent; therefore, the ERP for the control provides a measure of differences in activity caused by activating a group of unadapted neurons (i.e., adaptation-related difference). Subsequently, any remaining differences in ERPs between deviants and controls must then be because there is a rule in the oddball sequence (i.e., that the next stimulus will be a standard), but no such rule in the control sequence.

It is possible that adaptation (sometimes called stimulus-specific-adaptation, Ulanovsky, Las, & Nelken, 2003) is overestimated in the equiprobable control because the difference between random and control stimuli may be larger than that of the difference between standard and deviant stimuli (Jacobsen & Schröger, 2001; Näätänen & Alho, 1997). To avoid overestimating adaptation and, by doing so, underestimating (v)MMN, Ruhnau et al. (2012) proposed the cascadic control.

In the cascadic control, the control is equally infrequent as the deviant in the oddball sequence, but there is an uninterrupted regularity among all stimuli. For example, in the MMN, a control stimulus identical to a deviant (***italicized in boldface***) would be interspersed among a sequence of tones that rise and fall depending on the frequency (Hz) (e.g., 1072... 974... *886*... ***805***... *886*... 974... 1072... 1179... 1072... 974... *886*... ***805***...). Any differences in the ERPs between deviants and controls then are purely due to the predictability of the stimulus, because the only difference is that the deviant is not predictable in the oddball, but is predictable in the control sequence.

These controls allow one to exclude adaptation-related differences contributing to any observed ERP differences, thus revealing true ERP differences attributed to processing deviance. But in the absence of a control for adaptation, any magnitude of deviance effect could be due to differences in adaptation.

In effect, the relationship between magnitude of deviance and the vMMN is still unclear. Originally, I had planned to address this gap in the literature. However, in the course of reviewing the vMMN literature, it became clear that there were some inconsistencies in the low-level deviance research, warranting further attention.

## 2.4 Attention

When researchers began to explore the possibility of a visual analogue of the MMN, one of the pre-requisites was that it must also occur in the absence of

attention (Cammann, 1990). Accordingly, directing attention towards the stimulus of interest limits conclusions about whether the vMMN is a true analogue of the MMN, because the MMN occurs for unattended changes in auditory input (Näätänen et al., 1978; Näätänen, 1992). Furthermore, directing attention toward the stimulus of interest limits conclusions about which visual regularities and irregularities the brain can pre-attentively encode and detect, respectively.

Accordingly, it is common practice in vMMN research (as I will show) to direct attention away from the stimulus of interest. This usually involves asking participants to attend to an unrelated stimulus in the same modality, such as asking participants to respond when the size of a central fixation cross changes (e.g., Czigler, Balazs, & Pató, 2004), or in a different modality, such as listening to an audiobook (e.g., Astikainen, Lillstrang, & Ruusuvirta, 2008). Where attention has been on the stimulus of interest, this usually involves asking participants to make a decision about a regularity-irrelevant feature of the stimulus of interest, such as whether the stimulus appears for a long or short time (e.g., Berti et al., 2001; Berti & Schröger, 2004, 2006).

Directing attention toward the stimulus of interest can be problematic. Evidence suggests that the vMMN is affected by attention (Chen, Huang, Luo, Peng, & Liu, 2010; Wei et al., 2002). In fact, attention toward the deviant can often facilitate a vMMN to a deviant that would not produce a vMMN otherwise (e.g., Alho, Woods, Algazi, & Näätänen, 1992; Czigler & Csibra, 1990; Csibra & Czigler, 1991, 1992; Woods, Alho, & Algazi, 1992). The reason for this is not

entirely clear. One possibility is that deviance detection in vision differs from deviance detection in audition. The distinction would argue against the vMMN as a true analogue of the MMN. Alternatively, it may be that attention affects vMMN amplitudes because attention toward deviants amplifies ERP components within the vMMN time-window (e.g., N2b, Patel & Azzam, 2005). It follows that changes in negativity may reflect fluctuations in attention rather than deviance detection. Whatever the reason for the confounding effect of attention on the vMMN, these findings emphasize the importance of directing attention away from the stimulus of interest to delineate exactly which pre-attentive visual changes evoke the vMMN.

## 2.5 Types of Deviance

We can divide the vMMN literature into studies testing deviants that violate an established rule or category—abstract deviants—or studies testing deviants that differ from standards on a physical dimension—feature deviants.

### 2.5.1 Abstract Deviants

Abstract deviants differ from feature deviants because the physical properties of the stimulus do not define regularity. One can further divide vMMN abstract deviants into rule-based and categorical. Although belonging to a category is also a type of rule, whether a deviant is rule-based or categorical dictates the type of sequence in which the deviant appears. Rule-based deviants (***italicized in boldface***) are those that violate an established sequential rule or pattern among stimuli. For example, if the rule dictates that each stimulus

appears twice before changing, a third repetition of the stimulus would violate the rule, even though it is physically identical to the preceding stimulus (e.g., A... A... B... B... A... A... ***A***... B...). On the other hand, if the same deviant appears among a series of numbers, it would constitute a categorical deviant because, the numbers, although different, belong to the numeric category, whereas, the letter does not, so it evokes the vMMN (e.g., 6... 7... 5... 1... ***A***... 3...).

Czigler, Weisz, and Winkler (2006) showed participants red-black and green-black checkerboard patterns that alternated according to this rule and found that the irregular (third) repetition evoked the vMMN. In another study, Bubic, Bendixen, Schubotz, Jacobsen, and Schröger (2010) found that in sequences of circle stimuli regularly increasing in size thrice before returning to the smallest (initial) size, unpredicted size decrements evoked the vMMN. Kimura (2018) and Kimura and Takeda (2013; 2015) also found that rule-based orientation deviants evoked the vMMN when they interrupted a sequence of stimuli whose orientation changed predictably, such that the stimulus appeared to be rotating in one direction. For example, if each stimulus were oriented 32.7° in a clockwise direction from the previous stimulus, a stimulus that was oriented 32.7° in the opposite direction would violate the rule and evoke the vMMN (Kimura & Takeda, 2013; 2015).

Others have shown that the vMMN occurs for categorical violations using faces of different genders (Kecskés-Kovács, Sulykos, & Czigler, 2013b; Wang et al., 2016), facial expressions (Astikainen & Hietanen, 2009; Chang, Xu, Shi, Zhang, & Zhao, 2010; Csukly et al., 2013; Fujimura & Okanoya, 2013; Kovarski

et al., 2017; Kreegipuu et al., 2013; Stefanics, Csukly, Komlosi, Czobor, & Czigler, 2012; Zhao & Li, 2006, for a corresponding MEG study see, Susac, Ilmoniemi, Pihko, & Supek, 2004), and hand laterality (Stefanics & Czigler, 2012). Other abstract irregularities include asymmetries (Kecskés-Kovács, Sulykos, & Czigler, 2013a), object-based irregularities (Müller, Widmann, & Schröger, 2013; Müller et al., 2010), numeric irregularities (i.e., number of items expected to appear, Hesse, Schmitt, Klingenoefer, & Bremmer, 2017), and even semantic irregularities (Wei & Gillion-Downens, 2018). Clearly, the visual system can readily encode higher-order regularities such that their corresponding irregularity can evoke a vMMN.

### 2.5.2 Feature Deviants

Feature deviants are deviants that are different from standards by some physical property, such as orientation or colour. Table 2.1 gives parameters of studies examining vMMN to different feature deviants. I had four reasons for this table. It shows:

1. The kinds of feature deviants that have been used to evoke the vMMN.
2. The various magnitudes of deviance used to evoke the vMMN to feature deviants.
3. The approach to vMMN research.
4. Inconsistencies in the low-level deviance findings.

I address each of these in a section below (numbered accordingly). Most importantly, Table 2.1 allowed me to identify areas in which further research is essential.

I included all experiments that I am aware of that manipulated a single feature of the stimulus in a vMMN study or condition, provided there was ERP data from a healthy adult sample. Articles published after January 22, 2019, are not included. I also included studies returned in a Scopus search for journal articles containing specified search terms in either abstract, title, or keywords on this date "mismatch AND negativity AND (vision OR visual) AND [*insert deviant feature*]". For example, a Scopus search of "mismatch AND negativity AND (vision OR visual) AND [*spatial frequency*]" produced 14 results, but only two of these tested spatial frequency deviants in a vMMN study of healthy adults.

I also included details of studies in which authors described the increased negativity to deviants within the vMMN time-window as somethings other than vMMN. For example, Kenemans, Jong, and Verbaten (2003) were the first to describe the response to deviance as rareness-related negativity (see also Kenemans, Hebly, van den Heuvel, & Grent-'T-Jong, 2010). Others have described it as DRN (Alho et al., 1992; Clifford et al., 2010; Kimura et al., 2010; Kimura & Takeda, 2013; Lorenzo-López, Amenedo, Pazo-Alvarez, & Cadaveira, 2004; Pazo-Álvarez, Amenedo, & Cadaveira, 2004b; Pazo-Álvarez, Amenedo, Lorenzo-López, & Cadaveira, 2004a; Wei et al., 2002), change-

related negativity (Kimura, Katayama, & Murohashi, 2008), or N200/N2 difference (e.g., Berti, & Schröger, 2001, 2004, 2006).

The details for each deviant feature appear separately. For example, each feature deviant tested using the multi-feature paradigm (Näätänen, Pakarinen, Rinne, & Takegat, 2004) appears as a single entry. In the multi-feature paradigm, every second trial is a deviant trial because a feature, as opposed to the whole stimulus, determines whether the stimulus represents a standard or a deviant. Because all other (standard) features are unchanged, one deviant trial can represent a standard with respect to another feature and, in a multi-feature sequence of 12, six deviant trials are possible; two for three different deviants (e.g., S... ***D1***... S... ***D3***... S... ***D2***... S... ***D3***... S... ***D1***... S... ***D2*** ...). The ability to test different deviants within a short time is what makes the multi-feature paradigm an attractive alternative to the oddball paradigm.

In Table 2.1, studies appear chronologically for each deviant feature: orientation, contrast, luminance, spatial frequency, colour, shape or size, location, motion direction, duration, or omission. I am not aware of any vMMN study (excluding those described in the following Chapters) investigating phase deviance exclusively.

For each experiment or condition within a study, I give details about:

- The number of participants in the final data set (N).
- The stimulus(i).

- Stimulus size. Where the dimensions were not reported, I calculated size where possible. If there were multiple stimuli, I give the size of the smallest stimulus, thus revealing the smallest stimulus capable of evoking the vMMN.
- Location in the visual field and whether the stimulus appeared centrally or peripherally.
- Background (BG) colour.
- Whether the participant's task was visual, auditory, or manual.
- What occupied the participant's attention.
- The magnitude of the difference between the standard and the deviant.
- The duration of the stimulus(i) and ISI. If the duration or ISI was jittered or manipulated, I give the smallest duration and largest ISI ***italicized in boldface***.
- Deviant probability (Deviant Prob.) within an oddball sequence (as a proportion of 1).
- The minimum number of standards that separated each deviant stimulus (Min. S), if stipulated.
- Whether the authors compared physically identical stimuli.
- Whether there was a control for adaptation, such as the *equiprobable* control or the *cascadic* control. If there were multiple controls, I give the vMMN amplitude for the control in **boldface**.
- The chosen reference for the EEG data.

- Low-pass (LP) and high-pass (HP) filters used to process the EEG data (in Hz).
- The electrode or region of interest (ROI).
- The vMMN time-window (TW) used to extract mean amplitudes (in ms).
- Mean amplitude of the vMMN (in μV). Where the mean amplitude of the vMMN was not reported, I calculated the mean amplitude from difference waves (or ERPs if necessary) by dividing the maximum vMMN amplitude by the minimum vMMN amplitude within the vMMN time-window used to extract mean amplitudes.
- The time of maximum amplitude of the vMMN (in ms). Where the peak latency of the vMMN was not reported, the peak latency is estimated from the difference wave figure or is given as the mid-point of the time-window of interest.

Where all experimental conditions produced the vMMN, I favour positive results by giving the task, attention allocation, deviant probability, amplitude, latency, and electrode or ROI of the largest reported vMMN. I leave a blank where a piece of information was not available or was not applicable (e.g., there was no control for adaptation). Entries in red illustrate where the negativity was not significantly different from zero.

Table 2.1 *VMMN Research in which the Deviant is a Feature of Visual Input*

| Study | N | Stimulus(i) | Height (°VA) | Width (°VA) | BG Colour | Task Modality | Attention On | D and S Difference | Stimulus Duration | ISI | Deviant Prob. | Min. S | Physical Control | Adaptation Control | Reference | HP (Hz) | LP (Hz) | Electrode or ROI | TW (x–y ms) | vMMN A (μV) | vMMN PL (ms) |
|---|---|---|---|---|---|---|---|---|---|---|---|---|---|---|---|---|---|---|---|---|---|
| **Orientation** | | | | | | | | | | | | | | | | | | | | | |
| Czigler and Csibra (1990) | 9 | Central Chevrons | 0.77 | 1.27 | | Visual | Frame border | 180° | 83 | 417 | .20 | 2 | | | Linked-earlobes | 0.20 | 50 | Oz | 210–240 | –2.50 | 255 |
| Fu et al. (2003) | 12 | Central square-wave gratings | 3.20 | 3.20 | Black | Visual | Spatial frequency of gratings | 90° | 100 | ***100*** | .10 | 1 | Reverse roles | | Right mastoid | 0.10 | 40 | Occipital | 180–220 | –1.90 | 192 |
| Astikainen et al. (2004) | 8 | Central light bar | 3.40 | | Black | Auditory | Words | 90° | 50 | 450 | .10 | 2 | Deviant alone | | Linked-mastoids | 0.10 | 30 | Pz | 160–200 | –1.28 | 180 |
| Astikainen et al. (2008), 400 ms ISI | 10 | Central dark bar | 3.90 | | Grey | Auditory | Words | 36° | 100 | 400 | .10 | 2 | Reverse roles | Equi-probable | Average | 0.10 | 30 | Occipital | 185–205 | –0.69 | 195 |
| Astikainen et al. (2008), 1100 ms ISI | 10 | Central dark bar | 3.90 | | Grey | Auditory | Words | 36° | 100 | 1000 | .10 | 2 | Reverse roles | Equi-probable | Average | 0.10 | 30 | Occipital | 185–205 | 0.27 | 195 |
| Czigler and Pató (2009), Experiment 1 | 14 | Peripheral grid pattern | 9.30 | 13.10 | Grey | Visual | Target quadrangle width | 90° | 68 | 702 | .07 | 10 | | | Linked-mastoids | 0.10 | 30 | Right posterior | 270–290 | –1.01 | 280 |
| Kimura et al. (2009) | 12 | Central grey bar | 3.00 | 0.50 | Grey | Visual | Bar edges | 36° | 100 | 400 | .20 | 2 | Reverse roles | Equi-probable | Nose-tip | 0.10 | 30 | T6(P8) | 200–250 | –1.60 | 225 |
| Czigler and Sulykos (2010) | 24 | Peripheral line segments | 0.37 | 0.04 | Grey | Visual | Colour of central line segment | 30° | 70 | 280 | .15 | | Reverse roles | | Average mastoid | 0.15 | 30 | Oz | 162–170 | –0.60 | 166 |
| Sulykos and Czigler (2011) | 12 | Peripheral Gabor patches | 0.80 | 0.80 | Black | Visual | Spaceship task | 90° | 80 | 480 | .18 | | Reverse roles | | Linked-mastoids | 0.10 | 30 | Oz | 121–131 | –2.55 | 130 |

| Study | N | Stimulus(i) | Height (°VA) | Width (°VA) | BG Colour | Task Modality | Attention On | D and S Difference | Stimulus Duration | ISI | Deviant Prob. | Min. S | Physical Control | Adaptation Control | Reference | HP (Hz) | LP (Hz) | Electrode or ROI | TW (x–y ms) | vMMN A (μV) | vMMN PL (ms) |
|---|---|---|---|---|---|---|---|---|---|---|---|---|---|---|---|---|---|---|---|---|---|
| Kimura and Takeda (2013) | 22 | Peripheral grey bars | 3.00 | 0.40 | Grey | Visual | Fixation dot | 33° | 250 | 250 | .09 | 1 | Reverse roles | Equi-probable | Nose-tip | 1.00 | 30 | PO8 | 221–231 | –0.93 | 226 |
| Shi et al. (2013) | 12 | Peripheral red rectangles | 0.30 | 0.10 | White | Visual | Fixation cross | 90° | 50 | 550 | .10 | 1 | | | Nose-tip | 0.10 | 100 | Occipito-temporal | 150–250 | –1.60 | 200 |
| Sulykos et al. (2013) | 12 | Peripheral Gabor patches | 1.00 | 1.00 | Dark | Visual | Spaceship task | 30° | 70 | 610 | .07 | 12 | | Equi-probable | Average | 1.00 | | Parieto-occipital | 140–350 | –0.05 | 210 |
| Takács et al. (2013), Experiment 1 | 17 | Peripheral Gabor patches | 1.60 | 1.60 | Grey | Visual | Fixation dot | 50° | 100 | 350 | .12 | 3 | Reverse roles | | Average | 0.10 | 30 | Parieto-occipital | 120–140 | –0.51 | 134 |
| Takács et al. (2013), Experiment 2 | 19 | Peripheral Gabor patches | 1.60 | 1.60 | Grey | Visual | Fixation dot | 90° | 100 | 350 | .12 | 3 | Reverse roles | | Average | 0.10 | 30 | Parieto-occipital | 116–176 | –1.10 | 148 |
| Kimura and Takeda (2014), Experiment 1 | 23 | Central grey bar | | | Back | Manual | Button press | 22° | 250 | ***602*** | .10 | | Reverse roles | | Nose-tip | 1.50 | 30 | Right occipito-temporal | 200–250 | –1.19 | 225 |
| Kimura and Takeda (2014), Experiment 2 | 21 | Central grey bar | | | Black | Manual | Button press | 22° | 250 | ***607*** | .10 | | Reverse roles | | Nose-tip | 1.50 | 30 | Right occipito-temporal | 240–290 | –0.92 | 265 |
| Qian et al. (2014) | 14 | Peripheral red rectangles | 0.30 | 0.10 | White | Visual | Fixation cross | 90° | 50 | 550 | .10 | 1 | | | Nose-tip | 0.10 | 100 | Occipital-temporal | 150–250 | –1.13 | 200 |
| Noyce and Sekuler (2014) | 20 | Peripheral Chevrons | 1.40 | 1.40 | Grey | Visual | Central Chevron | 180° | 50 | 1000 | .10 | | | | Average | 0.25 | 60 | Posterior | 144–284 | –0.36 | 214 |
| Farkas et al. (2015) | 27 | Peripheral Gabor patches | 7.70 | 7.70 | Grey | Visual | Fixation cross | 90° | 200 | 450 | .20 | | Reverse roles | | Average | 0.10 | 30 | Sagital parieto-occipital | 90–200 | –0.30 | 145 |

| Study | N | Stimulus(i) | Height (°VA) | Width (°VA) | BG Colour | Task Modality | Attention On | D and S Difference | Stimulus Duration | ISI | Deviant Prob. | Min. S | Physical Control | Adaptation Control | Reference | HP (Hz) | LP (Hz) | Electrode or ROI | TW (x–y ms) | vMMN A (μV) | vMMN PL (ms) |
|---|---|---|---|---|---|---|---|---|---|---|---|---|---|---|---|---|---|---|---|---|---|
| Kimura and Takeda (2015), oddball | 22 | Peripheral grey bars | 3.00 | 0.40 | Grey | Visual | Fixation dot | 33° | 250 | 250 | .09 | 2 | Reverse roles | Equi-probable | Nose-tip | 0.10 | 30 | PO8 | 197–207 | –1.16 | 202 |
| Bodnár et al. (2017), Experiment 1 | 17 | Peripheral line texture | 1.26 | 0.09 | Black | Visual | Spaceship task | 90° | 100 | 400 | .12 | | **Reverse roles** and Standard only | | Nose-tip | 0.10 | 30 | Occipital | 112–132 | –1.56 | 123 |
| File et al. (2017), Experiment 1 | 15 | Peripheral line texture | 1.26 | 0.09 | Black | Visual | Spaceship task | 36° | 100 | 500 | .12 | 4 | Reverse roles | Equi-probable and **Cascadic** | Nose-tip | 0.10 | 30 | Parieto-occipital | 105–190 | –0.09 | 144 |
| Pesonen et al. (2017) | 16 | Central dark bar | 3.90 | | Grey | Auditory | Words | 36° | 100 | 1100 | .10 | 2 | | | Cz | 0.10 | 400 | Occipital | 100–300 | –1.02 | 210 |
| Yan et al. (2017) | 15 | Peripheral black arrows | 3.68 | 3.42 | White | Visual | Fixation cross | 90° | 100 | 500 | .20 | 2 | | | Nose-tip | 0.10 | 30 | Parieto-occipital | 100–300 | –2.60 | 200 |
| **Contrast** | | | | | | | | | | | | | | | | | | | | | |
| Nyman et al. (1990) | 9 | Peripheral square-wave gratings | 2.00 | 2.00 | | Visual | Fixation dot | -0.48 M | 100 | 490 | .10 | | Reverse roles | | Right mastoid | 0.10 | 100 | Oz | 100–200 | –0.28 | 150 |
| Wei et al. (2002) | 12 | Coloured scenery | 1.60 | 2.46 | Stimulus | Visual | Contrast increment | | | ***652*** | .15 | | | | Nose-tip | 0.10 | 40 | Oz | 150–200 | –1.20 | 152 |
| **Luminance** | | | | | | | | | | | | | | | | | | | | | |
| Stagg et al. (2004) | 12 | Peripheral white vertical bars | 2.23 | 0.34 | Black | Visual | Fixation square | 2.76 cd/m² | 200 | 612 | .06 | | Reverse roles | | Fz | 0.05 | 100 | Occipital | 210–400 | –1.67 | 305 |

| Study | N | Stimulus(i) | Height (°VA) | Width (°VA) | BG Colour | Task Modality | Attention On | D and S Difference | Stimulus Duration | ISI | Deviant Prob. | Min. S | Physical Control | Adaptation Control | Reference | HP (Hz) | LP (Hz) | Electrode or ROI | TW (x–y ms) | vMMN A (μV) | vMMN PL (ms) |
|---|---|---|---|---|---|---|---|---|---|---|---|---|---|---|---|---|---|---|---|---|---|
| Kimura et al. (2010a) | 12 | Peripheral discs | 2.50 | 2.50 | Black | Visual | Fixation cross | 76 cd/m$^2$ | 80 | ***720*** | .20 | 1 | Reverse roles | | Nose-tip | 1.00 | 35 | Oz | 150–200 | –5.29 | 175 |
| Kimura et al. (2010b) | 12 | Peripheral discs | 1.40 | 1.40 | Black | Visual | Fixation letter | 127.36 cd/m$^2$ | 150 | 450 | .20 | 4 | Reverse roles | | Nose-tip | | 35 | POz | 220–260 | –5.25 | 240 |
| Sulykos and Czigler (2014) | 14 | 3-ring concentric annuli | 2.29 | 2.29 | Blue-violet | Visual | Fixation cross | 6.3 cd/m$^2$ | 400 | ***322*** | .20 | 2 | Reverse roles | | Average | 0.10 | | Posterior | 180–220 | –0.64 | 201 |
| Jack et al. (2017) | 10 | Annular sine-wave grating | 3.20 | 3.20 | Black | Visual | Report binocular rivalry | 14.51 cd/m$^2$ | 100 | 100 | .06 | 10 | Reverse roles | | Average | 0.10 | 40 | Right posterior | 230–274 | –2.00 | 250 |
| **Spatial Frequency** | | | | | | | | | | | | | | | | | | | | | |
| Tales et al. (1999), Experiment 1 | 12 | Peripheral white vertical bars | 2.20 | 0.68 | Black | Visual | Fixation square | +0.6 cpd | 200 | ***642*** | .06 | 2 | | | Fz | | 70 | O2 | 250–400 | –4.00 | 325 |
| Tales et al. (1999), Experiment 2 | 12 | Peripheral white vertical bars | 2.20 | 0.68 | Black | Visual | Fixation square | -0.6 cpd | 200 | ***642*** | .06 | 2 | | | Fz | | 70 | O1 | 250–400 | –1.86 | 325 |
| Tales et al. (2002) | 24 | Peripheral white vertical bars | 2.20 | 0.68 | Black | Visual | Fixation square | -0.6 cpd | 200 | ***642*** | .06 | 2 | | | Fz | | 70 | O2 | 250–400 | –3.40 | 325 |
| Heslenfeld (2003) | 14 | Peripheral vertical square-wave gratings | 5.60 | 16.00 | Black | Visual | Visuo-motor task | 1.72 cpd | 17 | ***450*** | .20 | 1 | Reverse roles | | Average mastoids | 0.08 | 35 | Oz | 100–200 | –1.10 | 150 |
| Kenemans et al. (2003) | 12 | Peripheral vertical square-wave gratings | 5.20 | 5.40 | Black | Visual | Fixation cross | 1.8 cpd | 18 | 350 | .20 | | Deviant alone | | Right mastoid | 0.05 | 40 | Oz | 60–200 | –1.19 | 135 |

| Study | N | Stimulus(i) | Height (°VA) | Width (°VA) | BG Colour | Task Modality | Attention On | D and S Difference | Stimulus Duration | ISI | Deviant Prob. | Min. S | Physical Control | Adaptation Control | Reference | HP (Hz) | LP (Hz) | Electrode or ROI | TW (x–y ms) | vMMN A (μV) | vMMN PL (ms) |
|---|---|---|---|---|---|---|---|---|---|---|---|---|---|---|---|---|---|---|---|---|---|
| Stagg et al. (2004) | 12 | Peripheral white vertical bars | 2.23 | 0.34 | Black | Visual | Fixation square | 0.6 cpd | 200 | 612 | .06 | | Reverse roles | | Fz | 0.05 | 100 | Occipital | 210–400 | –3.73 | 305 |
| Maekawa et al. (2005) | 7 | Central windmill-pattern | 5.80 | 5.80 | Grey | Auditory and visual | Story and target windmill | 18 vanes | 200 | 800 | .10 | | Reverse roles | | Nose-tip | 0.05 | 50 | Oz | 230–320 | –4.50 | 245 |
| Tales and Butler (2006) | 11 | Peripheral white vertical bars | 2.20 | 0.68 | Black | Visual | Fixation square | +0.6 cpd | 200 | ***642*** | .06 | 2 | | | Fz | | 70 | T6(P8) | 250–400 | –3.90 | 300 |
| Maekawa et al. (2009), Experiment 1 | 10 | Central windmill-pattern | 5.80 | 5.80 | Grey | Auditory | Story | 18 vanes | 200 | 800 | .10 | 7 | Deviant block | | EGI average [126 127] | 0.05 | 30 | Oz | 150–300 | –6.33 | 252 |
| Maekawa et al. (2009), Experiment 2 | 8 | Central windmill-pattern | 5.80 | 5.80 | Grey | Auditory | Story | 18 vanes | 200 | 800 | .10 | 7 | Standard block | | EGI average [126 127] | 0.05 | 30 | Oz | 150–300 | –2.19 | 232 |
| Kenemans et al. (2010) | 16 | Peripheral vertical square-wave gratings | 5.20 | 5.40 | Black | Visual | Fixation cross | 1.8 cpd | 17 | 350 | .10 | | Reverse roles | | Right mastoid | 0.05 | 30 | Oz | 150–170 | –0.50 | 150 |
| Chang et al. (2011) | 14 | Peripheral white vertical bars | 2.23 | 0.34 | Black | Visual | Fixation square | 0.6 cpd | 200 | 612 | .12 | 2 | Reverse roles | Equi-probable | Nose-tip | 0.10 | 30 | Parieto-occipital | 150–250 | –1.25 | 200 |
| Sulykos and Czigler (2011) | 12 | Peripheral Gabor patches | 0.80 | 0.80 | Black | Visual | Spaceship task | 4 cpd | 80 | 480 | .18 | | Reverse roles | | Linked-mastoids | 0.10 | 30 | Oz | 135-145 | –1.18 | 136 |
| Cleary et al. (2013) | 20 | Background horizontal square-wave gratings | 14.48 | 10.88 | Stimulus | Visual | Fixation cross | 6 cpd | 1000 | 750 | .15 | | | | Right mastoid | 0.05 | 30 | O2 | 130–200 | –2.70 | 150 |
| Maekawa et al. (2013) | 20 | Central windmill-pattern | 5.80 | 5.80 | Grey | Auditory | Story | 18 vanes | 200 | 800 | .10 | | Reverse roles | | EGI average [126 127] | 0.05 | 30 | Oz | 150–350 | –1.25 | 280 |

| Study | N | Stimulus(i) | Height (°VA) | Width (°VA) | BG Colour | Task Modality | Attention On | D and S Difference | Stimulus Duration | ISI | Deviant Prob. | Min. S | Physical Control | Adaptation Control | Reference | HP (Hz) | LP (Hz) | Electrode or ROI | TW (x–y ms) | vMMN A (μV) | vMMN PL (ms) |
|---|---|---|---|---|---|---|---|---|---|---|---|---|---|---|---|---|---|---|---|---|---|
| Stothart and Kazanina (2013) | 39 | Peripheral white vertical bars | 4.47 | 1.37 | Black | Visual | Fixation square | 0.6 cpd | 200 | ***642*** | .06 | 2 | | | Average | | 40 | Parieto-occipital | 100–600 | –0.66 | 222 |
| Hedge et al. (2015) | 20 | Peripheral vertical square-wave gratings | 2.23 | 0.34 | Black | Visual | Fixation square | +0.6 cpd | 200 | 300 | .06 | 2 | Reverse roles | | Average | | 40 | Parieto-occipital | 161–329 | –0.94 | 265 |
| Hedge et al. (2015) | 20 | Peripheral vertical square-wave gratings | 2.23 | 0.34 | Black | Visual | Fixation square | -0.6 cpd | 200 | 300 | .06 | 2 | Reverse roles | | Average | | 40 | Parieto-occipital | 161–329 | –0.22 | 281 |
| Bodnár et al. (2017), Experiment 2 | 19 | Central windmill pattern | 13.82 | 13.82 | Grey | Visual | Centre tracking task | 6 vanes | 100 | 400 | .12 | | Reverse roles | | Nose-tip | 0.10 | 30 | Occipital | 198–218 | –1.73 | 203 |
| File et al. (2017), Experiment 2 | 23 | Central windmill-pattern | 13.82 | 13.82 | Grey | Visual | Spaceship task | 6 vanes | 200 | 800 | .10 | 7 | Reverse roles | Equi-probable | Average | 0.10 | 30 | Occipital | 200–340 | –1.49 | 269 |
| **Colour** | | | | | | | | | | | | | | | | | | | | | |
| Czigler et al. (2002) | 8 | Peripheral square-wave grating | 14.50 | 10.90 | Stimulus | Visual | Fixation cross | red-green | 17 | ***350*** | .12 | | Reverse roles | Equi-probable | Nose-tip | 0.10 | 30 | Occipital | 128–142 | –0.36 | 136 |
| Czigler et al. (2002) | 8 | Peripheral square-wave grating | 14.50 | 10.90 | Stimulus | Visual | Fixation cross | red-pink | 17 | ***350*** | .12 | | Reverse roles | Equi-probable | Nose-tip | 0.10 | 30 | Occipital | 128–142 | –0.07 | 136 |
| Horimoto et al. (2002), Experiment 1 | 11 | Central coloured square | | | | Auditory | Tones | blue-green blue | 1000 | ***250*** | .10 | | | | Linked-earlobes | 0.05 | 50 | Pz | 0–550 | –4.80 | 250 |
| Czigler et al. (2004) | 12 | Peripheral coloured-black checkerboard | | | Dark | Visual | Fixation cross | green-red | 17 | 350 | .10 | | Reverse roles | | Linked-mastoids | 0.10 | 30 | Oz | 140–200 | –1.36 | 170 |

| Study | N | Stimulus(i) | Height (°VA) | Width (°VA) | BG Colour | Task Modality | Attention On | D and S Difference | Stimulus Duration | ISI | Deviant Prob. | Min. S | Physical Control | Adaptation Control | Reference | HP (Hz) | LP (Hz) | Electrode or ROI | TW (x–y ms) | vMMN A (μV) | vMMN PL (ms) |
|---|---|---|---|---|---|---|---|---|---|---|---|---|---|---|---|---|---|---|---|---|---|
| Kimura et al. (2006c) | 12 | Peripheral discs | 2.50 | 2.50 | Black | Visual | Fixation shape | red-blue | 70 | 350 | .20 | | Reverse roles and **deviant block** | | Nose-tip | 0.10 | 30 | PO8 | 150–170 | –1.29 | 160 |
| Berti (2009), Experiment 1 | 8 | Peripheral triangle | | | Grey | Visual | Triangle orientation | red-green | ***200*** | 1300 | .18 | 3 | Reverse roles | | Nose-tip | 1.00 | 25 | P3 | 150–210 | –0.52 | 210 |
| Grimm et al. (2009) | 16 | Peripheral green triangles | 3.40 | 4.20 | Grey | Visual | Fixation target | green-red | 150 | 1450 | .11 | 2 | Reverse roles | | Nose-tip | 0.75 | 35 | Right occipital | 265–295 | –0.87 | 280 |
| Thierry et al. (2009) | 20 | Central disc | 2.00 | 2.00 | Grey | Visual | Shape change | green-green or blue-blue | 200 | 800 | .10 | 3 | Reverse roles | | Average | 0.10 | 20 | Parieto-occipital | 162–232 | –0.91 | 197 |
| Clifford et al. (2010) | 18 | Peripheral squares | 4.09 | 4.09 | Grey | Visual | Fixation cross | blue-green | 200 | ***1200*** | .20 | 1 | | | Average earlobes | 0.10 | 40 | Posterior | 250–350 | –1.14 | 300 |
| Czigler and Sulykos (2010) | 24 | Peripheral line segments | 0.37 | 0.04 | Grey | Visual | Central line segment | turquoise-yellow-green | 70 | 280 | .15 | | Reverse roles | | Average mastoids | 0.15 | 30 | POz | 137–145 | –0.60 | 141 |
| Stefanics et al. (2011), Experiment 1 | 13 | Peripheral discs | | | Grey | Visual | Fixation cross | red-green | 100 | 300 | .10[d] | | Reverse roles | | Average | 0.10 | 30 | Occipital | 100–400 | –0.66 | 222 |
| Stefanics et al. (2011), Experiment 2 | 15 | Peripheral discs | | | Grey | Visual | Fixation cross | red-green | 100 | ***300*** | .20 | | Reverse roles | | Average | 0.10 | 30 | Occipital | 100–400 | –1.16 | 214 |
| Mo et al. (2011) | 30 | Peripheral squares | 2.50 | 2.50 | Grey | Visual | Fixation cross | blue-green | 200 | 900 | .20 | | Reverse roles | | Nose-tip | 0.80 | 20 | Parieto-occipital | 130–190 | –1.03 | 160 |
| Müller et al. (2012) | 15 | Peripheral discs | 0.92 | 0.92 | Grey | Visual | Fixation cross | green-red | 120 | 600 | .10 | 1 | Reverse roles | | Nose-tip | 1.00 | 35 | Occipital | 240–280 | –1.57 | 260 |

| Study | N | Stimulus(i) | Height (°VA) | Width (°VA) | BG Colour | Task Modality | Attention On | D and S Difference | Stimulus Duration | ISI | Deviant Prob. | Min. S | Physical Control | Adaptation Control | Reference | HP (Hz) | LP (Hz) | Electrode or ROI | TW (x–y ms) | vMMN A (μV) | vMMN PL (ms) |
|---|---|---|---|---|---|---|---|---|---|---|---|---|---|---|---|---|---|---|---|---|---|
| Shi et al. (2013) | 12 | Peripheral red rectangles | 0.30 | 0.10 | White | Visual | Fixation cross | red-blue | 50 | 550 | .10 | 1 | | | Nose-tip | 0.10 | 100 | Occipito-temporal | 150–250 | –1.00 | 200 |
| Qian et al. (2014) | 14 | Peripheral red rectangles | 0.30 | 0.10 | White | Visual | Fixation cross | red-blue | 50 | 550 | .10 | 1 | | | Nose-tip | 0.10 | 100 | Occipito-temporal | 150–250 | –1.18 | 200 |
| Sysoeva et al. (2015) | 12 | Peripheral discs | 4.23 | 4.23 | Black | Visual | Peripheral line orientation | red-green | ***18*** | ***1611*** | .10 | | Reverse roles | | Average mastoids | 1.00 | 30 | O1 | 120–160 | –0.47 | 141 |
| Zhong et al. (2015) | 26 | Peripheral squares | 1.27 | 1.27 | Grey | Visual | Fixation cross | blue-green | 200 | 900 | .20 | 1 | | | Nose-tip | 0.80 | 20 | Parieto-occipital | 130–190 | –0.36 | 160 |
| Stefanics et al. (2018) | 34 | Peripheral faces | 5.40 | 3.80 | Grey | Visual | Fixation cross | red-green | 200 | ***600*** | .50 | 5 | Reverse roles | | Average | 0.05 | 30 | Occipito-temporal | 196–228 | –1.00 | 200 |
| **Shape or Size** | | | | | | | | | | | | | | | | | | | | | |
| Alho et al. (1992) | 12 | Central white vertical gratings | 4.40 | 3.90 | Black | Auditory and Visual | Deviants | -0.50° height | 50 | ***400*** | .20 | | Deviant alone | | Non-cephalic | 0.10 | 40 | Oz | | –2.00 | 200 |
| Woods et al. (1992), Experiment 2 | 12 | Peripheral vertical gratings | 4.40 | 3.90 | Black | Auditory and Visual | Deviants | -0.80° height | 50 | 300 | .10 | | | | Non-cephalic | 0.10 | 40 | Lateral occipital | 220–300 | –2.32 | 260 |
| Kimura et al. (2008) | 12 | Peripheral discs | 1.70 | 1.70 | Black | Visual | Fixation target | 0.9° diameter | 200 | 1600 | .16 | | Deviant block | | Nose-tip | 0.03 | 30 | Oz | 120–140 | –1.54 | 130 |
| Grimm et al. (2009) | 16 | Peripheral green triangles | 3.40 | 4.20 | Grey | Visual | Fixation target | Hexagon | 150 | 1450 | .11 | 2 | Reverse roles | | Nose-tip | 0.75 | 35 | Right occipital | 245–275 | –0.70 | 260 |

| Study | N | Stimulus(i) | Height (°VA) | Width (°VA) | BG Colour | Task Modality | Attention On | D and S Difference | Stimulus Duration | ISI | Deviant Prob. | Min. S | Physical Control | Adaptation Control | Reference | HP (Hz) | LP (Hz) | Electrode or ROI | TW (x–y ms) | vMMN A (μV) | vMMN PL (ms) |
|---|---|---|---|---|---|---|---|---|---|---|---|---|---|---|---|---|---|---|---|---|---|
| Bubrovszky and Thomas (2011) | 10 | Central "O" | | | | Visual | Fixation target | "X" | 200 | ***1200*** | .10 | | | | | 0.10 | 45 | Posterior | 185–232 | | 208 |
| Shi et al. (2013) | 12 | Peripheral red rectangles | 0.30 | 0.10 | White | Visual | Fixation cross | red-ellipses | 50 | 550 | .10 | 1 | | | Nose-tip | 0.10 | 100 | Occipito-temporal | 150–250 | –1.00 | 180 |
| Shi et al. (2013) | 12 | Peripheral red rectangles | 0.30 | 0.10 | White | Visual | Fixation cross | +0.06° width | 50 | 550 | .10 | 1 | | | Nose-tip | 0.10 | 100 | Occipito-temporal | 150–250 | –0.60 | 190 |
| Qian et al. (2014) | 14 | Peripheral red rectangles | 0.30 | 0.10 | White | Visual | Fixation cross | red-ellipses | 50 | 550 | .10 | 1 | | | Nose-tip | 0.10 | 100 | Occipito-temporal | 150–250 | –0.61 | 200 |
| Qian et al. (2014) | 14 | Peripheral red rectangles | 0.30 | 0.10 | White | Visual | Fixation cross | +0.06° width | 50 | 550 | .10 | 1 | | | Nose-tip | 0.10 | 100 | Occipito-temporal | 150–250 | –0.62 | 180 |
| Yu et al. (2017) | 23 | Peripheral novel polygons | | | White | Visual | Fixation cross | Different polygon | 200 | 900 | .20 | 1 | | | Nose-tip | 0.80 | 40 | Lateral parieto-occipital | 130–190 | –1.08 | 160 |
| **Location** | | | | | | | | | | | | | | | | | | | | | |
| Berti and Schröger (2004), Experiment 1 | 10 | Central grey triangles | | | Green square on grey | Visual | Stimulus duration | moved in green square | ***200*** | 1300 | .12 | | | | Nose-tip | 1.00 | 20 | P8 | 150–250 | –1.90 | 224 |
| Berti and Schröger (2004), Experiment 2 | 6 | Central grey triangles | | | Green square on grey | Visual | Stimulus duration | moved in green square | ***200*** | 1300 | .12 | | | Equi-probable | Nose-tip | 1.00 | 20 | Parieto-occipital | 220–300 | | 245 |
| Berti and Schröger (2006) | 8 | Central grey triangles | | | Green square on grey | Visual | Stimulus duration | moved in green square | ***200*** | 1300 | .12 | | | Equi-probable | Nose-tip | 1.00 | 20 | P8 | 170–300 | –0.57 | 200 |

| Study | N | Stimulus(i) | Height (°VA) | Width (°VA) | BG Colour | Task Modality | Attention On | D and S Difference | Stimulus Duration | ISI | Deviant Prob. | Min. S | Physical Control | Adaptation Control | Reference | HP (Hz) | LP (Hz) | Electrode or ROI | TW (x–y ms) | vMMN A (μV) | vMMN PL (ms) |
|---|---|---|---|---|---|---|---|---|---|---|---|---|---|---|---|---|---|---|---|---|---|
| Berti (2009), Experiment 1 | 8 | Peripheral green triangle | | | Grey | Visual | Triangle orientation | Laterally shifted | 200 | 1300 | .18 | 3 | Reverse roles | | Nose-tip | 1.00 | 25 | P3 | 150-210 | –2.74 | 190 |
| Berti (2009), Experiment 2 | 8 | Central green triangle | | | Grey | Visual | Number task | Laterally shifted | 200 | 1300 | .18 | 3 | Reverse roles | | Nose-tip | 1.00 | 25 | P3 | 150-210 | –2.37 | 200 |
| Boll and Berti (2009) | 11 | Peripheral red triangles | | | Grey | Auditory and Visual | | 0.42° skyward shift | 200 | ***1700*** | .19 | | | | Nose-tip | 1.00 | 20 | P8 | 170–250 | –0.86 | 200 |
| Grimm et al. (2009) | 16 | Peripheral green triangles | 3.40 | 4.20 | Grey | Visual | Fixation target | 2.4° vertically shifted | 150 | 1450 | .11 | 2 | Reverse roles | | Nose-tip | 0.75 | 35 | Right occipital | 230–260 | –0.93 | 245 |
| Berti (2011) | 10 | Upper-case consonants | | | Grey | Visual | Target detection | Vertically shifted | 100 | | .40 | 5 | | | Nose-tip | 1.00 | 30 | O2 | 260–300 | –2.36 | 280 |
| Schmitt et al. (2018) | 8 | Gabor pattern | 3.20 | 3.20 | Stimulus | Visual | Central or peripheral Gabor pattern | 9.4° left or right | 190 | ***210*** | .20 | | Reverse roles | Equi-probable | Average-mastoids | | 50 | Parieto-occipital | 140–170 | –1.21 | 160 |
| **Motion Direction** | | | | | | | | | | | | | | | | | | | | | |
| Lorenzo-Lopéz et al. (2004) | 7 | Peripheral horizontal sinusoidal grating | 4.13 | 4.13 | | Visual | Fixation number | 1.95°/s opposite direction | 133 | 665 | .20 | 1 | | | Nose-tip | 0.10 | 30 | Parieto-occipital | 165–205 | –2.26 | 155 |
| Pazo-Alvarez et al. (2004a) | 7 | Peripheral sinusoidal grating | 4.13 | 4.13 | | Visual | Fixation number | 1.95°/s opposite direction | 133 | 665 | .20 | 1 | Reverse roles | Equi-probable | Nose-tip | 0.10 | 30 | Occipital | 145–165 | –1.80 | 155 |
| Pazo-Alvarez et al. (2004b) | 12 | Peripheral sinusoidal grating | 4.13 | 4.13 | | Visual | Fixation number | 1.95°/s opposite direction | 133 | 665 | .20 | 1 | Reverse roles | | Nose-tip | 0.05 | 100 | Occipito-temporal | 100–225 | –0.53 | 150 |

| Study | N | Stimulus(i) | Height (°VA) | Width (°VA) | BG Colour | Task Modality | Attention On | D and S Difference | Stimulus Duration | ISI | Deviant Prob. | Min. S | Physical Control | Adaptation Control | Reference | HP (Hz) | LP (Hz) | Electrode or ROI | TW (x–y ms) | vMMN A (μV) | vMMN PL (ms) |
|---|---|---|---|---|---|---|---|---|---|---|---|---|---|---|---|---|---|---|---|---|---|
| Kremláček et al. (2006) | 9 | Peripheral horizontal sinusoidal grating | 30.0 | 42.0 | Stimulus | Visual | Fixation target | 50°/s opposite direction | 200 | 600 | .06 | 3 | | | Right earlobe | 0.30 | 30 | Occipital | 145-260 | –2.59 | 202 |
| Amenedo et al. (2007) | 12 | Peripheral sinusoidal grating | 4.13 | 4.13 | Stimulus | Visual | Fixation number | 1.95°/s opposite direction | 133 | 665 | .20 | 1 | | | Nose-tip | 0.10 | 30 | Posterior | 145–225 | –1.63 | 198 |
| Hosák et al. (2008) | 17 | Peripheral sinusoidal grating | 30.00 | 42.00 | Stimulus | Visual | Fixation target | 50°/s opposite direction | 200 | 600 | .06 | 3 | | | Right earlobe | 0.30 | 30 | Parieto-occipital | 120–240 | –1.60 | 180 |
| Kuldkepp et al. (2013) | 40 | Peripheral vertical sinusoidal gratings | 20.50 | 27.60 | Stimulus | Visual | Target motion | 1.6°/s opposite direction | 200 | 600 | .15 | 1 | | | Linked-earlobes | 1.00 | 30 | Parietal | 150–175 | –0.47 | 167 |
| **Duration or Omission** | | | | | | | | | | | | | | | | | | | | | |
| Chen et al. (2010) | 13 | Central red disc | 2.29 | 2.29 | Black | Auditory | Stimulus duration | -80 ms | 200 | ***1500*** | .15 | | Reverse roles | | Nose-tip | 0.10 | 24 | Parieto-occipital | 296–336 | | 316 |
| Khodanovich et al. (2010) | 10 | Green light-emitting diodes | 1.15 | 1.15 | | Visual | Deviant | -50 ms | 200 | ***2000*** | .20 | | Deviant block | | Average earlobes | 0.16 | 25 | Posterior temporal | 200–400 | –1.50 | 300 |
| Qiu et al. (2011) | 20 | Peripheral black squares | 3.80 | 4.00 | | Visual | Fixation cross | -100 ms | 150 | ***350*** | .20 | | Reverse roles | | Nose-tip | 0.10 | 100 | Occipital | 200–250 | –2.74 | 225 |
| Shi et al. (2013) | 12 | Peripheral red rectangles | 0.30 | 0.10 | White | Visual | Fixation Cross | +50 ms | 50 | 550 | .10 | 1 | | | Nose-tip | 0.10 | 100 | Occipito-temporal | 150–250 | –0.70 | 200 |
| Qian et al. (2014) | 14 | Peripheral red rectangles | 0.30 | 0.10 | White | Visual | Fixation Cross | +50 ms | 50 | 550 | .10 | 1 | | | Nose-tip | 0.10 | 100 | Occipito-temporal | 150–250 | –0.78 | 133 |

| Study | N | Stimulus(i) | Height (°VA) | Width (°VA) | BG Colour | Task Modality | Attention On | D and S Difference | Stimulus Duration | ISI | Deviant Prob. | Min. S | Physical Control | Adaptation Control | Reference | HP (Hz) | LP (Hz) | Electrode or ROI | TW (x–y ms) | vMMN A (μV) | vMMN PL (ms) |
|---|---|---|---|---|---|---|---|---|---|---|---|---|---|---|---|---|---|---|---|---|---|
| Si et al. (2014) | 15 | Peripheral red rectangles | 4.50 | 4.50 | | Visual | Fixation cross | +50 ms | 50 | 500 | .20 | 2 | | | Nose-tip | 0.10 | 30 | Occipito-temporal | 200–250 | –1.10 | 216 |
| Yang et al. (2016), increment | 21 | Peripheral black squares | 3.80 | 4.00 | | Visual | Fixation cross | +100 ms | 50 | 600 | .20 | 2 | | | Nose-tip | 1.00 | 30 | Occipital | 180–260 | –1.15 | 220 |
| Yang et al. (2016), decrement | 21 | Peripheral black squares | 3.80 | 4.00 | | Visual | Fixation cross | -100 ms | 150 | 600 | .20 | 2 | | | Nose-tip | 1.00 | 30 | Occipital | 180–260 | –0.49 | 200 |
| Durant et al. (2018), static decrement | 20 | Peripheral moving white dots | 0.15 | 0.15 | Grey | Visual | Spaceship task | -80 ms | 200 | ***600*** | .17 | 3 | | | Average | 0.50 | 30 | Parieto-occipital | 220–270 | –0.52 | 245 |
| Durant et al. (2018), static increment | 20 | Peripheral moving white dots | 0.15 | 0.15 | Grey | Visual | Spaceship task | +80 ms | 120 | ***600*** | .17 | 3 | | | Average | 0.50 | 30 | Parieto-occipital | 220–270 | | |
| Czigler et al. (2006), Experiment 1 | 10 | Peripheral matrix of squares | 0.50 | 0.50 | Grey | Visual | Fixation cross or omissions | -17 ms | 17 | ***127*** | .10 | 4 | | | Nose-tip | 0.10 | 30 | Oz | 100–200 | –1.97 | 190 |
| Czigler et al. (2006), Experiment 2 | 12 | Peripheral matrix of squares | 0.50 | 0.50 | Grey | Visual | Fixation cross | -17 ms | 17 | ***127*** | .10 | 4 | | | Nose-tip | 0.10 | 30 | O2 | 186–226 | –2.83 | 206 |

*Note*. N = number of participants in the final data set. ºVA = degrees of visual angle. BG = background. D = Deviant. S = Standard. ISI = Inter-stimulus-interval. Deviant Prob. = deviant probability within an oddball sequence. Min. S = minimum number of standards that separated each deviant stimulus. HP = high-pass. LP = low-pass. ROI = region of interest. TW = time-window used to calculate mean amplitude. vMMN A = mean amplitude of visual mismatch negativity. vMMN LP = visual mismatch negativity peak latency. Spaceship task = Sulykos and Czigler (2011) designed the Spaceship task to ensure absolute control of participants' attention. The task field occupies an area of the visual field opposite the stimulation of interest. Participants navigate a spaceship through a canyon—a rectangular object vertically and horizontally segmented giving the impression of depth and a horizon—while avoiding/catching colour-determined targets. These targets may be other spaceships (Sulykos, Kecskés-Kovács, & Czigler, 2015) or coloured doors (Sulykos & Czigler, 2011).

## 2.6 Low-level Deviance

### 2.6.1 Feature deviants that evoke the vMMN

Table 2.1 illustrates all the basic features of visual input that yield the vMMN. There are 24 entries for orientation, two for contrast, five for luminance, 20 for spatial frequency, 19 for colour, ten for shape and size, nine for location, seven for motion, and 12 for duration and omission. Contributing 22% of the 108 entries in Table 2.1, orientation is the most investigated feature deviant. Therefore, orientation appears to be the most robust property of visual input known for evoking the vMMN.

In Figure 2.1, I depict the relationship between my dependent variable (i.e., mean vMMN amplitude and peak latency) across all entries with available amplitude and peak latency data. There was a significant moderate negative relationship between vMMN amplitude and latency, $r$ (102) = –.352, $p$ < .001 (two-tailed), indicating that vMMNs with later peak latencies were also larger than vMMNs with earlier peak latencies.

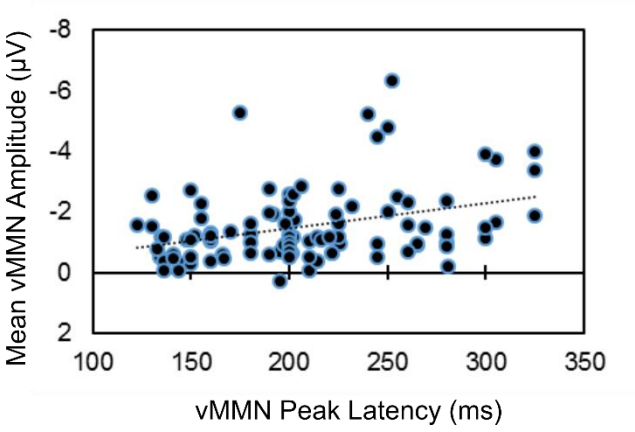


*Figure 2.1* Scatter plot depicts the correlation between vMMN peak latency and mean amplitude. Mean amplitude and peak latency data were available for only 104 of the 108 experiments or conditions within experiments in Table 2.1. Note the correlation is negative; the reversed values on the y-axis give the impression of a positive correlation. Black dotted line depicts the linear trend in the data.

### 2.6.2 Magnitude of deviance and the vMMN to feature deviants

To glean a meaningful relationship between the magnitude of deviance and mean vMMN amplitude or peak latency, I performed correlational and linear regression analyses of vMMN amplitude and latency using orientation entries in Table 2.1. I chose orientation for having the largest number of entries in Table 2.1 ($N$ = 24). I did not include all studies because magnitudes of deviance between the standard and deviant stimuli for other basic properties of visual input (e.g., location, motion direction, and duration) are less amenable to standardisation and their standardised differences may not equate across properties of visual input. I standardised the magnitude of deviance by calculating it as the difference between the deviant and the standard orientation, divided by 90 if it less than or equal to 90°, or minus 90 and then divided by 90 if it is more than 90°.[1]

In addition to the magnitude of deviance, I included covariates that others have shown affect the vMMN in my linear regression analyses. I discuss the evidence for this in detail in section 2.6.3. These are:

- attention (binary, towards versus away from the stimulus of interest),
- deviant probability (as a proportion of 1),
- ISI (in ms),

[1] If the deviant had an orientation of 90° and the standard had an orientation of 180°, the difference is 1.0. If the deviant had an orientation of 155° and the standard had an orientation of 45°, the difference is 0.22.

- control for adaptation (binary, yes or no).

Table 2.2 shows the correlations between these predictors and vMMN mean amplitude ($M$ = –1.10 µV, $SD$ = 0.77) or peak latency ($M$ = 194 ms, $SD$ = 42) for orientation deviants[2]. Deviant probability, whether there was a control for adaptation, and whether the participants' attention was on versus away from the stimulus of interest, predicted mean vMMN amplitude. The moderate positive correlation between adaptation control and vMMN amplitudes suggests that vMMN amplitudes were larger (more negative) when there was no control for adaptation compared to when there was. There was also a moderate negative correlation between attention and vMMN amplitude. This suggests that attention toward the changing stimulus evoked larger vMMN amplitudes than when attention was elsewhere. Furthermore, the negative moderate correlation between deviant probability and vMMN amplitude, suggests that deviants that are more frequent evoked larger vMMN amplitudes than less frequent deviants.

Attention also predicted vMMN peak latency. The moderate positive correlation suggests that peak latency is later when attention is on the changing stimulus compared to when it is not. No other predictor was significant and scatter plots did not reveal any (perhaps non-monotonic) relationship between the magnitude of deviance and mean vMMN amplitude or vMMN peak latency (Figure 2.2).

[2] Visual inspection of normal Q-Q-plots and detrended normal Q-Q-plots confirmed normality for variables in tables depicting bivariate Pearson's r correlation coefficients. Linearity and homoscedasticity between non-binary variables (e.g., amplitude, latency, magnitude of deviance, ISI, and deviant probability) was assessed via visual inspection of scatter plots. Although a linear relationship was not always evident, scatter plots did not reveal any non-linear relationships.

Table 2.2 *Bivariate Pearson's r Correlation Coefficients between Magnitude of Deviance, Attention, Deviant Probability, Inter-stimulus-interval (ISI), Adaptation Control, and vMMN Amplitude or Latency for Orientation Deviants*

| Measure | | 1 | 2 | 3 | 4 | 5 | 6 |
|---|---|---|---|---|---|---|---|
| 1. | Mean Amplitude/ Peak Latency | — | –.312 | **–.354*** | **–.486**** | .344 | **.417*** |
| 2. | Magnitude of Deviance | –.183 | — | –.168 | .207 | –.056 | –.423* |
| 3. | Attention | **.473*** | –.168 | — | .223 | –.188 | –.103 |
| 4. | Deviant Probability | –.240 | .207 | .223 | — | –.233 | –.188 |
| 5. | ISI | .283 | –.056 | –.188 | –.233 | — | –.068 |
| 6. | Adaptation Control | .081 | –.423* | –.103 | –.188 | –.068 | — |

*Note*. Correlations for mean amplitude appear above the diagonal and correlations for peak latency appear below the diagonal. *$p$ < .05 **$p$ < .01

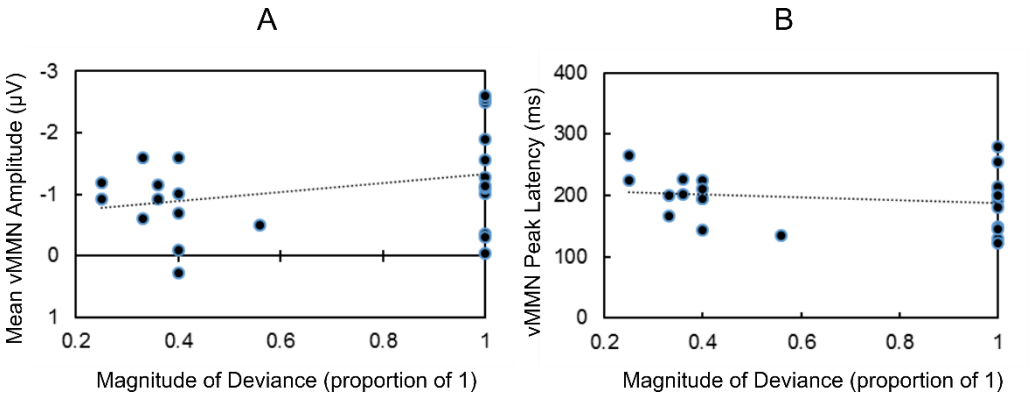


*Figure 2.2* Scatter plots depict the relationships between Magnitude of Deviance and mean vMMN amplitude (A) or vMMN peak latency (B) for orientation deviants ($p$ > .05). Black dotted lines depict the linear trends in the data.

I show un-standardised (*B*) and standardised (ß) regression coefficients and squared semi-partial (or 'part') correlations ($sr^2$) for each predictor in two linear regression analyses: one without (1) and one with (2) magnitude of deviance in Table 2.3. I also present the amount of variance explained by each regression equation ($R^2$), their effect sizes (Cohen's $f^2$), and the change in

variance explained ($\Delta R^2$) caused by adding magnitude of deviance. I analysed the mean vMMN amplitude and peak latency separately.

Table 2.3 *Un-standardised (B) and Standardised (ß) Regression Coefficients, and Squared Semi-Partial Correlations ($sr^2$) for each Predictor in the Linear Regression Analysis with and without Magnitude of Deviance with Variance Explained ($R^2$), Effect Size ($f^2$), and Change in Variance Explained ($\Delta R^2$) for vMMN Amplitudes and Latencies for Orientation Deviants (N = 24)*

| Measure | *B* | 95% CI of *B* | | ß | $sr^2$ | $R^2$ | $f^2$ | $\Delta R^2$ |
|---|---|---|---|---|---|---|---|---|
| Mean Amplitude | | | | | | | | |
| 1. Attention | –.371 | –1.055 | .315 | –.199 | .037 | .460* | .852 | |
| Deviant Probability | –5.783 | –12.690 | 1.125 | –.315 | .060 | | | |
| ISI | .001 | <.001 | .002 | .257 | .087 | | | |
| Adaptation Control | .591 | –.013 | 1.195 | .355 | .120 | | | |
| 2. Attention | –.450 | –1.173 | .274 | –.241 | .049 | .478* | .916 | .018 |
| Deviant Probability | –5.309 | –12.421 | 1.803 | –.289 | .052 | | | |
| ISI | .001 | < .001 | .002 | .241 | .071 | | | |
| Adaptation Control | .479 | –.201 | 1.159 | .288 | .064 | | | |
| Magnitude of Deviance | –.373 | –1.360 | .613 | –.158 | .018 | | | |
| Peak Latency | | | | | | | | |
| 1. **Attention **** | 62.061 | 24.758 | 99.364 | .610 | .345 | .460* | .852 | |
| Deviant Probability | –274.780 | –651.685 | 102.125 | –.274 | .106 | | | |
| ISI | .059 | –.005 | .124 | .342 | .066 | | | |
| Adaptation Control | 10.561 | –22.405 | 43.527 | .116 | .013 | | | |
| 2. **Attention **** | 63.742 | 23.686 | 103.799 | .627 | .333 | .463* | .862 | .003 |
| Deviant Probability | –284.906 | –678.727 | 108.914 | –.284 | .109 | | | |
| ISI | .060 | –.006 | .127 | .348 | .069 | | | |
| Adaptation Control | 12.957 | –24.705 | 50.618 | .143 | .016 | | | |
| Magnitude of Deviance | 7.986 | –46.648 | 62.620 | .062 | .003 | | | |

*Note*. CI = confidence interval. ISI = Inter-stimulus-interval. *$p$ < .05 **$p$ < .01

Table 2.3 shows that adding magnitude of deviance to the regression equation does not explain any more of the variance in the amplitude data either. Despite the significant correlations with vMMN amplitude in Table 2.2, no predictor explained a significant amount of the variance in either regression equation for mean vMMN amplitude (Table 2.3).

Similarly, adding magnitude of deviance to the regression equation did not significantly increase the variance explained in the peak latency data. Here, attention was the single greatest predictor of vMMN peak latency, explaining up to 34.5% of the variance.

To demarcate whether magnitude of deviance affects the vMMN peak latency for some feature deviants, such as spatial frequency (Maekawa et al., 2005), but not others, such as orientation, I performed a similar analysis on the data for spatial frequency deviants ($n$ = 20). Mean (*SD*) vMMN amplitude and peak latency for spatial frequency deviants was –2.21 μV (1.61) and 238 ms (66), respectively. Standardised magnitude of deviance was the difference between deviant and standard, divided by the larger spatial frequency.[3] Results for the correlations and linear regressions appear in Table 2.4 and Table 2.5, respectively.

[3] If the deviant had a spatial frequency of 1.2 cpd and the standard had a spatial frequency of 0.6 cpd, the difference is 0.5.

Table 2.4 *Bivariate Pearson's r Correlation Coefficients between Magnitude of Deviance, Attention, Deviant Probability, Inter-stimulus-interval (ISI), Adaptation Control, and vMMN Amplitude or Latency for Spatial Frequency Deviants (N = 20)*

| Measure | | 1 | 2 | 3 | 4 | 5 | 6 |
|---|---|---|---|---|---|---|---|
| 1. | Mean Amplitude/ Peak Latency | — | −.106 | −.336 | .236 | **−.580**** | .178 |
| 2. | Magnitude of Deviance | **−.471*** | — | .306 | .523** | .154 | −.277 |
| 3. | Attention | .027 | .306 | — | −.012 | .275 | −.076 |
| 4. | Deviant Probability | **−.853***** | .154 | −.012 | — | −.188 | .054 |
| 5. | ISI | .339 | .523 | .275 | −.188 | — | .220 |
| 6. | Adaptation Control | −.015 | −.277 | −.076 | .054 | .220 | — |

*Note*. Correlations for amplitude appear above the diagonal and correlations for peak latency appear below the diagonal. *$p < .05$ **$p < .01$ ***$p < .001$

The only significant correlate with mean vMMN amplitude was ISI. The moderately strong negative correlation suggests that longer ISIs yield larger vMMN amplitudes than shorter ISIs. Deviant probability and magnitude of deviance was negatively correlated with peak latency such that more frequent and smaller changes in deviants are related to earlier vMMNs.

Table 2.5 shows that despite a significant relationship between magnitude of deviance and peak latency in Table 2.4, magnitude of deviance did not explain a significant amount of variance in the peak latency data and the only significant predictor of vMMN peak latency was deviant probability. Similar to orientation, scatter plots did not reveal a relationship between magnitude of deviance and mean vMMN amplitude or peak latency (Figure 2.3).

Table 2.5 *Un-standardised (B) and Standardised (ß) Regression Coefficients, and Squared Semi-Partial Correlations ($sr^2$) for each Predictor in the Linear Regression Analysis with and without Magnitude of Deviance with Variance Explained ($R^2$), Effect Size ($f^2$), and Change in Variance Explained ($\Delta R^2$) for vMMN Amplitudes and Latencies for Spatial Frequency Deviants (N = 20)*

| Measure | *B* | 95% CI of *B* | | ß | $sr^2$ | $R^2$ | $f^2$ | $\Delta R^2$ |
|---|---|---|---|---|---|---|---|---|
| Mean Amplitude | | | | | | | | |
| 1. Attention | –1.098 | –4.147 | 1.950 | –.153 | .021 | | | |
| Deviant Probability | 3.719 | –10.332 | 17.769 | .109 | .011 | .466* | .873 | |
| **ISI *** | –.005 | –.009 | –.001 | –.581 | .280 | | | |
| Adaptation Control | 1.505 | –.687 | 3.697 | .288 | .076 | | | |
| 2. Attention | –1.262 | –4.544 | 2.020 | –.175 | .026 | | | |
| Deviant Probability | 1.473 | –17.572 | 20.517 | .043 | .001 | | | |
| **ISI *** | –.005 | –.010 | –.001 | –.613 | .273 | .471 | .890 | .006 |
| Adaptation Control | 1.710 | –.823 | 4.242 | .327 | .079 | | | |
| Magnitude of Deviance | 1.492 | –6.666 | 9.650 | .110 | .006 | | | |
| Peak Latency | | | | | | | | |
| 1. Attention | –11.901 | –95.676 | 71.874 | –.040 | .001 | | | |
| **Deviant Probability *** ** | –1146.358 | –1532.483 | –760.233 | –.815 | .632 | .763*** | 3.220 | |
| ISI | .074 | –.035 | .183 | .201 | .034 | | | |
| Adaptation Control | –3.956 | –64.194 | 56.282 | –.018 | <.001 | | | |
| 2. Attention | –3.251 | –92.105 | 85.603 | –.011 | <.001 | | | |
| **Deviant Probability ** ** | –1027.659 | –1543.219 | –512.099 | –.731 | .297 | | | |
| ISI | .089 | –.030 | .208 | .241 | .042 | .773*** | 3.405 | .010 |
| Adaptation Control | –14.794 | –83.350 | 53.763 | –.069 | .004 | | | |
| Magnitude of Deviance | –78.843 | –299.698 | 142.012 | –.141 | .010 | | | |

*Note*. CI = confidence interval. ISI = Inter-stimulus-interval. *$p$ < .05 **$p$ < .01 ***$p$ < .001

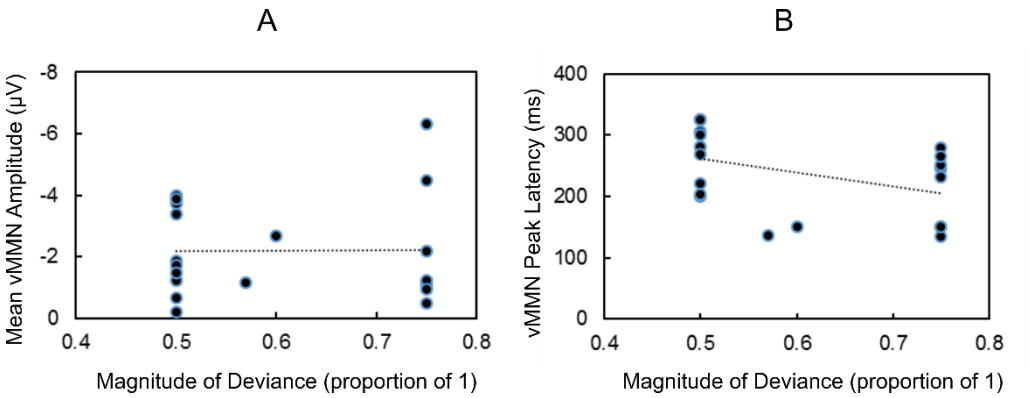


*Figure 2.3* Scatter plots depict the relationships between Magnitude of Deviance and mean vMMN amplitude (A) or vMMN peak latency (B) for spatial frequency deviants ($p > .05$). Black dotted lines depict the linear trends in the data.

To summarise, I did not find evidence supporting the magnitude of deviance effect on vMMN amplitudes that others have reported (Czigler et al., 2002; Czigler & Csibra, 1990; Takacs et al., 2013): that larger magnitudes of deviance evoke larger vMMNs. I also did not find the effect reported by Maekawa et al. (2005): that larger magnitudes of deviance evoke earlier vMMNs. This is despite analysing spatial frequency studies (Table 2.4 and 2.5) in addition to orientation studies (Table 2.2 and 2.3). Moreover, evidence that longer gaps between stimuli evoke larger vMMNs is not consistent with the existing literature (e.g. Astikainen, Lillstrang, & Ruusuvirta, 2008; Fu et al., 2003; Sysoeva, Lange, Sorokin, & Campbell, 2015). I discuss this further in section 2.6.3.5.

One explanation for this puzzling discrepancy is that the data in Table 2.1 do not reveal the true relationship between the magnitude of deviance and vMMN or between other predictors of vMMN amplitude and peak latency. This may be due to a combination of factors. I consider these next.

### 2.6.3 The approach to vMMN research

Although the brain encodes many kinds of visual regularities, evidenced by their respective irregularities evoking the vMMN, Table 2.1 also highlights the current approach to vMMN research. It shows how others have:

1. isolated and manipulated deviant features,
2. controlled for attention,
3. equated physical properties of stimuli for appropriate comparisons,
4. controlled for adaptation-related differences,
5. chosen their experimental design, and
6. chosen their EEG data pre-processing criteria.

As I will show next, most, if not all, of these differences can contribute to the observed differences in results, making it difficult to draw conclusions about feature deviance, let alone the magnitude of deviance effect.

#### 2.6.3.1 Isolating and manipulating deviant features

Consider that each visual stimulus contains a specific combination of visual features. All these features, as well as their combination, determine which neurons will respond to the stimulus. It is therefore not surprising that each visual stimulus evokes a particular ERP and changing even one feature will change the ERP. What is surprising is that most visual stimuli in Table 2.1 are not stimuli in which one can easily manipulate a single property of visual input without affecting others.

In one study, not included in Table 2.1 for having simultaneously manipulated two features of visual input to investigate low-level deviance, Mazza et al. (2005) compared ERPs to red triangle stimuli and green disc stimuli. These differ in colour, most likely in luminance (Mazza et al. did not report doing any procedure to ensure the stimuli were isoluminant), and in all the features that make their shapes different (e.g., in the orientation of their contours, in the areas of the retina stimulated, in spatial frequency). Any differences in their ERPs could be from one, or more, or all these differences, thus limiting conclusions one can draw about processing deviance associated with shape or colour alone.

A Gabor patch, however, is ideal for visual research. Firstly, Gabor patches are physiologically plausible visual stimuli because their profile resembles that of a visual cortex simple cell's receptive field (Field & Tolhurst, 1986; Fredericksen, Bex, & Verstraten, 1998; Marčelja, 1980). The second virtue of a Gabor patch is the separability of stimulus features it affords. Specifically, manipulating a single feature of a Gabor patch, such as orientation, will not affect any other feature of a Gabor patch, such as spatial frequency or luminance. This is especially true when the Gabor patch appears on a background with the same mean luminance as the Gabor patch itself. Thirdly, the Gabor patch is the most popular stimulus among visual psychophysicists (Fredericksen et al., 1998). Therefore, using Gabor patch stimuli in visual neuroscience facilitates translation of research findings from visual psychophysics into visual neuroscience (and vice versa).

A Gabor patch comprises a sinusoidal grating of a specified spatial frequency, phase, and orientation. The spatial frequency is how many complete cycles fit into one degree of visual angle, measured in cycles per degree (cpd). One complete cycle is the distance between the whitest peak of one bar and the whitest peak of the white bar closest to it. The phase value determines what part of the cycle occupies the centre of a display, measured in radians or degrees (°). In degrees, a 0° phase places the black-to-white crossing at the centre, a 90° phase places the whitest peak of the bar at the centre, a 180° phase places the white-to-black crossing at the centre, and so on.

In a Gabor patch, the contrast of the sinusoid decreases with distance from the centre of the grating according to a cumulative Gaussian function. The standard deviation of the Gaussian function, measured in degrees of visual angle, determines how much of the sinusoid is visible in a Gabor patch. Changing one of these properties, such as orientation, will not affect any other property such as the spatial frequency, phase, contrast, and luminance. To illustrate, I show two Gabor patches in Figure 2.4. They differ in orientation only. Figure 2.4 shows that all other features of the Gabor patch are unchanged when manipulating a single feature such as orientation.

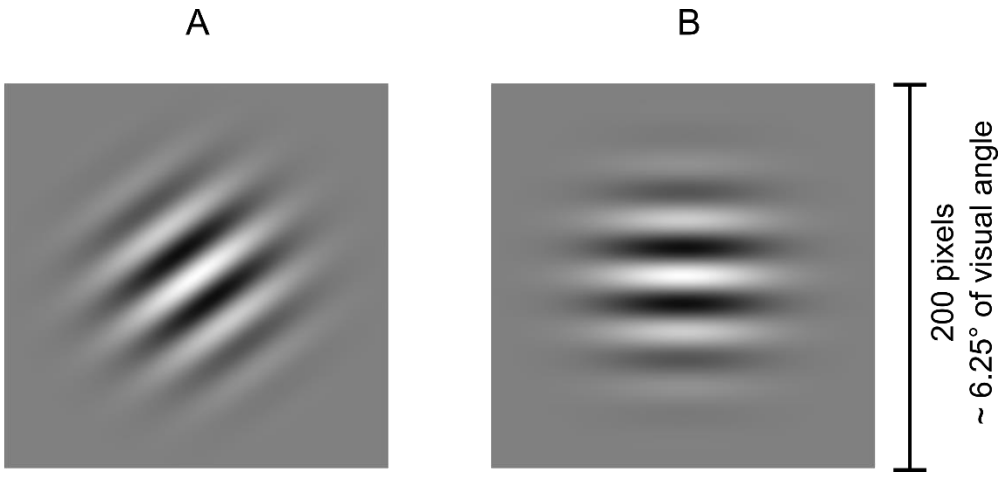


*Figure 2.4* Gabor patches. A. Gabor patch 54° clockwise from vertical 0°. B. Gabor patch 90° clockwise from vertical 0°. All other features are the same. The Michelson contrast (.99), phase (90°), spatial frequency (1 cpd of visual angle), mean luminance (41.8 cd/m$^2$), and SD of the Gaussian envelope (1° of visual angle) are identical. At a viewing distance of 57 cm on a monitor that shows 32 pixels per cm, each Gabor patch subtends approximately 4.5° of visual angle.

For these reasons, the Gabor patch is ideal for conducting low-level deviance research. Only 6% of the entries in Table 2.1 manipulated the deviant feature in a Gabor patch stimulus or pattern ($n$ = 7). Only 3% included a grey background ($n$ = 3). This inevitably limits the conclusions about low-level deviance one can draw from the literature.

#### 2.6.3.2 Controlling for attention

Table 2.1 shows that 81% of entries directed attention away from the stimulus of interest, the rest directed attention toward the stimulus of interest ($n$ = 87). This shows that it is common practice to direct attention away from the stimulus of interest in vMMN research.

Fixation tasks are also essential in vMMN research and directing attention to a task or stimulus in a different modality poses its own issues. Although this is not a problem in auditory research, because the participant's auditory system receives the auditory information regardless of what he or she is attending to, in

vision research, one must ensure that the eyes are open and the stimulus of interest appears in the participant's visual field, so that the visual system receives the change in input. One must also ensure that the eyes are fixated so that no other changes are contributing to the observed differences in brain activity.

Overall, 57% of the entries in Table 2.1 used some form of *central* fixation task ($n$ = 62). Of the 87 entries in which attention was directed away from the stimulus of interest, 71% used a fixation target, dot, square, cross, or fixation dot tracking task ($n$ = 62). Clearly, the vMMN community appreciates the importance of fixation.

#### 2.6.3.3 Equating physical properties of stimuli

It is essential to compare physically identical stimuli to know whether differences in processing reflect genuine deviance detection rather than differences due to differences in the physical properties of a stimulus. In this regard, the literature is consistent, with 57% of the entries in Table 2.1 having compared physically identical stimuli ($n$ = 62). This can be achieved by; having the deviants and standards *reverse roles* in different blocks; including a block containing a single *deviant alone*; including a *standard block,* in which multiple deviants appeared among standards, but not with the deviants having equal frequency to those in the oddball blocks; including a *deviant block*, in which only the deviant is repeated. However, these methods do not control for differences in the ERPs due to adaptation. For this, one must use a control for adaptation.

#### 2.6.3.4 Controlling for adaptation

Increased negativity to deviants compared to standards reflects both genuine deviance detection and adaptation-related differences due to the repetition of standards in oddball sequences. One can distinguish between the two by comparing oddball deviants with deviants that appear in either an equiprobable or a cascadic control. Otherwise, the resulting negativity represents deviant-related negativity (DRN), a combination of adaptation and genuine vMMN.

Considering all entries in Table 2.1, 14% included a control for adaptation ($n$ = 15). Of the 108 entries, 13 did not require a control for adaptation because the stimulus intensity (units over time) decreased on deviant trials; thus deviants did not excite different neurons or neurons to the same extent, so an adaptation control is not necessary here (Khodanovich, Esipenko, Svetlik, & Krutenkova, 2010; Qiu et al., 2011). Of the remaining 95 entries, only 16% discounted (i.e., isolated and removed) adaptation-related differences to distinguish genuine vMMN from effects of adaptation ($n$ = 15).

Notably, mean vMMN amplitudes were significantly larger for studies that did not use a control for adaptation ($M$ = –1.60 µV, $SD$ = 1.23, $n$ = 90) compared to those that did ($M$ = –.79 µV, $SD$ = .66, $n$ = 14[4]), $t$ (102) = 2.421, $p$ = .017 (two-tailed). Thus, when controlling for adaptation, the vMMN is much smaller. Logically, the combined adaptation-related and deviance-related differences

[4] One of the 15 entries that used a control for adaptation did not have amplitude data.

would yield a larger DRN than a genuine vMMN that is free from adaptation. One could argue that the –.82 μV difference illustrates the importance of controlling for adaptation and that only a small percentage of the existing low-level deviance literature reveals genuine deviance-related differences because all others may be differences due to adaptation. This seriously limits the conclusions we can draw about the effects of low-level deviance on the vMMN.

#### 2.6.3.5 Experimental design

Varying any aspect of an oddball sequence can affect the resulting vMMN. Here, I explore aspects known for affecting the vMMN as well as those that may affect the vMMN.

***Inter-stimulus-Interval (ISI)***

The mean ISI across all features was 663 ms (*SD* = 387 ms, *n* = 106). Others have found that shorter ISIs produce larger vMMNs than longer ISIs (Astikainen et al., 2008; Fu et al., 2003; Sysoeva et al., 2015). For example, as shown in Table 2.1, in one condition of their study, Astikainen et al. (2008) abolished the vMMN with 1000 ms ISI. This was arguably due to the duration of the sensory memory trace, which, according to behavioural research, is less than one second (Sperling, 1960; Averbach & Coriell, 1961; Sakitt, 1976).

However, also shown in Table 2.1, Pesonen, Savić, Kujala, and Tarkka (2017) found a vMMN for the same orientation deviant (36° difference), using bar stimuli like those used by Astikainen et al. (2008), and a longer 1100 ms ISI. It is difficult to reconcile how one study could find an orientation vMMN with

an ISI of 1100 ms (Pesonen et al., 2017) whereas a study using an ISI of 1000 ms could not (Astikainen et al., 2008). These kinds of inconsistencies may explain why ISI was not a significant predictor of vMMN amplitude for orientation deviants (Table 2.3) or why a correlational analysis including all entries with details of mean amplitude and ISI in Table 2.1 was not significant, $r$ (101) = .050, $p$ = .618 (two-tailed). Figure 2.5(A) depicts the results.

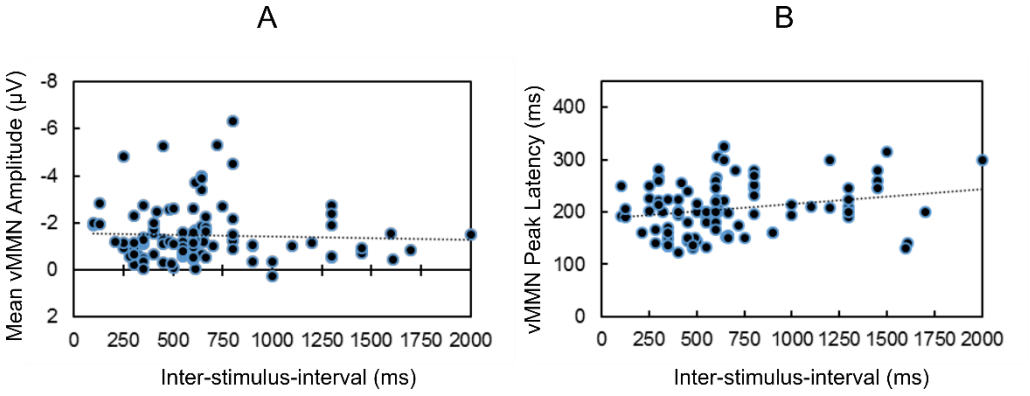


*Figure 2.5* Scatter plots depict the correlations between Inter-stimulus-interval (ISI) and mean vMMN amplitude (A) or vMMN peak latency (B). Only the weak positive correlation between ISI and vMMN peak latency is significant ($p$ < .05). Black dotted lines depict the linear trends in the data.

Figure 2.5(B) depicts the relationship between ISI and vMMN peak latency for all entries in Table 2.1. A correlational analysis revealed that shorter ISIs produced earlier vMMNs than longer ISIs, $r$ (104) = .217, $p$ = .026 (two-tailed). Although this does not agree with the results in Table 2.3 and 2.4—that longer gaps between stimuli evoke earlier vMMNs to spatial frequency deviants—this is consistent with Fu et al. (2003). Considering the inconsistencies in this review as well as previous findings, it seems that further research is necessary to elucidate the relationship between ISI and vMMN amplitude and peak latency. I erred on the side of caution and used ISIs of 400 ms or less in all feature deviant studies in this thesis.

### *Stimulus duration*

Overall, the mean stimulus duration in Table 2.1 is 149 ms (*SD* = 140 ms, *n* = 106). However, Table 2.6 shows that the mean (*SD*), minimum, and maximum stimulus durations capable of evoking the vMMN varies depending on the deviant feature.

Table 2.6 *Number of Experiments or Conditions within Experiments, Mean (Standard Deviation) Stimulus Duration (in ms), Along with Minimum and Maximum Stimulus Duration for each Deviant Feature in Table 2.1*

| Feature | N | Mean (*SD*) | Minimum | Maximum |
|---|---|---|---|---|
| Orientation | 24 | 115 (68) | 50 | 250 |
| Contrast | 1 | 100[a] | 100 | 100 |
| Luminance | 5 | 186 (128) | 80 | 400 |
| Spatial Frequency | 20 | 202 (201) | 17 | 1000 |
| Colour | 19 | 157 (217) | 17 | 1000 |
| Shape or Size | 10 | 105 (72) | 50 | 200 |
| Motion Direction | 15 | 178 (31) | 133 | 200 |
| Stimulus Duration | 12 | 105 (73) | 17 | 200 |

*Note*. [a] Only one of two contrast studies provided duration information.

Correlational analysis for stimulus duration and vMMN amplitude revealed that longer stimulus durations evoked smaller vMMNs than shorter stimulus durations, $r$ (101) = –.298, $p$ = .002 (two-tailed). There was also evidence that shorter stimulus durations produced earlier vMMNs than longer stimulus durations, $r$ (104) = .194, $p$ = .046 (two-tailed). I illustrate these relationships in Figure 2.6.

It should also be noted that longer stimulus durations may trigger eye movements away from fixation. According to Westheimer (1954), this can begin 120 ms after stimulus onset and reach peak acceleration at 160 ms. Therefore, a

shorter stimulus duration may be better for avoiding any confounds associated with eye movement, including muscle artifacts and differences in visual input.

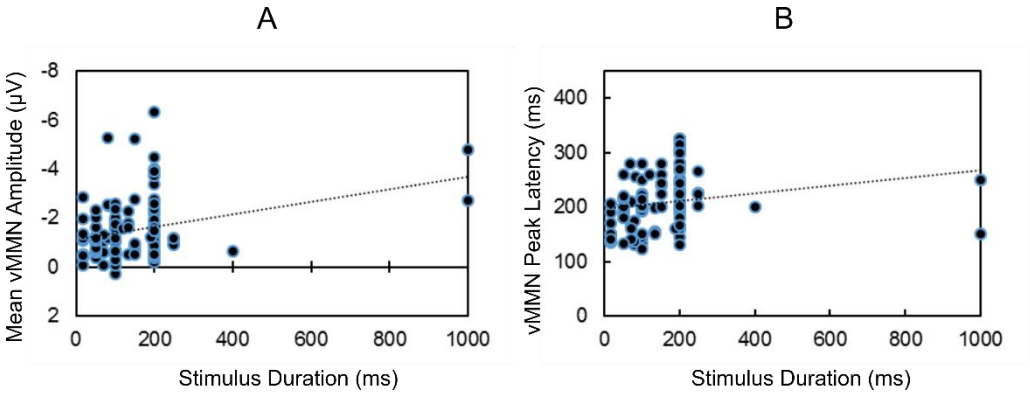


*Figure 2.6* Scatter plots depict the correlations between Stimulus Duration and mean vMMN amplitude (A) or vMMN peak latency (B). Note the correlation between Stimulus Duration and mean vMMN amplitude is negative; the reversed values on the y-axis give the impression of a positive correlation. Both correlations are significant ($p < .05$). Black dotted lines depict the linear trends in the data.

To maximise the likelihood of obtaining a vMMN and minimise eye movement artifacts, I used a stimulus duration of between 80 and 120 ms in all my studies, except when replicating the ISI of a previous study (Kimura & Takeda, 2015). In this instance, I used a 200 ms stimulus duration (450 ms stimulus-onset-asynchrony in Experiment 2 of Ch. 4).

### *Deviant probability*

Only two entries in Table 2.1 used a deviant probability of more than 20%. The mean deviant probability is 14% (*SD* = 7%) and there was no meaningful relationship between deviant probability and mean vMMN amplitude fot all entries in Table 2.1 with available data, $r$ (102) = .001, $p$ = .996 (two-tailed). There was, however, a significant weak negative correlation for peak latency data, $r$ (105) = –.221, $p$ = .022 (two-tailed), suggesting that deviants with a higher probability of occurring evoke earlier vMMNs (see Figure 2.7B). This is

consistent with the correlational and linear regression analyses in Table 2.4 and 2.5, respectively. Specifically, deviant probability was the only strong predictor of vMMN peak latency for spatial frequency deviants, with deviants that are more frequent having evoked earlier vMMNs than less frequent deviants.

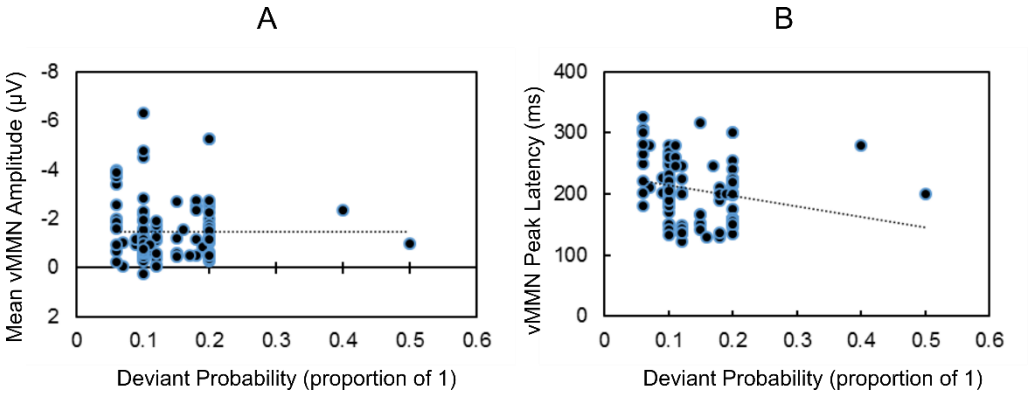


*Figure 2.7* Scatter plots depict the correlations between Deviant Probability and mean vMMN amplitude (A) or vMMN peak latency (B). Only the weak negative correlation between Deviant Probability and vMMN peak latency is significant ($p < .05$). Black dotted lines depict the linear trends in the data.

This is consistent with Stefanics et al. (2011) who examined deviant probability and found that deviants with a 10% probability evoked earlier vMMNs compared to deviants with a 30% probability. However, Stefanics et al. also found that deviants that are less probable deviants evoked larger vMMNs than deviants that are more probable. It seems that smaller deviant probabilities are optimal for evoking a larger vMMN (even if it is later). Furthermore, a deviant probability of 20% or less appears to be the most consistent approach to defining deviant probability. I used a deviant probability between 10% and 20% in all my studies.

### *Minimum number of standards preceding a deviant*

The standards within the oddball sequence establish regularity, making it vital for at least two standards to separate each deviant stimulus. If not, the deviant may not constitute a violation of a regularity. Despite this, of those studies that adopted the oddball paradigm ($n$ = 95)—not the multi-feature paradigm because at least one standard separates each deviant in this paradigm as per its design—only 57% of the experiments or conditions within experiments in Table 2.1 stipulated a minimum number of standards between deviants ($n$ = 55). It is unknown whether the stipulation was absent because there was no such stipulation in oddball sequences or because it was overlooked when writing the methodology. Only 44% studies mentioned that they stipulated more than one standard must separate deviants ($n$ = 42).

If only some deviant trials yield a vMMN (because two or more standards preceded the deviant on some trials and not others), the resulting vMMN will be smaller than that of a vMMN where all deviant trials yield the vMMN due to the averaging process. Horváth et al. (2008) described this effect in the context of magnitude of deviance in audition. Horváth et al. argued that as the audible discrimination of irregular tones approached discrimination threshold, the ratio of trials that *do not* evoke the MMN increases. On the other hand, the ratio of deviant trials evoking the MMN is unchanged when the deviant is easily discriminable. Averaging the trials for each deviant then gives the appearance of magnitude of deviance effect restricted to near discriminable differences. The same argument applies here. That is, some vMMN amplitudes in Table 2.1 may

have been larger if at least two standards had separated all deviants. This hinders comparisons of vMMNs across studies and may be another reason that the expected magnitude of deviance effect did not emerge in my analysis of the current data. In all my studies in which I used the oddball paradigm (Ch. 1–5 and Experiment 1 of Ch. 6), at least two standards separated deviants.

#### 2.6.3.6 Pre-processing criteria

Different pre-processing criteria often reflect the different EEG recording systems used. It is, however, pertinent to consider how some of these differences in criteria can affect findings.

##### *Chosen reference*

ERP components are electrical dipoles that manifest as positive voltages at one site on the scalp and negative voltages in another. However, the chosen reference can affect a component's peak (e.g., vMMN amplitude), its latency (e.g., time of maximum negativity), where it is largest (e.g., electrode or ROI), and even its polarity (Kayser & Tenke, 2010; Nunez, 2010). Dien (1998) described how one could bias data toward one hemisphere when using a unipolar reference (e.g., the left or *right earlobe* or *mastoid*) by producing enlarged ERP amplitudes opposite the recording site. Re-referencing the data to the average of left and right reference electrodes (e.g., earlobes or mastoids) helps to avoid this (Lopez-Calderon & Luck, 2014). This has been called *linked-earlobes* or *linked-mastoids reference*. However, linked-earlobes or linked-mastoids can also mean forcing the two sites to have the same voltage. The latter does not alleviate the

problem (Dien, 1998) and the choice of reference is not always clear, thus hindering comparisons between studies.

Historically, researchers considered the nose-tip electrically neutral as a non-cephalic reference (Dien, 1998). Now, re-referencing to the average of all electrodes is considered optimal, especially for a high-density recording montage (i.e., at least 32 electrodes) (Dien, 1998; Lopez-Calderon & Luck, 2014; Luck, 2005; Nunez, 2010). Of the 107 experiments or conditions within experiments that provide reference electrode details, only 7% used a unipolar reference ($n$ = 7), 52% used a nose-tip or non-cephalic reference ($n$ = 56), 18% used the *average reference* ($n$ = 19), and 17% used linked or averaged earlobes, mastoids, or electrodes as reference ($n$ = 18). I used the average reference for all my studies except when replicating analyses from other studies. In this instance (Ch. 6), I used the nose-tip as reference.

### *Filter frequency*

Widmann, Schröger, and Maess (2015) described temporal filtering as a process in which one attenuates signals (e.g., electrical noise or activity) that oscillates a specific number of times per second (i.e., rate), define by a frequency and measured in Hertz (Hz). Frequency cut-off values determine the range of frequencies to preserve. For example, power mains in Australia produce regularly oscillating electrical activity at around 50 time per second (50 Hz). A low-pass filter cut-off value of below 50 Hz (e.g., 40 Hz) will attenuate the effect of all signals at frequencies above this value, including 50 Hz signals. Ultimately, the goal of filtering is to increase the signal-to-noise ratio in the

electrophysiological data and filtering is common practice in EEG research (Widmann et al., 2015).

The general approach to selecting a low-pass filter cut-off frequency is relatively consistent. Of those that reported a low-pass filter ($n$ = 106), 47% used a 30 Hz cut-off ($n$ = 50). High-pass filter cut-off frequencies are more variable, ranging from 0.03 to 1.5 Hz. This is alarming because cut-off frequencies above 0.1 Hz can produce artifactual early negativities as early as 100 ms after onset (Acunzo, Mackenzie, & van Rossum, 2012; Kappenman & Luck, 2010; Luck, 2005; Tanner, Morgan-Short, & Luck, 2015, Widmann et al., 2015). This is problematic where DRN or vMMN calculations include all ERP values between 100 and 400 ms.

In keeping with best practice, I used a conservative 0.1 Hz high-pass filter cut-off frequency (Tanner et al., 2015; Widmann et al., 2015), accepting this may limit the comparability of results with existing findings. Low-pass cut-off frequencies were always 40 Hz as recommended by Widmann et al. (2015).

### 2.6.4 Inconsistencies in the findings

Table 2.1 revealed some inconsistencies in low-level deviance research findings. For example, there are differences in the chosen electrode or ROI (i.e., the location on the scalp), vMMN peak latency, and mean vMMN amplitude. Careful consideration of the literature also revealed some issues concerning the replicability of a vMMN to feature deviants.

#### 2.6.4.1 Peak electrode or ROI

The vMMN is generally largest at parieto-occipital regions on the scalp. For this reason, the electrode or ROI analysed is usually here. Table 2.1 verifies this. Small variations in the chosen electrode or ROI usually reflect differences in the site of maximal difference, perhaps owing to differences in the feature tested. In all my studies, I focused on the activity within the same ROIs at the left, midline, and right parieto-occipital ROIs, except when replicating a previous study (Kimura et al., 2009). In this instance, I used the same electrode Kimura et al. reported their main effects at—the P8 electrode.

#### 2.6.4.2 Mean amplitude

Given all complete entries in Table 2.1, the mean vMMN amplitude is –1.49 μV and the standard deviation is 1.20 μV. As I have already shown, amplitude variability can reflect difference in adaptation control, attentional manipulation, ISI, deviant probability, and even chosen reference. Amplitudes can differ even when investigating similar feature deviants. To illustrate, Kimura et al. (2009) reported a vMMN more than three times (–1.60 μV) the size of the vMMN reported by Astikainen et al. (2008) (–0.50 μV). Both studies used the equiprobable control, single bar stimuli, 36° orientation deviants, a minimum of 2 standards between deviants, 100 ms stimulus duration, 400 ms ISI, and filtered the data using 0.1–30 Hz filter. They differed in deviant probability (20% and 10%, respectively), chosen reference (nose-tip and common average), chosen electrode (T6/P8 and occipital), and task. According to Stefanics et al. (2010), the ratio Astikainen et al. (2008) used (90:10) should have produced the larger

vMMN. As this was not the case, perhaps then the difference in the size of the vMMN was due to some combination of chosen reference, chosen electrode, task, or some other aspect.

#### 2.6.4.3 Peak latency

The mean peak latency of the vMMN is 207 ms and the standard deviation is 51 ms for all entries in Table 2.1. This reflects various differences. One is the type of feature. For example, Table 2.1 shows that vMMN peak latencies occur as early as 130 ms for orientation (Sulykos & Czigler, 2011) or as late as 305 ms for spatial frequency (Stagg et al., 2004). However, there appear to be inconsistencies for identical stimuli. For example, Maekawa et al. (2005) reported a vMMN to windmill-like patterns at 185 ms whereas File et al. (2017) reported a vMMN for the same stimuli at least 70 ms later. Such timing differences are difficult to reconcile unless one accepts that other processes may be affecting one of the reported vMMNs. These processes may reflect genuine differences in deviance detection, such as the magnitude of deviance, or they may reflect processes outside of deviance detection, such as attention or adaptation. These unanswered questions encourage further research.

#### 2.6.4.4 Replicability of vMMN to feature deviants

Table 2.1 shows that feature deviance findings are sometimes difficult to replicate. Inconsistencies are not so surprising for rarely investigated features. For example, only two studies have investigated contrast deviance and one did not observe a vMMN. However, it is surprising to see inconsistencies in other frequently investigated low-level features, such as orientation and spatial

frequency. For example, Czigler and Sulykos (2010) found a vMMN to orientation deviants using peripherally presented line segments. However, File et al. (2017) were not able to replicate the orientation vMMN using line textures and controlling for adaptation. In the same study, File et al. observed that increases in spatial frequency evoked the vMMN, but decreases did not. File et al. reasoned that an increase in spatial frequency yields a vMMN because it represents a more complex change, necessitating prediction error; whereas, a decrease in spatial frequency does not yield a vMMN because it does not constitute a complex change. The alternative is that confounding changes in the stimuli, such as added orientation information for increases but not decreases in spatial frequency, may be contributing to the DRN in the former, but not the latter.

Findings for duration deviants are also contradictory. For example, Durant, Sulykos, and Czigler (2018) found a statistically significant vMMN for short duration deviants, but not for long duration deviants. Yang et al. (2016) found the opposite result—short duration deviants did not evoke the vMMN, but long duration deviants did. These conflicting findings suggest that some other facet(s) may predict whether a vMMN occurs for a feature deviant. These may or may not include confounding stimulus parameters.

The reasons for these inconsistencies are unknown. To determine whether feature deviants do indeed evoke a vMMN when isolating feature deviants in physiologically plausible stimuli, comparing physically identical stimuli, controlling for adaptation, and ensuring that the eyes are on the stimulus, further

research is essential. This is in part what drives the current research. The other part focuses on whether the local context of a deviant, such as the magnitude of deviance, affects the vMMN.

## 2.7 Conclusion

In summary, my review of the literature as summarised in Table 2.1 and elaborated on in the current Chapter shows that:

- Various parameters of experimental design can have an (intended or unintended) effect on the resulting vMMN. This can make it difficult to delineate the true effect of low-level deviance on the visual system, let alone show whether there is a monotonic relationship between the magnitude of deviance and the size of the vMMN.
- There are many inconsistencies in the existing vMMN literature concerning low-level deviance.

A unified approach to conducting vMMN research in the future may help to alleviate these two issues. The current review is especially useful in this respect as it outlines optimal parameters for future research in addition to exploring consequences for differing parameters of experimental design. To answer critical questions about magnitude of deviance or even conclude that changes in basic properties of visual input evoke the vMMN, further research is necessary. This is precisely the research I undertake in the following Chapters.

# CHAPTER 3

## DOES BRAIN PROCESSING OF UNPREDICTED VISUAL CHANGES INCREASE WITH THE SIZE OF CHANGE? A VISUAL MISMATCH NEGATIVITY (vMMN) STUDY

Based on the following manuscript in preparation

Male, A. G., Roeber, U., & O'Shea, R. P. (2019). Does brain processing of unpredicted visual changes increase with the size of the change? A visual mismatch negativity (vMMN) study.

# 3. DOES BRAIN PROCESSING OF UNPREDICTED VISUAL CHANGES INCREASE WITH THE SIZE OF CHANGE? A VISUAL MISMATCH NEGATIVITY (VMMN) STUDY.

## 3.1 Preface

In this Chapter, I investigate whether local context of an unexpected change can affect the brain's processing of it. I manipulated the size of change between the predicted input and actual input—this is the magnitude of deviance. I varied the magnitude of deviance by showing Gabor patches of a particular orientation as standards and otherwise identical Gabor patches of a different orientation as deviants in roving oddball sequences. I controlled for adaptation-related differences by comparing deviants with physically identical stimuli in equiprobable sequences.

This study tests one aspect of the first thesis question:

I. Does the magnitude of deviance of a pre-attentive change affect the vMMN to changes in a basic property of visual input?

## 3.2 Introduction

Predictive coding theory has been embraced enthusiastically and is considered a leading theory of how the brain deals with sensory input (Garrido, Kilner, Stephan, & Friston, 2009; Spratling, 2017). A fundamental assumption of predictive coding theory is that the brain uses experience (e.g., past sensory input) to generate predictive models of sensory input at various levels of the sensory pathway. If future inputs match the prediction, no further processing is required. If they do not match—a so-called prediction error—further processing occurs to update the model. In vision, the visual mismatch negativity (vMMN) represents a signature of the brain processing associated with prediction error (Clark, 2013; Garrido et al., 2008, 2009; Kimura et al., 2011; Stefanics, Astikainen, & Czigler, 2015; Stefanics, Kremláček, & Czigler, 2014). However, one unanswered question about how the brain processes sensory input remains unresolved: do larger changes in sensory input produce larger prediction errors than smaller changes in sensory input? We seek to answer this question by measuring the amplitude of vMMN to different magnitudes of difference (i.e., deviance).

The vMMN is revealed by event-related potentials (ERPs) derived from electroencephalography (EEG). The vMMN occurs when an unpredicted different (deviant) visual stimulus occurs in a sequence of identical (standard) visual stimuli. To show the vMMN, one typically uses the oddball paradigm (s. 1.3 in Ch. 1, Squires et al., 1975). The vMMN is characterised by increased negativity for the deviant relative to the standard and is largest between 150 and 300 ms after the onset of the deviant.

### 3.2.1 Magnitude of deviance and the vMMN

Many different types of change in visual input appear to produce a vMMN. These include changes in simple features, such as spatial frequency (Maekawa et al., 2005; Sulykos & Czigler, 2011), orientation (Astikainen, Lillstrang, & Ruusuvirta, 2008; Astikainen, Ruusuvirta, Wikgren, & Korhonen, 2004; Czigler, Balázs, & Winkler, 2002; Czigler & Csibra, 1990; Farkas, Stefanics, Marosi, & Csukly, 2015; Kimura, Katayama, Ohira, & Schröger, 2009; Kimura & Takeda, 2013, 2014, 2015; Yan, et al., 2017), and luminance (Jack et al., 2017; Kimura, Widmann, & Schröger, 2010; Stagg, Hindley, Tales, & Butler, 2004). More complex changes include deviations in the order of stimuli (Bubic, von Cramon, Jacobsen, Schröger, & Schubotz, 2009; Czigler & Pató, 2009; Kimura & Takeda, 2015), colour category (Clifford, Holmes, Davies, & Franklin, 2010; Fonteneau, & Davidoff, 2007; Thierry, Athanasopoulos, Wiggett, Dering, & Kuipers, 2009), emotional expression (Li, Lu, Sun, Gao, & Zhao, 2012), and the gender of facial stimuli (Kecskés-Kovács, Sulykos, & Czigler, 2013).

However, few studies have compared the vMMN of small versus large visual deviants (Czigler & Csibra, 1990; Czigler et al., 2002; Czigler & Sulykos, 2010; Flynn, Liasis, Gardner, Boyd, & Towell, 2009; Kimura et al., 2008; Maekawa et al., 2005; Takács et al., 2013). Critically, only one of these studies included an appropriate control for adaptation. Czigler et al. (2002) compared ERPs for red-black vertical square-wave gratings appearing among pink-black gratings (small deviant condition) or green-black gratings (large deviant condition) with ERPs for control stimuli appearing in equiprobable control sequences. Equiprobable control sequences include a mix of deviants, the

standard, and some number of equally frequent other stimuli (Schröger & Wolff, 1996). All stimuli in the control appear with the same frequency so that no regularity is established (i.e., no probability-related differences). Furthermore, neurons processing the deviants in the oddball sequence are equally adapted, if any, to those in the control sequence, removing adaptation as an explanation of any differences.

Czigler et al. (2002) found that large deviants produced a vMMN, but small deviants did not. One explanation for their finding is a magnitude of deviance effect (Czigler et al., 2002). The other explanation is that there is a minimum difference needed to observe a vMMN. Moreover, to determine the form of the relationship between the magnitude of deviance and the vMMN amplitude (e.g., linear vs. exponential), at least three magnitudes of deviance are needed. We improve on their design by employing three magnitudes of deviance in the present study.

To show whether larger changes produced larger vMMNs than smaller changes, we varied the orientation difference between the deviant and the standard stimuli in the oddball sequences. The difference was either small, medium, or large. To our surprise, we failed to show any vMMN at all. Instead, we found an early deviance-related positivity whose size was unrelated to the size of a difference in orientation.

### 3.2.2 The present study

We sought to clarify the relationship between the magnitude of deviance and the vMMN. We varied the size of an orientation change in otherwise

identical Gabor patches (s. 2.6.3.1 in Ch. 2). In this study, we use a Gabor patch for two reasons:

- Its profile resembles the receptive fields of visual cortical simple cells (Daugman, 1984; Field & Tolhurst, 1986; Fredericksen et al., 1998).
- We can isolate a single property, in our case orientation, without affecting others such as spatial frequency, contrast, or average luminance.

We compared ERPs to deviants from roving oddball blocks with identical controls from equiprobable blocks. Only a handful of (v)MMN studies have used the roving oddball paradigm (e.g., Cowan, Winkler, Teder, & Näätänen, 1993; Czigler & Pató, 2009; Fisher et al., 2010; Garrido et al., 2008; Leung, Greenwood, Michie, & Croft, 2015). The orientation difference between standard and deviant was either 15°, 30°, or 60°. We chose these orientation differences for two reasons.

- Even our smallest orientation difference of 15° is about 37 times greater than the discrimination threshold of about 0.4° (e.g., Burbeck & Regan, 1983). This allows us to see the predicted relationship between vMMN magnitude and size of deviant free from problems from being close to the detection threshold (e.g., Horváth et al., 2008, s. 2.6.3.5 in Ch. 2).
- Czigler and Sulykos (2010) used 30° and 60° deviants in a between-subject design where half of the participants saw the 30° deviant and

the other half saw the 60° deviant. They found that both orientation deviants produced a vMMN and vMMNs did not differ between participants. Their between-subject design may not have been powerful enough to show differences in vMMN. Moreover, they did not use a control for adaptation. We used a within-participant design with all three deviants in each oddball block to maximise the chances of our finding a relationship between magnitude of deviance and the vMMN

## 3.3 Method

### 3.3.1 Participants

To estimate our sample size, we used the mean (*SD*) difference in amplitude between the deviant and standard stimuli of –0.5 μV (0.68) for orientation deviants (colour and orientation task combined) at Oz ireported by Czigler and Sulykos (2010). According to G*Power (Faul, Erdfelder, Lang, & Buchner, 2007; Faul, Erdfelder, Buchner, & Lang, 2009), we needed 17 participants to achieve a power of .8.

Twenty-one self-declared healthy adults (8 males, 18 right-handed) with normal or corrected-to-normal vision participated in the experiment (power increased to .88). Mean age was 33 years with a range from 18 to 60 years. Most of the participants were undergraduate psychology students at Murdoch University. All participants provided their written informed consent and were free to withdraw from the experiment at any time. Participants received course credit or entry into a draw to win a $50 gift card in return for participation. The

Human Research Ethics Committee at Murdoch University approved the experiment (ethics permit 2015 208).

### 3.3.2 Apparatus

Participants sat in a light-attenuated chamber where they viewed a calibrated monitor (17-inch, colour cathode ray tube display; Sony Trinitron Multiscan E230) from 57 cm distance. The monitor showed 1280×1024 pixels (75 Hz refresh rate) and was the only source of light. A chin rest stabilized participants' head. Participants gave their responses by pressing a key on a 4-key response box with the index finger of their dominant hand.

A PC running Linux (v4.13.0), GNU Ubuntu (v16.04.4), Octave (v4.0.0) (Eaton, Bateman, Hauberg, & Wehbring, 2014), and Psychophysics Toolbox (v3.0.14) (Brainard, 1997; Kleiner, Brainard, & Pelli, 2007; Pelli, 1997) delivered the visual stimuli and recorded behavioural responses. An iMac running NetStation 5.2 (EGI) recorded EEG data.

### 3.3.3 Stimuli

All Gabor patches were achromatic (mean RGB values of 128 128 128) on a background of the same colour. Each patch had a contrast of .999, a phase of 0 radians (the black-to-white crossing was in the centre of the patch), a spatial frequency of 2.4 cycles per degree (cpd) of visual angle, and a standard deviation of the Gaussian of 3.84° of visual angle. The visible parts of each Gabor patch had a diameter of approximately 22° of visual angle. There were 12 possible orientations: 8°, 23°, 38°, 53°, 68°, 83°, 98°, 113°, 128°, 143°, 158°, and 173° clockwise from vertical (0°).

For the participants' primary task, capitalized letters were superimposed on the centre of the Gabor patch in cyan (mean RGB values of 0 255 255) in 30-point Courier font. Letters occupied 0.5° (width) × 0.6° (height) of visual angle. We used all 26 letters of the English alphabet. We give an illustration of this in Figure 3.1.

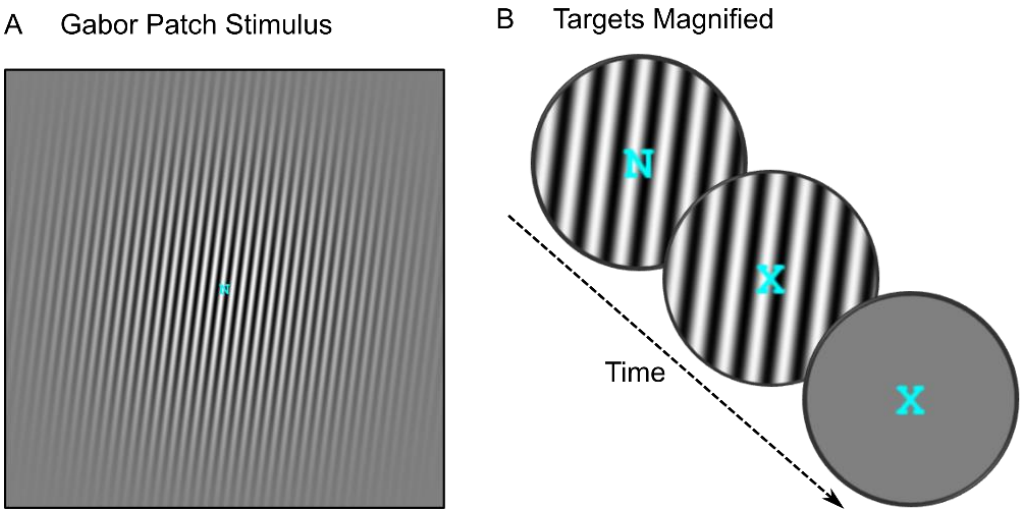


*Figure 3.1* Screenshots from the experiment of a Gabor patch, tilted 8° clockwise from vertical (0°), with a superimposed fixation letter. A. Gabor patch stimulus subtends 22° of visual angle from a 57cm viewing distance. B. Targets are magnified in the depicted fixation task to show the letter changes from a non-target N to a target X, requiring the participant to press a key. Each letter appeared for 600 ms before changing.

### 3.3.4 Procedure

There were 12 blocks of trials. There were 634 trials per block. Each trial lasted for 360 ms, comprising an 80 ms display of a Gabor patch and a 280 ms display of a blank field. Each block took less than four minutes to complete. Participants were free to take breaks between blocks.

There were two sorts of blocks:

1. Roving oddball blocks had 626 trials of which 114 (18%) were deviants (38 for each deviant). For each participant and block, we organised trials into random-length sequences containing at least 3 standards and no more than 22 standards followed by a deviant. On average, five standards separated each deviant. The deviant was randomly and equally 15°, 30°, or 60° from the standard. The first standard was one of 12 possible orientation values, chosen randomly for each participant. For example, the first few trials of one sequence might be 8°... 8°... 8°... *68°* (i.e., 60° deviant for the first sequence) then ...68°... 68°... 68°... *83°*... (i.e., 15° deviant for the second sequence). Figure 3.2(A) depicts such an oddball sequence.

2. Equiprobable blocks contained all possible orientations. All orientations appeared equally (8.3%) because no orientation represents a deviant in its own right. We also ensured that the stimulus (**in boldface**) preceding the control (underlined) was identical to the stimulus preceding the deviant in the oddball block (e.g., 23°... 113°... **8°**... 68°... 173°... 38°... **68°**... 83°... 143°...). Thus, we can discount the possibility that a difference in pairing (in the oddball vs. control sequences) is contributing to any deviance-related differences. Figure 3.2(B) depicts this equiprobable control sequence.

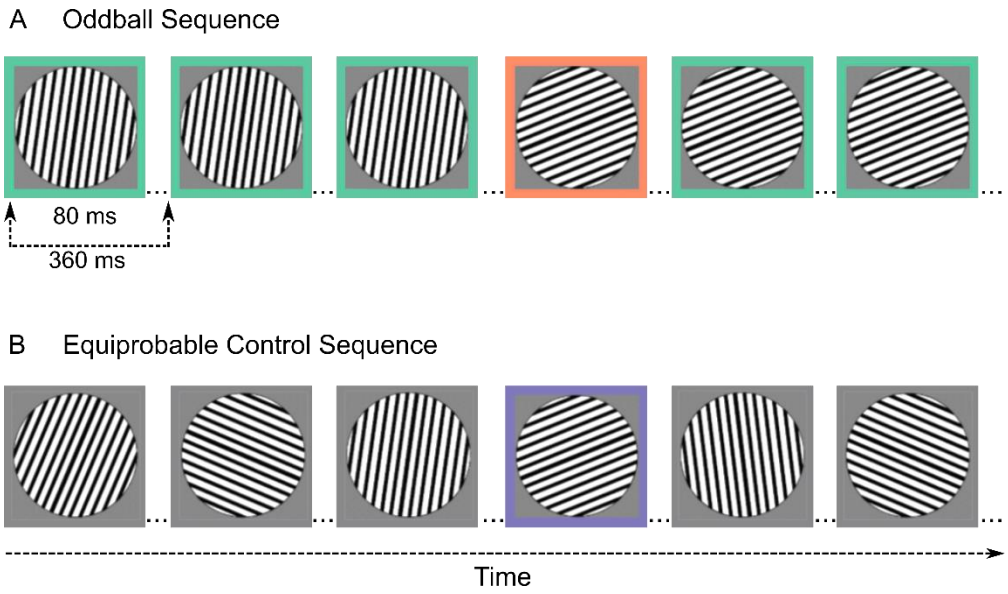


*Figure 3.2* Illustrations of part of a roving oddball sequence (top) and the same part of an equiprobable control sequence (bottom). A. In the oddball sequence, three identical trials comprising an 8° standard (outlined in green) precede the deviant of 68° (outlined in orange). The deviant becomes the first standard of the next sequence. B. In the equiprobable control sequence, the orientation of the stimulus varies randomly from trial to trial except that the stimuli preceding the deviant and the deviant (outlined in purple) are physically identical to the same two stimuli in the oddball sequence. We do not show the fixation task here and '...' denotes the 260-ms inter-stimulus-interval.

There were six oddball blocks and six equiprobable blocks. We randomized block order afresh for each participant and instructed participants to look at the centre of the screen where a continually changing sequence of letters appeared in all blocks. Each letter appeared for 600 ms. The onset and offset of the letter stimuli were desynchronised with the onset and offset of the Gabor patches. We asked participants to press a key with the dominant hand whenever an X appeared. If the participant responded between 0.15 and 1.2 s after target onset, the response was correct. There were 383 letter changes during a block. On average, there were 15 targets in each block; this varied between 7 and 25 targets per block.

### 3.3.5 EEG recording and analysis

We recorded the electroencephalogram (EEG) using an EGI 129-channel dense-array HydroCel geodesic sensor net. We recorded EEG at a 500 Hz sampling rate. Impedances were below 50 kΩ as recommended by Ferree, Luu, Russell, and Tucker (2001) for the high-input impedance amplifiers. All channels (i.e., electrodes) were referenced to Cz.

We processed the EEG data offline using MATLAB (2015b; Mathworks Inc., USA) and EEGLAB (14.1.1; Delorme & Makeig, 2004) and ERPLAB toolboxes (6.1.4; Lopez-Calderon & Luck, 2014). We re-referenced the signal of all electrodes to the common average and filtered the EEG with a low-pass 40 Hz Kaiser-windowed (beta 5.65) sinc finite impulse response (FIR) filter (order 184) followed by a high-pass 0.1 Hz Kaiser-windowed (beta 5.65) sinc FIR filter (order 9056). Epochs were 400 ms long. This featured a 50 ms pre-stimulus baseline, accommodating the short 360 ms stimulus-onset-asynchrony (SOA). We excluded epochs including amplitude changes exceeding 800 μV at any electrode.

We identified electrodes with unusually high deviations in EEG activity relative to the average standard deviation pooled from all electrodes using the method described by Bigdely-Shamlo, Mullen, Kothe, Su, and Robbins (2015). A robust z score was calculated for each electrode by replacing the mean by the median and the standard deviation by the robust standard deviation (0.7413 times the interquartile range). Any electrode with a z score exceeding 2.0 was deemed

as having poor signal to noise ratio. We removed these electrodes provided (at least) four others surrounded them.

We performed independent component analysis (ICA) with AMICA (Palmer, 2015). To improve the decomposition, we performed independent component analysis (ICA) on raw data (excluding bad electrodes) filtered by a 1 Hz high-pass (Kaiser-windowed sinc FIR filter, order 804, beta 5.65) and 40 Hz low-pass filter, segmented into epochs, but not baseline corrected (Groppe, Makeig, & Kutas, 2009). Winkler, Debener, Müller, and Tangermann (2015) have suggested and validated that a) high-pass filters do improve ICA decompositions (reliability, independence, and dipolarity) and b) one can apply the de-mixing matrix to a linearly transformed dataset. We simultaneously reduced the data to 32 components.

To ensure that those trials where participants moved their eyes or blinked were not included in the final analysis of the data, we bipolarized data from electrodes above and below the right eye (electrodes 8 and 126) and outer canthi of both eyes (electrodes 1 and 32) to achieve vertical and horizontal EOG channels, respectively (as recommended by Maekawa et al., 2013). We marked epochs containing amplitude changes exceeding ±60 μV at these EOG channels for rejection.

Before rejection, we applied the de-mixing matrix to the 0.1−40 Hz filtered data and used SASICA (Makeig, Bell, Jung, & Sejnowski, 1996) to identify which components exhibited low autocorrelation, low focal electrode or trial activity, high correlation with vertical or horizontal EOG, or met ADJUST

criteria (Mognon, Jovicich, Bruzzone, & Buiatti, 2011). We assessed the remaining components for consistency in the time course of single trials and in components' activity power spectrum (Chaumon, Bishop, & Busch, 2015). After removing components deemed as un-related to brain activity, we removed epochs previously marked for rejection and then removed epochs containing amplitude changes exceeding ±60 μV at any electrode. Finally, we interpolated data for rejected electrodes using spherical splines (Perrin, Pernier, Bertnard, Giard, & Echallier, 1987).

We averaged ERPs separately for the standard, deviant, and control trials and produced difference waves by subtracting ERPs to standards and ERPs to controls from ERPs to deviants. The mean numbers (*SD*) of epochs in each ERP appear in Table 3.1.

Table 3.1 *Mean Number (Standard Deviation) of Epochs per Participant in the Grand Average ERP for Standards, Deviants, and Controls (N = 21)*

| Magnitude of Deviance | Standard | Deviant | Control |
|---|---|---|---|
| 15° (small) | | 187 (26) | 187 (28) |
| 30° (medium) | {1994 (261)} | 186 (28) | 188 (30) |
| 60° (large) | | 188 (25) | 188 (27) |

We defined three regions of interest (ROIs) in each hemisphere and three along the scalp midline from frontal, central, and parieto-occipital regions on the scalp. Figure 3.3 shows electrodes averaged in each region.

We conducted temporal principal component analysis (PCA) on the individual average ERP data for deviant and control trials using the EP Toolkit (v2.64; Dien, Khoe, & Mangun, 2007). We used Promax orthogonal rotation (κ

= 3) with a covariance relationship matrix and Kaiser weighting as recommended by Dien, Beal, and Berg (2005). PCA reduces the data to those components explaining most of the observed data. The first component explains the greatest amount of signal and every component thereafter explains less of the data than the component before it. A component's loading (scaled by *SD*) shows how much of the data (activity) a component is responsible for over time (Dien, 2012).

Using PCA, one can identify separate components in the ERP waveform and extract an alternative measure of ERP component amplitudes for inferential testing (Carretié et al., 2004; Dien, 2010; Dien & Frishkoff, 2005). Each PCA component has a peak latency, a site of maximum positivity on the scalp (i.e., a component's positive pole), and a site of maximum negativity on the scalp (i.e., a component's negative pole). Plotting a topographical map of the microvolt-scaled PCA data of a single component at the time of its peak latency shows the component's positive and negative pole.

In our PCA of the data, we retained 13 components based on Horn's (1965) parallel test, explaining more than 95% of the variance. We extracted microvolt-scaled scores for components of interest only. These were components showing deviance-related difference at their respective positive and negative poles (see Figure S1 and S2 in Appendix A for details of all components). Extracting and comparing component scores from ROIs is similar to comparing mean amplitude in the ERP waveforms, but it is more precise because one can isolate the activity

from a single component, whereas mean amplitudes of traditional ERP components can contain activity from multiple components (Dien, 2012).

A vMMN component would emerge as a component that is largest (most negative) between 150–300 ms, based on previous orientation studies (e.g., 162–170 ms in Czigler & Sulykos, 2010; 200–250 ms in Kimura et al., 2009; 190–220 ms in Kimura & Takeda, 2015). A vMMN component should also yield scores that are more negative for deviants compared to controls at the component's negative pole in the parieto-occipital (PO) ROIs.

We compared scores for components of interest using traditional analyses of variance (ANOVAs) and paired *t*-tests. Where we found a significant main effect or interaction including deviance (deviants vs. control) as a factor, we performed Bayesian ANOVAs and Bayesian paired *t*-tests to determine the likelihood of obtaining the data. We used a medium prior (i.e., Cauchy prior whose width was set to 0.707) for all Bayesian analyses.

The model with the largest Bayes Factor ($BF_{10}$) is the model that best explains the data; this is the *favoured* model. According to Jefferys (1961) evidence for the alternative is anecdotal (or weak, Raftery, 1995) if a $BF_{10}$ is between 1 and 3. It is substantial between 3 and 10, strong between 10 and 30, very strong between 30 and 100, and decisive when it is greater than 100. We employed a more conservative approach for a $BF_{10}$ greater than 100. Evidence for the alternative is strong given a $BF_{10}$ between 100 and 150 or very strong given a $BF_{10}$ greater than 150 (Raftery, 1995).

The inclusion Bayes Factor ($BF_{Incl.}$) is the extent to which the data support the inclusion of a factor. The $BF_{Incl.}$ compares the prior probability with the factor versus without the factor. A $BF_{Incl.}$ of less than 1 suggests that including a factor or an interaction does not improve the likelihood of obtaining the data. We also performed Bayes Factor replication ($BF_{r0}$) tests (Verhagen & Wagenmakers, 2014). This illustrates the probability of obtaining the data given a prior informed by previous works. We compared mean amplitudes between 162 and 170 ms (as in Czigler & Sulykos, 2010) at each PO ROI given the effect size (Cohen's $d$ = –0.73) for the difference between standard and deviant orientations (averaged over both task conditions) at the Oz in Czigler and Sulykos (2010).

Where there are more than two levels for any factor or interaction between factors, we correct degree of freedom for all analyses (frequentist and Bayesian) using the Greenhouse-Geisser (ε). Eta squared ($\eta^2$) denote the estimated effect size and all paired *t*-tests were two-tailed unless explicitly stated.

## 3.4 Results

### 3.4.1 Behavioural results

The mean hit rate for detecting the central X was 98% and the false alarm rate was 0.1%, showing that participants paid attention to the task and did very well on it. Mean (*SD*) hit rate for oddball blocks was 98.2% (1.8%) and 98.2% (2.3%) for control blocks, $t$ (20) = 0.016, $p$ = .987, $BF_{10}$ = 0.228. Mean false alarm rates were also similar in the oddball ($M$ = 0.0007, $SD$ = 0.0007%) and control blocks ($M$ = 0.0005, $SD$ = 0.0005%), $t$ (20) = 1.678, $p$ = .109, $BF_{10}$ =

0.754. Mean (*SD*) reaction times were 545 ms (52 ms) in the oddball block and 545 ms (51 ms) for the control blocks, $t$ (20) = –0.025, $p$ = .981, $BF_{10}$ = 0.228.

### 3.4.2 Event-related potentials (ERPs) and difference waves

Figure 3.3 shows the grand average ERPs for each magnitude of deviance. We show the canonical P1, N1, P2, N2, and P3 components at the enlarged right parieto-occipital ROI for the 15° deviant condition (top panel). ERPs at the lateral PO ROIs—where the vMMN is usually largest—are typical for ERPs recorded by others in vMMN studies (e.g., Kimura & Takeda, 2015). The ERPs for standards (green) compared with ERPs to deviants (orange) or controls (purple) show smaller P2s and P3s. This is consistent with what one would expect from adaptation.

Within the vMMN time-window (150–300 ms), there was no greater negativity to deviants than to controls exceeding the 95% confidence intervals. We show the difference waves in Figure 3.4 at the left (L), midline (M), and right (R) frontal (F) and parieto-occipital (PO) ROIs. Opposite to a negativity, we observed a positive deviant-minus-standard and deviant-minus-control mean difference potential for all three magnitudes of deviance at the PO ROIs. This enhanced positivity (in place of negativity) explains why most of our replication tests provide strong evidence in favour of the null (i.e., $BF_{r0} < 0.2$ in Table 3.2). The negativity at the L PO in the deviant-minus-control difference wave for 30° deviants is the only instance in which we do not garner support for the null ($BF_{10}$ = 1.309, $BF_{r0}$ = 1.290). Still, the data provide only weak evidence for the alternative, our frequentist test is non-significant, the negativity does not exceed

our 95% confidence intervals, and we did not find a component consistent with a vMMN in our PCA of the data (below).

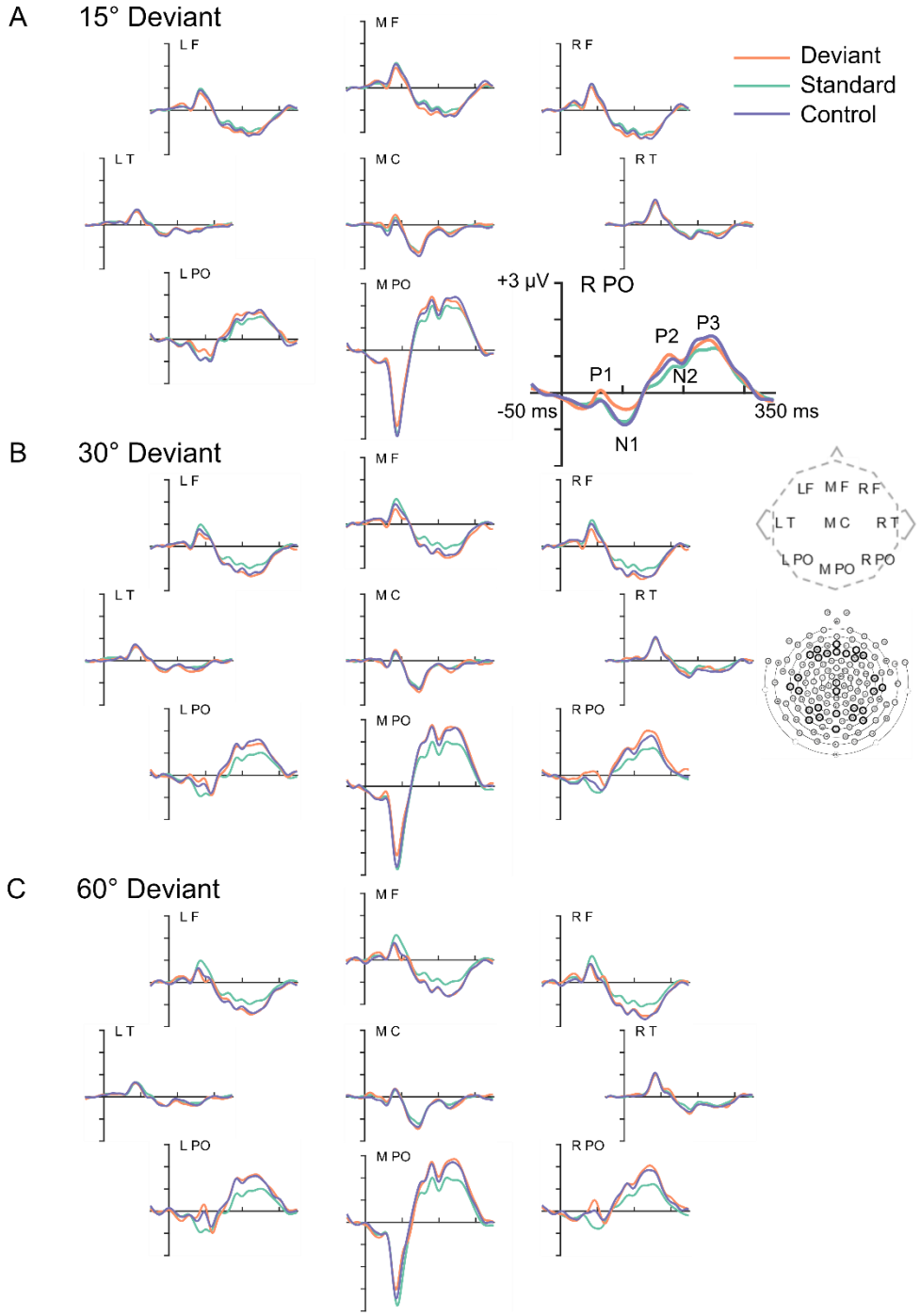


*Figure 3.3* Grand average ERPs for each magnitude of deviance. Standard (green), deviant (orange), and control (purple) ERPs plotted at left (L), midline (M), and right (R) frontal (F), and parieto-occipital (PO) regions. We also show ERPs at M central (C) and L and R temporal (T) regions. Electrode clusters in each region are depicted by the black circles on the diagram of the 129-channel net. We show the typical ERP components for the 15° orientation deviants at the R PO region. The distance between ticks is larger here for having enlarged the figure for illustration.

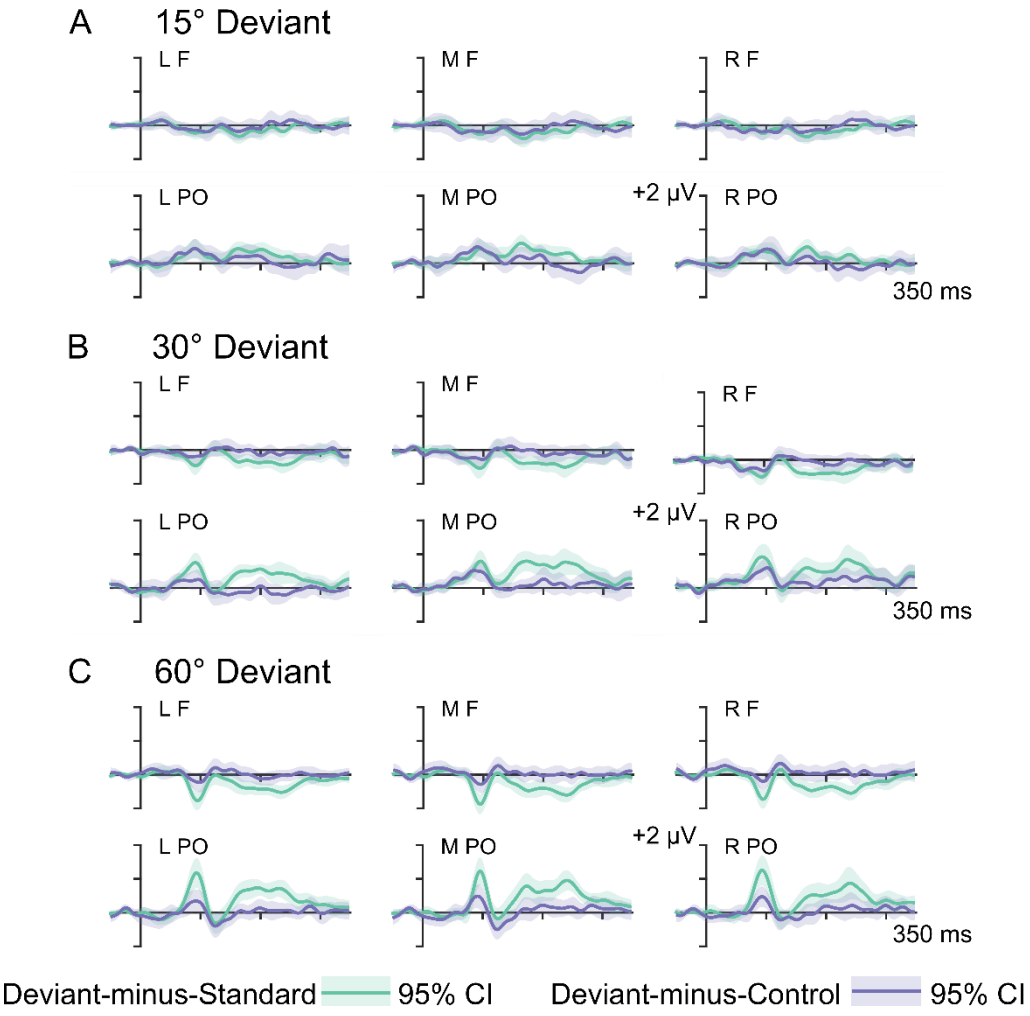


*Figure 3.4* Difference waves for each magnitude of deviance. We show the deviant-minus-standard (green) and deviant-minus-control (purple) difference waves at left (L), midline (M), and right (R), frontal (F), and parieto-occipital (PO) regions. The lighter green and purple around the deviant-minus-standard and deviant-minus-control difference wave, respectively, show the 95% confidence interval. No negativity exceeded the 95% confidence interval within the vMMN peak time-window (150–300 ms). The deviant-related positivity around 90 ms at the PO regions increases with the magnitude of deviance (A-C) in the deviant-minus-standard difference wave, but not in the deviant-minus-control difference wave when controlling for adaptation.

Outside the vMMN time-window, we observed a deviant-related positivity around 90 ms at all PO ROIs and a deviant-related negativity around 120 ms at the M PO ROI. The positivity appears to increase with the magnitude of deviance in the deviant-minus-standard difference wave, but not in the deviant-minus-control difference wave—when controlling for adaptation.

Table 3.2 *Directed Bayesian ($BF_{10}$ and $BF_{r0}$) t-tests (one-tailed) of the Difference in Mean Amplitude (μV) at Left, Middle, and Right Parieto-occipital regions between 162 and 170 ms for Each Difference Wave and Magnitude of Deviance (df = 20)*

| | Deviant vs. Standard | | | | | Deviant vs. Control | | | | |
|---|---|---|---|---|---|---|---|---|---|---|
| | **μV** | ***t*** | ***p*** | $BF_{10}$ | $BF_{r0}$ | **μV** | ***t*** | ***p*** | $BF_{10}$ | $BF_{r0}$ |
| 15° (small) | | | | | | | | | | |
| L PO | 0.42 | 3.822 | .999 | 0.061 | 0.006 | 0.20 | 1.325 | .900 | 0.109 | 0.011 |
| M PO | 0.58 | 4.910 | .999 | 0.055 | 0.006 | 0.20 | 1.361 | .906 | 0.107 | 0.011 |
| R PO | 0.47 | 4.292 | .999 | 0.058 | 0.005 | 0.20 | 1.669 | .945 | 0.096 | 0.009 |
| 30° (medium) | | | | | | | | | | |
| L PO | 0.48 | 4.754 | .999 | 0.055 | 0.006 | –0.13 | –1.625 | .060 | 1.309 | 1.290 |
| M PO | 0.77 | 5.217 | .999 | 0.025 | 0.006 | 0.06 | 0.588 | .719 | 0.155 | 0.023 |
| R PO | 0.59 | 3.856 | .999 | 0.061 | 0.005 | 0.15 | 1.251 | .887 | 0.112 | 0.012 |
| 60° (large) | | | | | | | | | | |
| L PO | 0.60 | 4.180 | .999 | 0.059 | 0.005 | 0.04 | 0.388 | .649 | 0.174 | 0.029 |
| M PO | 0.69 | 3.821 | .999 | 0.061 | 0.006 | 0.08 | 0.559 | .709 | 0.157 | 0.023 |
| R PO | 0.43 | 2.672 | .993 | 0.073 | 0.006 | –0.06 | –0.431 | .336 | 0.325 | 0.106 |

*Note*. L PO = left parieto-occipital region of interest. M PO = middle parieto-occipital region of interest. R PO = right parieto-occipital region of interest.

We compared ERPs to standard and random stimuli at varying positions in the sequence to see if there was any evidence of regularity encoding in the oddball sequences. Broadly speaking, repetition suppression (RS) appears as attenuated brain activity to repeated stimuli that reflects changes due to learning (for a review, see Grill-Spector, Henson, & Martin, 2006). For example, evidence suggests that smaller ERP amplitudes for repeated stimuli reflects evidence of regularity encoding (e.g., Baldeweg, 2006; Bendixen et al., 2007; Ethridge et al., 2016; Rigoulet et al., 2017; Summerfield et al., 2011; Tang, Smout, Arabzadeh, & Mattingley, 2018). We explored this possibility by clustering epochs based on the position of the stimulus within the oddball or

control sequences. The average number of epochs for positions 3–5 was 1396 for standards and 1404 for random stimuli, for positions 6–8 there were 478 for standards and 468 for random stimuli, and for positions 9 and above there were 120 for standards and 123 for random stimuli.

Figure 3.5(A) shows that N1 negativity in the standard ERPs decreases as the number of standards preceding it increases. As expected, this is absent for the random stimuli in control blocks as there is no repetition here (Figure 3.5B). Therefore, the data provide some evidence that the regularity in our roving oddball sequences was encoded.

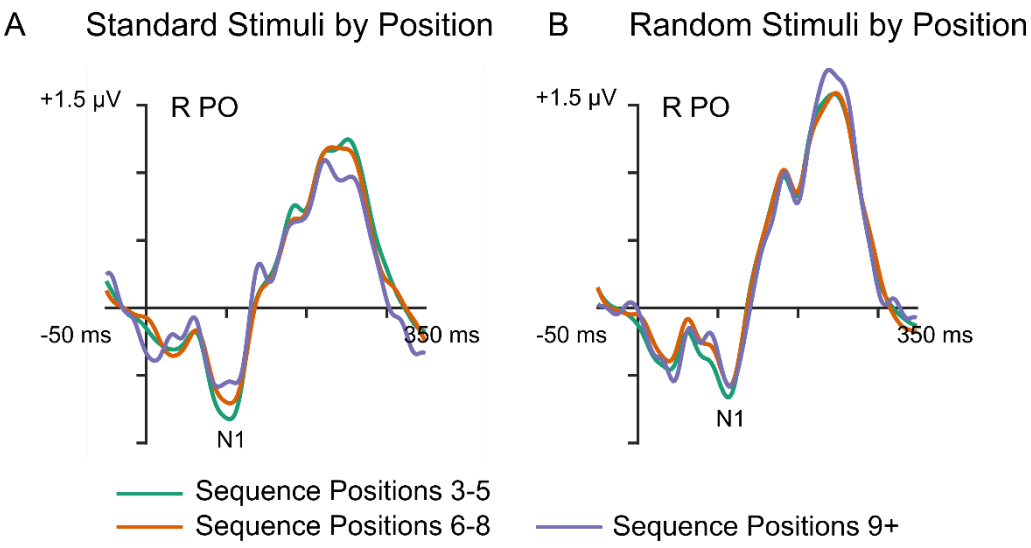


*Figure 3.5* ERPs for standard and random stimuli according to their position in oddball and control sequences, respectively. A. For standard ERPs, the average number of epochs in the ERP for positions 3–5 was 1396, 478 for positions 6–8, and 120 for positions 9 and above. B. For random ERPs, the average number of epochs in the ERP for positions 3–5 was 1404, 468 for positions 6–8, and 123 for positions 9 and above. The N1 suppression appears for repeated stimuli only and the strength of suppression increases with the number of repetitions. Note, however, that the signal to noise ratio is not equal across conditions.

### 3.4.3 Principal components analysis (PCA)

PCA revealed the components contributing to the deviant-related positivity observed in our difference waves were the P1 and N1 components seen in Figure 3.3. However, we did not find a component in which the deviant produced greater negativity than the control at its maximum (positive pole) or minimum (negative pole) with a peak latency between 100 and 150 ms that would explain the negativity at the M PO ROI in Figure 3.4 (see Figure S1 and S2 Appendix A for details of all components).

Figure 3.6 shows that the P1 (component 3) peaked at 90 ms in lateral PO electrodes. This was followed by an N1 (component 5) with a peak latency of 108 ms. N1 negative and positive poles were at occipital and lateral frontal electrodes, respectively. Figure 3.6 shows the P1 and N1 scalp topographies at their peak latencies, the P1 and N1 component loadings (scaled by *SD*), and their scores per condition at L PO, M PO, and R PO ROIs.

According to Figures 3.3 and 3.6, the negative pole of the P1 component (M PO ROI) is larger than the positive pole (R PO ROI). A simple dipole analysis, using the EP toolkit (Dien, 2010), FieldTrip's dipole analysis function (Oostenveld, Fries, Maris, & Schoffelen, 2011), and EEGLAB for visualising the results, confirmed that the pronounced negativity at the M PO ROI is due to the combined negative pole of both P1 components converging within close proximity.

We extracted the microvolt-scaled component score for deviant and control conditions and compared them statistically using a three-way repeated-measures ANOVA with region (left vs. midline vs. right), magnitude of deviance (small vs. medium vs. large), and deviance (deviant vs. control) as factors on N1 scores. The N1 did not differ among regions, $F$ (2, 40) = 1.261, $p$ = .293, $\varepsilon$ = 0.928, $\eta^2$ = .059, or among the three magnitudes of deviance, $F$ (2, 40) = 1.769, $p$ = .190, $\varepsilon$ = 0.844, $\eta^2$ = .081, or between deviants and controls, $F$ (1, 20) = 1.546, $p$ = .228, $\eta^2$ = .072. There was no significant interaction between these factors (see Appendix B, Table S1 for details of the full ANOVAs).

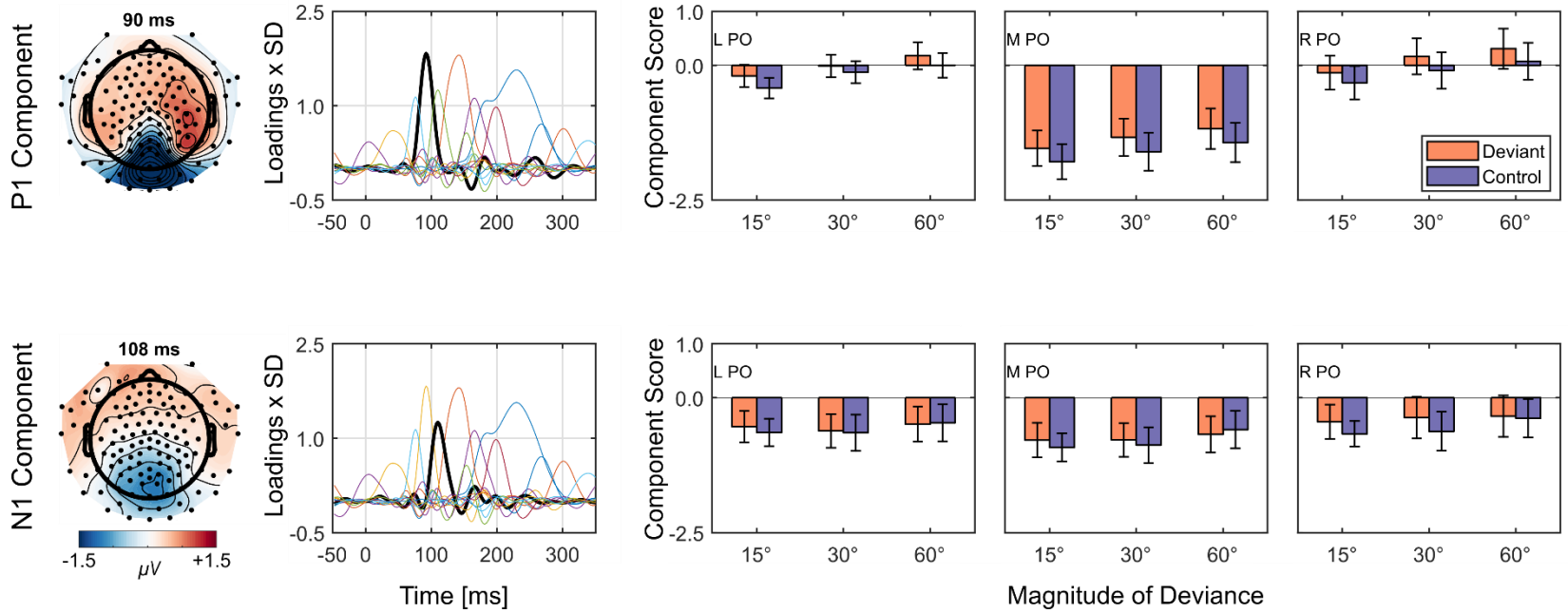


*Figure 3.6* PCA component details for the P1 and N1. The top panel shows details of the P1. The bottom panel shows details of the N1. In the leftmost column, we show the combined activity from deviant (orange) and control (purple) trials at peak latency of the P1 (top) and N1 (bottom). In the second column, we show the component loadings (scaled by *SD*) (thick black line) relative to all other components (thin multi-coloured lines). This illustrates the component's contribution to the overall evoked activity recorded from the scalp (e.g., the ERP). In columns three to six, we show the scores for deviant and control trials for each magnitude of deviance (15°, 30°, 60°) at the left (L), midline (M), and right (R) parieto-occipital (PO) ROI. Error bars depict ±1 standard error.

We did find that the P1 was affected by deviance. We compared P1 amplitudes in each PO ROI with magnitude of deviance (small vs. medium vs. large) and deviance (deviant vs. control) as factors because amplitudes were visibly different at each PO ROI. Magnitude of deviance was significant at the L PO: $F$ (2, 40) = 30.081, $p < .001$, $\varepsilon = 0.722$, $\eta^2 = .601$, M PO: $F$ (2, 40) = 17.667, $p < .001$, $\varepsilon = 0.672$, $\eta^2 = .469$, and R PO: $F$ (2, 40) = 17.294, $p < .001$, $\varepsilon = 0.686$, $\eta^2 = .464$. Significant positive linear trends in mean P1 voltage for deviants and controls (combined to perform trend analysis) in the L PO: $F$ (1, 20) = 36.888, $p < .001$, $\eta^2 = .648$, M PO: $F$ (1, 20) = 21.053, $p < .001$, $\eta^2 = .513$, and R PO: $F$ (1, 20) = 20.517, $p < .001$, $\eta^2 = .506$, show that larger magnitudes of deviance evoked larger P1 amplitudes than smaller magnitudes of deviance.

P1 amplitudes were also larger for deviants than for controls at the L PO: $F$ (1, 20) = 9.836, $p = .005$, $\eta^2 = .330$, M PO: $F$ (1, 20) = 14.065, $p = .001$, $\eta^2 = .413$, and R PO: $F$ (1, 20) = 16.966, $p < .001$, $\eta^2 = .459$. This is therefore is a deviance-related positivity.

The data provide very strong evidence for a favoured Bayesian model including both magnitude of deviance and deviance at the L PO: $BF_{10}$ = 4.221e+8, M PO: $BF_{10}$ = 1.879e+8, and R PO: $BF_{10}$ = 1.049e+9. However, there was no significant interaction between the magnitude of deviance and deviance (see Table S1 in Appendix B for details of the full ANOVAs) and the data provide strong evidence against including the interaction effect at the L PO: $BF_{\text{Incl.}} = 0.694$, M PO: $BF_{\text{Incl.}} = 0.498$, and R PO: $BF_{\text{Incl.}} = 0.614$, meaning that the difference between the control and deviant stimuli was not modulated by the

magnitude of deviance. Therefore, the P1 difference between the deviant and control (i.e., the deviant-minus-control difference) does not increase with the magnitude of deviance.

## 3.5 Discussion

We conducted this study to determine whether the size of the difference between an expected and unexpected visual input—magnitude of deviance—affects the brain's error response—the vMMN. However, we did not find evidence for a vMMN in any condition. Therefore, we could not confirm any sort of relationship between the magnitude of deviance and the vMMN. This result is especially surprising for the 30° and 60° orientation deviants, given that others have used similar orientation deviants to show the vMMN (e.g., 30 and 60° deviants, Czigler & Sulykos, 2010, 36° deviants, Kimura et al., 2009; 32.7° deviants, Kimura & Takeda, 2013, 2015; 22.51° deviants in Kimura & Takeda, 2014). Given the statistical power of the present study and our Bayesian analyses, we are confident that our orientation deviants do not yield the vMMN. Still, we consider alternative reasons for our results.

### 3.5.1 Alternative reasons for our results

Alternative reasons for our results include:

#### 3.5.1.1 Poor signal-noise ratio

This is always a possibility. However, our ERPs are clear and show the ERP components we typically find for visual stimuli (Clark, Fan, & Hillyard, 1995). Moreover, we did find an effect on the P1 of magnitude of deviance and

for deviants compared with standards. These findings suggest our signal-noise ratio was not so weak that it disguised any robust vMMN to orientation changes.

#### 3.5.1.2 Use of Gabor patches

We used Gabor patches because they are better for isolating a single, low-level feature of visual input—orientation in this case—than bars and gratings. We are aware of three studies that have found a vMMN for orientation deviants using Gabor patch stimuli (Farkas et al., 2015; Sulykos & Czigler, 2011; Takács et al., 2013). Perhaps there are so few because Gabor stimuli are suboptimal for vMMN research.

Alternatively, it is possible that the vMMNs in some studies showing orientation vMMNs to other visual stimuli contain unrelated ERP differences due to changes in other properties of visual stimuli, such as a bar's stimulating new parts of the retina. We describe in more detail below (s 3.5.2) how co-varying changes in visual input with orientation may be contributing to previously reported orientation vMMNs.

#### 3.5.1.3 Stimulus duration

Our stimulus duration was 80 ms. Although our stimulus duration was less than 115 ms—the mean stimulus duration calculated from 24 orientation studies in Chapter 2 (Table 2.6)—others have found a vMMN to orientation deviants using presentation times as short as 50 ms (Astikainen et al., 2004). This suggests that a presentation time as short as ours should still produce a vMMN if one were to occur.

Moreover, long presentation times have their own problems. This is because the appearance of a deviant might trigger a saccadic eye movement away from fixation, as the participant tries to explore the new stimulus. Saccadic eye movements can start after 120 ms and reach peak acceleration after 160 ms (Westheimer, 1954), putting them into the vMMN time-window.

I am grateful to my examiner for this thought-provoking question. Indeed, there are several issues that must be considered in visual research and, to date, the best means for ensuring minimal effect on the stimulus of interest is to direct attention elsewhere. This does not ensure that attentional blink will not occur, but at the very least, occur to same degree for all unattended stimuli such that the trend in the results should be unchanged.

#### 3.5.1.4 Long inter-stimulus intervals (ISIs)

There is evidence that longer ISIs reduce (or abolish) the vMMN (Astikainen et al., 2008; Fu et al., 2003). For example, Astikainen et al. (2008) compared vMMNs for orientation deviants appearing in sequences in which the ISI was 400 or 1100 ms. They found that only the shorter ISI produced a vMMN. Our ISI was 280 ms. This is shorter than the ISI several other studies have used to evoke a vMMN, with many using an ISI of 350 ms or more (Amenedo, Pazo-Alvarez, & Cadaveira, 2007; Czigler et al., 2002; Stagg et al., 2004; Sulykos & Czigler, 2011). Therefore, it does not seem likely that our chosen ISI is the reason for our failing to show a vMMN.

#### 3.5.1.5 Randomised block order

Evidence suggests that when the environment is highly unstable or volatile, there is greater variation in the size of the vMMN (Frost, Winkler, Provost, Todd, 2016; Todd, Provost, Cooper, 2011; Lieder et al., 2013). We randomised block order such that blocks testing different magnitudes of deviance were intermixed, therefore, environmental volatility was high. Perhaps then, even if any error response did occur, it was so reduced by volatility that it could not be measured. This explanation, however, does not account for others inability to find a genuine vMMN to orientation changes occurring in less volatile settings (e.g., File et al., 2017).

#### 3.5.1.6 Use of roving standard

In the roving oddball paradigm, there are fewer identical standards than in ordinary oddball sequences because there is a new standard in each oddball sequence. Essentially, in the roving paradigm, there is less time for the brain to become accustomed to a regularity. However, auditory mismatch studies have used the roving oddball paradigm to yield the MMN (e.g., Fisher et al., 2010; Garrido et al., 2008; Leung, Greenwood, Michie, & Croft, 2015). Huotilainen, Kujala, and Alku (2001) have also shown that relatively few repetitions of a standard—only two to three repetitions—are required for the MMN to occur for deviant vowels in the roving paradigm. Moreover, the MMN amplitude did not increase beyond four or five repetitions (Huotilainen et al., 2001).

Still, the minimum number of standards required for yielding the vMMN in the roving paradigm is currently unknown. Czigler and Pató (2009) used the roving paradigm to show the vMMN to 90° orientation deviants. They showed at least 10 standards before each deviant. Smout et al. (2019) tested orientation deviants using the roving oddball paradigm and found classic and genuine vMMNs when participants paid attention to the stimulus. The number of standard repetitions was between 4 and 11.

In our roving oddball blocks, we had a minimum of three standards preceding each deviant and an average of five standards separated each deviant. Therefore, the number of standards should (at least according to roving MMN and vMMN studies) have been enough for yielding a vMMN.

Although we cannot rule out that our use of the roving paradigm contributed to our failure to find the vMMN to orientation deviants, we have to say that this cannot be the only cause, because we have conducted other studies with ordinary oddball sequences and failed to show any vMMN (Male et al. 2018; Ch. 5–6).

#### 3.5.1.7 Attention

There is evidence to suggest that some deviants will not produce a vMMN unless participants actively attend to the deviants (e.g., Czigler & Csibra, 1990; Csibra & Czigler, 1991, 1992; Smout et al., 2019). In a paradigm similar to ours, Smout et al. (2019) recorded ERPs to attended and unattended deviants. In the ERP data, they found a clear vMMN only for attended deviants. Perhaps we

might have observed a vMMN if participants attended to the Gabor patches. However, if attention is required for a vMMN to occur, this could suggest that the vMMN is not pre-attentive and therefore not a true analogue of the MMN.

### 3.5.2 Why other studies have reported a vMMN to orientation deviants

If we accept that our failure to find a vMMN to orientation deviants is not due to our chosen parameters, we must resolve why other studies have found a vMMN to orientation deviants. Of those that controlled for adaptation and still found a vMMN to *oddball* orientation deviants, all three studies used bar stimuli with deviants that were at least 32° different from standards.

Astikainen et al. (2008) showed participants bars that changed by 36° on deviant trials while they listened to a story. Kimura et al. (2009) asked participants to respond to bars whose corners were rounded. In both studies, participants had no incentive to fixate on the visual stimuli, even less so when there was no visual task (e.g., Astikainen et al., 2008). We replicated Kimura et al. and found that participants looked towards the ends of the bars during oddball blocks, which is the location of the information for the participants' task, and that they looked at the centre of the bars during control blocks. We suspect that our participants fixated more than those who participated in Kimura et al.'s study given we had additional fixation conditions and we used eye-tracking. This means that on deviant trials in oddball blocks, participants in Kimura et al.'s study were seeing multiple changes in visual input, not just the orientation change. For example, there is an additional change in orientation (of the bar's

end) and luminance that occurs toward the end of the bar that does not occur at the centre of the bar.

In the oddball condition of another orientation study, participants responded to central fixation dot changes while eight light grey bars appeared in the periphery on a black background (Kimura & Takeda, 2015). The bar's orientation changed by 32.7° on deviant trials and each stimulus appeared for 250 ms. Our participants only saw each stimulus for 80 ms. We have already described the problem with longer presentation times due to participants being more likely to shift their gaze toward other positions on the screen (where the bars were). It would be useful to monitor and compare eye movements for long versus short stimulus durations to establish whether this affects the resulting vMMN.

### 3.5.3 Deviant-related positivity and the P1

Although we did not find a vMMN, we did find deviant-related positivity from the P1 positivity. We found a similar result in other experiments (Male et al., 2018, Ch. 6). The trend in the P1 amplitudes is identical in both studies, with all deviants' producing significantly larger, more positive, P1s than identical, equally probable controls. This enhanced P1 could be likened to change-related positivity for change stimuli in visual S1–S2 matching tasks (Kimura, Katayama, & Murohashi, 2005, 2006, 2008). However, these studies did not control for adaptation and without a control for adaptation, it difficult to draw conclusions about what the positivity represents. In the present study, we discounted adaptation as a potential explanation for the deviant-related positivity.

Possibly discrepancies between predicted and unpredicted input in low-level visual features are resolved earlier than the vMMN in a process revealed by this early deviant-related positivity. One other study found a significant deviance-related P1 difference and no vMMN when comparing 30°deviants with equiprobable controls. Although Sulykos and Czigler (2013) reasoned that their orientation deviants failed to reactivate the memory for a previous standard, it is possible that the early deviant-related positivity they observed represents an earlier index of error. Clearly, further research is essential to establish whether there is an early prediction error for basic properties of visual input like orientation and whether this then affects whether a vMMN also occurs.

## 3.6 Conclusion

We found an early deviance-related positivity to orientation deviants, but we did not find a vMMN. If this positivity is a neural correlate of prediction error in vision, then there is evidence to suggest that prediction error does not increase with the magnitude of deviance, because its amplitude was unaffected by it. Still, further research is essential to confirm whether an earlier electrophysiological index of prediction error exists for low-level changes in visual input.

# CHAPTER 4

## PRECISION OF VISUAL PREDICTIONS: A STUDY OF DEVIANT-RELATED NEGATIVITY (DRN) FOR UNPREDICTED ORIENTATION CHANGES.

Based on the following manuscript in preparation

Male, A. G., Roeber, U., & O'Shea, R. P. (2019). Precision of visual predictions: A study of deviant-related negativity (DRN) for unpredicted orientation changes.

# 4. PRECISION OF VISUAL PREDICTIONS: A STUDY OF DEVIANT-RELATED NEGATIVITY (DRN) FOR UNPREDICTED ORIENTATION CHANGES.

## 4.1 Preface

In this Chapter, I investigate whether local context of a change affects the brain's processing of it by manipulating magnitude of deviance. However, unlike the study in Chapter 3, I used a sequential rule to establish regularity; deviants violated the rule, making them rule-based deviants.

In two experiments, I manipulate the orientation difference between the predicted and unpredicted input and measure the deviant-related negativity (DRN)—increased negativity owing to adaptation-related difference (e.g., N1 difference) and negativity owing to prediction error (e.g., the vMMN). There were four different rule-based deviants. This allowed me to test one derivative of my thesis as well as a second question. These were:

I. Does the magnitude of deviance of a pre-attentive change affect the DRN to violations of abstract regularities in visual input?

II. Do adaptation-related differences and deviance-related differences contribute to DRN equally?

## 4.2 Introduction

Chalky beads of washing liquid hug the frame of freshly cleaned glass. Through the glass, in the distance, the brilliantly white tin roof of the building opposite is competing with the green and brown foliage of a tall gum tree. There are books piled high beneath the windowsill, a miniature fan atop it, its blades constantly revolving. Although one does not see these objects, one still knows they are there, because at some stage, they were seen, and logic dictates that objects do not just disappear, unexpectedly and without cause. This understanding is rooted in the probabilistic way in which the brain represents its environment.

Although these objects are not being attended to, the brain would also detect any kind of change in these objects; for example, if the humming of the fan became louder or its blades began to rotate more quickly. This is because unexpected sensory input produces a different pattern of activity in the brain when compared with expected input (Näätänen, Gaillard, & Mäntysalo, 1978). We can show this by measuring the brain's electrical activity via electrodes placed on the scalp—electroencephalography (EEG)—and averaging EEG activity that is time-locked to the onset of sensory input over many events to produce event-related potentials (ERPs). Näätänen et al. (1978) compared ERPs from irregular, different tones with ERPs from a series of regular, identical tones and found that between 120 and 400 ms, irregular tones produced a more negative voltage (i.e. negativity) than regular tones. They called this negativity the mismatch negativity (MMN).

In the paradigm most commonly used to show the MMN—the oddball paradigm (Squires et al., 1975)—irregular *deviants* interrupt regularly occurring *standard*s. Standards occur more frequently than deviants do; therefore, standards establish the regularity and deviants violate it. A violation can only occur where regularity is already established; therefore, at least two standards should separate each deviant (s 2.5.8.4, Ch. 2).

Various unattended irregularities can yield the MMN, including simple deviants like changes in tone frequency (e.g., Jacobsen & Schröger, 2003; Näätänen, 1990, 1992). Irregularities that are more complex also yield the MMN, including irregular tonal repetitions and excursions from tonal patterns (e.g., Tervaniemi, Maury, & Näätänen, 1994) and analogues of the MMN exist in other sensory modalities, including vision (Cammann, 1990). The visual MMN (i.e., vMMN) is largest between 150 and 300 ms and, similar to the MMN, irregular repetitions and excursions from patterns of visual input produce a vMMN (Bubic, Bendixen, Schubotz, Jacobsen, & Schröger, 2010; Czigler & Pató, 2009; Czigler, Weisz, & Winkler, 2006; Kimura, Widmann, & Schröger, 2010). Therefore, an unpredicted change in a fan's sound or speed is likely to evoke a sensory specific mismatch, showing that the brain detects such changes in unattended objects.

What is unclear, however, is whether the amount of change will affect the brain's processing of the change and what this difference in brain processing represents. This is what we are concerned with in the present study.

### 4.2.1 Magnitude of deviance and deviant-related negativity (DRN)

Many consider the (v)MMN a neural correlate of prediction error (Clark, 2013; Garrido et al., 2008, 2009; Stefanics, Astikainen, & Czigler, 2015; Stefanics, Kremláček, & Czigler, 2014). However, it is unknown whether the magnitude of deviance affects the (v)MMN. This is primarily because most of the evidence for a monotonic relationship between magnitude of deviance and (v)MMN is based on MMN research and most of these studies did not control for adaptation (s. 2.1, Ch. 2). Therefore, most MMN studies measured deviant-related negativity (DRN, Kimura et al. 2009) and the DRN contains differences in ERP amplitudes due to adaptation (i.e., adaptation-related differences) as well as deviance (i.e., deviance-related differences). Only the latter pertains to genuine deviance detection (e.g., vMMN) and because adaptation-related differences increase with the size of the difference between inputs (i.e., magnitude of difference), adaptation-related differences can give the appearance of a magnitude of deviance effect (e.g., Ch. 3).

Moreover, the evidence for a magnitude of deviance effect on the vMMN is inconsistent (Czigler, Balázs, & Winkler, 2002; Czigler & Csibra, 1990; Czigler & Sulykos, 2010; Flynn, Liasis, Gardner, Boyd, & Towell, 2009; Kimura, 2018; Maekawa et al., 2005; Smout et al., 2019; Takács et al., 2013). So, the question remains; does the magnitude of deviance affect the vMMN and, if not, is it because existing reports of the magnitude of *deviance* effect are driven by magnitude of *difference* effect? We seek to address this is the present study.

### 4.2.2 The present study

We sought to determine whether the brain's response to unexpected visual changes (i.e., DRN) shares some relationship with how unexpected (magnitude of deviance) or different (magnitude of difference) the input is from the predicted or preceding input, respectively. We manipulated orientation in a rotating-oddball paradigm. This allowed us to manipulate magnitude of deviance with respect to the predicted input and magnitude of difference with respect to the preceding stimulus.

For example, a stimulus will have a particular orientation (e.g., 90°). The following stimulus will have rotated clockwise or anticlockwise by some angle (e.g., clockwise 30°). Each standard that follows adheres to this pattern by rotating in the same direction (e.g., clockwise) by the same angle (e.g., 30°). At some point thereafter, a stimulus that does not adhere to this pattern will appear; this is the deviant. The orientation of this stimulus will be different from the predicted stimulus orientation by some angle and different from the previous stimulus by another angle. The two angles of difference are not equal.

Others have used similar rule-based orientation deviants to show the vMMN (e.g., Kimura, 2018; Kimura & Takeda, 2015). In their regularity condition, Kimura and Takeda (2015) showed participants eight light grey bars (each 0.5°×3.0° of visual field) arranged at eight peripheral locations on a black background. The orientation of these bars changed by 32.7° in a clockwise or anticlockwise direction (depending on the block) on each trial until a deviant interrupted the sequence. Deviants were rotated 32.7° in the opposite direction.

They observed a vMMN to these deviants even after separating adaptation-related differences from DRN.

We defined four deviants. The relative difference in orientation of each deviant appears in Table 4.1. Figure 4.1 shows the expected trend in DRN amplitudes if the magnitude of deviance and difference similarly (A) or distinctly (B–C) affects mean DRN amplitude. For example, if both magnitude of difference and magnitude of deviance contribute to DRN equally, then Deviants 1 and 2 should produce similar DRNs (Figure 4.1A). If one contributes to DRN more than the other, the two DRNs would differ (Figure 4.1B–C).

To our surprise, we did not observe a difference between any deviant and standard stimuli in Experiment 1. We tested different stimuli and performed Experiment 2 to confirm that our results genuinely reflect the effect of our orientation manipulation. Still, we found no DRN.

Table 4.1 *Relative Orientation Difference for each Rule-based Deviant*

| Deviant | Magnitude of Difference (°) | Magnitude of Deviance (°) |
|---|---|---|
| Deviant 1 | +10 | –20 |
| Deviant 2 | +20 | –10 |
| Deviant 3 | +40 | +10 |
| Deviant 4 | +50 | +20 |

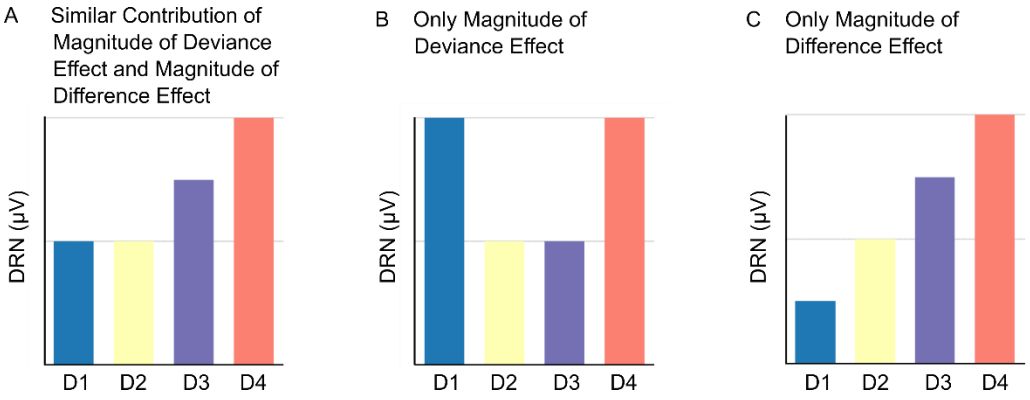


*Figure 4.1* Estimated effect of magnitude of deviance and magnitude of difference on mean deviant-related negativity (DRN) amplitudes. Deviant 1 (D1) is the least different from the preceding orientation, but most different to the predicted. Deviant 2 (D2) is more different from the preceding orientation but least different to the predicted orientation. Deviant 3 (D3) is even more different from the preceding orientation but least different to the predicted orientation. Deviant 4 (D4) is the most different from the preceding orientation and most different to the predicted orientation. A. The expected trend in DRN amplitudes if the magnitude of deviance and difference equally affect DRN. B. The expected trend in DRN amplitudes if the magnitude of deviance affects the DRN, but not magnitude of difference. C. The expected trend in DRN amplitudes if the magnitude of difference affects DRN, but magnitude of deviance does not.

## 4.3 Experiment 1

### 4.3.1 Method

#### 4.3.1.1 Participants

Twenty-five self-declared neurologically healthy participants (14 males, 23 right-handed) with normal or corrected-to-normal vision volunteered in return for course credit or the chance to win a $50 (AUD) voucher. Mean age was 25 years with a range from 18 – 43. Most of the participants were undergraduate psychology students at Murdoch University. All participants provided their written informed consent and were free to withdraw from the experiment at any time. The Murdoch University Ethics Committee approved the study (ethics permit 2016 117).

#### 4.3.1.2 Apparatus

Apparatus details are the same as those used in Chapter 3 (s. 3.3.2).

#### 4.3.1.3 Stimuli

We chose to use Gabor stimuli for reasons previously outlined in Chapter 2 (s. 2.5.4). All stimuli appeared on an achromatic background (mean RGB of 128 128 128). Gabor patches varied in either colour or orientation. Other features of Gabor patches, including phase (0 radians), spatial frequency (2.4 cycles per degree of visual angle, cpd), and standard deviation of the Gaussian (3.84° of visual angle) remained the same. Each Gabor patch subtended a visual angle of 24°, but the visible parts of the Gabor patch had a diameter of approximately 22°. There was a white central fixation cross. The length of each bar of the fixation cross was .6° of visual angle; the width was .03° of visual angle.

The orientation of the first Gabor patch in a block was one of 17 possible orientations between 15° and 175° (10° separation) clockwise from vertical (0°). Selection was random. The orientation of each new Gabor patch changed by 30° in a clockwise or anti-clockwise direction (alternating between blocks), until a deviant interrupted the sequence. There were four rule-based deviants (see Table 4.1 for orientation details). Therefore, a sequential rule determined whether a stimulus represented a standard or deviant within a sequence. There was no apparent motion; thus, the regularity we instantiate is about orientation, not motion. This is similar to what others have done to evoke DRN to rule-based orientation deviants (e.g., no apparent motion in Kimura, 2018; Kimura & Takeda, 2013, 2014, 2015).

#### 4.3.1.4 Procedure

There were 12 oddball blocks of trials in this experiment. Half of the blocks were clockwise rotation blocks; half were anti-clockwise rotation blocks. Each block housed 275 trials; 44 trials (16%) were deviants (11 per deviant). We randomised the deviant's position provided that three standards separated each deviant. The length of a sequence ranged between 4 and 16 trials. The mean number of trials per sequence was six. We randomised block order afresh for each participant. Each trial lasted 800 ms featuring a 680 ms inter-stimulus-interval (ISI). Figure 4.2 shows an example of a sequence containing Deviant 4 (outlined in pink).

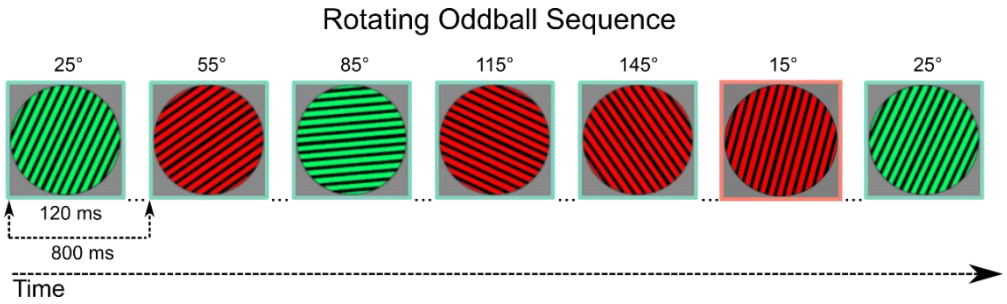


*Figure 4.2* Illustration of a rotating oddball sequence in Experiment 1. In the depicted sequence, orientation is changing in a clockwise direction. Five standards (outlined in green) precede the deviant (outlined in pink) that is rotated 50° from the previous Gabor patch and 20° from the predicted Gabor patch—Deviant 4. The orientation of each stimulus in degrees (°) appears above it (all from vertical 0°). Participants respond to a target colour (50:50) assigned at the beginning of the experiment. We do not show the fixation cross in this illustration and '...' denotes the 680-ms inter-stimulus-interval.

The task-relevant feature was Gabor patch colour. The colour was either red or green (50:50) (Figure 4.2). We asked participants to look at an always-present white fixation cross and to respond only when a Gabor patch with the target colour (counterbalanced across participants) appeared. A response was correct if it occurred between 0.15 and 2 s after stimulus onset. Participants took

self-timed breaks between blocks and all participants completed all blocks within 1 hour (3.67 minutes per block).

#### 4.3.1.5 EEG recording and analysis

All EEG recording and analysis was identical to Chapter 3 (s. 3.3.5), except that epochs commenced 100 ms prior to stimulus onset and ended 400 ms post-stimulus onset and we excluded electrodes with a z score exceeding 3.0 (instead of 2.0). We averaged ERPs for all standards and each deviant. The mean (*SD*) number of epochs for each ERP was 1939 (150) for Standards, 115 (10) for Deviant 1, 116 (10) for Deviant 2, 116 (11) for Deviant 3, and 115 (9) for Deviant 4. We obtained our difference waves by subtracting the standard ERP from each deviant ERP.

Regions of interest (ROIs) were identical to Chapter 3 and included left (L), and right (R) frontal (F), temporal (T), and parieto-occipital (PO) regions. We also defined a midline frontal (M F), midline central (M C), and midline parieto-occipital (M PO) ROI. Figure 4.3(A) shows electrodes in each ROI.

We performed temporal principal component analysis (PCA) on the individual average ERP data for Standard, Deviant 1, Deviant 2, Deviant 3, and Deviant 4 trials using the EP Toolkit (v2.64; Dien, Khoe, & Mangun, 2007) so that we could isolate the constituents of the ERP waveform (Carretié et al., 2004; Dien, 2010; Dien & Frishkoff, 2005).[5] We used the same parameters used in

[5] PCA produces a single score per component and condition; this represents the activity of a component (as if all other components that contribute to the EEG activity are absent), over all participants, in a single condition, at a specified electrode or region of interest (Dien, 2012).

Chapter 3 (s. 3.3.5). We retained nine principal components according to Horn's (1965) parallel test, explaining more than 95% of the variance.

We extracted the microvolt-scaled component scores for each stimulus type (i.e., Standard, Deviant 1, Deviant 2, Deviant 3, and Deviant 4) for all components with a single peak latency between 70 and 350 ms because DRN typically occurs between 150−350 ms and is largest (i.e., most negative) over the PO regions on the scalp (e.g., Kimura et al., 2010). We searched for components meeting these criteria. As we did not find any, we did not perform statistical analysis on the PCA data.

We performed paired Bayesian *t*-tests to examine the probability of obtaining our behavioural data, using a medium prior (i.e., Cauchy prior whose width was set to 0.707), and all paired tests are two-tailed.[6]

### 4.3.2 Results

#### 4.3.2.1 Behavioural results

Accuracy (d′) and reaction time (RT) results for detecting target colours (from 25 participants) as well as comparisons between standard and deviant trials using Bayesian *t*-tests appear in Table 4.2. We analysed correct response RT only and calculated d′ using a log-linear correction (Stanislaw & Todorov, 1999). There was no difference in RT, but accuracy was better for deviants compared to standards. Possibly the irregularity combined with target colour roused

[6] A $BF_{10}$ between 1 and 3 provides weak evidence for the alternative (or null) hypothesis. A $BF_{10}$ larger than 3 provides moderate evidence in favour of the alternative or strong evidence if a $BF_{10}$ is larger than 10 (Lee & Wagenmakers, 2013).

participants' attention. The high d′ for both trial types suggests that participants were attending to the task regardless of trial type.

Table 4.2 *Bayesian Factors ($BF_{10}$) and Paired t-tests for Mean (Standard Deviation) Accuracy and Reaction Time for Standards and Deviants (df = 24)*

| | **Standard** | **Deviant** | ***t*** | ***p*** | ***BF*$_{10}$** |
|---|---|---|---|---|---|
| Accuracy (*d*′) | 4.71 (.82) | 5.18 (.50) | 5.745 | < .001 | 3248.831 |
| Reaction Time (ms) | 287 (24) | 287 (23) | 0.964 | .344 | 0.321 |

#### 4.3.2.2 Event-related potentials (ERPs) and difference waves

Visual inspection of the ERPs revealed that deviant ERPs were similar to one another. The PCA (below) confirms this. Thus, we combined the ERPs from all four deviants to produce one ERP and one deviant-minus-standard difference wave for all four deviants. Figure 4.3(A) shows the ERPs for standards (green) and deviants (orange) as well as the deviant-minus-standard difference wave (black) at each ROI.

We show the canonical P1, posterior N1 (pN1), and P2 at the enlarged R PO ROI. We also show the anterior N1 (aN1) here and at the R F ROI. Others have described this as a late P1 component (e.g., Friedman, Sehatpour, Dias, Perrin, & Javitt, 2012); however, PCA (Figure 4.3B) distinguishes it from the P1. The P3 appears at the M C.

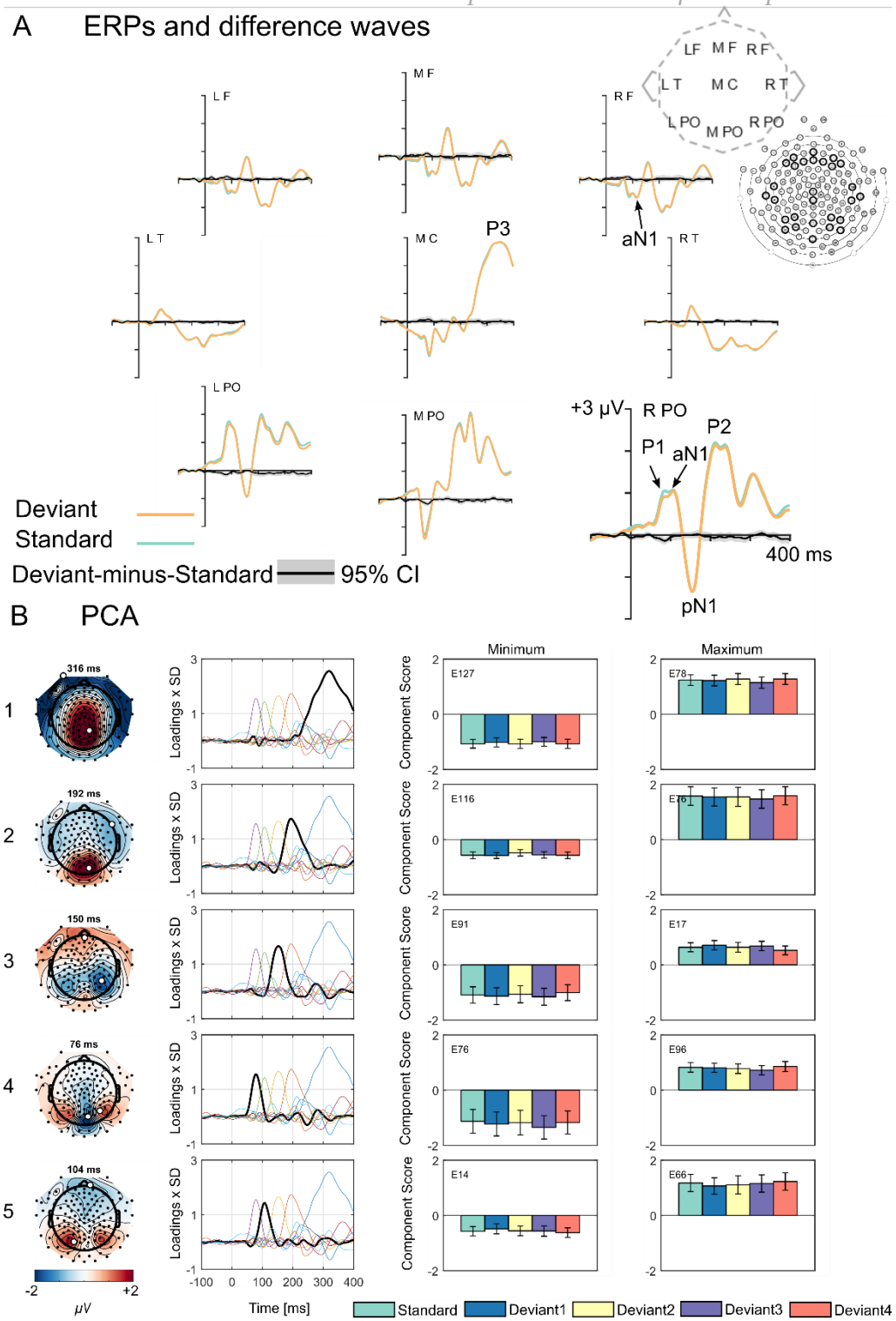


*Figure 4.3* Experiment Results 1 ($N$ = 25). A. Grand average ERPs and deviant-minus-standard difference waves. One ERP for standards (green) and all deviants combined (orange) and one deviant-minus-standard (black) difference wave at the left (L), midline (M), and right (R) frontal (F) and parieto-occipital (PO) regions of interest (ROIs). We also show ERPs at M central (C) and L and R temporal (T) ROIs. The grey around each difference wave shows the 95% confidence interval (CI). Electrode clusters in each ROI are depicted by the black circles on the diagram of the 129-channel net. B. PCA results. From left to right, we show: the component number, topographical maps (combined activity from deviant and standard trials at peak latency), component loadings (a component's contribution as a thick black line to the overall evoked activity relative to all other components as thin lines of different colours), component score for minimum, and component score for maximum. The last two, the bar graphs, show means for each deviant and standard conditions, ±1 standard-error bars, and electrode numbers. We show the location of these electrodes on the topographical maps by white disks.

Figure 4.3(A) shows that the P1 at the L PO and R PO peaks at approximately 80 ms. The pronounced occipital negativity at the M PO at the same time reflects the combined negative poles from both P1s. There is a similar result in Chapter 3. Possibly, the pronounced negativity is due to the large visual field excited by the stimulus subtending 22° of visual angle. No negativity exceeded the 95% confidence intervals within the DRN time-window (150–350, Kimura et al., 2010). In effect, we did not find any evidence of DRN or any deviance-related differences in our ERPs.

#### 4.3.2.3 Principal component analysis (PCA)

In Figure 4.3(B), we show details of the components shown in Figure 4.3(A) (also the only components with a single peak between 70 and 350 ms). These are the P1 (component 4), aN1 (component 5), pN1 (component 3), P2 (component 2), and P3 (component 1). The P3's posterior-parietal distribution (Kok, 2001; Polich, 2003) suggests it reflects target processing (e.g., P3b). No component was temporally or topographically consistent with DRN.

#### 4.3.2.4 Follow-up with different stimuli

We conducted a follow-up to confirm whether we would find a difference between our standard and deviant ERPs with different smaller stimuli. We tested four new participants (1 male, mean age 27 years, range 25 – 30, all right-handed) with stimuli previously used by Jack et al. (2017) in a binocular rivalry experiment that showed a classic vMMN to unattended swaps of the stimuli between the two eyes. We illustrate the stimuli in Figure 4.4.

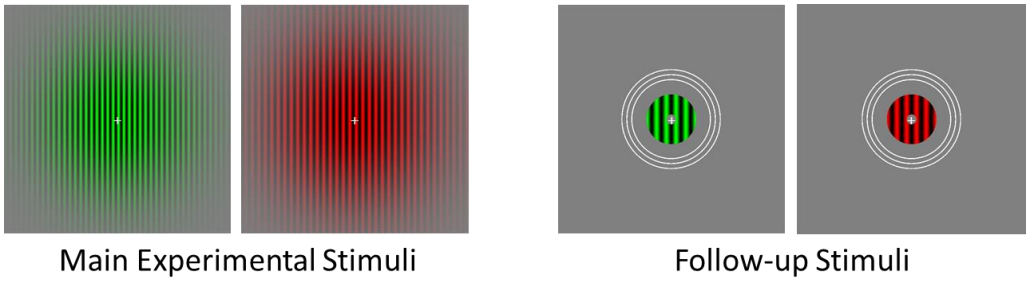


*Figure 4.4* Screenshots of stimuli used in the main experiment (left) and follow-up (right). We modified the stimuli from Jack et al. (2017) to suit our task. Jack et al. (2017) used black-to-white gratings and a red fixation cross. All other parameters of the stimuli were identical to theirs.

#### 4.3.2.5 Behavioural results

Table 4.3 shows mean (*SD*) d′ and RT results for detecting target colours (from 4 participants) as well as comparisons between standard and deviant trials.

Table 4.3 *Bayesian Factors ($BF_{10}$) and Paired t-tests for Mean (Standard Deviation) Accuracy and Reaction Time for Standards and Deviants (df = 3)*

| | **Standard** | **Deviant** | ***t*** | ***p*** | ***$BF_{10}$*** |
|---|---|---|---|---|---|
| Accuracy (*d'*) | 4.03 (.37) | 4.77 (.12) | 4.968 | .016 | 5.210 |
| Reaction Time (ms) | 280 (31) | 280 (34) | 0.301 | .783 | 0.444 |

Similar to the main experiment, accuracy was better for deviants compared to standards and there was no difference in RT between standards and deviants. The similar task performance in follow-up testing, suggests participants' engagement in the colour task was unaffected by the different stimuli.

#### 4.3.2.6 EEG recording and analysis, event-related potentials (ERPs), difference waves, and principal component analysis (PCA)

All EEG recording and analysis of the data were identical to the main experiment. The mean (*SD*) number of epochs for each ERP was 1768 (221) for Standards, 104 (15) for Deviant 1, 105 (14) for Deviant 2, 109 (14) for Deviant 3, and 106 (15) for Deviant 4. We created four difference waves by subtracting

the standard ERP from each deviant ERP before combining all four deviants to produce one deviant ERP and one deviant-minus-standard difference wave because ERPs for the different deviants did not differ.

ERPs from follow-up testing (Figure 4.5A) were similar to the ERPs from the main experiment, especially those recorded from the PO ROIs. The P1, pN1, P2, and P3 are clear despite having so few participants. Difference wave amplitudes did not exceed the 95% confidence interval in either direction at any ROI (Figure 4.5A). We retained eight components according to Horn's (1965) parallel test, explaining more than 95% of the variance.

Figure 4.5(B) shows the details of the components shown in Figure 4.5(A) only. These are the P1 (component 3), pN1 (component 7), P2 (component 1), and P3 (component 6). The details of all components with a single peak latency between 70 and 350 ms appear in Figure S3 in Appendix C.

Figure 4.5(B) shows that the P1 and P2 were larger than those in the main experiment (cf. Figure 4.4 and 4.2). This may be due to the sharper edges of the gratings. Nevertheless, we did not find a component that was topographically and temporally consistent with DRN. This suggests that the use of Gabor patches was not responsible for the null result of the main experiment. Next, we consider what we learned from the main experiment.

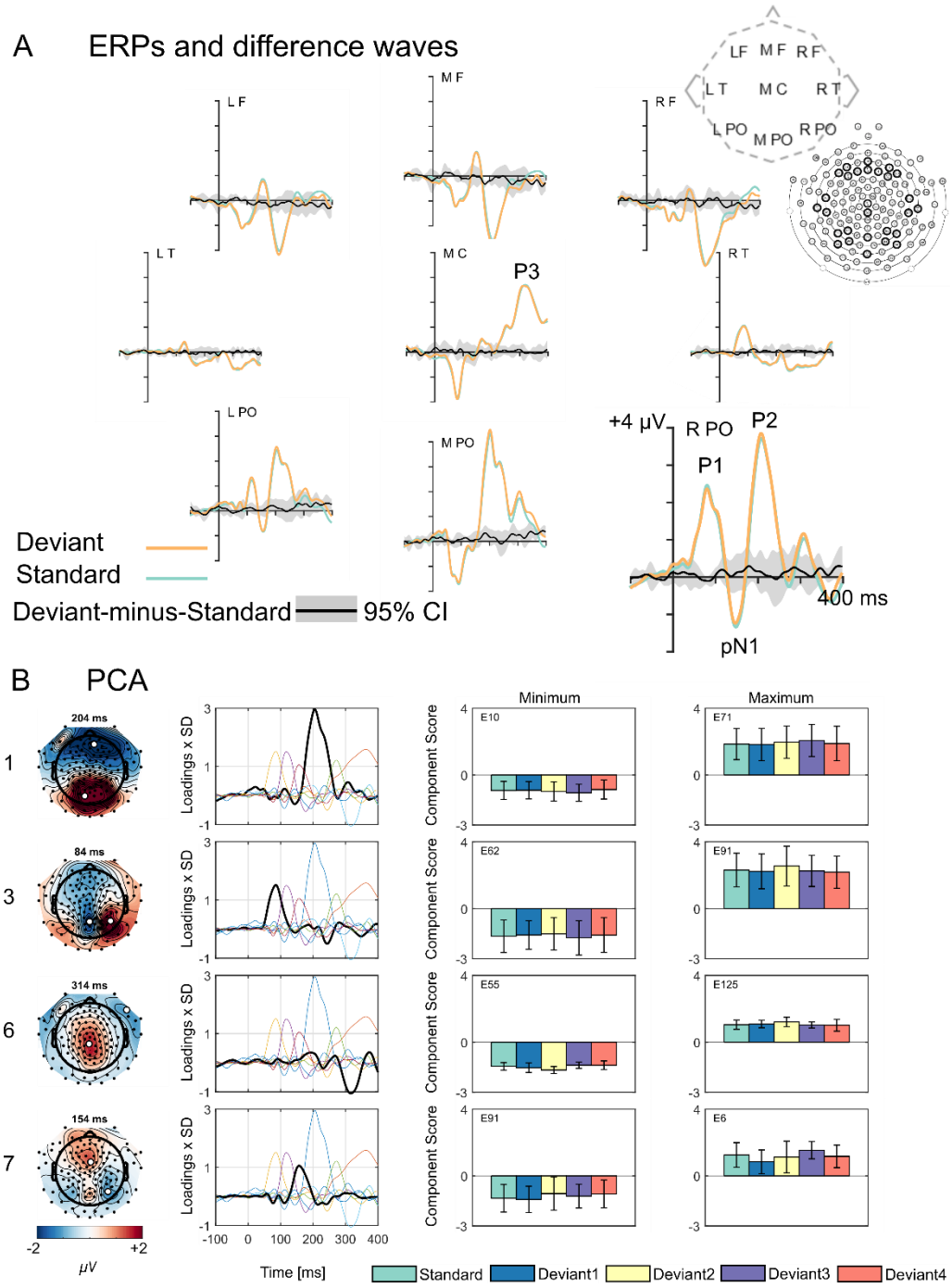


*Figure 4.5* Results from Experiment 1 follow-up ($N$ = 4). Stimuli are gratings. A. Grand average ERPs and deviant-minus-standard difference waves. One ERP for standards (green) and all deviants combined (orange) and one deviant-minus-standard (black) difference wave at the left (L), midline (M), and right (R) frontal (F) and parieto-occipital (PO) regions of interest (ROIs). We also show ERPs at M central (C) and L and R temporal (T) ROIs. The grey around each difference wave shows the 95% confidence interval (CI). Electrode clusters in each ROI are depicted by the black circles on the diagram of the 129-channel net. B. PCA results. From left to right, we show: the component number, topographical maps (combined activity from deviant and standard trials at peak latency), component loadings (a component's contribution as a thick black line to the overall evoked activity relative to all other components as thin lines of different colours), component score for minimum, and component score for maximum. The last two, the bar graphs, show means for each deviant and standard conditions, ±1 standard-error bars, and electrode numbers. We show the location of these electrodes on the topographical maps by white disks.

### 4.3.3 Discussion

We tested whether different magnitudes of rule-based orientation deviants produced different DRNs. We tested this with Gabor patches in the main experiment and gratings in a follow-up, but we did not find a DRN in either. This finding is surprising given the similarities between our experiment and the regularity condition in Kimura and Takeda (2015). We discuss the differences between these two experiments.

#### 4.3.3.1 Stimulus differences

One major difference between these two studies is the stimulus used. Kimura and Takeda (2015) showed their participants eight bars (each 3º×.4º of visual angle)—evenly separated at eight peripheral locations. The eccentricity of the furthermost bars end was 5.9º of visual angle. We showed participants a single large Gabor patch occupying approximately 22° of visual angle. Therefore, our Gabor patch stimuli (and their orientations) occupied similar peripheral locations to the bars in Kimura and Takeda. A further difference is that a second orientation appears at the right angle of each bar—at its ends. Therefore, predictions are likely to include predictions about both orientations.

In addition, our stimuli were coloured whereas Kimura and Takeda used achromatic stimuli. Perhaps the visual system prioritises colour categorization over encoding orientation regularity because colour categorization occurs at higher levels in the visual system, beyond the primary visual cortices (V1) (e.g., V4, Siok et al., 2009). This presupposes that the visual system cannot encode regularity in low-level feature dimensions such as orientation while participants

are engaged in colour categorizations. We are not aware of any evidence of this; therefore, we tested this in a subsequent experiment (Experiment 2).

#### 4.3.3.2 Task-related differences

Our participants attended to the colour of the stimulus of interest whereas Kimura and Takeda's participants attended to changes in a central fixation dot. Perhaps, in order to show a vMMN, attention must be away from the stimulus of interest altogether. Although this is not consistent with research showing that attention toward a visual deviant can facilitate a vMMN rather than inhibit it (e.g., Alho, Woods, Algazi, & Näätänen, 1992; Czigler & Csibra, 1990; Csibra & Czigler, 1991, 1992; Woods, Alho, & Algazi, 1992), we tested this notion in Experiment 2.

Another task-related difference is that target frequency in Kimura and Takeda was lower than ours. Perhaps our high target frequency was too taxing and this diminished the resources available for encoding a rotating regularity like ours. We also tested this in Experiment 2.

#### 4.3.3.3 SOA differences

Our SOA (800 ms) and ISI (680 ms) were longer than those used by Kimura and Takeda (500 ms and 250 ms respectively). We used a longer ISI to give participants enough time to respond to frequent targets. However, longer ISIs are thought to reduce vMMN amplitude (e.g., Astikainen et al., 2008; Fu et al., 2003) and deviants that appear among jittered, non-identical, standards (compared to identical standards) produce smaller MMNs (Daikhin & Ahissar, 2012). It seems that how we instantiate regularity affects the vMMN. Perhaps,

our ISI was too long and prevented participants from encoding the regularity needed for detecting irregularity. To confirm this, we reduced the ISI to that used by Kimura and Takeda in Experiment 2.

#### 4.3.3.4 Magnitudes of deviance differences

The magnitude of deviance in our experiment—our largest was 20° from predicted—is smaller than that of Kimura and Takeda's regularity condition—a 65.4° reversal of the rotation. In another rule-based orientation regularity study, Kimura's (2018) orientation difference was a 36° reversal from the predicted orientation. Perhaps, to show DRN to rule-based orientation deviants, a reversal is required, or the difference between predicted and shown orientations needs to be larger than we used, or both. Pattern reversals, unfortunately, would not have allowed us to test our hypothesis regarding adaptation-related and deviance-related contribution to DRN so, at the risk of being unable to discount this explanation for our findings, we maintained our orientation manipulation.

#### 4.3.3.5 Summary

Because we did not find DRN in any condition and Kimura and Takeda (2015) found a vMMN to similar rule-based orientation deviants, we must entertain the possibility that differences between our studies are the cause. To address this, we conducted Experiment 2. Its task and ISI were the same as those used by Kimura and Takeda.

## 4.4 Experiment 2

We conducted Experiment 2 to test whether aspects of Experiment 1 were preventing us from finding DRN to rule-based orientation deviants. We adopted

a fixation dot task, reduced the frequency of targets, and used shorter SOAs and ISIs. We maintained the orientation manipulation so that we might still show whether the magnitude of deviance, the magnitude of difference, or both, determine the size of DRN. We also included a post-test in which participants attended to the sequence regularity. The results of Experiment 2 would confirm whether colour, ISI, task, or target-related effects might have affected our results in Experiment 1. It turned out that none of these changes yielded a DRN.

### 4.4.1 Method

Some aspects of Experiment 2 were identical to those of Experiment 1. These were inclusion criteria for participants, EEG apparatus and data collection, the phase, spatial frequency, standard deviation of the Gaussian of our Gabor patches, our orientation manipulation, and our counterbalancing and randomisation. The differences were that all stimuli were black-to-white Gabor patches; thus colour (mean RGB of 128, 128, 128), luminance (42 cd/m$^2$), and contrast (.999) did not change across trials.

We used G*Power (Faul, Erdfelder, Lang, & Buchner, 2007; Faul, Erdfelder, Buchner, & Lang, 2009) to estimate the sample size needed to replicate the deviant-minus-control difference at PO8 in Kimura and Takeda's (2015) rotating oddball condition given a mean difference of −0.73 μV and a *SE* of .19 (*SD* = .89, *N* = 22). We needed 18 participants to achieve a statistical power of .95. We tested 20 new participants (9 males, 17 right-handed) with a mean age of 28 years and a range of 20 – 54, giving us a power of .97.

#### 4.4.1.1 Procedure

There were 14 blocks. We reduced the length of each trial to 450 ms and the ISI was 250 ms (same ISI as Kimura & Takeda, 2015). Each block contained 533 trials; 64 of these trials were deviants (16 per deviant). Each block took 4 minutes to complete. Participants were free to take breaks between blocks.

There were two sorts of blocks:

1. There were 12 experimental blocks of trials. In half of the blocks, the orientation of the Gabor patches changed in a clockwise direction. In the other half of the blocks, the orientation of the Gabor patches changed in an anti-clockwise direction. In the experimental blocks, Gabor patches were task-irrelevant. We asked participants to press a key whenever the (always-present) cyan fixation dot doubled in size (from .12° of visual angle to .24° of visual angle). These were the targets. There were 10 – 14 targets per block. We randomised target position in each block and block order afresh for each participant. We give an illustration of a target and non-target trial in Figure 4.6. We separated all deviants by at least three standards; Kimura and Takeda (2015) separated deviants by at least two standards. The length of a sequence in our experiment was between 4 and 30 trials and the mean number of trials in each sequence was eight.

2. There were two post-test blocks of trials at the end of the experiment. Gabor patch orientation changed in a clockwise direction in one

block and in the opposite direction in the other. We explained sequence regularity to each participant, giving them verbal examples for each kind of irregularity (i.e. deviant type) before they completed these blocks. We asked participants to respond to any instance of irregularity (i.e. a deviant) by pressing a key on a 4-key response box with the index finger of their dominant hand while fixating on the always-present cyan central fixation dot.

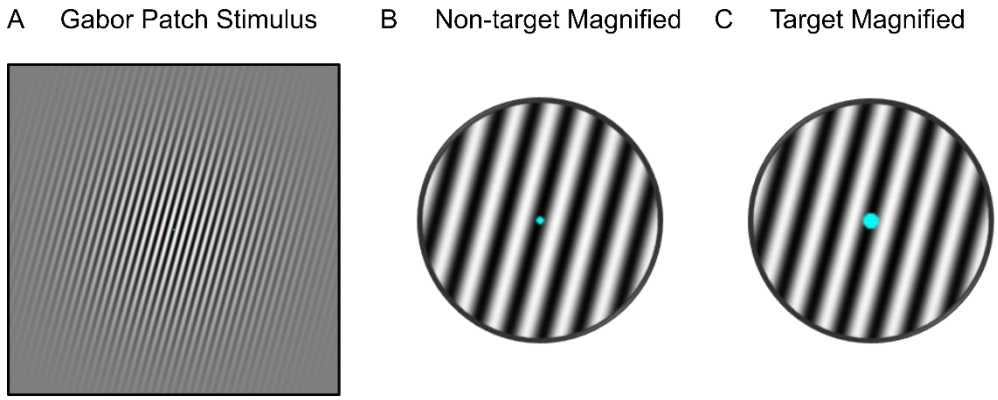


*Figure 4.6* Screenshots from the experiment of a 15° Gabor patch with a superimposed fixation dot. A. Complete Gabor patch stimulus. B. Non-target magnified. C. Target magnified. In the depicted fixation task, the dot doubles in size on target trials (C), requiring the participant to press a key.

#### 4.4.1.2 EEG recording and analysis

Most EEG-recording and EEG pre-processing steps were identical to Experiment 1 except that we reduced our epoch size to 400 ms with a 50 ms baseline to accommodate the shorter SOA (450 ms). The mean (*SD*) number of epochs for each ERP was 3655 (985) for Standards, 143 (38) for Deviant 1, 144 (41) for Deviant 2, 143 (41) for Deviant 3, and 145 (41) for Deviant 4. The shorter SOA allowed us to collect data from more trials. In our PCA of the ERP data, we retained 12 components according to Horn's (1965) parallel test, explaining more than 95% of the variance.

We also performed Bayes Factor[7] replication tests ($BF_{r0}$) (Verhagen & Wagenmakers, 2014) on the mean amplitudes between 270 and 280 ms at PO ROIs because this is the time-window in which Kimura and Takeda (2015) found the vMMN to regularity deviants. We also performed repeated-measures Bayesian analysis of variances (ANOVAs); Bayesian paired *t*-tests; traditional repeated-measures ANOVAs and paired *t*-tests. All *t*-tests are two-tailed unless explicitly stated and all Bayesian analyses are calculated using a medium prior (Cauchy prior whose width was set to 0.707).

### 4.4.2 Results

#### 4.4.2.1 Behavioural results

Mean (*SD*) hit rate and RT for detecting increases in the size of the fixation dot (from 20 participants) was 95% (4.8) and 491 ms (60), respectively. We applied a log-linear correction (Stanislaw & Todorov, 1999) to obtain a d′ for each deviant and participant in the post-test. The post-test results appear in Figure 4.7. No d′ exceeded 1 and all participants expressed how difficult they found the post-test blocks to complete. In fact, d′ was negative for four participants for Deviant 2 (D2) and Deviant 4 (D4). For Deviant 3 (D3), d′ was negative for five participants. All d′s were positive for Deviant 1 (D1). This is reflected in the effect of deviant type on accuracy, $F$ (3, 57) = 5.056, $p$ = .004,

[7] The model with the largest Bayes Factor ($BF_{10}$) is the *favoured model*. A $BF_{10}$ between 1 and 3 provides weak evidence in favour of the alternative hypothesis (and against the null hypothesis), a $BF_{10}$ between 3 and 10 provides moderate evidence, a $BF_{10}$ between 100 and 150 provides strong evidence, and a $BF_{10}$ of more than 150 provides very strong evidence (Raftery, 1995). Following Lee and Wagenmakers (2013), we took as substantial evidence for the *null* if $BF_{10}$ was between 0.33 and 0.1, and strong evidence if the $BF_{10}$ was less than 0.1.

$\eta^2$ = .210, $BF_{10}$ = 10.615, and the higher accuracy for D1 compared to D2 and D3, but not D4 (shown in Figure 4.7).

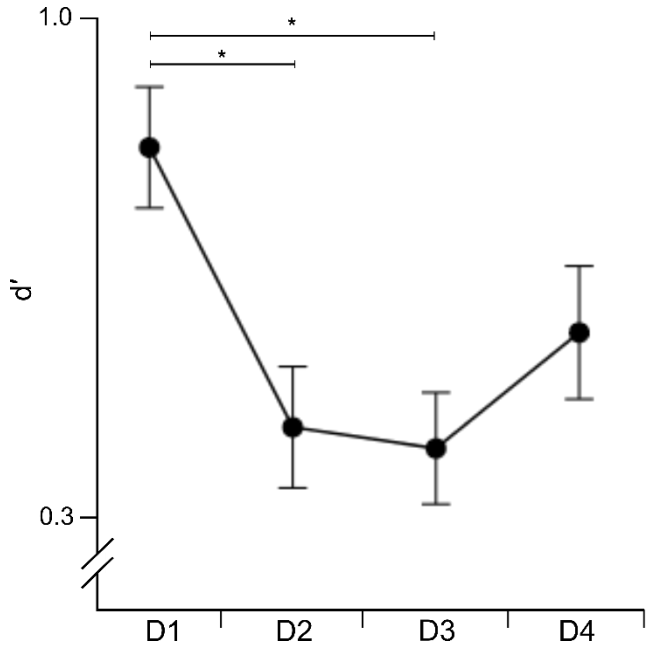


*Figure 4.7* Accuracy (d′) results from irregularity detection post-test blocks. Asterisks denote significant pairwise comparisons ($p < .05$). We corrected $p$ using the Bonferroni correction for multiple comparisons. Accuracy was better for Deviant 1 (D1) compared to Deviant 2 (D2), and Deviant 3 (D3), but not compared to Deviant 4 (D4). No other paired comparisons were significant.

#### 4.4.2.2 Event-related potentials (ERPs) and difference waves

Similar to Experiment 1, ERPs for the different deviants were similar for each deviant type, so we combined the ERPs from all four deviants to produce one ERP and one deviant-minus-standard difference wave. Figure 4.8(A) shows the ERPs for standards, deviants, and the deviant-minus-standard difference wave at each ROI. The ERPs in Experiment 2 are different from Experiment 1 (cf. Figure 4.3A and 4.8A). We label early ERP components at the R PO (enlarged for demonstrative purposes).

Figure 4.8(A) shows that the P1 is smaller than in Experiment 1. The negativity at the M PO from the combined negative dipoles of the left and right

P1 is also smaller than in Experiment 1 (cf. Figure 4.8A and 4.3A). This may be because attention to a stimulus amplifies early ERP components, like the P1 and N1 (Posner & Driver 1992, for a discussion on component amplification, see Hillyard et al., 1998). Our P2 and P3 components have all but disappeared. Contrast increments yield larger P2 amplitudes (Nyman et al., 1990) and the absence of clear P2 may be a consequence of having made all stimuli achromatic, thereby removing the luminance and contrast increments between ISI and Gabor patch stimuli. The reduced P3 is a result of having substantially fewer targets in Experiment 2 compared to Experiment 1. Despite all these differences in ERPs between studies, we did not observe negativity exceeding the 95% confidence intervals.

In Figure 4.8(B), we give details of the components illustrated in Figure 4.8(A) (for details of all components with a single peak latency between 70 and 350 ms, see Figure S4 in Appendix D). We did not find a component whose topography and temporal profile was typical of DRN.

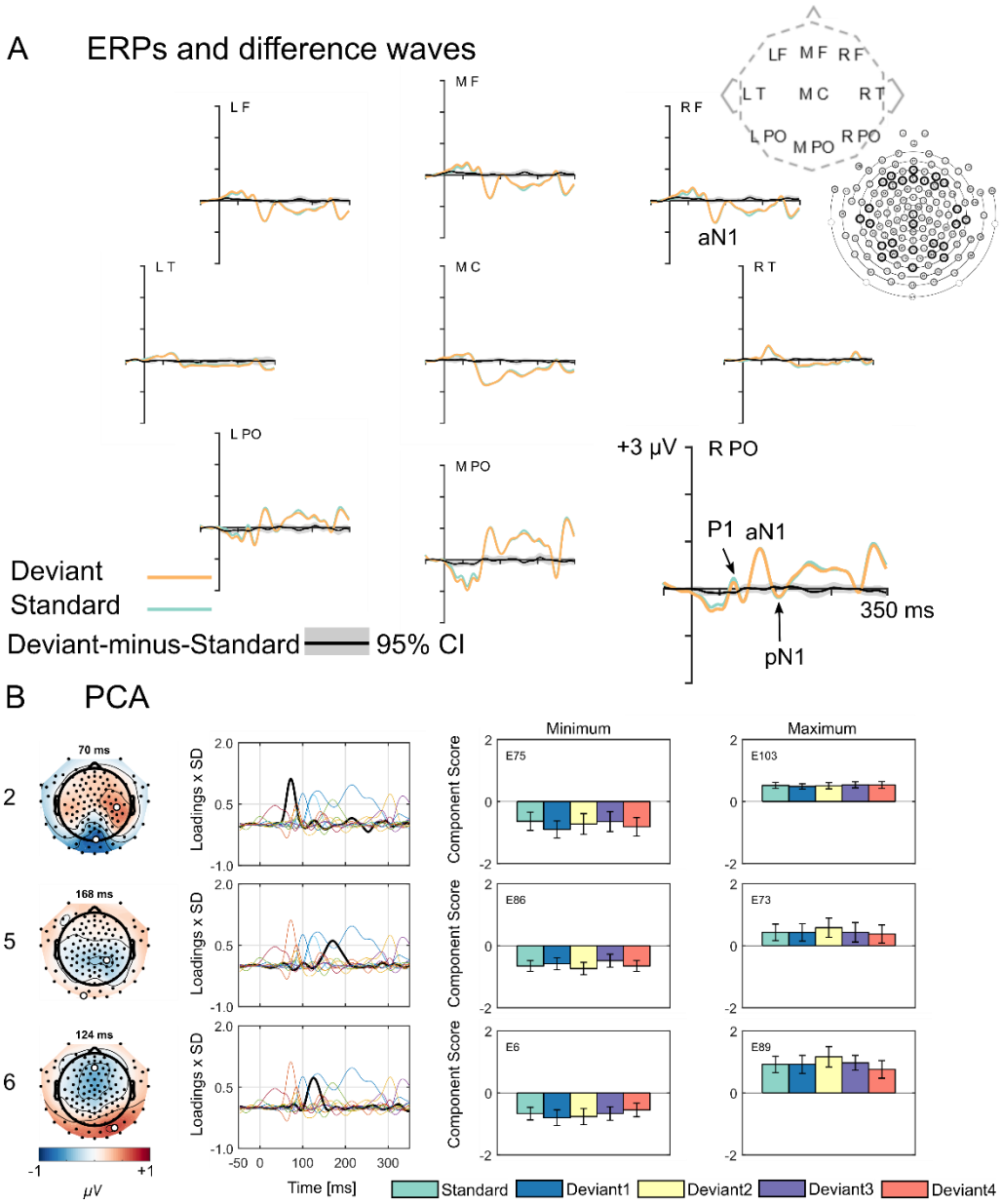


*Figure 4.8* Results from Experiment 2 (*N* = 20). Stimuli are Gabor patches. A. Grand average ERPs and deviant-minus-standard difference waves. One ERP for standards (green) and all deviants combined (orange) and one deviant-minus-standard (black) difference wave at the left (L), midline (M), and right (R) frontal (F) and parieto-occipital (PO) regions of interest (ROIs). We also show ERPs at M central (C) and L and R temporal (T) ROIs. The grey around each difference wave shows the 95% confidence interval (CI). Electrode clusters in each ROI are depicted by the black circles on the diagram of the 129-channel net. B. PCA results. From left to right, we show: the component number, topographical maps (combined activity from deviant and standard trials at peak latency), component loadings (a component's contribution as a thick black line to the overall evoked activity relative to all other components as thin lines of different colours), component score for minimum, and component score for maximum. The last two, the bar graphs, show means for each deviant and standard conditions, ±1 standard-error bars, and electrode numbers. We show the location of these electrodes on the topographical maps by white disks.

To be sure, we replicated the relevant *t*-tests reported by Kimura and Takeda (2015) given the mean amplitude difference of –.73 µV (*SE* = .19, t = –3.84) at PO8 in their regularity condition. We found no difference between all deviants (combined) and standard stimuli at the left and right PO ROIs, one-tailed; L PO: $t$ (19) = –0.256, $p$ = .400, $BF_{10}$ = 0.285, $BF_{r0}$ = 0.053; R PO: $t$ (19) = –0.064, $p$ = .475, $BF_{10}$ = 0244, $BF_{r0}$ = 0.038. Table 4.4 shows the results for each deviant versus the standard at the L PO and R PO ROIs. Our Bayes Factor tests provide strong evidence in favour of the null hypothesis (all $BF_{10}$ and $BF_{r0}$ < 1).

Table 4.4 *Directed Bayesian ($BF_{10}$ and $BF_{r0}$) t-tests (one-tailed) of the Difference in Mean Amplitude (µV) at Left and Right Parieto-occipital regions between 270 and 280 ms for Each Deviant compared with the Standard (df = 19)*

| | L PO | | | | | R PO | | | | |
|---|---|---|---|---|---|---|---|---|---|---|
| | **µV** | ***t*** | ***p*** | $BF_{10}$ | $BF_{r0}$ | **µV** | ***t*** | ***p*** | $BF_{10}$ | $BF_{r0}$ |
| Deviant 1 | 0.01 | 0.080 | .531 | 0.219 | 0.030 | –0.08 | –0.927 | .183 | 0.547 | 0.203 |
| Deviant 2 | –0.08 | –0.589 | .282 | 0.385 | 0.101 | 0.09 | 0.655 | .740 | 0.152 | 0.013 |
| Deviant 3 | 0.01 | 0.132 | .552 | 0.211 | 0.028 | 0.01 | 0.127 | .550 | 0.212 | 0.028 |
| Deviant 4 | 0.01 | 0.100 | .539 | 0.216 | 0.029 | –0.03 | –0.346 | .367 | 0.303 | 0.063 |

*Note*. L PO = left parieto–occipital region of interest. R PO = right parieto–occipital region of interest.

PCA confirmed smaller amplitudes for early components as compared with Experiment 1. Figure 4.8(B) shows that the P1 (component 2) has a peak latency of 70 ms and this is similar to Experiment 1 (76 ms, component 4, Figure 4.3B). The positive pole of the aN1 (component 6) appeared to be larger (i.e., more positive) for Deviant 2 compared to the standard; however, this difference was not statistically significant according to our frequentist test and our Bayesian

test was very weak, $t$ (19) = 1.929, $p$ = .069, $BF_{10}$ = 1.085. Therefore, we did not find any conclusive evidence for deviant-related differences.

### 4.4.3 Discussion

We conducted Experiment 2 to explore whether colour, ISI, or target frequency contributed our findings in Experiment 1: no DRN to any rule-based orientation deviant. We removed colour and modified the SOA and task to be comparable to that of Kimura and Takeda (2015) because they found a vMMN where the relationship between standards was similar to the relationship between standards in the present study. Nevertheless, we did not find DRN for any deviant. In fact, we did not find any conclusive evidence for a deviance-related difference in any component. We can, therefore, conclude that parameters in Experiment 1 were not responsible for the difference in our findings and those reported by Kimura and Takeda. We consider what might be responsible next.

## 4.5 General Discussion

We did not find DRN in either Experiment, despite making Experiment 2 more similar to the regularity condition in a study that did find a vMMN to rule-based orientation deviants (Kimura & Takeda, 2015). Our achieved power (.97) and our Bayesian replication tests provide strong evidence that we would not have been able to find DRN in Experiment 2. We consider what remaining differences between the studies could be preventing us from showing DRN and why.

### 4.5.1 Detecting violations and magnitudes of deviance

It is possible that our largest magnitude of deviance was not larger enough to evoke DRN. Although Kimura and Takeda (2014) found DRN to 22° orientation changes, perhaps the orientation change in the present study was too small because an abstract rule governed the relationship between stimuli and a much larger change is needed in such instances.

Our participants found it extremely difficult to detect the deviants in our post-test in Experiment 2. Moreover, all rule-based orientation deviants that have evoked a vMMN have been, exclusively, pattern reversals. Perhaps then, for DRN to occur, an appreciable violation, such as a pattern reversal, is required. This is explanation 1.

Although attention towards, or even conscious appreciation of, irregularity is *not* necessary for the vMMN to occur (Bubic et al., 2010; Czigler & Pató, 2009; Müller et al., 2010, 2013), perhaps a violation must be discriminable when attention is on it for the violation to be able to evoke a mismatch response when attention is elsewhere. There is evidence to suggest that discriminability affects the size of the (v)MMN (Horváth et al. 2008; Winkler, Reinikainen, & Näätänen, 1993; Woods, 1990). For example, Horváth et al. (2008) argued that the combination of trials that evoke the MMN with those that do not is what yields the supposed magnitude of deviance effect when the deviant is near the discrimination threshold. That is when the deviant is near threshold, only some trials evoke the MMN, but as the detection ratio increases, more trials evoke the MMN. The implication is that some deviants do not evoke the MMN because they are not perceived as different from standards (i.e., do not exceed the

discrimination threshold). Therefore, although a discriminable change will evoke a mismatch response (Garrido et al., 2009), it is unknown whether the same can be said for deviants that are not easily distinguished from standards.

Another possibility is that the regularity needed for detecting irregularity was not encoded and therefore a DRN was not possible. This is explanation 2. It is not clear from our post-test results whether participants found the task so difficult because they did not detect the regularity necessary for this or because they did detect some regularity, but they did not perceive violations (explanation 1). However, the orientation difference between regular stimuli in our study (i.e., 30°) is very similar to what Kimura and Takeda (2015) used in their regularity condition (i.e., 32.7°). Therefore, it is not likely that the orientation difference in this study is what might have affected the ease with which regularity was encoded. For this, we address the remaining difference between the two studies: the stimuli used.

### 4.5.2 Encoding regularity and stimuli

To date, all rule-based orientation studies that have found a vMMN showed participants grey bar stimuli on a black background. Possibly a rotating regularity is more obvious (and more easily encoded) when bars are used in place of Gabor patches (explanation 2). It may also be easier, then, to detect regularity violations regardless of how big the violation is (explanation 1). It would be useful to compare bar and Gabor patch stimuli in a rule-based orientation deviant paradigm to delineate this. Alternatively, including a measure of appreciable regularity and irregularity would help to explore whether DRN did not occur

because participants did not encode the regularity needed for detecting deviants or because they did detect regularity but did not detect the deviants.

### 4.5.3 Alternative explanation

Alternatively, perhaps orientation deviants (rule-based or otherwise) do not yield a vMMN. This is explanation 3. A growing number of studies show that feature deviants, like orientation, do not yield a vMMN (Sulykos, Kecskés-Kovács, & Czigler, 2013; File et al., 2017; Male et al., 2018). After having found that 15°, 30°, or 60° orientation deviants did not yield a vMMN in a traditional oddball paradigm in Chapter 3, we argued that perhaps well-controlled orientation deviants do not yield a vMMN. We have tested this in the present study using rule-based deviants and our findings could favour the argument that well-controlled rule-based orientation deviants do not yield a vMMN either. However, in light of previous findings and our post-test results, it would be premature to suggest that rule-based orientation deviants do not yield a vMMN or DRN. For this, further research is essential. Instead, it is more likely that our findings show that some degree of appreciable irregularity (at least) is essential for showing DRN.

## 4.6 Conclusion

We found that rule-based orientation deviants do not produce DRN. This may be because a large violation is required to yield DRN or because appreciable regularity is also required for successful deviance detection. It is clear further research is essential given the inconsistencies in rule-based orientation deviance research outlined.

# CHAPTER 5

## DOES THE BRAIN PROCESS UNEXPECTED CHANGES IN ORIENTATION AND CONTRAST DIFFERENTLY?

Based on the following manuscript in preparation

Male, A. G., Roeber, U., & O'Shea, R. P. (2019). Does the brain process unexpected changes in orientation and contrast differently?

# 5. DOES THE BRAIN PROCESS UNEXPECTED CHANGES IN ORIENTATION AND CONTRAST DIFFERENTLY?

## 5.1 Preface

In this Chapter, I investigate whether the brain processes unexpected changes in orientation or contrast differently, given that a change in orientation may represent a greater threat than a change in contrast, evolutionarily speaking. I also manipulate the visual field in which the change occurs, showing stimuli to the central (CVF) or lower visual field (LVF), to investigate whether this type of manipulation affects deviance processing.

It was essential for my hypotheses to manipulate basic properties of visual input. The chosen visual properties also reflect my desire to ascertain whether orientation changes do evoke the vMMN, given that I am yet to find the vMMN or DRN, and my desire to test this against a not-so-established change that should, theoretically, evoke a vMMN. The questions motivating this research are derivatives of my original and revised thesis:

I. Do changes in contrast or orientation produce a vMMN?

II. Does the vMMN to orientation and contrast changes differ?

III. Does manipulating visual field presentation affect how the visual system processes contrast and orientation changes?

## 5.2 Introduction

Imagine one of our evolutionary ancestors moving through open forest on a windy day, looking for fruit. Its visual system and possibly attention are occupied primarily by the search for fruit of a certain shape and colour. Nevertheless, its visual system must remain attuned to the properties of the background, including the orientation of grasses and reeds, and the leaves, stems, and branches of trees that are constantly changing in the wind. Our ancestor needs to be able to detect alterations of those properties, such as a systematic change of the orientation of stems in one part of its visual field that might warn, for example, of the movements of a dangerous predator. It is likely that our ancestor's brain had separate processes for finding food and for monitoring the visual scene for changes. It is the latter we are interested in.

Predictive models of sensory processing are integral to how the brain processes changes in the visual scene (Friston, 2003; Rao, 1999; Rao & Ballard, 1997). The first important feature of such models is that the brain uses them to predict future sensory input. Supposedly, the brain does this, because that which is predictable requires little additional processing or processes like attention. The second feature is that the brain compares incoming input with that which the brain decides is predictable based on these models. If the incoming input is congruent with the predicted input, the brain maintains the model, but if the incoming input is incongruent with the predicted input, a prediction error occurs and the brain updates the model.

We are interested in how the brain processes different kinds of change in the visual scene. Specifically, we are interested in whether larger error signals occur in the brain if one kind of change is more important for survival than another kind of change. One of the most frequently cited arguments for prediction error is that it facilitates the constant need to adapt to one's ever-changing environment (e.g., Berti, Roeber, & Schröger, 2004; Berti & Schröger, 2001; He, Hu, Pakarinen, Li, & Zhou, 2014; Stagg, Hindley, Tales, & Butler, 2004). The truism is often accompanied by a reference to survival or biological threat (e.g., Astikainen, Lillstrang, & Ruusuvirta, 2008; Bubic, von Cramon, Jacobsen, Schröger, & Schubotz, 2009; Grimm, Bendixen, Deouell, & Schröger, 2009; Kovarski et al., 2017; Kreegipuu, Raidvee, Näätänen, & Allik, 2013; Qian et al., 2014; Tugin, Hernandez-Pavon, Ilmoniemi, & Nikulin, 2016). However, to our knowledge, no one has explored the possibility that differences in the magnitude of prediction error are based on how biologically important the change is. We rectify this in the present study by comparing prediction errors to orientation changes—the more important change, with contrast changes—the less important change.

Näätänen, Gaillard, and Mäntysalo (1978) discovered a neural correlate of prediction error. They found that, even though participants were not attending to the tones, event-related potentials (ERPs) from rare, different, unpredicted, *deviant*, tones produced a more negative voltage (i.e., negativity) than ERPs from a series of identical, *standard*, tones; this is the mismatch negativity (MMN). To show the MMN, Näätänen et al. (1978) produced difference waves

by subtracting the ERP to frequent standard tones from the ERP to infrequent deviant tones.

These techniques have revealed analogues of the MMN in other sensory modalities, including vision (Czigler & Csibra, 1990). The visual analogue of the MMN is the visual MMN (i.e., vMMN) and occurs when a deviant visual input is detected, such as a change in colour (Czigler, Balázs, & Winkler, 2002) or orientation (Astikainen et al., 2008; Astikainen, Ruusuvirta, Wikgren, & Korhonen, 2004; Czigler, Balázs, & Winkler, 2002; Czigler & Csibra, 1990; Farkas, Stefanics, Marosi, & Csukly, 2015; Kimura, Katayama, Ohira,O & Schröger, 2009; Kimura & Takeda, 2015). This makes the vMMN ideal for investigating different types of change in the visual scene.

Supposedly, the vMMN does not require attention to, or even consciousness of, deviance to occur (Czigler, Weisz, & Winkler, 2006). Intuitively, this makes sense. Returning to our earlier example, our ancestor's brain must have had a means for detecting changes in the orientation of stems that could predict danger, even when occupied by foraging. The vMMN is clearly an excellent candidate for a prediction error in vision (Stefanics, Kremláček, & Czigler, 2014).

One important unanswered question is whether some deviants yield larger prediction errors (i.e., vMMNs) than others. A second important question is why this could be the case.

### 5.2.1 Do different deviants produce different vMMNs?

We propose two reasons that one change might yield a larger prediction error than another. One reason is that the appreciable difference between the standard and deviant in one case (e.g., an orientation difference) is larger than the appreciable difference between the standard and deviant in another case (e.g., a contrast difference). For example, Takács et al. (2013) showed, using the oblique effect, that an orientation difference that is *perceived* as larger can yield larger, more sustained vMMNs, even when the size of the orientation difference is identical. Evidently, units of a difference do not necessarily correspond to perceived difference and the relationship between units of difference is not necessarily linear (Stevens, 1975). Instead, an exponential rule usually governs the relationship (Stevens, 1975). This is why estimation of perceived differences is necessary to conclude whether differences arise because of dissimilarity in appreciable differences or because of some other aspect. We used a form of magnitude estimation in the present study to control for this.

The second reason one change might yield a larger prediction error than another is that the size of prediction error corresponds to biological importance. A larger prediction error may be more likely to trigger later processes, such as reorienting attention. Attention toward a change is often a necessary precursor for adapting behaviour and attention capture was one of the originally proposed purposes for the MMN (Schröger, 1996).

Only a handful of studies have tested different deviants in the same participants (e.g., Grimm et al., 2009; He et al., 2014; Kreegipuu et al., 2013;

Qian et al., 2014; Shi, Wu, Sun, Dang, & Zhao, 2013; Sulykos, & Czigler, 2011). In one study, Qian et al. (2014) manipulated five dimensions of visual input and found the largest vMMN for orientation deviants compared to colour, duration, shape, and size. Sulykos and Czigler (2011) also reported a larger vMMN for orientation deviants compared with the vMMN for spatial-frequency deviants. Unfortunately, these studies did not control for adaptation. This is problematic where the deviant is physically different from the standard—as is the case in these studies—as a deviant yields a larger response from unadapted neurons, compared to the smaller response from adapted neurons for the repeated standard.

One method for separating out adaptation-related differences to leave only difference owing to deviance detection is the equiprobable control (s.2.2. in Ch. 2, Schröger & Wolff, 1996). Grimm et al. (2009) compared three different deviant types with equiprobable controls and found that location deviants produced the largest vMMN, followed by colour, then shape. Possibly, a change in location is more important than a change in colour or shape, because the location change almost certainly signals that something in the visual scene has moved. We propose differences in the size of the vMMN for orientation and contrast deviants in this study based on this axiom.

### 5.2.2 The present study

There is some evidence to suggest that orientation deviants yield larger vMMNs than other deviant features. We used orientation deviants in the present study to test this. We also used contrast deviants. Contrast is another low-level

feature of visual input that is potentially associated with a lower level of threat than orientation. Furthermore, only two studies have investigated contrast deviance. Nyman et al. (1990) found no vMMN to deviants with a lower Michelson contrast (.24) than the standard (.72). Wei, Chan, and Luo (2002) found a vMMN for deviants whose contrast was greater than that of the standard. However, Wei et al. (2002) did not control for adaptation; therefore, it is still unclear whether contrast deviants evoke a vMMN when controlling for adaptation. We have the opportunity to test this.

We propose that, if the size of prediction error reflects biological importance, orientation deviants will produce larger vMMNs compared to contrast deviants. This is because changes in orientation signal greater threat, such as movement or the presence of a novel element within the visual scene, such as a predator or the edge of a cliff, whereas contrast changes signal a change in the clarity of something that is already present in the environment. Such changes could be due to a cloud-cast shadow, fog, or smoke.

To demarcate whether local context of a change might have affected the level of perceived threat of orientation and contrast changes differently for our foraging ancestors, we compared changes in the lower visual field (LVF) and central visual field (CVF). We expected a bigger vMMN for change in the LVF compared to the CVF, because the former is more likely to represent a change in the near distance (i.e., in front of our feet). In the case of orientation, it might be from the movement of a snake or of the terrain. In the case of contrast, it might

be from fog starting to cover the ground. Both kinds of deviants give earlier warning of hazards when we are walking than central vision.

Deviants appearing in the LVF tend to produce bigger vMMNs compared with deviants appearing in the upper visual field (UVF) (Czigler, Balázs, & Pato, 2004; Sulykos, & Czigler, 2011). There are also reasons other than ours to expect an advantage for the LVF. For example, Masland (2017) found that the cones in the peripheral part of the monkey retina respond 30 ms faster than cones in central vision. Moreover, so-called transient retinal ganglion cells, which have large receptive fields and preferentially respond to changes, disproportionately exist in the peripheral parts of the retina (e.g., Nelson, 2007). We aim to confirm whether the vMMN revealed by the differences between ERPs are larger in the LVF compared to CVF. This is not to be confused with the size of ERP amplitudes, as these will be smaller for peripherally presented stimuli compared to centrally presented stimuli due to more area in the visual cortices dedicated to processing foveal, compared to peripheral, information (Talbot & Marshall, 1941).

In sum, we compared orientation and contrast changes, after equating appreciable differences for each, and the same change in the LVF and CVF. Nevertheless, we did not observe a vMMN in any condition for either visual feature, despite increasing the number of participants to increase our statistical power to .99.

## 5.3 Method

### 5.3.1 Participants

According to our calculation using G*Power (Faul, Erdfelder, Lang, & Buchner, 2007; Faul, Erdfelder, Buchner, & Lang, 2009), we needed at least 14 participants to replicate the orientation vMMN reported by Kimura and Takeda (2015) in their oddball condition at PO8 (–1.16 μV, *SE* = .34, *SD* = 1.59) to achieve a power of .8. We chose Kimura and Takeda (2015) for the similarities in orientation deviance (details below) across studies.

We tested sixteen self-declared neurologically healthy participants (6 males, 15 right-handed) with normal or corrected-to-normal vision, increasing the power of our study to .87. Participants volunteered in return for course credit or the chance to win a $50 AUD voucher. We excluded two additional datasets from further analysis due to excessive noise in the data and insufficient trials in one or more conditions. Mean age was 31.7 years with a range 18 – 48. The Murdoch University ethics committee approved the study (ethics permit 2015 208).

### 5.3.2 Apparatus

Participants sat in a light-attenuated chamber facing a photometrically calibrated, 17-inch, colour, CRT monitor (Sony Trinitron Multiscan E230). The monitor showed 1280×1024 pixels at 100 Hz refresh rate. All other apparatus details were identical to Chapter 3 (s. 3.3.2).

### 5.3.3 Stimuli

Our Gabor patches had a spatial frequency of 1.6 cycles per degree (cpd), a phase of one-quarter of a cycle (the centre of a white bar appeared in the centre of the screen), and a standard deviation of the Gaussian of 1° of visual angle. The visible part of the Gabor patch was approximately 4°. The Gabor patch edge was .5° from the centre of the fixation cross in the LVF condition.

To ensure equal perceptual differences between orientation and contrast stimuli we conducted a study pilot using categorical magnitude estimation (Anderson, 1972; Stevens, 1975). Categorical magnitude estimation is similar to magnitude estimation in most respects, except that the values assigned to stimulus intensity are limited as opposed to unrestricted as is the case in magnitude estimation (Stevens, 1975). Exponents and constants from the pilot data allowed us to choose values of our orientation and contrast stimuli (for details of the pilot see Appendix E). We adopted three additional constraints in designing our experimental stimuli. These were:

1. The difference between the standard and deviant orientation stimuli should be at least 33° because others have found a vMMN with orientation differences of 32.7° (Kimura & Takeda, 2015).
2. The deviant's contrast should be less than the standard's contrast to control for any adaptation-related differences—a lower contrast will not excite any unadapted neurons. This is also what Nyman et al. (1990) did in their study.

3. The contrast of all orientation stimuli should be equal to that of the deviant contrast stimulus.

To achieve a difference in Michelson contrast that was equal to that of a 33° orientation difference in our contrast blocks, the contrast of our standard was .846 and the contrast of our deviant was .393. The remaining Michelson contrast values for the equiprobable control were .242, .544, .695, and .997. For orientation blocks, the Michelson contrast of the Gabor patch was always .393. The orientation of the standard and deviant was 128° and 95°. These alternated in different blocks. The remaining orientation values were 84°, 106°, 117°, and 139°.

There was a white central fixation cross. The length of each bar of the fixation cross was .60° of visual angle; the width was .03° of visual angle. On target trials, the vertical bar of the cross grew in length (.60°×.66° of visual angle).

### 5.3.4 Procedure

Each block ($n$ = 12) contained 480 trials and took 2.4 minutes to complete; each trial lasted for 500 ms and the inter-stimulus-interval (ISI) was 400 ms. Participants were free to take breaks between blocks.

There were four oddball blocks per feature each containing 80 deviant trials (17%). The standard and deviant orientations reversed roles in half of the orientation oddball blocks; the standard and deviant contrasts did not. We randomised the position of the deviant provided at least four standards separated

each deviant. In equiprobable blocks (two per feature), all six values for a given feature appeared pseudo-randomly (i.e., repetitions not possible). In half of the blocks, all stimuli appeared in the CVF. In the other half, all stimuli appeared in the LVF. We randomised block order afresh for each participant.

We asked participants to fixate on the always-present white fixation cross. Fixation-cross changes lasted 120 ms and onset was not synchronised with Gabor patch onset and offset. A response was correct when it occurred between 150 and 1000 ms after target onset.

### 5.3.5 EEG recording and analysis

All EEG recording and analyses were identical to Experiment 1 in Chapter 4 (s. 4.7.1.5).

We averaged ERPs separately for the standard, deviant, and control stimuli in CVF and LVF before subtracting ERPs to controls and ERPs to standards from ERPs to deviants to produce two difference waves for each visual field and feature. Traditionally, the deviant-minus-standard difference wave reveals enhanced negativity due to a break from adaptation and prediction error (e.g., DRN), whereas the deviant-minus-control difference wave reveals prediction error only (e.g., vMMN). However, because the contrast deviant is always a contrast decrement and a lower contrast stimulus does not excite different neurons, there are no adaptation-related differences to control for and DRN in the deviant-minus-standard difference wave for contrast deviants could also represent a vMMN.

We show the mean number (*SD*) of epochs of each ERP in Table 5.1. We obtained twice the number of controls for orientation compared to contrast stimuli because both versions of the orientation deviant appeared with equal probability among four other orientations. Both versions of the deviant are included in the control ERP.

Table 5.1 *Mean Number (Standard Deviation) of Epochs per Participant in the Grand Average ERP for Standards, Deviants, and Controls (N = 16)*

| Condition | Standard | Deviant | Control |
|---|---|---|---|
| Orientation-CVF | 477 (101) | 120 (27) | 121 (30) |
| Orientation-LVF | 498 (87) | 124 (24) | 127 (20) |
| Contrast-CVF | 502 (103) | 125 (27) | 66 (10) |
| Contrast-LVF | 508 (71) | 125 (18) | 63 (11) |

Figure 5.1 shows the electrodes in each region (these are identical to Ch. 3 and Ch. 4). We compared difference wave amplitudes with point-by-point *t-test*s using the Mass Univariate ERP Toolbox (Groppe, Urbach, & Kutas, 2011). Significance criterion was five consecutive significant time points (totalling 10 ms) 150–300 ms after stimulus onset.

We conducted PCA for each feature and visual field separately, allowing for topographical differences in PCA components owing to the visual field manipulation. All PCA parameters were identical to Chapter 3 (s. 3.3.5). For each orientation PCA, we included deviant and control trials only. For each contrast PCA, we included standards, deviants, and controls. A vMMN component would be characterised by a negative deviant-minus-control difference score for orientation conditions or a negative deviant-minus-standard

difference score for contrast conditions at the component's minimum (typically PO regions) and would be largest between 150 and 300 ms.

We retained 14 principal components according to Horn's (1965) parallel test, explaining more than 95% of the variance, in all four conditions except for the contrast-LVF condition. Here, we retained 17 principal components. We extracted microvolt-scaled component scores from our components of interest for statistical comparisons. We submitted these scores to traditional analysis of variance (ANOVA) and paired *t*-tests as well as Bayesian ANOVAs and paired *t*-tests, using a medium prior (i.e., Cauchy prior whose width was set to 0.707). All paired tests are two-tailed. We report significant results for ERP and PCA results only, applying the Greenhouse-Geisser correction (ε) where necessary. Eta squared ($\eta^2$) denotes the estimated effect size.

## 5.4 Results

### 5.4.1 Behavioural results

Table 5.2 shows mean (*SD*) hit rates and reaction times (correct responses only) for detecting increases in the size of the fixation cross for each condition. A 2×2×2 ANOVA with feature (orientation vs. contrast), visual field (CVF vs. LVF), and block type (oddball vs. control) revealed participants performed better during LVF conditions (80.7% ±15.5%, 472.9 ±87.4 ms) compared to CVF conditions (70.9% ±17.3%, 521.5 ±78.2 ms), perhaps because stimuli appearing behind the fixation cross made fixation cross changes more difficult to see. The model with the highest $BF_{10}$ (the favoured model) was the model containing only

the main effect of visual field for hit rate, $F$ (1, 15) = 8.933, $p$ = .009, $\eta^2$ = .373, $BF_{10}$ = 489.680, and reaction time, $F$ (1, 15) = 13.426, $p$ = .002, $\eta^2$ = .472, $BF_{10}$ = 40800.105, and there was strong evidence against including all other factors (all $BF_{Incl} < 0.2$).[8] All other effects and interactions were non-significant (see Appendix F, Table S2 for details of the full ANOVAs).

Table 5.2 *Mean (Standard Deviation) Hit Rate (%) and Reaction Time (ms) for each Block Type and Condition (df = 15)*

| Condition | Oddball | Equiprobable |
|---|---|---|
| Hit Rate (%) | | |
| Orientation-CVF | 67.5 (20.4) | 72.1 (16.6) |
| Orientation-LVF | 80.6 (14.5) | 82.2 (16.0) |
| Contrast-CVF | 71.4 (16.8) | 72.5 (15.5) |
| Contrast-LVF | 78.3 (14.3) | 81.5 (17.4) |
| Reaction Time (ms) | | |
| Orientation-CVF | 526.4 (86.2) | 519.9 (76.9) |
| Orientation-LVF | 479.4 (86.4) | 471.5 (90.0) |
| Contrast-CVF | 531.8 (76.8) | 508.0 (73.0) |
| Contrast-LVF | 470.6 (83.6) | 470.3 (89.6) |

### 5.4.2 Event-related potentials (ERPs) and differences waves

#### 5.4.2.1 Orientation ERPs

Figure 5.1 shows the ERPs for the standard (green), deviant (orange), and control (purple) orientation stimuli in the CVF (A) and LVF (B) conditions. We

[8] The model with the largest Bayes Factor ($BF_{10}$) is the *favoured model*. The main effects and interactions within such a model are important for explaining the data. The data provide moderate evidence for the alternative hypothesis (and against the null hypothesis) if $BF_{10}$ was larger than 3 or strong evidence if $BF_{10}$ was larger than 10 (Lee & Wagenmakers, 2013). $BF_{10}$ between 1 and 3 provide weak evidence (Raftery, 1961). The inclusion Bayes Factor ($BF_{Incl.}$) is the extent to which the data support inclusion of the factor of interest. The $BF_{Incl.}$ compares the posterior probability of matched models including vs. excluding the effect or interaction. $BF_{Incl}$ larger than 1 provides moderate evidence for including the factor of interest.

illustrate the canonical ERP components at the enlarged right parieto-occipital (R PO) plot in the orientation-CVF condition (Figure 5.1A). We also show the anterior N1 (aN1) here as well as its reversed polarity (i.e., the negative pole) at the right frontal (R F) ROI (Figure 5.1A). The smaller ERP components in the LVF condition (Figure 5.1B) reflects less cortical activity for peripherally presented stimuli (Talbot & Marshall, 1941).

#### 5.4.2.2 Contrast ERPs

Figure 5.2 shows the ERPs for the standard (green), deviant (orange), and control (purple) contrast stimuli in the CVF (A) and LVF (B) conditions. Again, we show the P1, aN1, pN1, and P2 at the enlarged R PO plot in the CVF condition (Figure 5.2A) as well as the aN1 at the R F ROI. The P2 is the largest component in both CVF (~1.5 μV) and LVF (~0.8 μV) conditions (Figure 5.2A and B, respectively). Comparing CVF conditions across features (cf. Figure 5.1A and 5.2A), the P2 amplitude for contrast standards is at least 50% bigger than the P2 for orientation standards (~1 μV). This undoubtedly reflects the higher Michelson contrast of the standard stimuli in the contrast condition compared to all other stimuli.

Figure 5.3 shows the deviant-minus-standard and deviant-minus-control difference waves for each condition. For each orientation difference wave in the CVF and LVF conditions (Figure 5.3A and C), point-by-point *t*-tests revealed amplitudes were not significantly different from zero in our time-window of interest (150–300 ms) for at least 10 ms. For the contrast-CVF condition (Figure 5.3B), point-by-point *t*-tests revealed that the increased negativity and positivity

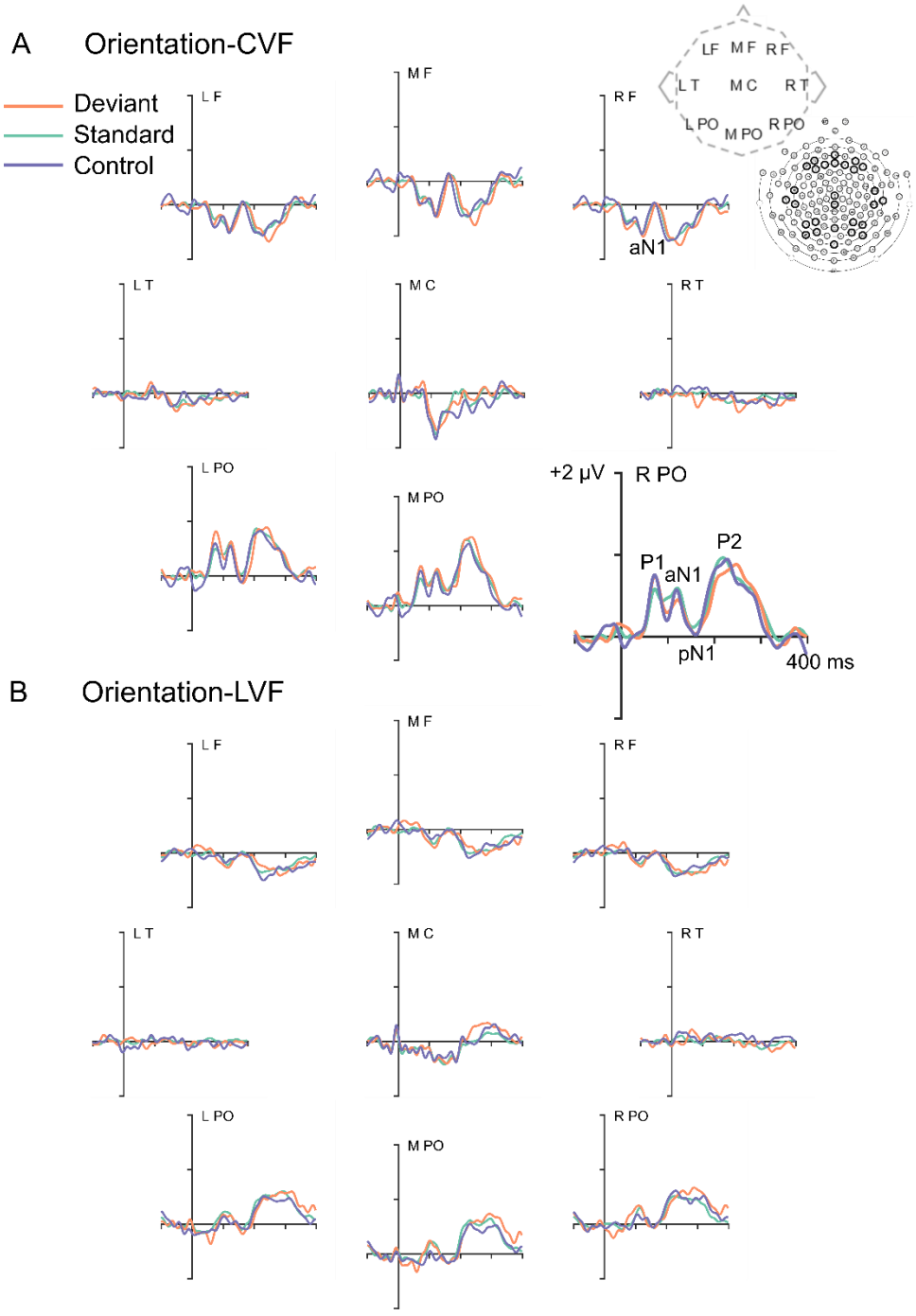


*Figure 5.1* Grand average ERPs for orientation stimuli. A. ERPs from the central visual field (CVF) condition. B. ERPs from the lower visual field (LVF). We show ERPs for standard (green), deviant (orange), and control (purple) trials at the left (L), midline (M), and right (R) frontal (F) and parieto-occipital (PO) regions of interest (ROIs). We also show ERPs at M central (C) and L and R temporal (T) ROIs. Electrode clusters within each region are depicted by the black circles on the diagram of the 129-channel net.

in the PO and F regions (respectively) were significant for the deviant-minus-standard difference wave only.

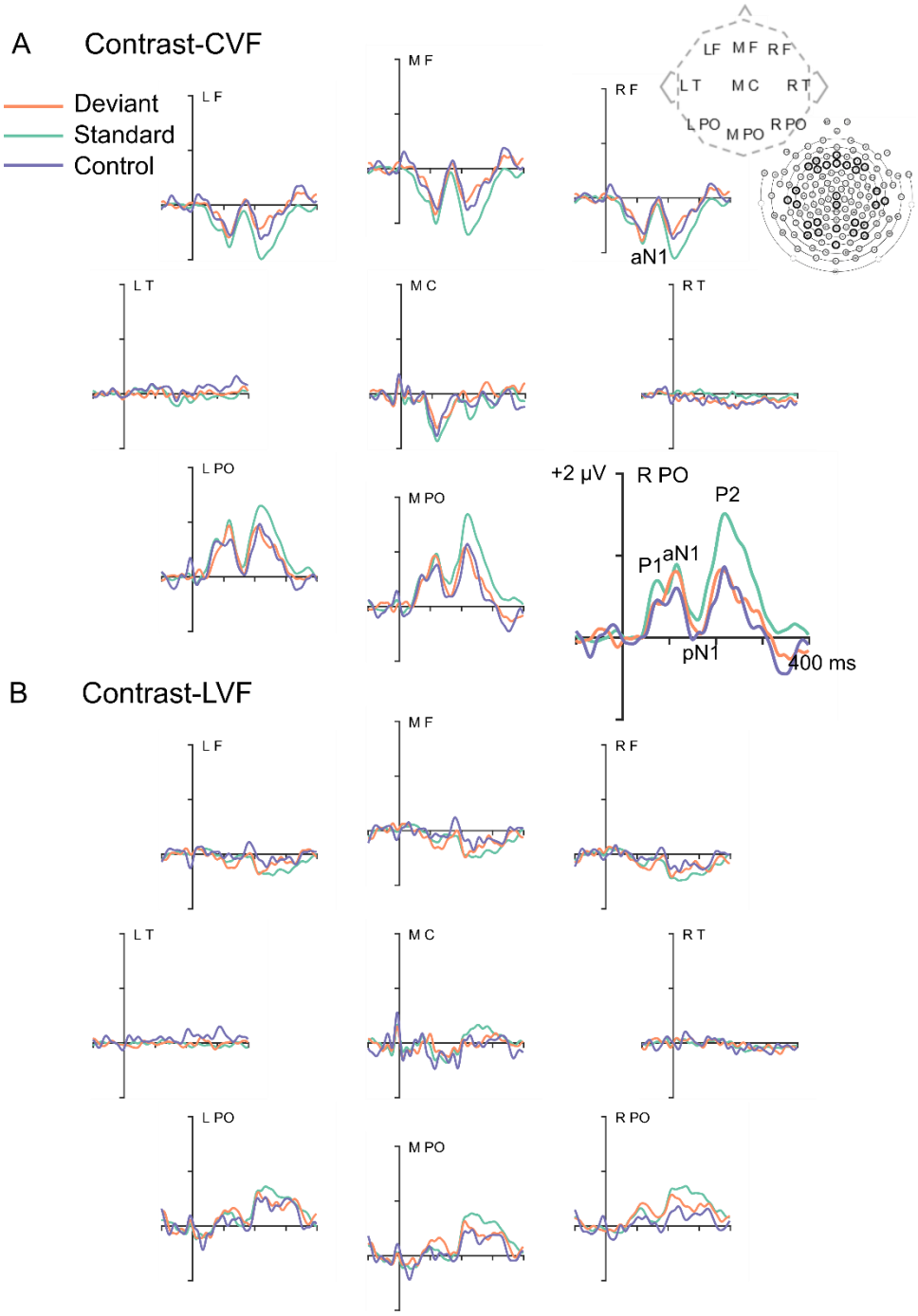


*Figure 5.2* Grand average ERPs for contrast stimuli. We show ERPs for standard (green), deviant (orange), and control (purple) trials at the left (L), midline (M), and right (R) frontal (F) and parieto-occipital (PO) regions of interest (ROIs). We also show ERPs at M central (C) and L and R temporal (T) ROIs. Electrode clusters within each region are depicted by the black circles on the diagram of the 129-channel net. A. ERPs from the central visual field (CVF) condition. B. ERPs from the lower visual field (LVF) condition. Electrode clusters within each region are depicted by the black circles on the diagram of the 129-channel net.

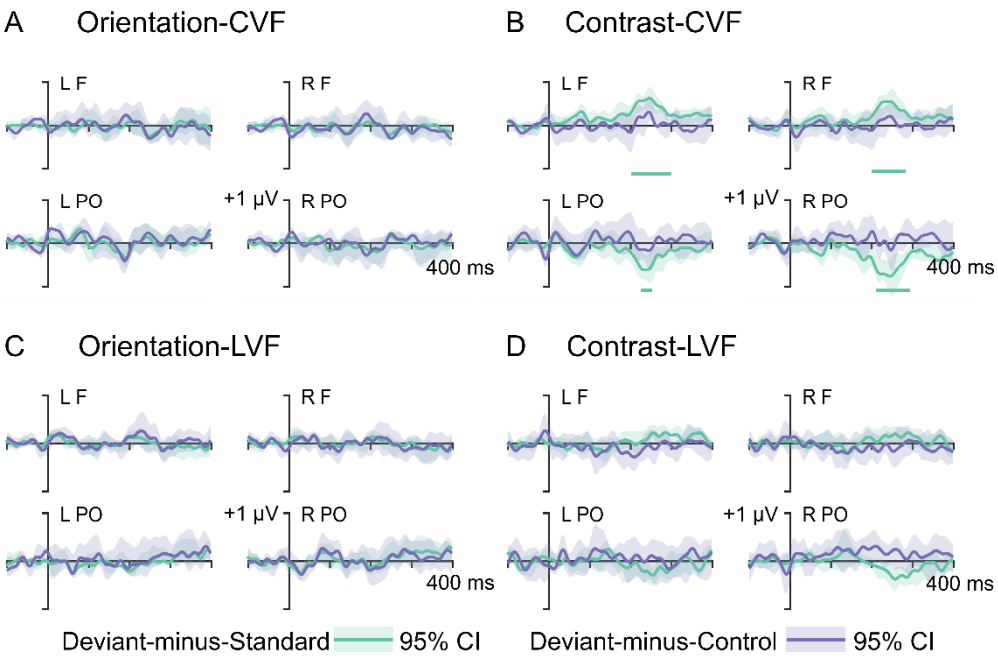


*Figure 5.3* Difference waves for each deviant feature appearing in central (CVF) and lower visual field (LVF). A. Orientation-CVF. B. Contrast-CVF. C. Orientation-LVF. D. Contrast-LVF. The lighter green and purple around the deviant-minus-standard (purple) and deviant-minus-control (green) difference wave, respectively, show the 95% confidence interval. We show difference waves at left (L) and right (R) frontal (F) and parieto-occipital (PO) regions. Horizontal bars illustrate where the deviant-minus-standard difference waves are significantly different from zero for at least 5 consecutive time points (10 ms).

### 5.4.3 Principal components analysis (PCA)

We performed temporal principal component analysis (PCA) to confirm the negativity in the deviant-minus-standard difference wave for contrast stimuli was indeed a vMMN. For each condition, we show details for each component identified in the corresponding CVF ERP figure. We also give details for components with a single peak latency between 70 and 300 ms whose scores are significantly different between deviants and controls (or standards for contrast conditions) at component minimum (negative pole) or maximum (positive pole)—not necessarily one of the ROIs depicted in our ERP figures.

#### 5.4.3.1 Orientation PCAs

Figure 5.4 shows details of each component identified in the corresponding ERP figure and components with a single peak latency between 70 and 300 ms whose scores differ between deviants and controls in the CVF (A) and LVF (B) condition. We provide summaries of our statistical comparisons of these components in Table 5.3.

To our surprise, no component was temporally or topographically consistent with DRN, for either orientation condition. In the orientation-CVF condition (Figure 5.4A), one component (component 9) was more negative for deviants than for controls at its negative pole. The topography of this component is like the aN1 (component 2), but its activity is only weakly correlated with the aN1 ($r$ = .22). In Chapter 3, we found evidence for deviant-related differences in the aN1 component.

Table 5.3 shows that no other *negative* component produced a significant negative deviant-minus-control difference score at its negative pole in the orientation-CVF condition. Instead, we found a significant negative deviant-minus-control difference at the negative pole of the P1 (component 4). We have previously observed deviant-related differences in the P1 (Ch. 3). P2 proper (component 1) did not differ for control and deviant stimuli, but another component's amplitudes, whose topography was similar to the P2 (component 5), were smaller for deviants than for controls at its positive pole and negative pole (Table 5.3). This component may be an earlier subcomponent of the P2 (e.g., P2a; Qin et al., 2016).

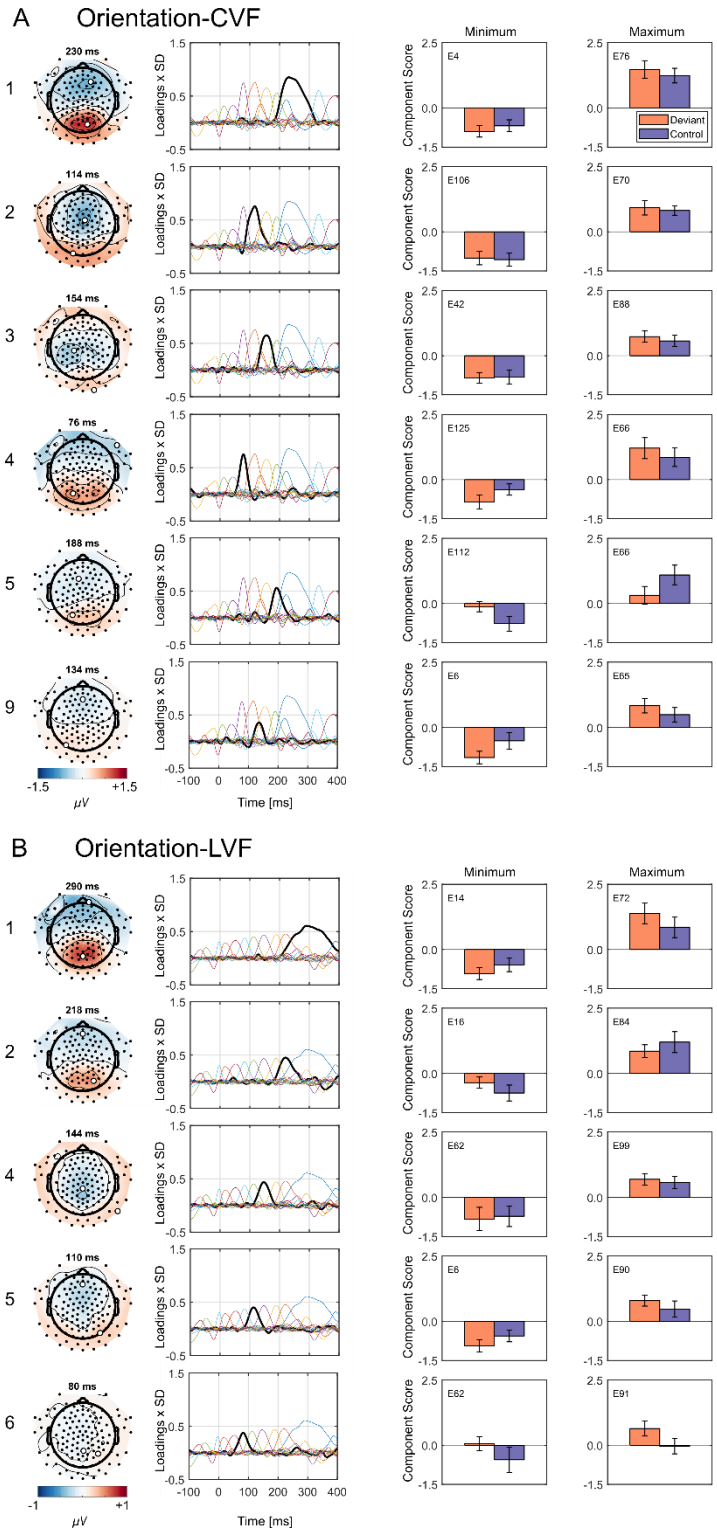


*Figure 5.4* PCA results for orientation stimuli. A. PCA for the central visual field (CVF) condition. B. PCA for the lower visual field (LVF) condition. We give details of a) each component identified in the corresponding ERP figure, and b) the components with a single peak latency between 70 and 300 ms whose scores are significantly different between deviants and controls at component minimum or maximum. From left to right, we show: the component number, topographical maps (combined activity from deviant and control trials at peak latency), component loadings (a component's contribution as a thick black line to the overall evoked activity relative to all other components as thin lines of different colours), component score for minimum, and component score for maximum. The last two, the bar graphs, show means for deviant (orange) and control (purple), ±1 standard-error bars, and electrode numbers. We show the location of these electrodes on the topographical maps by white disks.

*Table 5.3 Bayesian ($BF_{10}$) t-tests (two-tailed) of Deviant and Control Component Scores for Components of Interest in each Orientation Condition (df = 15)*

| Component | Max/Min | *t* | *p* | $BF_{10}$ |
|---|---|---|---|---|
| CVF | | | | |
| Component 1 (P2) | Max | 1.030 | .319 | 0.403 |
| | Min | −1.020 | .324 | 0.400 |
| Component 2 (aN1) | Max | 0.472 | .643 | 0.282 |
| | Min | 0.242 | .812 | 0.262 |
| Component 3 (pN1) | Max | 0.932 | .366 | 0.372 |
| | Min | −0.203 | .842 | 0.260 |
| Component 4 (P1) | Max | 1.748 | .101 | 0.884 |
| | Min | −2.184 | .045 | 1.624 |
| Component 5 | Max | −3.615 | .003 | 17.218 |
| | Min | 2.430 | .028 | 2.363 |
| Component 9 | Max | 0.912 | .376 | 0.367 |
| | Min | −2.742 | .015 | 3.895 |
| LVF | | | | |
| Component 1 (P3) | Max | 2.143 | .049 | 1.528 |
| | Min | −1.216 | .243 | 0.479 |
| Component 2 (P2) | Max | −1.143 | .271 | 0.447 |
| | Min | 1.286 | .218 | 0.514 |
| Component 4 (pN1) | Max | 0.650 | .525 | 0.308 |
| | Min | −0.423 | .679 | 0.276 |
| Component 5 (aN1) | Max | 1.122 | .279 | 0.438 |
| | Min | −1.571 | .137 | 0.708 |
| Component 6 (P1) | Max | 2.004 | .064 | 1.251 |
| | Min | 1.498 | .155 | 0.649 |

*Note.* Max = Maximum. Min = Minimum. CVF = central visual field. LVF = lower visual field. We highlight the Max or Min in grey depending on whether the component is decidedly positive or negative, respectively.

No component produced a significant negative deviant-minus-control difference in the orientation-LVF condition (Figure 5.4B). One significant difference emerged owing to the bigger P3 (component 1) for deviants compared to controls at its positive pole.

#### 5.4.3.2 Contrast PCAs

Figure 5.5 shows details of each component identified in the corresponding ERP figure and components with a single peak latency between 70 and 300 ms whose scores differ in the CVF (A) and LVF (B) condition. Summaries of statistical comparisons of the components for the CVF and LVF condition appear in Table 5.4 and 5.5, respectively. No negative component produced a significant deviant-minus-standard (D vs. S) or deviant-minus-control (D vs. C) difference at its negative pole (Min) in either contrast condition. Therefore, we did not find any component that was temporally or topographically consistent with a vMMN for either contrast condition.

Instead, in the contrast-CVF condition (Figure 5.5A), at the positive pole of one component (component 2), standards produced larger amplitudes than controls (but not deviants). The temporal profile of this component is similar to the pN1; its topography is not. P2 (component 1) and P3 (component 8) amplitudes were larger for standards compared to deviants at their positive poles. We did not find any significant difference between deviants and controls and only the P2 (not the P3) was larger for standards compared to controls here (Table 5.4). These results reflect greater stimulus intensity (i.e., Michelson contrast) for standards compared to deviants and controls.

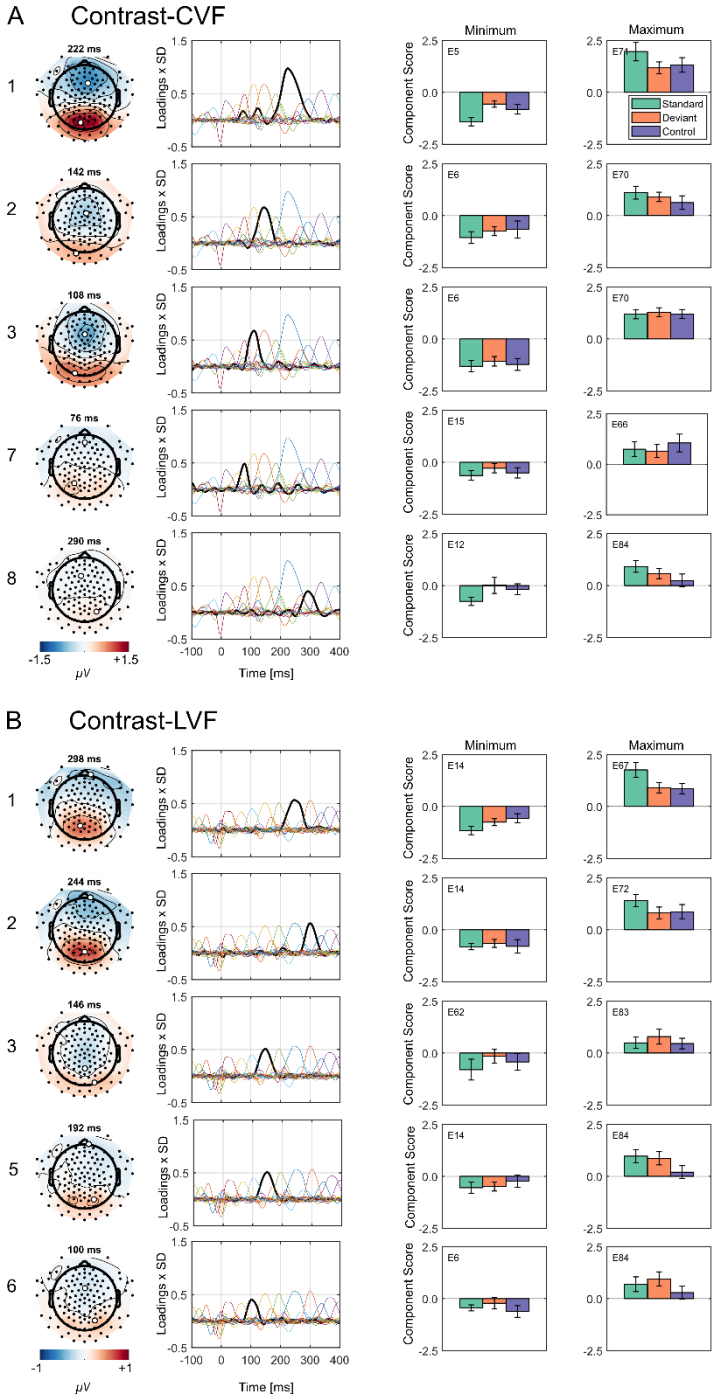


*Figure 5.5* PCA results for contrast stimuli. A. PCA for the central visual field (CVF) condition. B. PCA for the lower visual field (LVF) condition. We give details of a) each component identified in the corresponding ERP figure, and b) the components with a single peak latency between 70 and 300 ms whose scores are significantly different between standards, deviants, and controls at component minimum or maximum. From left to right, we show: the component number, topographical maps (combined activity from deviant and control trials at peak latency), component loadings (a component's contribution as a thick black line to the overall evoked activity relative to all other components as thin lines of different colours), component score for minimum, and component score for maximum. The last two, the bar graphs, show means for deviant (orange) and control (purple), ±1 standard-error bars, and electrode numbers. We show the location of these electrodes on the topographical maps by white disks.

Table 5.4 *Bayesian ($BF_{10}$) t-tests (two-tailed) of Component Scores for Standards, Deviants, and Controls for Components of Interest in the Contrast-CVF Condition (df = 15)*

| Component | Pair | Max/Min | *t* | *p* | $BF_{10}$ |
|---|---|---|---|---|---|
| Component 1 (P2) | D vs. C | Max | −0.836 | .416 | 0.346 |
| | | Min | 1.172 | .259 | 0.459 |
| | D vs. S | Max | −3.801 | .002 | 23.811 |
| | | Min | 5.199 | < .001 | 266.531 |
| | C vs. S | Max | −3.409 | .004 | 12.031 |
| | | Min | 4.416 | < .001 | 69.546 |
| Component 2 | D vs. C | Max | 1.744 | .102 | 0.879 |
| | | Min | −0.288 | .777 | 0.265 |
| | D vs. S | Max | −1.329 | .204 | 0.538 |
| | | Min | 1.856 | .083 | 1.020 |
| | C vs. S | Max | −2.320 | .035 | 1.993 |
| | | Min | 1.372 | .190 | 0.564 |
| Component 3 (aN1) | D vs. C | Max | 0.897 | .384 | 0.362 |
| | | Min | 0.637 | .533 | 0.305 |
| | D vs. S | Max | 0.595 | .560 | 0.299 |
| | | Min | 1.315 | .208 | 0.530 |
| | C vs. S | Max | 0.028 | .978 | 0.256 |
| | | Min | 0.316 | .756 | 0.267 |
| Component 7 (P1) | D vs. C | Max | 1.135 | .274 | 0.443 |
| | | Min | −0.814 | .428 | 0.341 |
| | D vs. S | Max | −0.390 | .702 | 0.273 |
| | | Min | 2.112 | .052 | 1.460 |
| | C vs. S | Max | 1.135 | .274 | 0.443 |
| | | Min | −0.814 | .428 | 0.341 |
| Component 8 (P3) | D vs. C | Max | 0.912 | .376 | 0.367 |
| | | Min | 0.525 | .607 | 0.289 |
| | D vs. S | Max | −3.004 | .009 | 6.022 |
| | | Min | 2.321 | .035 | 1.996 |
| | C vs. S | Max | −1.757 | .099 | 0.895 |
| | | Min | 2.331 | .034 | 2.028 |

*Note.* Max = Maximum. Min = Minimum. S = Standard. D = Deviant. C = Control. We highlight the Max or Min in grey depending on whether the component is decidedly positive or negative, respectively.

Table 5.5 *Bayesian ($BF_{10}$) t-tests (two-tailed) of Component Scores for Standards, Deviants, and Controls for Components of Interest in the Contrast-LVF Condition (df = 15)*

| Component | Pair | Max/Min | *t* | *p* | $BF_{10}$ |
|---|---|---|---|---|---|
| Component 1 (P2) | D vs. C | Max | 0.151 | .882 | 0.258 |
| | | Min | –0.958 | .353 | 0.380 |
| | D vs. S | Max | –3.703 | .002 | 20.071 |
| | | Min | 2.478 | .026 | 2.548 |
| | C vs. S | Max | –2.638 | .019 | 3.286 |
| | | Min | 2.162 | .047 | 1.572 |
| Component 2 (P3) | D. vs. C | Max | –0.149 | .883 | 0.258 |
| | | Min | 0.454 | .656 | 0.280 |
| | D vs. S | Max | –2.296 | .037 | 1.921 |
| | | Min | 0.882 | .392 | 0.358 |
| | C vs. S | Max | –1.403 | .181 | 0.538 |
| | | Min | 0.039 | .969 | 0.256 |
| Component 3 (pN1) | D vs. C | Max | 0.909 | .378 | 0.366 |
| | | Min | 0.816 | .427 | 0.341 |
| | D vs. S | Max | 1.037 | .316 | 0.406 |
| | | Min | 2.455 | .027 | 2.458 |
| | C vs. S | Max | –0.189 | .853 | 0.260 |
| | | Min | 0.948 | .358 | 0.377 |
| Component 5 | D vs. C | Max | 2.255 | .039 | 1.807 |
| | | Min | –1.089 | .294 | 0.425 |
| | D vs. S | Max | –1.121 | .280 | 0.437 |
| | | Min | 0.398 | .696 | 0.274 |
| | C vs. S | Max | –2.586 | .021 | 3.027 |
| | | Min | 1.115 | .283 | 0.435 |
| Component 6 (P1 or aN1) | D vs. C | Max | 1.847 | .084 | 1.008 |
| | | Min | 1.133 | .275 | 0.443 |
| | D vs. S | Max | 0.998 | .334 | 0.393 |
| | | Min | 0.923 | .371 | 0.370 |
| | C vs. S | Max | –1.216 | .243 | 0.479 |
| | | Min | –0.577 | .572 | 0.296 |

*Note.* Max = Maximum. Min = Minimum. S = Standard. D = Deviant. C = Control. We highlight the Max or Min in grey depending on whether the component is decidedly positive or negative, respectively.

Similar to the CVF condition, the P2 and P3 were larger for standards compared to deviants at their respective positive poles in the contrast-LVF condition (Figure 5.5B). Only the P2 (not the P3) was larger for standards compared to controls.

We also found larger negativity for standards than for deviants at the pN1's (component 3) negative pole. There was no difference between standards and controls here or between any stimuli at its positive pole. Component 5 amplitudes were more positive for standards and deviants compared to controls at its positive pole. This component is similar to the P2 in this condition and in the orientation-CVF condition. Possibly, it is a subcomponent of our P2 proper (component 1).

Overall, contrast standards evoked larger amplitudes from negative ERP components (i.e., more negative at the negative pole) as well as positive ERP components (i.e., more positive at the positive pole). We did not find any negative component that produced a negative deviant-minus-control or a deviant-minus-standard difference at its negative pole in either visual field condition. Therefore, the negativity in the contrast-CVF deviant-minus-standard difference wave in Figure 5.3(B) at the R PO is not due to a vMMN, but rather a larger P2, and possibly P3, for standards.

## 5.5 Discussion

We investigated whether orientation changes produced larger prediction errors (i.e., vMMNs) than equally different contrast decrements based on the

axiom that orientation changes represent greater biological threat than contrast decrements. We also investigated whether visual field affects the vMMN. However, we did not garner support for our hypothesized differences, because we did not find a vMMN in any condition.

Surprisingly, our orientation deviants did not produce a vMMN in either visual field despite using a similar orientation difference to those used by Kimura and Takeda (2015). In fact, we did not find a classic deviant-minus-standard vMMN for orientation deviants where others have. This may reflect the differences in stimuli across studies. For example, Qian et al. (2014) used red rectangular bars whose orientation changed by 90° on deviant trials. The change from red to the grey of the background (and vice versa) would produce a difference in the response from neurons whose receptive fields corresponds with the visual field in which the red bar appears on standard trials only. There were no such changes in luminance in the orientation conditions of the present study.

On initial inspection of the ERP data, we observed a negative-going difference that was characteristic of a vMMN in the deviant-minus-standard difference wave in the contrast-CVF condition (Figure 5.4A). This difference was not significant in the LVF condition. We suspect reduced signal intensity of LVF stimuli—due to having excited peripheral cells, not foveal cells—affected the overall signal to noise ratio in the visual cortices, obscuring deviance-related difference. It would be useful to increase the size of the LVF stimuli in future research. Nevertheless, our PCAs revealed that the DRN in the contrast-CVF condition reflects a larger P2, and possibly P3, for higher contrast stimuli

compared to lower contrast stimuli. Nyman et al. (1990) reported a similarly enhanced positivity to higher contrast standards 200 ms after onset.

Given that the difference in the deviant-minus-standard difference wave in the contrast-CVF condition was due to larger P2 amplitudes for (higher contrast) standards compared to (lower contrast) deviants and that higher contrast stimuli evoke larger P2 amplitudes than lower contrast stimuli (Nyman et al., 1990), the DRN here most likely reflects a contrast effect. Therefore, we did not find a vMMN for contrast changes either. This interpretation corroborates the findings of Nyman et al. Ours is not the first to find that low-level feature deviants fail to produce a vMMN. Undoubtedly, there is a means by which the visual system is processing these low-level changes. If not, it would be unlikely that our foraging ancestor would have been able to detect those systematic changes in visual properties, possibly warning that a predator was approaching. Perhaps the vMMN does not reveal their processing.

It is not likely that our ISI and stimulus duration is responsible for our failing to find the vMMN as it is identical to what others have used to test orientation deviance (Bodnár et al., 2017; Astikainen et al., 2008, Kimura et al. 2009). Moreover, we purposely selected an orientation difference that is slightly larger than the orientation difference used by Kimura and Takeda (2015) in their oddball condition to ensure our magnitude of deviance was enough for evoking a vMMN to orientation changes.

However, ours is one of the few studies that has used Gabor patches to investigate changes in basic properties of visual input (Ch. 2). Perhaps this is

because Gabor patches are not ideal for evoking the vMMN. Perhaps when a change is isolated to one property of visual input, it does not evoke a vMMN. We are not aware of any other visual stimulus that affords this level of control over all stimulus parameters.

Outside of the vMMN time-window, we found a difference between deviants and controls in the P1 (and possibly a later aN1) for orientation-CVF. We have previously observed such differences at the parieto-occipital regions for well-controlled orientation changes (Ch. 3 and 6). In Chapter 3, we found these differences in the P1 at around 90 ms. Unlike our other experiments (Ch. 3 and 6), deviance-related differences for orientation deviants only occurred at the negative poles of these components. The deviant-related positivities at the positive poles were not significant.

Possibly, the reduced stimulus contrast in this experiment compared to our other experiments is responsible. In the present study, orientation stimuli had a Michelson contrast of only 0.393: equal to the contrast of deviant stimuli in the contrast conditions. In our other experiments, the Michelson contrast of orientation stimuli was closer to 0.99 in two experiments (Ch. 3 and Ch. 6, Experiment 1) and 0.6 in another (Ch. 6, Experiment 2). The smaller P1 amplitudes in the orientation condition compared with the standards in the contrast conditions illustrate the effect of having reduced the contrast of our stimuli in the present study. We suspect that to show deviant-related differences, stimulus-to-noise ratio must be high and this reaches ceiling when contrast is high and stimuli appear in the CVF.

There was no difference in either P1 or aN1 components for contrast deviants compared to standards in either visual field. We speculate that adaptation and deviance differences in the contrast conditions cancelled each other out in this study because lower contrast deviants normally yield smaller early ERP amplitudes than higher contrast stimuli whereas deviants would normally produce larger early ERP amplitudes (Ch. 3 and Ch. 6). One could test this theory by reversing the standard and deviant contrast values and comparing ERPs to deviant with ERPs to a control stimulus (Ch. 6).

The growing number of studies failing to show a vMMN when investigating low-level feature changes in well-controlled visual input encourages continued investigation into how else these changes in visual input are resolved in the brain or, alternatively, closer inspection of the facets that predict a vMMN to low-level changes.

## 5.6 Conclusion

We propose that orientation and contrast deviants do not yield a vMMN in the CVF or LVF. The reason for this is not entirely clear. There is however research to suggest early deviant-related differences may be involved. Clearly, continued investigation of low-level visual deviance is needed.

# CHAPTER 6

## THE QUEST FOR THE VISUAL MISMATCH NEGATIVITY (VMMN): EVENT-RELATED POTENTIAL INDICATIONS OF DEVIANCE DETECTION FOR LOW-LEVEL VISUAL FEATURES.

Based on the following submitted manuscript

Male, A. G., O'Shea, R. P., Schröger, E., Müller, D., Roeber, U., & Widmann, A. (2019). The quest for the visual mismatch negativity (vMMN): Event-related potential indications of deviance detection for low-level visual features.

# 6. THE QUEST FOR THE VISUAL MISMATCH NEGATIVITY (VMMN): EVENT-RELATED POTENTIAL INDICATIONS OF DEVIANCE DETECTION FOR LOW-LEVEL VISUAL FEATURES

## 6.1 Preface

In this Chapter, I investigate whether changes in low-level features of visual input can evoke the vMMN. It contains two experiments. In the first experiment, I investigate whether other aspects of experimental design affect or predict the vMMN to orientation changes. I manipulate attentional focus and stimulus type in a 2×2 design, producing four conditions. One condition was a replication of a well-known orientation-deviant study by Kimura, Katayama, Ohira, and Schröger (2009). In keeping with their design, I compare each deviant from oddball sequences with its counterpart from corresponding equiprobable sequences. In the second experiment, I investigate whether changes in orientation, contrast, phase, and spatial frequency can evoke a vMMN using the multi-feature paradigm. Only five vMMN studies have tested the multi-feature paradigm and only one of these used a control for adaptation. Therefore, in addition to addressing the questions motivating this thesis, this experiment provides an opportunity to test the paradigm while controlling for adaptation (using the cascadic control). Together, these two experiments seek to show:

I. Whether isolated changes in different basic properties of visual input can evoke a vMMN.

## 6.2 Introduction

Sights, sounds, touches, tastes, and smells flood our senses at every moment. Yet we do not experience all this information, if only because it would require lots of energy for our brains to process it completely. Instead, our brains preferentially process unexpected changes in sensory input.

One signature of the processing of changes is the mismatch negativity (MMN), discovered by Näätänen, Gaillard, and Mäntysalo (1978) in the auditory modality. It is a brain response to rare, unpredicted, different, *deviant* tones in a sequence of identical *standard* tones, a so-called *oddball sequence*. One derives the MMN by comparing event-related potentials (ERPs) from deviants and standards collected with electroencephalography (EEG). It occurs sometime between 100 and 300 ms after the onset of the deviant and it does not require attention towards the deviant.

Various kinds of deviants produce the MMN, from simple feature deviants such as the pitch, intensity, or duration of tones, to increasingly complex and abstract deviants, such as unexpected repetition in a series of ever-changing tones. For a review, see Näätänen, Paavilainen, Rinne, and Alho (2007).

Analogues of the MMN have been reported for other sensory modalities, including olfaction (Krauel et al., 1999), touch (Kekoni et al., 1997), and vision (Cammann, 1990; Czigler & Csibra, 1990). Our concern in this paper is with vision: the visual mismatch negativity (vMMN). There is a presupposition that all analogues of the MMN should adhere to at least four principals:

1. The MMN reflects processes beyond simple adaptation (called "refractoriness" in older MMN literature: O'Shea, 2015), such as memory comparison, model updating, or prediction error. Such a MMN is sometimes called "genuine" (e.g., Paavilainen, Alho, Reinikainen, Sams, & Näätänen, 1991, p. 477).
2. The MMN occurs in response to regularity violations in well-isolated low-level, physiologically plausible, sensory features (Näätänen et al., 2007).
3. The MMN does not require attention (Näätänen, 1992).
4. The MMN is not due to physical differences of the stimuli (Kujala, Tervaniemi, & Schröger, 2007).

Here, we discuss whether these presuppositions are supported by present vMMN research. Although there exist hundreds of vMMN studies on many different types of deviants, we focused on changes in orientation, contrast, phase, and spatial frequency because, according to Graham (1989), these are among the key dimensions for describing the appearance of images viewed with both eyes and they are processed in the visual cortex or earlier. We reviewed all studies we found examining vMMN to these low-level visual features and list relevant parameters and results in Table 6.1. We then develop a paradigm to test these presuppositions for vMMN.

In Table 6.1, entries appear chronologically for each deviant feature: orientation, contrast, and spatial frequency (we were unable to find any studies that varied phase). If a single study conducted multiple experiments, we give the

details of each separately. Likewise, if an experiment tested two features separately, we give details for each condition separately.

For each experiment or condition, we provide details about:

- Number (N) of participants contributing to the final data set.
- The stimulus(i) used.
- Difference between the deviant and standard in units measured. In studies with more than one deviant size, we give the smallest difference that produced the vMMN.
- Whether the participant's task was visual, auditory, or manual.
- What participants attended to in order to perform their task.
- Whether there was any control comparing deviants with physically identical standards. This is achieved by having deviants and standards *reverse roles* in different blocks, by including a block containing a single *deviant alone*, by including a *deviant block* in which the deviant repeats, or by including a *standard block,* in which multiple deviants appear among standards, but not with a different frequency to the oddball blocks.
- Whether there was any control for adaptation (typically including control for physical differences), such as the *equiprobable* control or the *cascadic* control (see later).
- The latency of maximum amplitude of the vMMN (in ms).
- The electrode or region of interest.

- The mean amplitude of the classic, deviant (D) minus standard (S) vMMN, containing adaptation effects as well as prediction error (in μV).
- The mean amplitude of the genuine, D minus control (C) vMMN (μV; where applicable).
- The effect size of the classic vMMN (in Cohen's *d*; Cohen, 1977).
- The effect size of the genuine vMMN (*d*; where applicable).

We give any vMMN amplitude in red if it was not statistically significant. Where a piece of information was not reported, could not be calculated from the information available, or was not applicable (e.g., there was no control for adaptation), we leave a blank. We preserved the sign of Cohen's *d*s: all reported negativities should be negative.

Table 6.1 *VMMN Research in which the Deviant Differs from Standards in Orientation, Contrast, or Spatial Frequency*

| Study | N | Stimulus(i) | Smallest Difference | Task Modality | Attention On | Physical Control[a] | Adaptation Control[a] | Time of Maximum Negativity (ms) | Electrode or ROI | Classic vMMN Amplitude (μV) | Classic Effect Size (Cohen's *d*) | Genuine vMMN Amplitude (μV) | Genuine Effect Size (Cohen's *d*) |
|---|---|---|---|---|---|---|---|---|---|---|---|---|---|
| **Orientation** | | | | | | | | | | | | | |
| Fu et al. (2003) | 12 | Square-wave grating | 90° | Visual | Spatial frequency of gratings | Reverse roles | | 192 | Occipital | –1.90[c] | | | |
| Astikainen et al. (2004) | 8 | Light bar | 90° | Auditory | Words | Deviant alone | | 180[b] | Pz | –1.28[c] | –1.79 | | |
| Astikainen et al. (2008) | 10 | Dark bar | 36° | Auditory | Words | Reverse roles | Equi-probable | 195[b] | Occipital | –1.13[c] | –2.06 | –0.69[c] | –0.79 |
| Czigler and Pató (2009), Experiment 1 | 14 | Grid pattern | 90° | Visual | Quadrangle width | | | 280[b] | Right posterior | –1.01[c] | –0.64 | | |
| Kimura et al. (2009) | 12 | Grey bar | 36° | Visual | Bar-edges | Reverse roles | Equi-probable | 225[b] | T6(P8) | –2.25[c] | –1.60 | –1.60[c] | –1.78 |
| Czigler and Sulykos (2010) | 24 | Peripheral line segments | 30° | Visual | Central line segment | Reverse roles | | 166 | Oz | –0.60 | –0.87 | | |
| Sulykos and Czigler (2011) | 12 | Gabor patches | 90° | Visual | Spaceship task[d] | Reverse roles | | 130 | Oz | –2.55 | –1.60 | | |
| Kimura and Takeda (2013) | 22 | Grey bars | 33° | Visual | Fixation dot | Reverse roles | Equi-probable | 226[b] | PO8 | –2.62 | –2.39 | –0.93 | –0.63 |

| Study | N | Stimulus(i) | Smallest Difference | Task Modality | Attention On | Physical Control[a] | Adaptation Control[a] | Time of Maximum Negativity (ms) | Electrode or ROI | Classic vMMN Amplitude (μV) | Classic Effect Size (Cohen's *d*) | Genuine vMMN Amplitude (μV) | Genuine Effect Size (Cohen's *d*) |
|---|---|---|---|---|---|---|---|---|---|---|---|---|---|
| Shi et al. (2013) | 12 | Red rectangles | 90° | Visual | Fixation cross | | | 200[b] | Occipito-temporal | –1.60 | | | |
| Sulykos et al. (2013) | 12 | Gabor patches | 30° | Visual | Spaceship task[d] | | Equi-probable | 210[c] | Parieto-occipital | | | –0.05[c] | |
| Takács et al. (2013), Experiment 1 | 17 | Gabor patches | 50° | Visual | Fixation dot | Reverse roles | | 134 | Parieto-occipital | –0.51 | | | |
| Takács et al. (2013), Experiment 2 | 19 | Gabor patches | 90° | Visual | Fixation dot | Reverse roles | | 148 | Parieto-occipital | –1.10 | | | |
| Kimura and Takeda (2014), Experiment 1 | 23 | Grey bar | 22° | Manual | Button press | Reverse roles | | 225[b] | Right occipito-temporal | –1.19 | –1.30 | | |
| Kimura and Takeda (2014), Experiment 2 | 21 | Grey bar | 22° | Manual | Button press | Reverse roles | | 265[b] | Right occipito-temporal | –0.92 | –0.97 | | |
| Qian et al. (2014) | 14 | Red rectangles | 90° | Visual | Fixation cross | | | 200 | Occipito-temporal | –1.13 | | | |
| Farkas et al. (2015) | 27 | Gabor patches | 90° | Visual | Fixation cross | Reverse roles | | 145[b] | Saggital parieto-occipital | –0.30 | –0.72 | | |
| Kimura and Takeda (2015) | 22 | Grey bars | 33° | Visual | Fixation dot | Reverse roles | Equi-probable | 202[b] | PO8 | | | –1.16 | –0.72 |
| Bodnár et al. (2017), Experiment 1 | 17 | Line texture | 90° | Visual | Spaceship task[d] | Reverse roles | | 264[c] | Occipital | 0.04[c] | 0.02 | | |

| Study | N | Stimulus(i) | Smallest Difference | Task Modality | Attention On | Physical Control[a] | Adaptation Control[a] | Time of Maximum Negativity (ms) | Electrode or ROI | Classic vMMN Amplitude (μV) | Classic Effect Size (Cohen's *d*) | Genuine vMMN Amplitude (μV) | Genuine Effect Size (Cohen's *d*) |
|---|---|---|---|---|---|---|---|---|---|---|---|---|---|
| File et al. (2017), Experiment 1 | 15 | Line texture | 36° | Visual | Spaceship task[d] | Reverse roles | Cascadic | 144 | Parieto-occipital | –0.67 | –1.15 | –0.09 | –0.26 |
| Pesonen et al. (2017) | 16 | Dark bar | 36° | Auditory | Words | | | 210 | Occipital | –1.02[c] | | | |
| Yan et al. (2017) | 15 | Black arrows | 90° | Visual | Fixation cross | Reverse roles | | 200[c] | Parieto-occipital | –2.60[c] | | | |
| **Contrast** | | | | | | | | | | | | | |
| Nyman et al. (1990) | 9 | Square-wave gratings | -0.48 M | Visual | Fixation dot | Reverse roles | | 150[b] | Oz | –0.28 | –0.11 | | |
| Wei et al. (2002) | 12 | Colour scenery | | Auditory or Visual | Tones or contrast increment | | | 152[b] | O2 | –1.20 | –2.07 | | |
| **Spatial frequency** | | | | | | | | | | | | | |
| Tales et al. (1999), Experiment 1 | 12 | White vertical rectangles | +0.6 cpd | Visual | Fixation square | | | 325[b] | O2 | –4.00[c] | | | |
| Tales et al. (1999), Experiment 2 | 12 | White vertical rectangles | -0.6 cpd | Visual | Fixation square | | | 325[b] | O1 | –1.86[c] | | | |
| Tales et al. (2002) | 24 | White vertical rectangles | -0.6 cpd | Visual | Fixation square | | | 325[b] | O2 | –3.40[c] | | | |

| Study | N | Stimulus(i) | Smallest Difference | Task Modality | Attention On | Physical Control[a] | Adaptation Control[a] | Time of Maximum Negativity (ms) | Electrode or ROI | Classic vMMN Amplitude (μV) | Classic Effect Size (Cohen's *d*) | Genuine vMMN Amplitude (μV) | Genuine Effect Size (Cohen's *d*) |
|---|---|---|---|---|---|---|---|---|---|---|---|---|---|
| Heslenfeld (2003) | 14 | Vertical gratings | 1.72 cpd | Visual | Visuomotor task | Reverse roles | | 150[b] | Oz | –1.10 | –2.10 | | |
| Kenemans et al. (2003) | 12 | Vertical square-wave gratings | 1.8 cpd | Visual | Fixation cross | Deviant alone | | 135 | Oz | –1.19[c] | | | |
| Stagg et al. (2004) | 12 | White vertical rectangles | 0.6 cpd | Visual | Fixation square | Reverse roles | | 305[b] | Occipital | –3.73[c] | | | |
| Maekawa et al. (2005) | 7 | Windmill pattern | 18 vanes | Auditory and Visual | Story and target windmill | Reverse roles | | 245[c] | Oz | –4.50[c] | –2.12 | | |
| Tales and Butler (2006) | 11 | White vertical rectangles | +0.6 cpd | Visual | Fixation square | | | 300[b] | T6(P8) | –3.90[c] | | | |
| Maekawa et al. (2009), Experiment 1 | 10 | Windmill pattern | 18 vanes | Auditory | Story | Deviant block | | 252[c] | Oz | –6.33[c] | | | |
| Maekawa et al. (2009), Experiment 2 | 8 | Windmill pattern | 18 vanes | Auditory | Story | Standard block | | 232[c] | Oz | –2.19[c] | –1.20 | | |
| Kenemans et al. (2010) | 16 | Vertical square-wave gratings | 1.8 cpd | Visual | Fixation cross | Reverse roles | | 160[b] | Oz | –0.50[c] | –0.63 | | |
| Chang et al. (2011) | 14 | White vertical rectangles | 0.6 cpd | Visual | Fixation square | Reverse roles | Equi-probable | 200[b] | Parieto-occipital | –0.95 | –1.02 | –1.25 | –0.95 |
| Sulykos and Czigler (2011) | 12 | Gabor patches | 4 cpd | Visual | Spaceship task[d] | Reverse roles | | 136 | Oz | –1.18 | –1.10 | | |

| Study | N | Stimulus(i) | Smallest Difference | Task Modality | Attention On | Physical Control[a] | Adaptation Control[a] | Time of Maximum Negativity (ms) | Electrode or ROI | Classic vMMN Amplitude (μV) | Classic Effect Size (Cohen's *d*) | Genuine vMMN Amplitude (μV) | Genuine Effect Size (Cohen's *d*) |
|---|---|---|---|---|---|---|---|---|---|---|---|---|---|
| Cleary et al. (2013) | 20 | Horizontal square-wave gratings | -6 cpd | Visual | Fixation cross | | | 150 | O2 | –2.70 | –1.03 | | |
| Maekawa et al. (2013) | 20 | Windmill pattern | 18 vanes | Visual | Target windmill | Reverse roles | | 280[b] | Oz | –1.25[c] | | | |
| Stothart and Kazanina (2013) | 39 | White vertical rectangles | +0.6 cpd | Visual | Fixation square | | | 222[c] | Parieto-occipital | –0.66[c] | | | |
| Hedge et al. (2015) | 20 | Vertical square-wave gratings | 6 cpd | Visual | Fixation square | Reverse roles | | 265[b] | Parieto-occipital | –0.94 | –0.55 | | |
| Bodnár et al. (2017), Experiment 2 | 19 | Windmill pattern | 6 vanes | Visual | Fixation dot | Reverse roles | | 203 | Occipital | –1.73 | –0.77 | | |
| File et al. (2017), Experiment 2 | 23 | Windmill pattern | 6 vanes | Visual | Spaceship task[d] | Reverse roles | Equi-probable | 269 | Occipital | –1.46 | –1.17 | –1.49 | –1.19 |

*Note.* [a] See text for explanation of categories. [b] This value represents the midpoint of the time-window used to calculate mean amplitude. [c] This value was calculated from the studies' figures. [d] Spaceship task: Sulykos and Czigler (2011) designed the Spaceship task to ensure absolute control of participants' attention. The task field occupies an area of the visual field opposite the stimulation of interest. Participants navigate a spaceship through a canyon—a rectangular object vertically and horizontally segmented giving the impression of depth and a horizon—while avoiding/catching colour-determined targets. These targets may be other spaceships (Sulykos, Kecskés-Kovács, & Czigler, 2015) or coloured doors (Sulykos & Czigler, 2011).

Next, we relate vMMN to the four MMN presuppositions.

### 6.2.1 Adaptation

ERP responses to repeated stimuli are typically smaller in amplitude, reflecting adaptation. Therefore, the greater negativity to deviants could come solely or partly from adaptation by the repetition of standards in oddball sequences (for thorough discussion see May & Tiitinen, 2009).

To disentangle adaptation from genuine detection of deviants, Schröger and Wolff (1996) developed a control, *equiprobable*, technique. In control sequences, different stimuli, including stimuli physically identical to the deviant, appear in random order, preventing any regularity, each with a frequency equal to that of the deviant in oddball sequences, equalizing adaptation. Schröger and Wolff argued that the comparison of deviants and physically identical control stimuli reflect the detection of regularity violations. We used this control in Experiment 1.

Ruhnau, Herrmann, and Schröger (2012) argued that with the equiprobable control adaptation is potentially overestimated. They proposed a sequence in which the stimulus changes regularly in a feature of interest (e.g., orientation) from trial to trial. One such stimulus is physically identical to the deviant; its overall frequency is the same as that of the deviant in each oddball block. This allows an expectation of the control stimulus to be established while keeping an adaptation level comparable with the one for the deviant in the oddball block.

We used this control in Experiment 2 to ensure our findings were unrelated to overestimated adaptation.

Table 6.1 shows that only 8 out of 50 (16%) vMMN experiments or conditions used either control, seriously limiting the conclusions about genuine vMMN effects we can draw from the literature.

### 6.2.2 Isolation and physiological plausibility of feature manipulations

Most stimuli used for vMMN research are not suited for manipulating low-level visual features. For example, a bar contains one orientation along its length and another, at right angles, at its end. Any stimulus with sharp edges necessarily stimulates wide bands of spatial frequencies.

Gabor patches, on the other hand, are ideal for isolating single low-level features. A Gabor patch comprises a sinusoidal grating of a particular frequency, phase, and orientation whose contrast reduces with distance from the centre of the grating by a Gaussian function whose size is expressed as the standard deviation in degrees of visual angle. That is, the orientation, spatial frequency, and luminance of a Gabor patch are as specified, without any other orientations, spatial frequencies, or luminances. Most importantly, using Gabor patches we can manipulate isolated features without affecting other low-level visual features.

Gabor patches are physiologically plausible because their profile resembles that of a simple cell in the visual cortex (Daugman, 1985; Field & Tolhurst, 1986; Fredericksen, Bex, & Verstraten, 1998). A simple cell has a

preferred orientation and spatial frequency; its receptive field dictates the stimuli to which it responds. An appropriate Gabor patch will ideally excite that cell. Only 4 of 43 vMMN experiments or conditions used Gabor patches (9%), again limiting the conclusions about vMMN we can draw from the literature.

### 6.2.3 Attention

One of the defining features of the MMN is that it occurs without attention. Inherent differences between the sensory modalities make it difficult to equate the allocation of attention across auditory and visual modalities. In vision, the eyes must be on the stimulus even if it is not task-relevant; in audition, the ears cannot be other than on the stimulus.

Table 6.1 shows the various ways in which attention has been manipulated in vMMN research. Attention can be on the stimulus of interest (e.g., Kimura et al., 2009), on some unrelated distractor stimulus (e.g., Sulykos & Czigler, 2013), or on stimulation in another modality (e.g., Astikainen, Lillstrang, & Ruusuvirta, 2008). To conclude whether the vMMN is "pre-attentive"—as the auditory MMN is—the stimulus of interest should not be task-relevant. However, one must ensure that participants are looking consistently at the stimulus of interest without attending to it. We find that 21 experiments or conditions (42%) used a central fixation stimulus that is not part of the stimuli of interest.

### 6.2.4 Comparison of physically identical stimuli

Physically different stimuli may elicit different ERPs, making it impossible to attribute differences to the detection of regularity violations. One

can compare physically identical stimuli by administering oddball blocks in which the standard and deviant reverse roles. Other methods, such as administering blocks containing only deviants, produce unexpectedly large classic vMMNs (e.g., Maekawa et al., 2005). Although 30 experiments and conditions did compare physically identical stimuli, only 7 of them (23%) also had an appropriate control for adaptation, again seriously limiting the conclusions about vMMN that can be drawn from the literature.

### 6.2.5 Other Issues

Table 6.1 also shows two inconsistencies in research into low-level deviants:

#### 6.2.5.1 VMMN peak latency

VMMN peak latencies have been reported as early as 130 ms (*orientation*: Sulykos & Czigler, 2011) or as late as 305 ms (*spatial frequency*: Stagg et al., 2004). Inconsistencies exist even with similar stimuli. For example, Maekawa et al. (2005) reported a vMMN to windmill-like patterns at 185 ms whereas File et al. (2017) reported a vMMN to the same patterns at least 70 ms later. Such timing differences are difficult to reconcile unless we accept that other processes may be affecting one of the reported vMMNs.

#### 6.2.5.2 Replicability of some vMMNs

Seven studies showed a vMMN to orientation deviants in bars, whereas three failed to show a vMMN to orientation deviants in line textures or Gabor patches (all controlling for adaptation). Two studies found that spatial frequency

deviants produced a vMMN only when deviants had higher spatial frequencies than the standard (File et al., 2017; Hedge et al., 2015). File et al. manipulated spatial frequency by changing the number of vanes in their sharp-edged radial gratings—windmill-like patterns—on deviant trials and argued that the deviant with fewer vanes did not produce a vMMN, because it was less complex. However, increasing the number of vanes also confoundingly increases the number of orientations in the stimulus.

These inconsistencies suggest that some other facet may predict whether a vMMN occurs. A key question is whether low-level feature deviants yield a vMMN when one controls for adaptation, uses physiologically plausible stimuli isolating the manipulated feature, manipulates task-irrelevant stimuli while ensuring the eyes are on the stimulus, and compares physically identical stimuli at the same time in the same experiment. We address these questions in two experiments.

### 6.2.6 The present study

In Experiment 1, we replicated an experiment by Kimura, Katayama, Ohira, and Schröger (2009) reporting a vMMN for orientation deviants with the equiprobable control. We selected this study because it was methodologically sound, reported large effects that were very well-controlled for adaptation effects (a necessity when one is interested in the underlying mismatch mechanisms), and because one of us (ES) was involved in the 2009 study. Kimura et al. used bars and had their participants press a button whenever the ends of the bars had rounded corners. We added conditions to tease apart potential contributors to the

vMMN they reported by testing the same orientation change with Gabor patches and by testing conditions in which the participants' attention/task was not on the ends of the stimuli but on a central fixation dot. We also measured where participants looked on the stimuli using a remote eye-tracker.

In Experiment 2, we tested orientation, contrast, phase, and spatial frequency deviants with Gabor patches using a multi-feature paradigm (Näätänen, Pakarinen, Rinne, & Takegata, 2004). In this paradigm, a feature of the stimulus, rather than the whole stimulus, can change to give a deviant for that feature and a standard for others. Similarly, all other stimuli are standards for that feature even though they may be deviants for others. One complete standard separates each deviant and each deviant feature appears once per set of four standard/deviant pairs of four trials in a pseudo-randomized order. This gives a probability of any feature similar to that of a traditional oddball sequence (here 12.5%). The advantage of this approach is that one can test multiple deviants within a short time.

## 6.3 Experiment 1

We replicated Kimura et al.'s (2009) study of orientation deviants using single bars (Figure 6.1A, I). We added three conditions, giving a 2×2 design of stimulus type: *bar* condition (Figure 6.1A, I-II) versus *Gabor* condition (Figure 6.1A, III-IV), and whether attention was on the edges of the stimuli to give the *edge* condition (Figure 6.1A, I and III) versus whether attention was on a central fixation dot to give the *fixation* condition (Figure 6.1A, II and IV). We also

measured participants' eye positions, fearing that when participants were attending to the bar ends their eyes might wander towards them, even though we

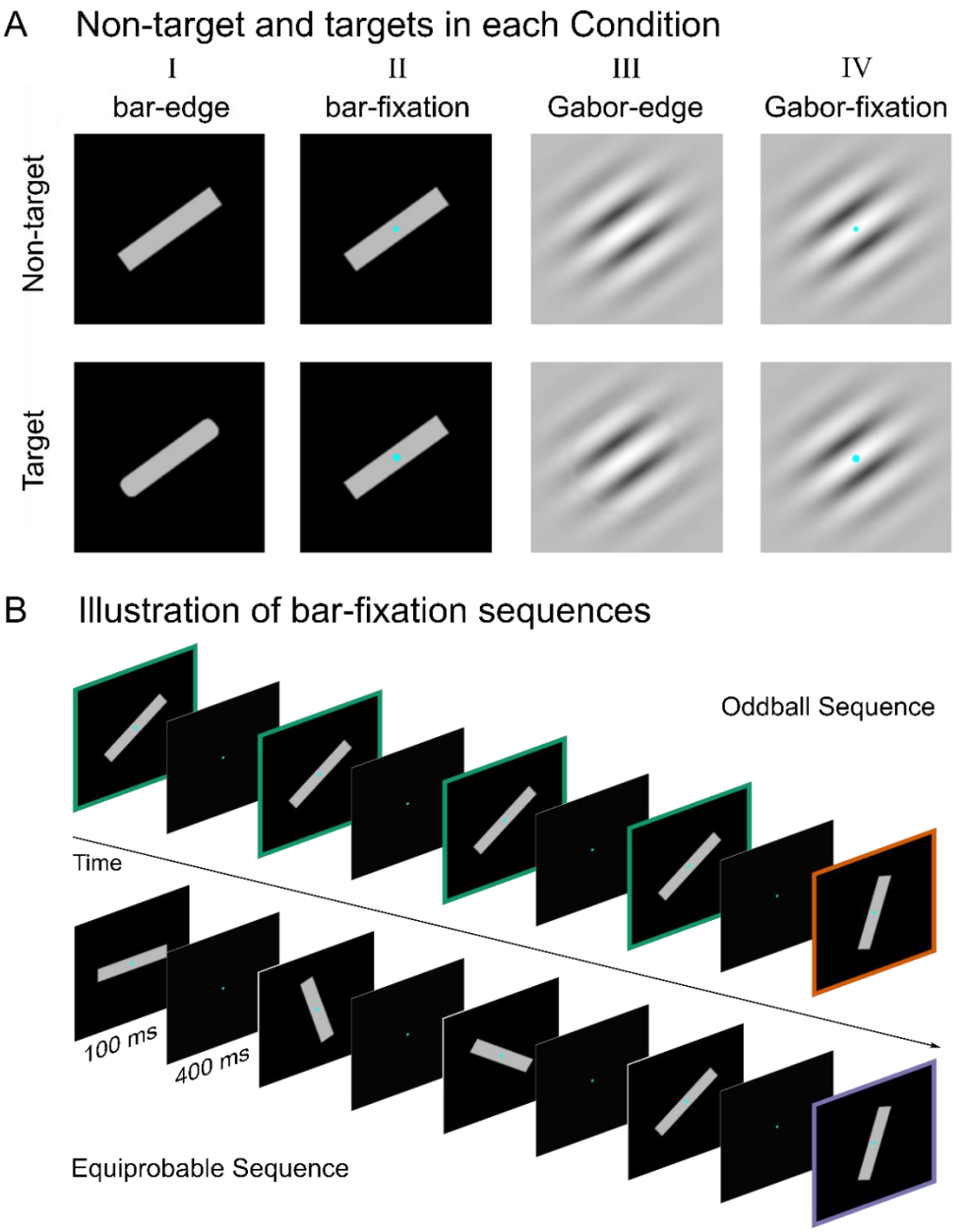


*Figure 6.1* Experiment 1. A. Examples of stimuli for the 2×2 design of Experiment 1. In this case, the orientation of non-target stimuli (top panel) and target stimuli (bottom panel) is 36° anticlockwise from horizontal, 0°. Stimuli were either bars (left two columns: I and II) or Gabor patches (right two columns: III and IV). Participants either paid attention to the edges of the stimuli (edge task: columns I and III) or to a fixation dot (fixation task: columns II and IV). B. Example of an oddball and an equiprobable-control sequence for the bar-fixation condition. The deviant (in orange) and control (in purple) have a probability of 20%. In the oddball sequence, the standards (in green) have a probability of 80%.

instructed them to keep their eyes in the centre of the screen (as Kimura et al., 2009, did).

### 6.3.1 Method

#### 6.3.1.1 Participants

Using G*Power (Faul, Erdfelder, Lang, & Buchner, 2007; Faul, Erdfelder, Buchner, & Lang, 2009), we estimated the sample size needed to achieve a power of .9 given the effect size found by Kimura et al. (2009): 5 participants. To optimize the likelihood of finding their effect, we tested 24 self-declared healthy adults (10 males, 20 right-handed) with normal or corrected-to-normal vision for a power of .99. Mean age was 24.20 years with a range from 19 – 49. The Murdoch University Ethics Committee approved the experiments (2015/208). All participants provided their written informed consent and were free to withdraw from the experiment at any time. Participants received monetary compensation or course credit in return for participation. The experiment took place in the BioCog laboratories of Leipzig University.

#### 6.3.1.2 Apparatus

Participants sat in an electrically shielded, sound-attenuated, light-attenuated chamber. They viewed stimuli on a photometrically linearized, 19-inch, colour, CRT monitor (Viewsonic G90fB) from 60 cm. The monitor showed 1024×768 pixels at a refresh rate of 100 Hz; it was the only source of light. A forehead-and- chin rest stabilized participants' heads. Participants gave their responses by pressing a key on a 4-key response pad connected to a response

registration device (RTBox; Li, Liang, Kleiner, & Lu, 2010). A PC with Ubuntu Linux v16.04.1, Octave v4.0, and Psychophysics Toolbox 3.0.14 (Brainard, 1997; Kleiner, 2013; Pelli, 1997) presented stimuli and recorded responses. We used an EyeLink 1000 (SR Research, Ottawa, Ontario, Canada) remote eye-tracker.

#### 6.3.1.3 Stimuli

In two conditions, we presented bar stimuli; in the remaining two conditions, we presented Gabor stimuli. For the bar stimuli, we used the original stimuli from Kimura et al. (2009): rectangular grey bars with a length of 3° visual angle and a width of 0.5° visual angle. The bars had a luminance of 41.7 candles per square meter (cd/m$^2$) (Kimura et al., 2009: 42 cd/m$^2$) on a black background with a luminance of 0.01 cd/m$^2$. This gave them a Michelson contrast greater than .99. Non-target bars had right-angled corners at their ends; target bars had rounded corners (Figure 6.1A, I).

Gabor patches comprised a grating with a Michelson contrast of .99, a phase of 0.5π radians (i.e., a white peak at the centre of the monitor), a spatial frequency of 1 cycle per degree (cpd) of visual angle, a mean luminance of 41.8 cd/m$^2$, and a peak luminance of 83.8 cd/m$^2$. The background had the same mean luminance. The Gaussian envelope had a standard deviation (SD) of 1° visual angle.

Target Gabor patches in the edge condition had a circular, raised-cosine-window-shaped margin with a radius of 1.5° visual angle where the contrast was

reduced from full to 30% over 0.33°. It appeared as a grey ring (Figure 6.1A, III). Bar and Gabor stimuli had an orientation of 0°, 36°, 72°, 108°, or 144° clockwise from horizontal.

In the fixation conditions, bars and Gabor patches had a central, cyan, circular fixation dot with a diameter of 0.13° visual angle and a luminance of 33.1 cd/$m^2$ for the bars and 64.2 cd/$m^2$ for the Gabor patches (Figure 6.1A, II and IV). Target fixation dot size was 0.26° visual angle. In the edge conditions, there was no fixation dot.

#### 6.3.1.4 Procedure

There were two stimulus and two task conditions each, arranged in a 2×2 design giving four conditions (see Figure 6.1A). We counter-balanced the order of conditions across participants.

Each condition started with written instruction and consisted of 12 blocks each taking 55 s to complete 110 trials. Participants were free to take breaks between blocks. To complete all 48 blocks took an average of 44 minutes. Ten of the 12 blocks per condition were oddball blocks and 2 were equiprobable control blocks. We randomized block order within each condition afresh for each participant and condition. Oddball blocks had 80% of standard trials and 20% of deviant trials (see Figure 6.1B).

Standard and deviant trials were pseudo-randomized for each participant and block except that at least two standards separated deviants. Each of the five possible orientations represented a standard orientation in two of the oddball

blocks. The deviant orientation was +36° from that of the standards in one block and –36° in the other block. Equiprobable blocks contained 20% each of the five possible orientations in pseudo-randomised order: there were no repetitions of orientation within these blocks.

Stimulus-onset-asynchrony (SOA) was 500 ms, featuring a 400 ms inter-stimulus-interval (ISI). In fixation conditions, the fixation dot was always present (see Figure 6.1B). All stimuli appeared at the centre of the screen. We instructed participants to look at the centre of the screen during all trials, whether there was a fixation dot or not. The first block of each condition and any blocks following a break began with a 9-point eye-tracker calibration and validation routine.

In all conditions, 9% of the stimuli (8 standards, 2 deviants in oddball blocks; 10 in equiprobable blocks) were targets. We asked participants to press a key as fast as possible with the index finger of the right hand whenever they detected a target. For a response to be correct, it had to be between 100 and 800 ms after target onset. There were always at least two non-target trials between target trials, but we did not explicitly inform participants about this contingency. In fixation conditions, fixation dot increments had a duration of 100 ms with a random onset asynchrony of 50, 150, 250, 350, or 450 ms from stimulus onset. There were equal numbers of the different onset asynchronies. Participants completed all the blocks for one condition before moving onto another.

#### 6.3.1.5 Eye tracking recording and analysis

The participant's head was stabilized. The eye-tracker monitored gaze positions of both eyes at a sampling rate of 500 Hz. We analysed gaze position at stimulus onset for standard, deviant, and control stimuli in each condition. We excluded gaze data for the first two stimulus events in each block, for target trials, and for trials that immediately followed a target or deviant stimulus. To correct for any systematic bias of the eye-tracker, we calculated the median of gaze position in bar-fixation condition and the median of gaze position in Gabor-fixation using standard and deviant trials in oddball blocks per eye and participant. We then corrected the gaze position by the mean of these two medians in all conditions.

We averaged gaze data over eyes and normalized data across trials by rotating gaze data by the degrees of difference between the bar's orientation (in a trial) and a bar stimulus with an orientation of 36° anticlockwise from horizontal. We excluded from further analysis blinks and eye movements—any gaze positions horizontally or vertically exceeding +/–3° visual angle from fixation. We computed probability density maps for each condition and block type by accumulating gaze positions across trials and blocks per condition and block type normalized by the number of included trials. We filtered probability density maps by a Gaussian kernel with an SD of 0.25° visual angle.

#### 6.3.1.6 EEG recording and analysis

We recorded the electroencephalogram (EEG) from 29 silver-silver chloride electrodes attached to an electrode cap (actiCAP). We placed electrodes

at AF3, AF4, F3, Fz, F4, F5, F6, FC1, FC2, FC5, FC6, C3, Cz, C4, T7, T8, CP1, CP2, CP5, CP6, P3, Pz, P4, P7, P8, O1, and O2 according to the extended international 10–20 system and at the left and right earlobe. We recorded EEG at a 500 Hz sampling rate and a time constant of 10 s with a BrainAmp DC system (Brain Products, Gilching, Germany). We recorded the electrooculogram (EOG) from electrodes placed lateral to the outer canthi of both eyes and an electrode placed below the left eye. Impedances were kept below 20 kΩ. We placed the ground electrode on the upper forehead and the reference electrode on the nose-tip (same as Kimura et al. 2009).

We completed pre-processing using MATLAB (2015b; MathWorks Inc.), EEGLAB (14.1.1; Delorme & Makeig, 2004), and ERPLAB (6.1.4; Lopez-Calderon & Luck, 2014). We filtered the continuous EEG and EOG activity with a high-pass 0.1 Hz Kaiser-windowed (beta 5.65) sinc FIR filter (order 9056) and low-pass 40 Hz Kaiser-windowed (beta 5.65) sinc FIR filter (order 184). Epochs were 500 ms long, including a 100 ms pre-stimulus baseline. We excluded the first two trials in each block, target trials, trials that immediately followed a target, trials that immediately followed a deviant stimulus, and epochs including amplitude changes exceeding 800 μV at any channel excluding EOG channels.

We identified noisy channels using the technique recommended by Bigdely-Shamlo, Mullen, Kothe, Su, and Robbins (2015). That is, we excluded channels with unusually high deviations in EEG activity (calculated as a z score exceeding 3.0 with a standard deviation of 0.7413 times the interquartile range). This affected no more than 3 electrodes per participant in 7 participants.

We corrected data for artifacts using independent component analysis (ICA) with AMICA (Palmer, 2015). To improve the decomposition, we computed the ICA on the raw data (excluding bad channels) filtered by a 1-Hz high-pass (Kaiser windowed sinc FIR filter, order 804, beta 5.65) and 40 Hz low-pass filter and epoched, but not baseline corrected (Groppe, Makeig, & Kutas, 2009). We then applied the obtained de-mixing matrix to the 0.1−40 Hz filtered data. Winkler, Debener, Müller, and Tangermann (2015) have validated that high-pass filters improve ICA decompositions (reliability, independence, and dipolarity) and the de-mixing matrix can be applied to a linearly transformed dataset.

We removed artifactual independent components from each participant's data by using SASICA (Chaumon, Bishop, & Busch, 2015; Makeig, Bell, Jung, & Sejnowski, 1996) to determine which exhibited low autocorrelation, low focal channel or trial activity, high correlation with vertical or horizontal EOG, or met ADJUST criteria (Mognon, Jovicich, Bruzzone, & Buiatti, 2011). We manually removed artifactual components using Chaumon et al.'s (2015) criteria, retaining those with any sign of neural activity based on consistent activity time-locked to stimulus onset, on topography, or on a 1/f-like power spectrum.

We next excluded any epochs containing amplitude changes exceeding ±100 μV at any channel. We interpolated noisy channels using spherical splines (Perrin, Pernier, Bertnard, Giard, & Echallier, 1987). We averaged event-related potentials (ERPs) separately for the standard, deviant, and control stimuli in each condition. The average number of epochs in each ERP appears in Table 6.2.

We then subtracted ERPs to controls and ERPs to standards from ERPs to deviants to produce a deviant-minus-control difference wave, revealing the genuine vMMN, and a deviant-minus-standard difference wave, revealing the classic vMMN.

Table 6.2 *Mean Number (Standard Deviation) of Epochs per Participant in the Grand Average ERP for each Condition and Type of Trial*

| Condition | Standard | Deviant | Control |
|---|---|---|---|
| bar-edge | 495 (19) | 194 (6) | 171 (5) |
| bar-fixation | 488 (28) | 190 (8) | 169 (8) |
| Gabor-edge | 486 (33) | 188 (15) | 167 (12) |
| Gabor-fixation | 484 (34) | 188 (13) | 168 (9) |

We conducted temporal principal component analysis (PCA) on the ERP data using the EP toolkit (v2.64; Dien et al., 2007). The structure of exogenous components was considerably different between bar and Gabor conditions. Therefore, we conducted PCA separately for bar and Gabor conditions on the individual average ERP data in deviant and control trials. We used Promax rotation ($\kappa = 3$) with a covariance relationship matrix and Kaiser weighting. Based on Horn's (1965) parallel test, we retained 12 components, explaining more than 95% of the variance.

To examine the probability of obtaining our data given a large effect size prior (informed from Kimura et al., 2009), we performed Bayes Factor replication tests (Verhagen & Wagenmakers, 2014) on the mean amplitudes between 200 and 250 ms at P7 and P8 (as in Kimura et al., 2009). We also

performed repeated-measures Bayesian analysis of variances (ANOVAs)[9]; Bayesian paired *t*-tests; traditional repeated-measures ANOVAs and paired *t*-tests on deviant-related amplitude differences in component scores at sites of component peak (e.g., P8 and O2). All *t*-tests are two-tailed unless explicitly stated and all Bayesian analyses are calculated using a medium effect size prior unless explicitly stated. We employed the Greenhouse-Geisser correction (ε) for degrees of freedom where appropriate. Eta squared ($\eta^2$) denotes the estimated effect size.

### 6.3.1 Results

#### 6.3.1.1 Behavioural performance

Over both tasks, mean hit rates were 88% (SD ±5%) and false alarm rates were 0.33% (SD ±0.32%). To determine whether there were any differences in task performance, we performed paired *t*-tests and Bayesian *t*-tests on hit rates and false alarm rates. Hit rates were marginally better for the edge task (90% ±7%) than for the fixation task (85% ±6%), $t$ (23) = 2.759, $p$ = .011, $BF_{10}$ = 4.409; there was no difference in false alarm rates between the two tasks (0.37% ±0.34% and 0.29% ±0.38%), $t$ (23) = 1.266, $p$ = .218, $BF_{10}$ = 0.437. The

[9] The model with the largest Bayes Factor ($BF_{10}$) is the *favoured model*. The main effects and interactions within such a model are therefore important for explaining the data. The inclusion Bayes Factor ($BF_{Incl.}$) is the extent to which the data support inclusion of the factor of interest. The $BF_{Incl.}$ compares the posterior probability of matched models including versus excluding the effect or interaction. We took as moderate evidence for the alternative hypothesis (and against the null hypothesis) if $BF_{10}$ was larger than 3, or strong evidence if $BF_{10}$ was larger than 10 (Lee & Wagenmakers, 2013). $BF_{10}$ between 0.33 and 3 provide weak evidence. $BF_{10}$ less than 0.33 provide substantial, and $BF_{10}$ less than 0.1 strong, evidence for the null model.

differences in hit rates are unlikely to have affected the ERPs because we excluded trials including targets or responses.

In our experiment, the difference between hit rates in standard and deviant trials in the bar-edge condition was –0.3% (standard trials: 92.2% ±7.0%, deviant trials: 92.5% ±7.0%). In Kimura et al.'s experiment, the difference was 4.2% (standard trials: 93.1% ±6.2%, deviant trials: 88.9% ±14.8%). The difference between false alarm rates in standard and deviant trials was –0.3% in our bar-edge condition (standard trials: 0.3% ±0.3%, deviant trials: 0.6% ±0.9%) and –0.6% in Kimura et al.'s (standard trials: 0.1% ±0.2%, deviant trials: 0.7% ±0.8%).

#### 6.3.1.2 Eye movement behaviour

In Figure 6.2 we show probability density maps for the fixation positions for all trials accumulated across all participants according to block type (oddball vs. equiprobable control), stimulus (bar vs. Gabor), and task (edge vs. fixation). Figure 6.2 shows that task and stimulus type predict gaze position. If participants followed the instructions to look at the centre of the stimuli, the majority of eye positions should be there, but this is true only when we had the central fixation task. When the participants' task was at the edge of the stimuli, their eye positions were more variable.

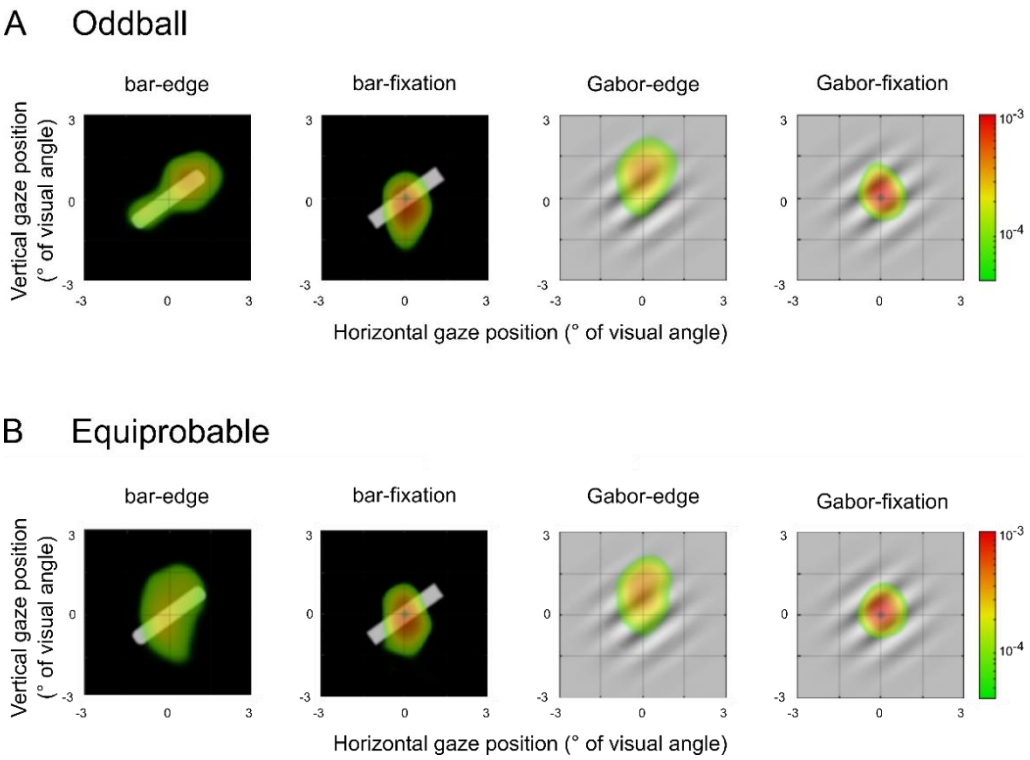


*Figure 6.2* Probability density maps for aggregated gaze data from all participants in Experiment 1. Coordinates for all accepted trials from each condition are standardized relative to individual gaze position and the orientation of an example stimulus (illustrated). Colours reflect the probability of that location being fixated at stimulus onset across trials in this condition. A. Results from oddball trials. B. Results from equiprobable control trials.

#### 6.3.1.3 Event-related potentials (ERPs) and difference waves

Figure 6.3 shows the ERPs and difference waves for each condition. Our ERPs are typical of ERPs recorded from the parieto-occipital regions on the scalp in other vMMN studies (e.g., Kimura & Takeda, 2015). We show the canonical ERP components at the P8 electrode Gabor-fixation condition in Figure 6.3.

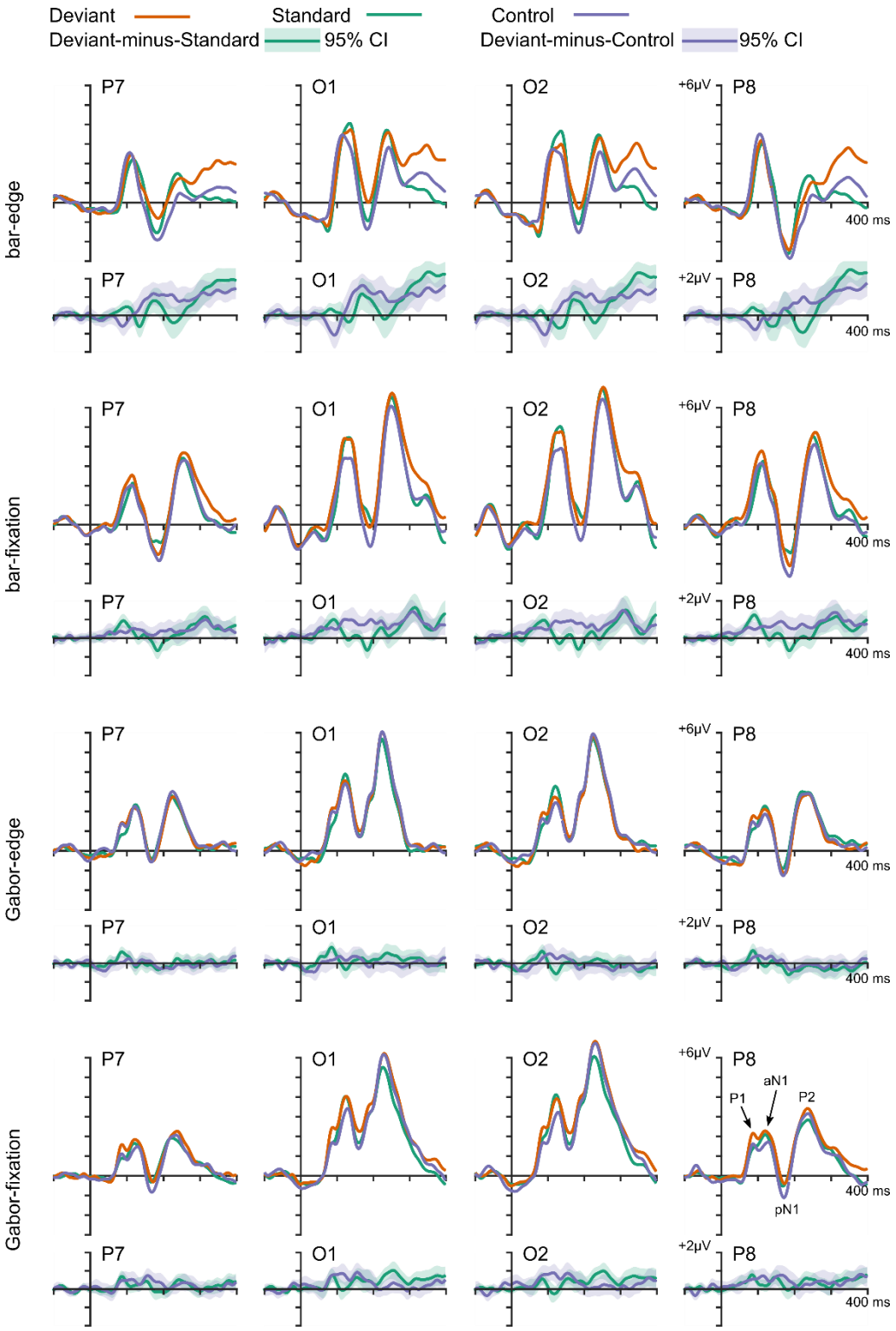


*Figure 6.3* ERPs and difference waves from P7, O1, O2, and P8 electrodes from Experiment 1. We illustrate the P1, positive pole of the anterior N1 (aN1), posterior N1 (pN1), and P2 at P8 electrode, Gabor-fixation condition.

The difference waves in Figure 6.3 are green for deviant-minus-standards and purple for deviant-minus-controls. The figure also shows the 95% confidence intervals. The green traces show some negativities in the vMMN time-window (100–300 ms), especially from electrode P8 from the bar-edge condition; these could be classic vMMNs (i.e., contributed to by adaptation).

Purple traces are positive for the entire vMMN time-window for bars and fluctuate randomly around zero for Gabor patches, showing no genuine vMMN (i.e., free from adaptation). We did not anticipate the early positivity commencing about 80 ms after stimulus onset that was larger for deviants than for controls at occipital electrodes in our fixations and bar-edge conditions. We explore this later.

***VMMN in the bar-edge condition (replication of Kimura et al., 2009)***

We conducted the relevant one-tailed *t*-tests reported by Kimura et al. (2009) (i.e., always testing for a negativity). We summarise these for key electrodes in Table S3 for the 100–150-ms time window and in Table S4 for the 200–250 ms time window. In contrast to Kimura et al., we did not find a genuine vMMN in that or any other electrode for the same (200–250 ms) time window. Instead, there was a positive difference potential[10].

Given the very large effect size reported by Kimura et al., the data provide strong evidence for the null hypothesis in Bayes Factor replication tests. The data also provide strong evidence for the null hypothesis when employing the

[10] PCA results suggest the enhanced positivity is due to enhanced P2, PCA component 1, peak latency 262 ms, and P3 related components, PCA components 4 and 7, peak latencies 320 and 370 ms, to deviant compared to control stimuli.

default medium effect size prior in a directed Bayesian *t*-test. We found similar results in a separate analysis of data in which we replicated Kimura et al.'s ERP analysis pipeline as closely as possible (Table S5 and S6).

***VMMN in the bar-fixation task***

In the bar-fixation task condition there was a similar positive deviant-minus-control mean difference potential in the vMMN time-window at the selected electrode locations. Once again, the data provide strong evidence for the null hypothesis in Bayes Factor replication tests (P7: $BF_{r0}$ = 0.002, P8: $BF_{r0}$ = 0.0005) and directed Bayesian *t*-tests, one-tailed; P7: 0.39 µV, $t$ (23) = 1.567, $p$ = .935, $BF_{10}$ = 0.093; P8: 0.62 µV, $t$ (23) = 2.293, $p$ = .984, $BF_{10}$ = 0.074.

***VMMN in the Gabor-edge task***

In the Gabor-edge task condition there was a small and statistically non-significant negative deviant-minus-control mean difference potential at the vMMN time-window and electrode locations. The data provide strong evidence for the null hypothesis in Bayes Factor replication tests (P7: $BF_{r0}$ = 0.110, P8: $BF_{r0}$ = 0.003), but do not provide conclusive evidence in directed Bayesian *t*-tests, one-tailed; P7: –0.20 µV, $t$ (23) = –1.575, $p$ = .065, $BF_{10}$ = 1.171; P8: –0.13 µV, $t$ (23) = –0.625, $p$ = .269, $BF_{10}$ = 0.370.

***VMMN in the Gabor-fixation task***

In the Gabor-fixation task condition there was a similar small positive deviant-minus-control mean difference potential in the vMMN time-window and electrode locations. The data provide strong evidence for the null hypothesis in Bayes Factor replication tests (P7: $BF_{r0}$ = 0.002, P8: $BF_{r0}$ = 0.0005) and

substantial evidence for the null hypothesis in directed Bayesian *t*-tests, one-tailed; P7: 0.15 µV, $t$ (23) = 0.751, $p$ = .770, $BF_{10}$ = 0.133; P8: 0.18 µV, $t$ (23) = 0.790, $p$ = .781, $BF_{10}$ = 0.130.

***Outside the vMMN time-window***

Outside the vMMN time-window, we did not observe any relevant negative deflections of the deviant-minus-control ERP difference wave exceeding the 95% confidence interval (except for the P1 effect in the bar-edge condition; see below and Figure 6.4). To detect any potential vMMN PCA component we computed ANOVAs for all components with a peak latency between 100 and 300 ms and a negative deviant minus control difference score in at least one condition or task at the peak electrode location—often parieto-occipital electrode. We did not find any significant main effect of stimulus type or interaction effect including stimulus type (all $BF_{10} < 0.5$; except for P1 in the bar conditions; see below). Although we did not identify any component that was temporally or spatially characteristic of the vMMN, we did find some PCA components sensitive to deviants.

#### 6.3.1.4 Principal components analysis (PCA)

PCA of the data confirmed early differences in amplitude seen in our ERPs (80–200 ms in Figure 6.3). Figure 6.4 shows that the temporal and topographical profiles of the P1 and N1 components were different between bar and Gabor conditions. In the bar conditions, the P1 component had a peak latency of 110 ms (maximal over parieto-lateral electrodes). An anterior N1 component with a peak latency of 146 ms (minimal over fronto-central electrodes and maximal over occipito-lateral electrodes) and a posterior N1 component with a peak

latency of 200 ms (minimal over parieto-lateral electrodes and maximal over fronto-central electrodes) followed. In the Gabor conditions, the P1 peak latency was 86 ms (maximal over occipito-lateral electrodes), an anterior N1 component with a peak latency of 126 ms (minimal over fronto-lateral electrodes and maximal over occipito-lateral electrodes), and a posterior N1 component with a peak latency of 170 ms (minimal over parieto-lateral and maximal over occipito-lateral electrodes) followed.

***P1***

In the bar conditions, we found an interaction between task and stimulus type, $F$ (1, 23) = 9.339, $p$ = .006, $\eta^2$ = .289, $BF_{Incl}$ = 1.641. Paired tests revealed marginally smaller P1 (PCA component 5) amplitudes for deviants than for controls in the edge task, $t$ (23) = –1.808, $p$ = .084, $BF_{10}$ = 0.872, but significantly larger P1 amplitudes for deviants than controls in the fixation task, $t$ (23) = 2.781, $p$ = .011, $BF_{10}$ = 4.600 (see Figure 6.4 top panel, left). Possibly, an unpredicted input (i.e., a deviant) yields a larger P1 than the predicted input (i.e., the standard), but only when the attention and fixation is well controlled, for example, when gaze is less variable—as in the fixation condition (cf. Figure 6.3).

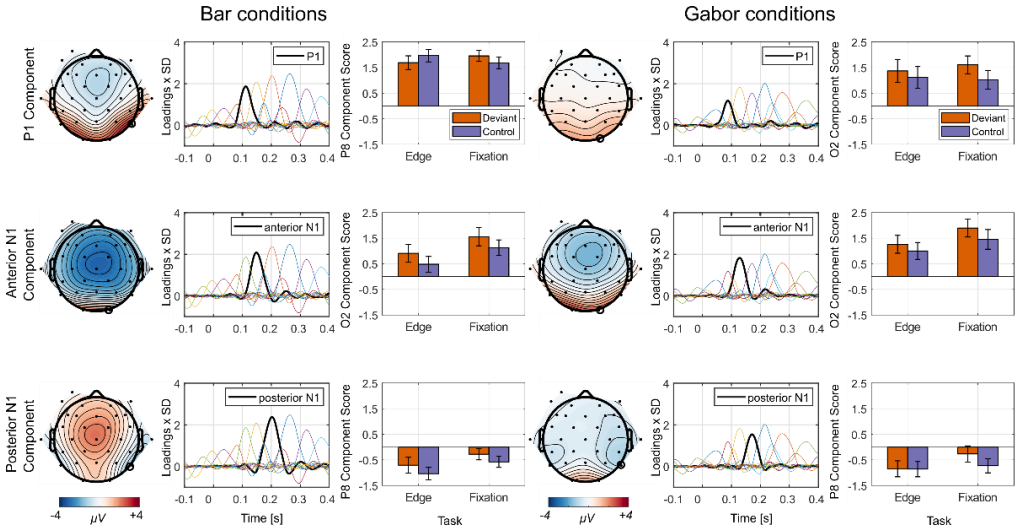


*Figure 6.4* Principal components contributing to early increased positivity in deviant-minus-control difference wave for bar and Gabor conditions in Experiment 1. The top row shows details of the P1 in the bar (left three panels) and Gabor (right three panels) conditions. The middle row shows details of the anterior N1 in the same conditions. The bottom row shows details of the posterior N1. Columns 1 and 4 show topographical maps of the average activity from deviant and control trials at peak latency. Columns 2 and 5 show component loadings (scaled by SD) against the time course of each component's contribution (thick black line) to the overall evoked activity recorded from the scalp relative to all other components (thin multi-coloured lines). Columns 3 and 6 show component scores for deviant and control trials in each stimulus and task condition at the electrode illustrated on the corresponding topographical map. Error bars depict ±1 standard error.

In the Gabor conditions, P1 (PCA component 7) amplitudes were larger for deviants than controls, however, the data do not provide conclusive evidence for the favoured model including the stimulus type main effect, $F$ (1, 23) = 4.463, $p$ = .046, $\eta^2$ = .163, $BF_{10}$ = 1.332 (see Figure 6.4 top panel, right).

### *Anterior N1*

In the bar conditions, at occipital electrodes, the anterior N1 (PCA component 3, shown as aN1 in Figure 6.3) amplitude was more positive in the fixation task than in the edge task, $F$ (1, 23) = 10.984, $p$ = .003, $\eta^2$ = .323. Amplitudes were also more positive for deviants than for controls, $F$ (1, 23) = 11.576, $p$ = .002, $\eta^2$ = .335 (see Figure 6.4, middle panel, left). The data provide strong evidence for the favoured model including both main effects ($BF_{10}$ =

2619.138) as well as substantial evidence against a moderation of the stimulus type effect by the task ($BF_{Incl}$ = 0.319).

Also, in the Gabor conditions, at occipital electrodes, the anterior N1 (PCA component 3) amplitudes were more positive in the fixation task than in the edge task, $F$ (1, 23) = 8.281, $p$ = .009, $\eta^2$ = .265, and for deviants than for controls, $F$ (1, 23) = 16.834, $p$ < .001, $\eta^2$ = .423 (see Figure 6.4, middle panel, right). The data provide strong evidence for the favoured model including both main effects ($BF_{10}$ = 537.932) as well as substantial evidence against a moderation of the stimulus type effect by the task ($BF_{Incl}$ = 0.345).

As a result, the data show that the stimulus type (i.e., deviant vs. control) determines anterior N1 positivity at occipital electrodes with deviants producing larger positivities than controls and this occurs for bar and Gabor stimuli regardless of the task, because task did not moderate the effect for either.

***Posterior N1***

In the bar conditions, the posterior N1 (PCA component 2) amplitude was more positive in the fixation task than in the edge task, $F$ (1, 23) = 6.189, $p$ = .021, $\eta^2$ = .212, and more positive for deviants than for controls, $F$ (1, 23) = 6.947, $p$ = .015, $\eta^2$ = .232 (see Figure 6.4, bottom panel, left). The data provide strong evidence for the favoured model including both main effects ($BF_{10}$ = 36.845) as well as substantial evidence against a moderation of the stimulus type effect by the task ($BF_{Incl}$ = 0.282).

In the Gabor conditions, we observed an interaction of stimulus type and task on the posterior N1 (PCA component 4) in the frequentist statistics, $F$ (1,

23) = 7.968, $p$ = .010, $\eta^2$ = .257. However, the Bayes factor analysis is inconclusive and rather provides weak evidence for this interaction ($BF_{Incl}$ = 0.525). The N1 amplitude was more positive for deviants compared to controls in the fixation task, $t$ (23) = 2.593, $p$ = .016, $BF_{10}$ = 3.226, but there was no difference between deviants and controls in the edge task, $t$ (23) = 0.124, $p$ = .903, $BF_{10}$ = 0.216 (see Figure 6.4, bottom panel, right). Further, the data do not provide conclusive evidence for any of the models (all $BF_{10}$ < 0.5).

### 6.3.1 Discussion

We could not find any convincing indication of a vMMN in any condition. This is particularly surprising because we replicated Kimura et al.'s (2009) stimuli and procedure in our bar-edge condition. There were three major differences in the method of the two studies:

1. We monitored participants' eye positions whereas Kimura et al. did not.
2. We also had the fixation (and Gabor) conditions whereas Kimura et al. did not.
3. We had a fewer control trials than Kimura et al. had.

#### 6.3.1.1 We monitored eye positions

We found that participants fixated on the centre of the stimuli when that was where their task was located, but participants' gaze positions were more variable in the edge task. In the Gabor-edge condition, gaze positions were altogether more variable and concentrated slightly off-centre, however, in the bar-edge condition, gaze positions tended to be widely spread around the bars.

Gaze position is also most different between control and oddball blocks in this condition. We suspect this is because gaze behaviour differed in each block type.

In oddball blocks, looking towards the bar's end would help target detection—the probability of looking at the correct location is high—whereas in the control blocks, looking towards the bar's end would not—the probability of looking at the correct location is low. This is because in the control blocks the orientation of the bars changed on every trial. The eyes would have been fruitlessly pursuing the location of the task-relevant information, always one trial behind its location. We suspect this is why, just from averaging, we see more central fixation in the control blocks compared with the oddball blocks in the bar-edge condition.

It seems that despite instruction, having the task-relevant information for bars at their ends was enough to cause participants' eyes to stray towards the bar ends on some trials, although the high variability suggests that participants did adhere to instruction on some trials. If our participants, who knew we were monitoring their gaze, looked strategically at different parts of the stimuli depending on the task, then it is quite possible that Kimura et al.'s participants, whose eye positions were not monitored, looked even more strategically than ours did, at the bar ends.

#### 6.3.1.2 We had other fixation (and stimulus) conditions

Our fixation conditions gave our participants practice at fixating centrally. This may well have transferred to our edge conditions, leading to more accurate central fixation than in Kimura et al.'s participants.

Consider the stimuli during the oddball sequence for Kimura et al.'s participants if they consistently looked at the bar ends. During the standard trials, a grey bar-end filled their foveas. We define the fovea as "the cross diameter … from foveal rim to foveal rim" (Kolb, Fernandez, & Nelson, 1997). During deviant trials, the black background filled the fovea. This turns an orientation deviant into a large decrement in luminance for the fovea. About 50% of the area of the visual cortex is devoted to processing input from the fovea, which will, therefore, have a much greater influence on ERPs than that processing the remaining 99.84% of the area of the retina (Kolb, Fernandez, & Nelson, 2018). This combined change in orientation and luminance may be sufficient for yielding the vMMN while a change in orientation alone is not.

Possibly our participants did not show a vMMN because we assume they fixated more centrally on more trials than Kimura et al.'s did. We discuss below why we think our participants did not show an orientation vMMN.

The observation of considerable differences between hit and false alarm rates in standard and deviant trials in the bar-edge condition in our experiment compared to the original experiment by Kimura et al. (2009) supports our interpretation of differences in fixation behaviour. With increasing gaze eccentricity along the bar, the hit rate is expected to increase in standard trials due to higher discriminability as the bar end moves towards the fovea but to decrease for deviant trials and vice versa for the false alarm rate. This is the pattern we observe in the data. The remarkably high inter-individual variability of the hit rate in deviant trials in Kimura et al.'s study might indicate that participants' fixation behaviour possibly followed different strategies.

Other studies of the orientation vMMN with bars might have involved a similar confounding of orientation with luminance, possibly explaining why some have found the vMMN using bar stimuli while others have not. For example, Astikainen et al. (2008), who did find a vMMN to bars, forced their participants to focus their attention on auditory stimuli, such that participants could have easily fixated on the ends of the bar stimuli. In contrast, File et al., who did not find a vMMN, used a demanding fixation task—thus, probably shielding participants from fixating on the ends of the bar stimuli.

#### 6.3.1.3 We had fewer control trials

We do not expect our lower number of control trials than Kimura et al.'s (2009) affected the vMMN measurement because signal-to-noise ratio (SNR) in the difference wave is limited by the condition with fewest trials. In Kimura et al. (2009) this is the deviant condition. The number of trials in our deviant ERP (maximum 200 trials) is about 67% of theirs (maximum 300 trials) and the SNR of our control ERPs is very good across all conditions. The Bayesian replication tests clearly support the notion that our failure to observe a vMMN was not due to lack of power or noise in the data. Furthermore, we were able to detect deviant-related differences in other components: the P1, anterior N1, and posterior N1.

We found that, except for the bar-edge condition, P1 amplitudes are larger for deviants than for controls. Perhaps the larger variance in gaze position (cf. Figure 6.2) disguised the true effect of deviants on P1 amplitudes. Of course, the variance in our post-hoc analyses of P1 amplitudes could be due to other factors we have not considered.

We also found that, according to our probabilistic and frequentist analyses, the positive pole of the anterior N1 is larger for deviants than controls and this is consistent across all conditions, suggesting it may be a reliable marker for deviance-related activity.

To examine whether vMMN can be observed for other properly isolated low-level visual features if controlled for adaptation effects and to conclude with greater certainty that our results were truly reflective of changes in low-level properties of visual stimuli, we conducted a second experiment.

## 6.4 Experiment 2

In addition to testing, again, whether orientation differences of 36° yield a vMMN, we also wanted to test other low-level differences. We searched for vMMNs for changes in orientation, Michelson contrast, phase, and spatial frequency. We carefully manipulated each low-level feature of visual input without affecting other features using Gabor patches. We compared ERPs to standards and deviants from multi-feature blocks and ERPs to control deviants from cascadic-control blocks (Ruhnau et al., 2012).

### 6.4.1 Method

Some aspects of the method of Experiment 2 were identical to those of Experiment 1, including the number of participants, inclusion criteria, the EEG apparatus, most properties of the Gabor patches, all properties of the fixation dots, the central fixation task, the EEG-recording, EEG pre-processing, and statistical analysis of the ERP data. The mean age of our 24 new participants was 23.13 years with a range of 18 – 38 years (9 males, 23 right-handed). The method

differed in that we used a multi-feature paradigm, a cascadic-control condition, and we did not measure participants' gaze positions.

#### 6.4.1.1 Stimuli

We manipulated the orientation, contrast, phase, and spatial frequency of the Gabor patches. In the multi-feature paradigm, standard Gabor patches had an orientation of 9° anticlockwise from horizontal, a Michelson contrast of .6, a phase of 0.5π radians, and a spatial frequency of 1.2 cpd of visual angle. Deviant stimuli had an orientation of 45° anticlockwise, or a Michelson contrast of .99, or a phase of 1.7π radians, or a spatial frequency of 0.9 cpd, but were identical to standard stimuli in all other features (see Figure 6.5A).

In the cascadic control, Gabor patches had an orientation of 45°, 9°, 333° (= 153°), 297° (= 117°), or 261° (= 81°) from horizontal (changing by 36° per trial), a Michelson contrast of .99, .6, .36, .22, or .13 (changing by 40% per trial), a phase of 1.7π, 0.5π, 1.3π, 0.1π, or 0.9π radians (changing by 1.2π radians per trial), and a spatial frequency of 0.9, 1.2, 1.6, 2.1, or 2.8 cpd visual angle (changing by 33% per trial).

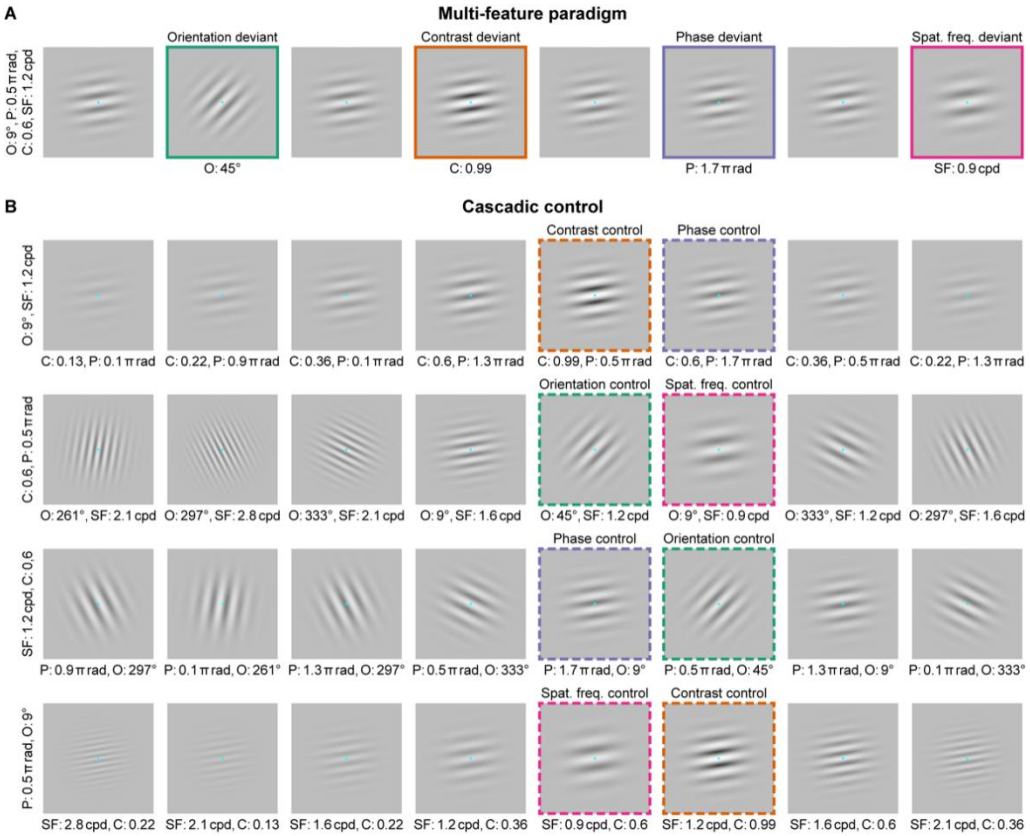


*Figure 6.5* Illustration of the stimuli and procedure of Experiment 2. A. Example of eight trials of a multi-feature block. The first panel shows the standard. The next panel, outlined in green, shows an orientation deviant (36° orientation difference from the standard). The next deviant panel, outlined in orange, shows a contrast deviant (.33 greater than the standard). The next deviant panel, outlined in violet, shows a phase deviant (1.2π radians difference from the standard). The final deviant panel, outlined in magenta, shows a spatial frequency deviant (33% less than the standard). B. Examples of eight trials of four kinds of cascadic-control blocks. The top row shows stimuli that change regularly in contrast and phase from trial to trial. The control stimuli for contrast and phase—physically identical to the deviants from the multi-feature blocks—are outlined in dashed orange and dashed violet. The remaining rows of panels show other combinations of stimulus features with stimuli that serve as controls for other deviants. The colour scheme is the same as in A. For each control stimulus, we show its orientation (O; °), Michelson contrast (C), phase (P; radians), and spatial frequency (SF; cpd).

#### 6.4.1.2 Procedure

The experiment started with written instruction and consisted of eight multi-feature blocks and eight cascadic-control blocks. We randomized block order. In the multi-feature blocks, standard and deviant stimuli appeared on alternate trials (Figure 6.5A). Each deviant feature appeared once per set of four standard/deviant pairs of trials in pseudo-randomized order with the constraint that the same deviant feature never appeared in two subsequent pairs of trials.

That is, for each set of eight stimuli, for each visual feature the local probability for the occurrence of a deviant was 12.5%, and of a standard 87.5% (similar to the regular oddball paradigm). In each of the multi-feature blocks, there were 128 standards and 128 deviants resulting in 256 deviants per visual feature.

In the cascadic-control blocks (illustrated in Figure 6.5B), we interspersed physically identical standard and control stimuli within a sequence in which the deviant stimulus feature was varied in a regular ascending and descending sequence (e.g., 1-2-3-4-5-4-3-2-1). We combined two features per block (contrast and phase, orientation and spatial frequency, phase and orientation, contrast and spatial frequency—see Figure 6.5(B). We did not combine phase and spatial frequency because both features would interact, obscuring regularity, and we did not combine contrast and orientation for a balanced design. The two-feature cascades had an offset of one trial: each feature led once in one of two blocks, resulting in eight cascadic-control blocks. This design allowed the corresponding multi-feature standard feature to precede each control stimulus. In each of the cascadic-control blocks, there were 256 stimuli including 32 control stimuli per feature resulting in 128 control stimuli per visual feature.

We included post-test blocks to assess the discriminability of each deviant stimulus in a two-interval, two-alternative, forced choice task. Participants were asked to look at the Gabor patches and to judge whether two successively presented Gabor patches were the same or different. Each Gabor patch was presented for 100 ms separated by an ISI of 400 ms. The fixation dot was always present. The next trial started 400 ms after the response. There were 128 pairs per block, 64 pairs were the same (both standard Gabor patches from the multi-

feature paradigm), and 64 pairs were different (16 per deviant feature from the multi-feature paradigm balanced between first and second interval). Participants responded by pressing a *same* button with the index finger of one hand and a *different* button with the index finger of other hand (counterbalanced across participants).

There was no reaction time limit for this task; however, we considered responses only between 0.1 and 2 s to remove instances in which participants took an impromptu break between trials. This resulted in a mean loss of about 2 trials in 19 participants (ranging from 1 to 8 trials) and none in the other five participants.

#### 6.4.1.3 EEG recording and analysis

In Table 6.3, we give the average number of epochs in each ERP for 24 participants. We performed PCA on the individual average ERP data in deviant and control trials. We retained 14 components (explaining more than 95% of the variance) based on Horn's (1965) parallel test.

Table 6.3 *Mean Number (Standard Deviation) of Epochs per Participant in the Grand Average ERP for each Deviant Feature and Trial Type*

| Condition | Standard | Deviant | Control |
|---|---|---|---|
| Orientation | { 784 (26) } | 196 (7) | 88 (11) |
| Contrast | | 197 (9) | 88 (9) |
| Phase | | 195 (8) | 88 (9) |
| Spatial Frequency | | 197 (10) | 88 (10) |

### 6.4.2 Results

#### 6.4.2.1 Behavioural performance

Performance on the fixation task for multi-feature (*hit rate:* 93% ±6%, *false alarm rate:* 0.75% ±0.65%) and cascadic blocks (*hit rate:* 93% ±6%, *false alarm rate:* 0.71% ±0.58%) was very similar: for hit rate, $t$ (23) = –.598, $p$ = .556, $BF_{10}$ = 0.253; for false alarm rate, $t$ (23) = .598, $p$ = .556, $BF_{10}$ = 0.253). Hit rates were high (93%) and false alarm rates were low (0.73%), showing that participants devoted themselves to the task.

To derive a d-prime (d′) for each deviant feature in our discriminability blocks we log-linear corrected (Stanislaw & Todorov, 1999). Sensitivity was worst for phase (d′ = 2.5 ±0.9 SD), better and about equal for contrast (d′ = 2.8 ±0.8) and spatial frequency (d′ = 2.8 ±0.7), and best for orientation (d′ = 3.5 ±0.7), $F$ (3, 69) = 23.913, $p$ < .001, ε = .929, $\eta^2$ = .510, $BF_{10}$ = 7.567e+7. All paired comparisons, aside for contrast versus spatial frequency, $t$ (23) = 2.781, $p$ = .854, $BF_{10}$ = 0.218, were significant. Overall performance accuracy (d′ = 2.8) suggests participants were able to perceive most deviants.

#### 6.4.2.2 Event-related potentials (ERPs) and difference waves

Figure 6.6 shows the ERPs and deviant-minus-control difference waves for each feature deviant. ERPs and their constituents to orientation conditions are similar to those of Experiment 1 (top panel). The ERPs to the other conditions are similar to those for orientation and to ERPs reported by others. We highlight the same ERP components at P8 in the orientation condition; these are the most similar across experiments.

***VMMN***

We did not find a vMMN in the 200–250 ms time-window (as in Kimura et al., 2009) in any of the four deviant feature conditions. Table 6.4 shows that the data provide very strong evidence for the null hypothesis. Instead, Figure 6.6 shows a positive deviant-minus-control mean difference potential in the vMMN time-window at P7 and P8 electrode locations for all four deviant feature conditions.

Table 6.4 *Directed Bayesian ($BF_{10}$) t-tests (one-tailed) of Mean Amplitudes (μV) between 200 and 250 ms at P7 and P8 Electrodes for Each Deviant Feature (df = 23)*

| | Electrode | | | | | | | |
|---|---|---|---|---|---|---|---|---|
| | P7 | | | | P8 | | | |
| **Condition** | **μV** | ***t*** | ***p*** | ***$BF_{10}$*** | **μV** | ***t*** | ***p*** | ***$BF_{10}$*** |
| Orientation | 0.28 | 1.554 | .933 | 0.093 | 0.25 | 1.199 | .879 | 0.107 |
| Contrast | 0.78 | 3.133 | .998 | 0.062 | 1.00 | 3.595 | .999 | 0.058 |
| Phase | 0.30 | 1.409 | .914 | 0.099 | 0.41 | 2.295 | .984 | 0.074 |
| Spatial Frequency | 0.98 | 4.988 | .999 | 0.049 | 1.16 | 5.905 | .999 | 0.046 |

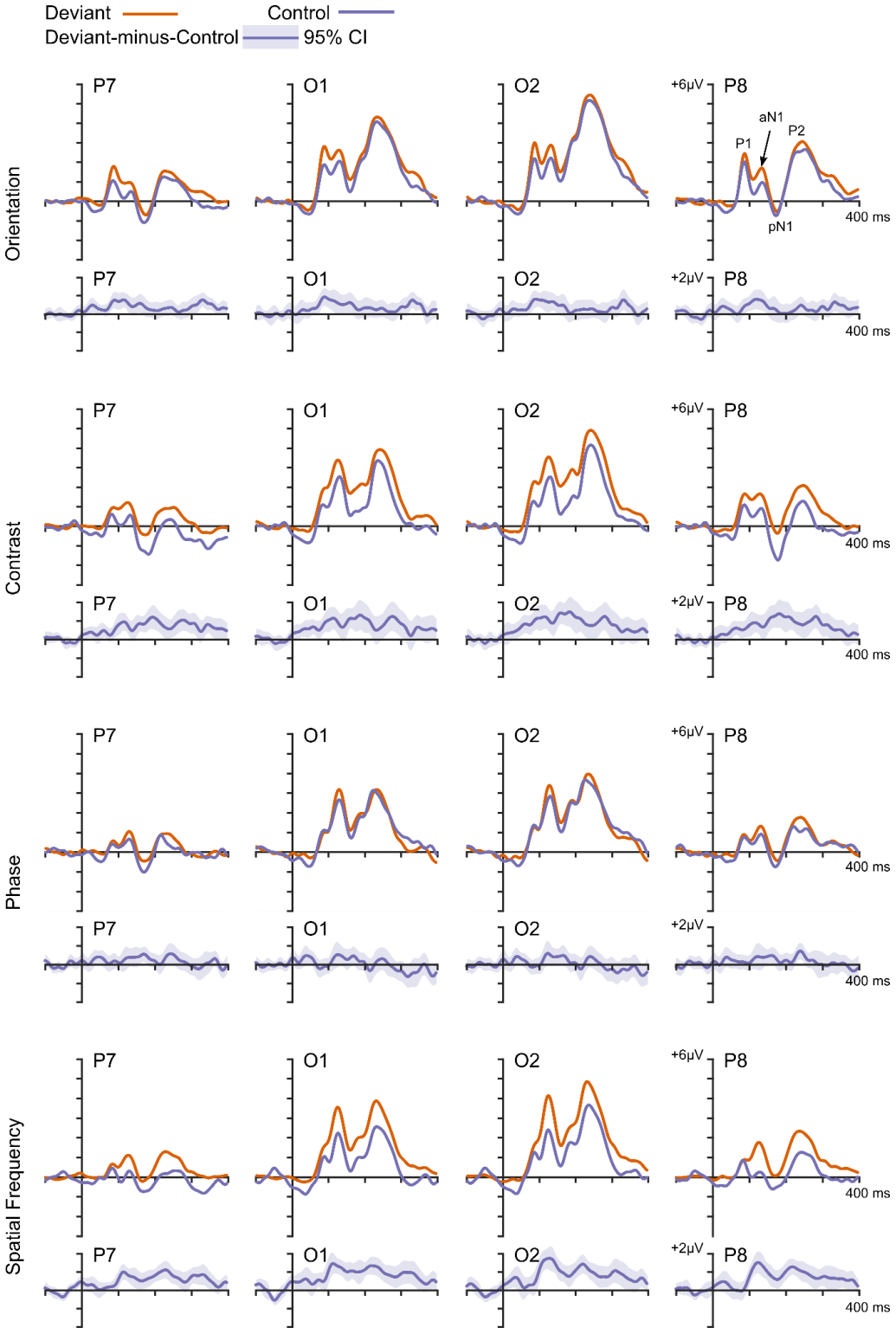


*Figure 6.6* ERPs and difference waves from P7, O1, O2, and P8 electrodes from Experiment 2. We did not observe any relevant negative deflections of the deviant-minus-control ERP difference wave exceeding the 95% confidence interval (but only positive).

#### 6.4.2.1 Principal components analysis (PCA)

***VMMN time-window***

To detect any potential vMMN PCA component we computed ANOVAs for all components with a peak latency between 100 and 300 ms and a negative deviant minus control difference score for at least one deviant feature at the occipito-parietal component peak electrode. We found a significant interaction between stimulus type and deviant feature in two components, but all follow-up tests were not significant (all $BF_{10} < 0.5$). We did not find any significant main effect of *stimulus type* or interaction effect including *stimulus type* in any other component (all $BF_{10} < 0.5$). That is, we did not find any PCA component corresponding to the vMMN.

Although we did not find a vMMN, we did observe increased early positivity to deviants compared with controls. Our PCA confirmed that this positivity was due to three separate components, as in Experiment 1. The components' structure and topography were highly similar to the ones observed in the Gabor conditions of Experiment 1. The peak latencies of P1 (94 ms), anterior N1 (132), and posterior N1 components (182 ms) were minimally later than in Experiment 1 (Figure 6.7).

***P1***

The P1 (PCA component 6) amplitude was more positive for deviants than for controls, $F$ (1, 23) = 15.209, $p < .001$, $\eta^2 = .398$, but the effect was modulated by an interaction with deviant feature, $F$ (3, 69) = 3.782, $p = .028$, $\varepsilon = 0.693$, $\eta^2$

= 0.141 (see Figure 6.7, top panel). All features, except for phase, produced a significant positive deviant minus control difference score (Table 6.5). However, the data provide very strong evidence for the favoured model including the main effect of stimulus types and deviant feature, $F$ (1, 23) = 2.831, $p$ = .045, $\eta^2$ = .110, $BF_{Incl}$ = 2.291 ($BF_{10}$ = 288.813). The data provide inconclusive evidence against including any interaction between stimulus type and deviant feature ($BF_{Incl}$ = 0.807).

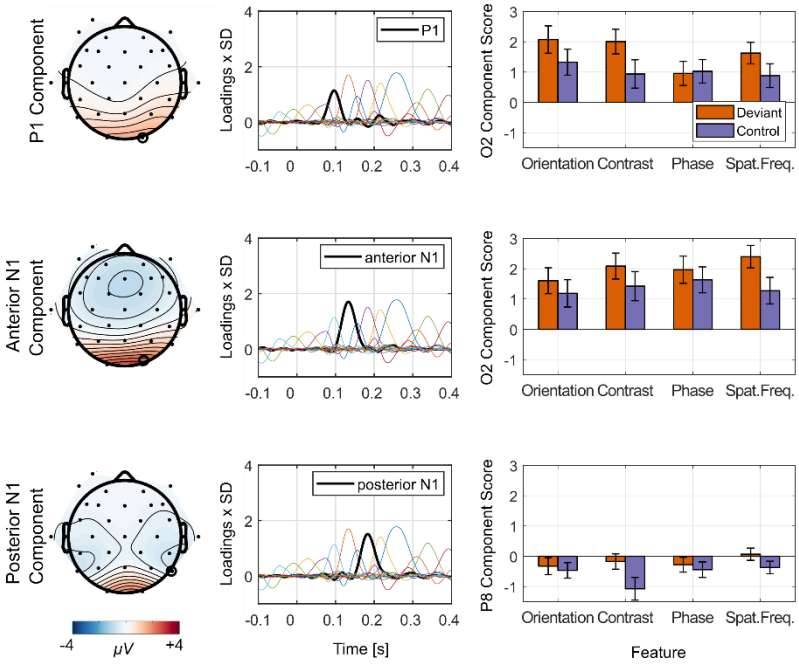


*Figure 6.7* Principal components contributing to early increased positivity in deviant-minus-control difference waves in Experiment 2. The top panel shows details of the P1. The middle panel shows details of the anterior N1. The bottom panel shows details of the posterior N1. The leftmost column shows topographical maps of combined activity from deviant and control trials at peak latency. The middle column shows loadings of each component's contribution (thick black line) to the overall evoked activity recorded from the scalp relative to all other components (thin lines of different colours). The rightmost column shows bar graphs of component scores for deviant and control trials for each deviant feature at the electrode illustrated on the corresponding topographical map. Error bars depict ±1 standard error.

Table 6.5 *Interactions with Deviant Feature examined with Paired Sample and Bayesian ($BF_{10}$) t-tests (two-tailed) for the P1, anterior N1 (aN1), and posterior N1 (pN1) (df = 23)*

| Deviant Feature | Electrode | *t* | *p* | $BF_{10}$ |
|---|---|---|---|---|
| P1 | | | | |
| Orientation | O2 | 3.378 | .003 | 15.313 |
| Contrast | O2 | 3.411 | .002 | 16.394 |
| Phase | O2 | -0.345 | .733 | 0.227 |
| Spatial Frequency | O2 | 2.328 | .029 | 2.005 |
| aN1 | | | | |
| Orientation | O2 | 2.720 | .012 | 4.095 |
| Contrast | O2 | 3.527 | .002 | 20.967 |
| Phase | O2 | 1.839 | .079 | 0.913 |
| Spatial Frequency | O2 | 5.908 | < .001 | 4040.549 |
| pN1 | | | | |
| Orientation | P8 | 0.704 | .489 | 0.269 |
| Contrast | P8 | 3.820 | < .001 | 39.248 |
| Phase | P8 | 1.198 | .243 | 0.406 |
| Spatial Frequency | P8 | 2.824 | .010 | 5.002 |

### *Anterior N1*

The anterior N1 (PCA component 2) amplitude at occipital electrodes was more positive for deviants than controls, $F$ (1, 23) = 33.139, $p < .001$, $\eta^2 = .590$ (see Figure 6.7, middle panel). Similar to the P1, this main effect interacted with deviant feature, $F$ (3, 69) = 4.745, $p = .007$, $\varepsilon = .884$, $\eta^2 = .171$. That is, all features, except for phase, produced a significant positive deviant minus control difference score (Table 6.5). The Bayesian ANOVA favoured the model including both main effects and the interaction ($BF_{10}$ = 955559.701). The data provide very strong evidence for an effect of stimulus type ($BF_{\text{Incl}}$ =

457240.641), but only some evidence for including effects of deviant feature ($BF_{Incl}$ = 2.095) and the interaction effect ($BF_{Incl}$ = 1.546).

***Posterior N1***

The posterior N1 (PCA component 4) amplitude was more positive for deviants than for controls, $F$ (1, 23) = 22.623, $p$ < .001, $\eta^2$ = .496, and significantly different among deviant features, $F$ (3, 69) = 3.818, $p$ = .024, $\varepsilon$ = 0.757, $\eta^2$ = .142. The stimulus type effect was, significantly modulated by deviant feature, $F$ (3, 69) = 3.501, $p$ = .031, $\varepsilon$ = .773, $\eta^2$ = .132 (see Figure 6.7, bottom panel). That is, the posterior N1 amplitude was more positive for deviants than for controls for contrast, and spatial frequency deviants, but not for orientation or phase deviants (Table 6.5). The Bayesian ANOVA favoured the model including both main effects and the interaction ($BF_{10}$ = 2332.248). The data also provide very strong evidence for including deviant feature ($BF_{Incl}$ = 403.809), strong evidence for including stimulus type ($BF_{Incl}$ = 3.021), and some evidence for including the interaction effect ($BF_{Incl}$ = 2.583).

Using the effect sizes for the deviant versus control Gabor-fixation stimuli at O2 (for P1 and aN1) and P8 (for pN1) in Experiment 1, we performed Bayes Factor replication tests comparing deviant and control orientation stimuli. The data provide strong evidence for the alternative for the P1 (O2: $BF_{r0}$ = 69.019) and aN1 (O2: $BF_{r0}$ = 17.718), but not the pN1 (P8: $BF_{r0}$ = 0.385).

### 6.4.3 Discussion

Our Bayes Factor tests provide strong evidence of no vMMN in Experiment 2. This confirms our finding from Experiment 1 that orientation deviants do not yield a vMMN when using physiologically plausible visual stimuli and controlling for adaptation and allocation of attention. Our findings also suggest that deviants in contrast, phase, and spatial frequency do not yield the vMMN.

One possibility we can discount is that the size of the deviants we used was too small. Except for phase, the differences we used are all many times greater than the respective discrimination thresholds: at least several tens of times for orientation (Regan & Price, 1986), and 5 to 10 times for contrast (Snowden & Hammett, 1998) and for spatial frequency (Webster, De Valois, & Switkes, 1990). We discuss phase below.

The absence of a vMMN to contrast-deviants corroborates Nyman et al. (1990), who also searched fruitlessly for one. Wei et al. (2002), however, concluded that there is a vMMN to contrast changes. But they did not control for the physical differences between lower and higher contrast stimuli as we and Nyman et al. did.

As far as we can tell, we are the first to test phase as a deviant feature for the vMMN. Phase information is essential in human vision. For example, Piotrowski and Campbell (1982) showed that one image's spatial frequency spectrum combined with the phase spectrum of a different image yields an image

that looks like the latter and not at all like the former. But Piotrowski and Campbell also showed that this phenomenon survives with the coarse encoding of phase, for example into only two levels. Consistent with this, psychophysical studies of phase discrimination show that highly trained observers can have thresholds ranging from about one third of (Burr, 1980), to half of (Caelli & Bevan, 1982), to about equal to (Troscianko & Harris, 1988), the difference we used. In any case, our post-test results suggest our participants could see the phase changes.

We also failed to find a vMMN to spatial-frequency deviants. File et al. (2017) also failed to find a vMMN to decreases in spatial frequency, admittedly of complex, windmill patterns that also vary in orientation content. They did find a vMMN when they increased spatial frequency in the same patterns, suggesting that a genuine vMMN arises only if there is a combination of features that increase, in this case of orientation and spatial frequency. Others reporting spatial-frequency vMMNs omitted any control for adaptation (e.g., Kenemans et al., 2003; Stagg et al., 2004; Maekawa et al., 2005, 2009, 2013).

One could argue that we did not find a vMMN to any deviant feature because the multi-feature paradigm is not ideal for showing the vMMN. Although the multi-feature paradigm is well established in the auditory literature, the paradigm has been adopted in only a handful of vMMN experiments (e.g., Grimm, Bendixen, Deouell, & Schröger, 2009; He, Hu, Pakarinen, Li, & Zhou, 2014; Kreegipuu et al., 2013; Qian et al., 2014; Shi, Wu, Sun, Dang, & Zhao, 2013). It would be useful to compare deviants appearing in

both a traditional oddball paradigm and a multi-feature paradigm with suitable controls. Given that Grimm et al. used the multi-feature paradigm to show a genuine vMMN, we suspect that we did not find a vMMN because we manipulated single, low-level properties of visual input, whereas Grimm et al. manipulated properties that combine features (e.g., luminance with colour).

Although we did not find evidence for a vMMN, in further exploration of the data we did find an early deviance-related positivity. According to our PCA, the components contributing to this early deviant-related positivity are the P1, anterior N1, and posterior N1. These differences are significant for the P1 and anterior N1 in all feature deviants, except for phase deviants. This could reflect phase invariance in complex cells in V1 (De Valois, Albrecht, & Thorell, 1982). Given these components are sensitive to stimulus type; we propose these deviant-related positivities may reflect the first instance of prediction error in vision. We discuss this further below but make clear that we did not predict such findings; therefore, they are exploratory.

## 6.5 General Discussion

We conducted two experiments to test whether low-level feature deviants yield the vMMN. This is becoming increasingly important considering some inconsistent findings in research into low-level deviance. In both experiments, we isolated and manipulated features of visual input based on our understanding of the visual system's physiology, we separated adaptation effects from genuine deviance detection, and we controlled for attention.

In Experiment 1, we replicated Kimura et al. (2009) and incorporated three additional conditions to examine the effect of using physiologically plausible versus implausible stimuli and attention on versus away from the stimulus of interest; no condition produced a vMMN. Our data provide very strong evidence for the null hypothesis. Therefore, we could not replicate the orientation vMMN results of Kimura et al. (2009) and it is not likely we would be able to do so given the effect size reported by Kimura et al. (2009) and power of this experiment (= .99). Although we carefully replicated the forerunner study, we had a larger number of participants than Kimura et al., and our Bayesian statistics show that it is reasonable to conclude that there is no orientation vMMN; we searched again for it, along with vMMNs to other basic properties of visual stimuli, in Experiment 2. This time, we used the multi-feature paradigm and cascadic control. Still, we did not find a vMMN for any deviant feature and instead, we replicated strong evidence for the null hypothesis when testing orientation as in Experiment 1 and found very strong evidence for the null hypothesis when testing contrast, phase, and spatial frequency deviants as well.

Although our findings are different from some existing research, we suspect that our rigorous design and controls have allowed us to isolate and determine the true effect of low-level deviance on the visual system. We propose that some experiments do not enact suitable controls for attention and adaptation (also determined by the stimulus used), whereas others do, which is why some experiments of low-level deviants show a vMMN whereas others do not. Nevertheless, existing feature-deviance research has been vital to appreciate how

the brain encodes and detects regularity and irregularity, respectively, even when attention is elsewhere. Our findings merely add to the appreciation of which types of visual deviants yield the vMMN and why.

The eye-tracking data in Experiment 1 were essential in this regard. They are consistent with the notion that a vMMN is more likely for deviants in which multiple dimensions of visual input change, suggesting that perhaps the vMMN is concerned with detecting deviants involving higher-order features or feature-combinations encoded to perceptual objects.

If so, our findings point to a difference between the vMMN and the MMN: one of the principal features of the MMN is that it occurs in response to regularity violations in well-isolated, low-level, physiologically plausible, sensory features. It is possible that existing vMMN paradigms are not suited to test low-level deviants because the visual system is equally (if not more) concerned with spatial order than temporal order.

Another possibility is that the visual system detects low-level deviance in a process that is not revealed by the vMMN. We observed what might be an index for detecting low-level visual irregularities in both experiments: amplitudes were more positive for deviants compared to identical equiprobable controls at occipito-parieto-lateral electrodes between 80–200 ms. We found strong and converging evidence for deviance-related effects for the anterior N1 PCA component at occipital locations (i.e., with a positive deviant minus control difference potential) in both experiments and in all conditions with the only exception of phase in Experiment 2 (in which the evidence was inconclusive).

We also found substantial evidence for deviance-related effects for the P1 and posterior N1 PCA components in some conditions. These were, however, not consistent across experiments and conditions and further research is needed to establish if these P1 and posterior N1 differences can be replicated.

If we accept that these early deviant-related positivities are meaningful, we could then consider these early positivities as the first instance of prediction error in vision perhaps comparable to the pre-MMN error signals reported for the auditory middle-latency response (MLR). In the MLR, there are positive (i.e., Pa at 30 ms, Slabu, Escera, Grimm, & Costa-Faidella, 2010) and negative (Nb at 40 ms) components that are sensitive to simple acoustic-feature irregularities (Alho, Grimm, Mateo-León, Costa-Faidella, & Escera, 2012; Althen, Grimm, & Escera, 2013; Grimm, Escera, Slabu, & Costa-Faidella, 2011; Leung, Cornella, Grimm, & Escera, 2012; Recasens, Grimm, Capilla, Nowak, & Escera, 2014) even if controlled for effects of adaptation. These components are different from the MMN in terms of origin (Recasens et al. 2014) and in what evokes them. The latter is because simple auditory changes produce the deviance-related MLR response; whereas, complex irregularities, such as feature conjunctions, do not (Cornella, Leung, Grimm, & Escera, 2012).

Although there are reports of increased positivity to deviants (Berti & Schröger, 2004; Chen et al., 2010; Fu, Fan, & Chen, 2003; Kimura et al., 2006b; Müller et al., 2012; Sulykos & Czigler, 2013; Sysoeva, Lange, Sorokin, & Campbell, 2015), we are the first to propose this early positivity as a marker for prediction error. In one study, Sulykos and Czigler (2013) found a positive

difference in amplitudes between 108 and 118 ms in the absence of a vMMN. Sulykos and Czigler (2013) explained their results in terms of a failure to reactivate memory for a previous standard and suggested that the deviant-related positivity is akin to change-related positivity (CRP, Kimura, Katayama, & Murohashi, 2005, 2006a, 2006b, 2006c; Wang et al., 2003).

The theoretical basis of, and evidence for, CRP, however, is different from the deviant-related positivity we observed. This is because CRP is thought to reflect a mismatch between two stimuli, irrespective of predictability. Perhaps some of the CRP reported in other studies does include some deviant-related positivity (e.g., Kimura et al., 2006b); however, in order to test this, one would need to isolate adaptation-related and deviant-related differences as we have done.

A pre-vMMN prediction error is consistent with an earlier prediction error sensitive for low-level changes in sensory input (Escera et al., 2014) and may have broader implications for how we conceptualize visual processing within the predictive coding framework. For example, it may be that deviant-related positivity reflects an earlier prediction error sensitive to differences in basic dimensions of visual input. It could be promising to investigate this pre-vMMN (positive) prediction error further.

## 6.6 Conclusions

Our results indicate that low-level feature deviants do not yield the vMMN if properly controlled for effects of adaptation, allocation of overt and covert

attention, physiological plausibility, and isolation of manipulated feature. We surprisingly failed to replicate findings by Kimura et al. (2009) and discovered what appears to be a pre-vMMN positive index of prediction error reserved for low-level changes in visual input. This may reflect differential processing for different visual changes and we encourage others to search for a pre-vMMN prediction error signal. In sum, we confirm that we can only realize the true effect of deviance on the low-level visual system and thus be able to identify other (also non-negative) indicators of deviant detection in vision when adequately controlling for adaptation and how attention is allocated during visual experiments.

# CHAPTER 7

## GENERAL DISCUSSION

# 7. GENERAL DISCUSSION

## 7.1 Overview

I attempted to measure genuine vMMN (Ch. 3, 5, and 6) and DRN (Ch. 4): increased negativity in the ERP waveform for unexpected changes in visual input. I asked whether local context of a change, such as the magnitude of deviance, affect the vMMN and DRN. This was a seemingly simple objective. However, my findings revealed that such an objective was not possible due to some unexpected findings. One finding, in particular, caused me to revise my thesis to show that changes in basic properties of visual input do not evoke the vMMN.

## 7.2 Summary of Findings

I conducted four low-level deviance experiments (Ch. 3, 5, and 6) in which I tested four feature deviants—deviants that differ from standards by a physical property of visual input as described by Graham (1989). These were orientation, contrast, phase, and spatial frequency. I also conducted two high-level deviance experiments (Ch. 4) in which I tested abstract deviants in the orientation specified by the rule of the preceding standards. I found that neither kind of deviant evoked a measurable vMMN or DRN. Instead, I found that feature deviants produced more positive early ERP amplitudes than equally probable, identical controls at parieto-occipital regions in three of the four low-level feature deviance experiments. I consider these findings, their explanations, and their implications.

## 7.3 Explanations Only for Abstract Deviance Findings

In Chapter 4, I failed to show DRN to rule-based orientation deviants. Having discounted the possibility that some of my chosen parameters were responsible for this result, I argued that the result was because:

1. participants did not encode the regularity necessary for detecting irregularity,
2. participants did encode the regularity necessary for detecting irregularity, but did not detect the irregularity (perhaps because it was too small a deviant), or
3. rule-based orientation deviants do not evoke DRN.

In light of other research showing the vMMN to rule-based orientation deviants (Kimura & Takeda, 2013, 2015; Kimura, 2018) and participants' performance when asked to detect deviants in my experiments, explanations 1 or 2 are more likely than explanation 3. The implications of explanations 1 and 2 are that some appreciation of either, or both, regularity and irregularity is required for DRN. This suggests there are limits to the kinds of regularity or irregularity that the visual system encodes or detects, respectively.

Existing evidence favours explanation 2. For example, Czigler et al (2002) showed that large deviants evoked the genuine vMMN; small deviants did not. However, others have found that when participants attend to small changes in orientation and shape or size, they then evoke DRN (Czigler & Csibra, 1990; Alho et al., 1992; Woods et al., 1992). Perhaps increased response sensitivity of

neurons in the V1 (e.g., Luck, Chelazzi, Hillyard, & Desimone, 1997; Thiele, Pooresmaeili, Delicato, Herrero, & Roelfsema, 2009) are responsible for the moderating effect of attention on small magnitudes of deviance. This would suggest that in the absence of attention (and increased sensitivity) the brain does not detect such deviances or that our measure is not sensitive enough to detect such small differences in electrophysiology.

Clearly, further research is vital to substantiate whether participants are able to encode regularity (explanation 2) or not (explanation 1). For example, a DRN to a pattern reversal would provide support for explanation 2. It would also be prudent to examine why attention determines the effect of small magnitudes of deviance on the visual system. One could test whether similar rule-based orientation deviants produced DRN when participants attended to them as they did during the post-test in Experiment 2 of Chapter 4.

## 7.4 Explanations Only for Low-level Feature Deviance Findings

I did not observe a vMMN for any low-level feature deviant in any of the four experiments in Chapters 3, 5, and 6 testing low-level feature deviance. Therefore, I propose that changes in basic properties of visual input do not evoke a vMMN. These findings, and indeed this proposal, contradict most of the existing low-level deviance vMMN literature. I propose that having used physiologically plausible well-controlled stimuli (only seven other experiments or conditions within experiments have done this, s. 2.8.1) in addition to having

controlled for, and separated, adaptation-related differences (only one other experiment has done both), has allowed me to show the true effect of low-level deviance on the visual system. I also propose that low-level deviance in the visual system is resolved in a process not revealed by the vMMN, but early deviant-related positivity.

### 7.4.1 Evidence for a pre-vMMN positive prediction error

In three of the four low-level feature deviance experiments, I observed significant deviant-related positivity at parieto-occipital scalp regions. In one experiment (Ch. 5), differences were restricted to the orientation-CVF condition because of the reduced signal-to-noise ratio (reduced contrast and LVF conditions) compared to other experiments. If any (or all) of the components contributing to this early positivity are sensitive to deviance, then this positivity is the earliest neural correlate of a cortically generated prediction error signal in vision.

I reviewed vMMN studies of low-level, feature deviants to determine whether others had documented (perhaps unknowingly) a similar early parieto-occipital deviance-related positivity. I found deviant-related positivity for orientation (Bodnár et al., 2017; Farkas et al., 2015; Fu et al., 2003; Kimura & Takeda, 2013, 2014, 2015; Qian et al., 2014; Sulykos et al., 2013; Takács et al., 2013), luminance (Sulykos & Czigler, 2014), spatial frequency (Cleary, Donkers, Evans, & Belger, 2013; File et al., 2017; for a corresponding MEG study see Susac, Heslenfeld, Huonker, & Supek, 2014), colour (Kimura et al.,

2006c; Müller et al., 2012; Sysoeva et al., 2015), and for duration (Berti & Schröger, 2004). Seven of these studies addressed the deviant-related positivity.

Fu et al. (2003) found a significant P84 deviant-related positivity and likened the result to change-related positivity (CRP, Kimura, Katayama, & Murohashi, 2005, 2006a, 2006b, 2006c; Wang et al., 2003). According to Kimura et al. (2006a, 2006b, 2008), CRP occurs because there is a difference between the memory trace of the previous stimulus and the current stimulus. This explanation does not distinguish CRP from adaptation or the original mismatch hypothesis proposed for the MMN (Näätänen, 1992). However, traditional paradigms used to show CRP (e.g., S1 – S2 matching) do not control for adaptation or instantiate regularity by repeating a stimulus; therefore, existing CRP paradigms (e.g., Kimura et al. 2006a, 2006b, 2006c) are not appropriate for investigating whether CRP reflects processes beyond adaptation.

Sulykos et al. (2013) compared orientation deviants with controls and used Gabor patch stimuli. They found no vMMN, but they did find an early positivity. They also likened the positivity to change-related positivity (CRP). Similarly, Kimura et al. (2006c), Sysoeva et al. (2015), and Müller et al. (2012) described the significant deviant-related positivity to colour deviants as CRP. Müller et al. also found that the size of the early positivity was inversely related to the size of the vMMN. Perhaps this is because the predictive framework governs both.

In another study, Chen et al. (2010) reported deviant-related positivity to duration deviants. They argued that the early positivity could reflect a feature specific change system, but conceded that the paradigm used was not appropriate

for testing this. Furthermore, Berti and Schröger (2004) found deviant-related positivity to location deviants compared with equally probable controls but argued that the stimuli they used limited conclusions about whether the P1 difference they observed was due to the predictability or eccentricity of the stimulus.

Having isolated and removed adaptation-related differences in all my low-level deviance experiments, I have shown that adaptation or CRP—as it is currently defined and tested—cannot explain the early deviant-related positivity to changes in basic properties of visual input. Instead, I suggest that the deviant-related positivity in the current thesis is comparable to the middle-latency response (MLR)—a neural correlate of an early prediction error signal in the auditory domain—that occurs *uniquely* for low-level deviants, such as frequency deviants (Slabu, Escera, Grimm, & Costa-Faidella, 2010; Alho, Grimm, Mateo-León, Costa-Faidella, & Escera, 2012; Althen, Grimm, & Escera, 2013; Grimm, Escera, Slabu, & Costa-Faidella, 2011; Leung, Cornella, Grimm, & Escera, 2012; Recasens, Grimm, Capilla, Nowak, & Escera, 2014). I consider the theoretical basis and implications for an early prediction error in vision.

### 7.4.2 Theoretical basis for a pre-vMMN positive prediction error

According to predictive coding theory, the brain's sensory systems are hierarchical. Processing of basic properties of sensory input happens at low levels and processing of properties that are more abstract happens at higher levels (Bastos et al., 2012; Clark, 2013; Friston, 2003, 2005, 2010; Huang & Rao, 2011; Lee & Mumford, 2003; Rao & Ballard, 1999; Rao, 1997). Predictive

models at each level contain information about the statistical probability of sensory input occurring. Abstract models pass predictive constraints to lower models so that they can formulate feature-specific predictions about incoming input. Lower levels, on the other hand, propagate prediction errors up the hierarchy.

When input conflicts with prediction, prediction error occurs, causing changes in the areas above *until* input and prediction are harmonised (Friston, 2003). When input and prediction are harmonised, the brain suppresses prediction error (Friston, 2003). Now, consider that the vMMN is only one reflection of prediction error. With this in mind, I propose that the vMMN represents a prediction error for higher-order irregularities whereas early deviant-related positivity represents a prediction error for low-level feature deviances. If we accept that these early deviant-related positivities reflect prediction error, possibly low-level feature deviants do not evoke a vMMN because:

i. prediction errors exist to prompt model updating (Friston, 2003; Kremláček et al., 2016),
ii. the brain suppresses prediction error at higher levels if discrepancy is resolved at lower levels (Friston, 2003), and
iii. the model responsible for predicting feature-specific properties of future visual input is already updated following the generation of prediction error in the level prior.

Resolution in this way is only possible where deviance is isolated to a single basic property of visual input. If, however, multiple properties of a visual stimulus change on deviant trials, then the deviant is no longer just a low-level feature deviant, in which case increasingly abstract models of sensory input may govern the predictability of the stimulus and a vMMN is possible if the input does not agree with such predictions.

For example, in Kimura and Takeda (2014; 2015) participants responded to fixation dot changes while the orientation of the bars arranged in the shape of a square on a black background changed by 32.7° on deviant trials (Kimura & Takeda, 2014). A vMMN followed early deviance-related positivity. Due to the physical properties of the bar stimuli, orientation changes also produced multiple differences in orientation and luminance, thus representing a more complex change in visual input. Subsequently, the brain compares input with predictions governed by increasingly abstract models and if the input disagrees with prediction, a further prediction error is possible. Essentially, even if the deviant-related positivity occurs for a simple orientation difference, a further prediction error may occur for the complex change.

Although this is the first report of a pre-vMMN prediction error, File et al. (2017) expressed a similar idea about different levels of resolution after having found that orientation deviants did not produce a vMMN whereas windmill-like deviants did. File et al. suggested that it might not be effective to establish a memory trace for a particular orientation given that adapted neurons already encode this information; whereas, regularities that are more complex are not

encoded at this level of neuronal adaptation. The current thesis, however, demonstrates a deviant-related positivity separate from adaptation.

### 7.4.3 A Note on Magnitude of Deviance

One of my original objectives was to determine whether the type and size of irregularity (i.e., deviance) in visual input affected the brain's processing of it. Although I cannot comment on the relationship between the magnitude of deviance and the vMMN or DRN, because I did not yield either, I have shown that the deviant-related positivity—regarded as a neural correlate of an earlier prediction error in the current thesis—obeys some all-or-nothing criteria. This is because it does not increase with the magnitude of deviance (Ch. 3).

It would be curious if the neural correlate of one prediction error (e.g., deviant-related positivity) was characterised by some all-or-nothing criteria, but another (e.g., vMMN) was not. I hope that others will continue to delve into the relationship between the magnitude of deviance research and the vMMN, as there is a paucity in the literature here. It is also crucial to conduct further research on the deviant-related positivity to confirm that its amplitude is unchanged by the magnitude of deviance. This is especially true for other types of low-level deviance, such as spatial frequency and contrast.

## 7.5 Alternative Explanations for all Findings

Of course, it is also possible that the deviants I have tested would normally evoke the vMMN and DRN and that I did not observe either for some other reason. I consider this next.

### 7.5.1 Magnitude of deviance

Perhaps the reason that my deviants did not evoke the vMMN is that the difference between predicted and unpredicted input was not sufficient. Sams, Paavilainen, Alho, and Näätänen (1985) and Alho et al. (1992) first expressed the idea that differences between the standard and deviant may need to be substantially larger for visual input than for auditory input in order for a vMMN to occur. Unfortunately, it is not clear from existing research what magnitudes of deviance are appropriate for deviance research due to inconsistencies in this regard. For example, Durant et al. (2017) and File et al. (2017) used the same 36° orientation difference as Astikainen et al. (2008) and Kimura et al. (2009), but they could not replicate the vMMN Astikainen et al. and Kimura et al. found.

Moreover, the smallest orientation deviant used to show a classic vMMN is 22° (Kimura & Takeda, 2014). In all the current feature deviant experiments, at least one orientation was greater than this (30° and 60° in Ch. 3, 33° in Ch. 5, and 36° in Ch. 5). Possibly additional aspects predict whether a low-level deviant produces a vMMN.

### 7.5.2 Stimuli

The studies informing our chosen magnitudes of deviance (e.g., Astikainen et al., 2008; Kimura et al., 2009; Czigler & Sulykos, 2010) did not use physiologically plausible stimuli, such as Gabor patches. Initially, this was not a concern because, if the reported vMMN was due to deviance, then it should still occur for changes in Gabor patches. However, a vMMN was not detected in any

of the five known experiments that used Gabor patches, controlled for adaptation, and directed attention away from Gabor patches (including mine).

I also compared bar and Gabor patch stimuli in otherwise identical conditions in Experiment 1 of Chapter 6. I did not find a vMMN for either stimulus type. However, I also emphasized fixation more than others who have used bar stimuli to evoke the vMMN (e.g., Kimura et al. 2009) by measuring eye-movement. Perhaps then, the reason that different stimuli can evoke the vMMN is because the type of visual stimulus determines where participants look and whether they fixate, and this determines the visual input reaching the visual cortices.

### 7.5.3 Experimental paradigms

Existing vMMN paradigms are descendent from MMN paradigms and emphasize temporal order. Perhaps some deviants determined by temporal order (a stimulus occurring at a time) do not evoke the vMMN because they do not constitute a deviance with which the visual system is overly concerned. Näätänen (1990) was the first to emphasize that only when considering the unique properties of the visual system would we find a visual analogue of the MMN.

In Chapter 6, I argued that temporal regularity is more important in auditory than visual input. This is because temporal information also contributes to auditory spatial localization and temporal regularity usually determines auditory anomalies whereas temporal regularity does not inform spatial

regularity (a stimulus occurring at a predictable position) in vision and spatial information is equally important for visual input. Perhaps for the visual system to consider some instances of deviance important, *where* a stimulus appears should (also) determine deviance.

### 7.5.4 Experimental settings

I discussed limitations in comparing findings across studies that used different EEG pre-processing parameters in my review of the vMMN literature (Ch. 2). Although the effects associated with varying these parameters on measures of the vMMN have not yet been reported, others have shown that different pre-processing parameters—upper and lower filter frequency cut-off limits, for example—can affect EEG/ERP results (Acunzo et al., 2012; Kappenman & Luck, 2010; Luck, 2005; Tanner et al., 2015; Widmann et al., 2015).

In Chapter 6, I compared results from two different EEG pre-processing pipelines. In a second analysis of the data, I replicated the pipeline used by Kimura et al. (2009) to ensure that this was not the cause of my failure to replicate their findings—a vMMN to orientation changes. Although the trend in the results were similar in both analyses (i.e., no vMMN in any condition), some differences were exaggerated in the second analysis compared to the first, such as the difference in mean amplitudes to control vs. standard stimuli. Therefore, although it is not likely that my chosen pre-processing parameters prevented me from revealing a true vMMN, these results do illustrate how differences in pre-processing parameters can affect findings. Considering this, it may be

worthwhile investigating how differences in experimental hardware, as well as pre-processing parameters, affect neuroimaging results. Ideally, the findings presented here will encourage others to a) investigate, or at least consider, the possibility that different experimental hardware or pre-processing parameters (i.e. experimental settings) can produce observable differences in the data across studies, and b) adopt a more consistent approach to selecting pre-processing criteria in vMMN research to facilitate comparisons across studies.

## 7.6 Implications and Significance for vMMN Research

The practical implications of the current findings are three-fold. First, these findings show that the data will only reveal what irregularities yield the vMMN when exerting control over a) attention; preferably by employing a fixation task, b) adaptation; by employing suitable controls for adaptation, and c) stimulus parameters; by employing well-controlled, physiologically plausible stimuli. Controlling for each of these parameters of experimental design would make comparisons between studies easier—as argued in Chapter 2—and may reconcile some of the inconsistencies in the vMMN literature, such as variances in peak amplitudes and latencies and reproducibility. This would facilitate a better understanding of the different types of visual regularities and irregularities the brain can encode and detect, respectively.

Second, these findings show it is equally important to document stimulus deviance that does not yield a vMMN. There may be many other unpublished findings of failed attempts to show vMMNs to low-level deviants. The difficulty in disseminating null results is common knowledge; however, my findings

illustrate the importance of disseminating all findings. An increasingly popular means for ensuring that findings are disseminated regardless of the result is to pre-register the study. Given the current state of the vMMN literature, it seems prudent to do so. However, pre-registration is relatively new, and few journals offered pre-registration prior to 2013 (Chambers, 2019). I cannot help but wonder what other failed vMMN studies showed deviant-related positivity, especially because the only other reported early deviance-related positivity for deviants compared to controls occurred when the vMMN was absent (Sulykos et al., 2013). Perhaps the deviant-related positivity reported in the current thesis would have been discovered sooner if there were a concerted effort to publish all findings, null results included.

The third practical implication of the current findings regards the increasing number of studies using the vMMN to infer differences in early visual processing in the dysfunctional brain. Reduced amplitude of the vMMN has been shown for schizophrenia (Csukly, Stefanics, Komlósi, Czigler, & Czobor, 2013; Farkas et al., 2015; Urban et al., 2008; Neuhaus, Brandt, Goldberg, Bates, & Malhotra, 2013), depression (Chang et al., 2011; Qiu et al., 2011), bipolar disorder (Maekawa et al., 2013), substance abuse (*alcohol*: Kenemans, Hebly, van den Heuvel, & Grent-'T-Jong, 2010; He, Hu, Pakarinen, Li, & Zhou, 2014; *nicotine*: Fisher et al., 2010; *methamphetamine*: Hosák, Kremláček, Kuba, Libiger, & Čížek, 2008), and neurodegenerative disorders (*Alzheimer's disease*: Tales & Butler, 2006; Tales, Haworth, Wilcock, Newton, & Butler, 2008). The number of studies is expected to grow given the appeal of identifying pre-

attentive, non-invasively measured neural correlates (or markers) of symptom severity and processing capacity (Kremláček et al., 2016).

However, most conclusions about visual processing deficits come from studies that did not control for adaptation (Farkas et al., 2015), did not isolate the deviant feature by using well-controlled visual stimuli (Chang et al., 2011), or both (Qiu et al., 2011; Maekawa et al., 2013; Neuhaus et al., 2013; Kenemans, et al., 2010; Tales et al., 2008; Tales & Butler, 2006). It is prudent that we do not confuse deficits in how the brain learns about environmental regularities with differences in adaptation. The current findings emphasize the importance of controlling for adaptation, fixation, attention, and stimulus parameters when proposing early visual processing deficits based on the vMMN to low-level feature deviants (e.g., Farkas et al., 2015; Kenemans et al., 2010; Maekawa et al., 2013) because any of these can affect the resulting vMMN (Ch. 2).

Using the vMMN to infer early processing deficits is also problematic if it is unknown how different kinds of deviance reveal themselves in the visual system. That is, there may be a better candidate for discerning such deficiencies. Visual P1 deficits are common in schizophrenia and are thought to reflect deficits in early visual processing (Butler et al., 2001, 2005; Friedman, Sehatpour, Dias, Perrin, & Javitt, 2012; Javitt, Spencer, Thaker, Winterer, & Hajos, 2008). Freidman et al. (2012) argued that P1 is a better index of schizophrenic pathology than the vMMN. Glutamatergic dysfunction, particularly at NDMA receptors, contributes to deficits in the MMN and the P1 (Butler et al., 2005; Javitt et al., 2008).

I have found that low-level feature deviance affects the P1 (Ch. 3, 5, and 6). Perhaps, then, visual P1 deficits are more common in schizophrenia than vMMN deficits because P1 deficits (as they are described) reflect deficits in the first instance of processes involved in generating prediction error in vision (i.e., deviant-related positivity). If so, then prediction error in the dysfunctional brain may be similarly affected in vision and audition, but is reflected in the visual system as P1 deficits and in the auditory system as MMN deficits. It would be useful to test whether NDMA antagonists—known for affecting the MMN for auditory deviants and the visual P1 (Butler et al., 2005; Javitt et al., 2008)—similarly affect the early deviant-related positivity identified in the current thesis. If deviant-related positivity was similarly affected, this would show that the mechanisms underlying it are comparable to those underlying the MMN and P1.

In sum, I have demonstrated that low-level feature deviants do not evoke the vMMN when adaptation-related differences are separated, and well-controlled physiologically plausible stimuli are used. I have also shown that a pre-vMMN positive prediction error may exist for low-level visual feature deviants.

In doing so, I:

- Encourage a uniform and controlled approach to vMMN research.

- Argue for the dissemination of all findings.
- Encourage others investigating electrophysiological biomarkers for neurocognitive dysfunction to carefully consider the conclusions drawn from measures of the vMMN in the absence of suitable controls, and to entertain the possibility of positive indices of prediction error.

## 7.7 Broader Implications and Further Research

It is clear from the current thesis findings that, to appreciate how the brain encodes and detects regularity and irregularity, respectively, one must control for attention (Ch. 2), fixation (Ch. 6), and adaptation (Ch. 2–6). This appreciation is fundamental for models of vision and has implications for neuro-rehabilitative efforts. For example, monitoring changes in the brain's capacity to extract statistical regularities (evidenced by irregularities evoking a vMMN) will only reveal real differences when all these aspects are controlled.

My findings that rule-based irregularities do not produce any deviant-related differences suggest that the visual system does not pre-attentively encode or detect regularity and irregularity, respectively, under certain conditions (e.g., small magnitudes of deviance). Possibly, the visual system is limited in this regard. Further research is essential to determine what these limitations are, if other aspects affect them, and indeed what types of visual abstractions, including rule-based regularities, the brain encodes. I have recommended that future studies incorporate a behavioural measure of regularity (as well as irregularity) and consider an attentional manipulation (on vs. away from the stimulus of

interest) to delineate its effect on encoding and detecting such regularities and irregularities, respectively.

It is also clear that the visual system detects and resolves low-level disparities between predicted and unpredicted input earlier than previously thought. This was evident by the deviant-related positivity to low-level feature deviants. The absence of a vMMN in all low-level feature deviance studies could suggest that once input and prediction are harmonised, no further prediction errors occur.

Because I did not predict the early positivity, my research is exploratory. To confirm these findings, it is necessary to conduct further low-level deviance research. It would be useful to examine whether changes in other basic properties of visual input, such as luminance, evoke the deviant-related positivity. This would confirm the current findings and help show that the deviant-related positivity does reflect a neural correlate of prediction error in vision for low-level feature deviants.

Furthermore, an experiment comparing ERPs to changes in a single low-level feature or changes in multiple low-level features would help to elucidate a) whether deviant-related positivity exclusively reflects low-level deviance processing and b) whether a vMMN can follow deviant-related positivity when low-level feature and high-level abstract deviance occur. If the vMMN occurred where multiple properties of visual input changed on deviant trials only and deviant-related positivity occurred in both instances, this would show that

multiple prediction errors can occur and would explain why Kimura and Takeda (2015) show deviant-related positivity and a vMMN.

Still, evidence that different error signals exist for different levels in the visual hierarchy encourages one to question how differences are reconciled once the visual system detects a disparity. The answers to such questions have important implications for models of sensory processing. For example, forward connections from lower to higher levels of the visual hierarchy may terminate when low-level deviances are detected and resolved (at lower levels). In such a case, models that are more abstract do not receive the discrepant input, perhaps because no higher order regularities were available for encoding and there is no potential for input to disagree with increasingly complex models of input. This seems consistent with the predictive coding ideology that the brain is resolved to process differences and disparities only (Huang & Rao, 2011). Clearly, a second earlier neural correlate of prediction error in vision reserved for feature deviants gives rise to more questions than answers. Nevertheless, equipped with this understanding, we are in a better position to reveal how the brain processes visual irregularities.

## 7.8 Conclusion

In my quest for the vMMN and DRN, I happened upon some unexpected findings. These are:

I. Well-controlled low-level feature deviants do not evoke the vMMN.

II. A pre-vMMN positive prediction error exists for low-level visual deviants and it does not scale with the size of deviance.

III. For abstract, rule-based orientation deviants to evoke DRN, some appreciation of regularity, irregularity, or both, may be required.

I have shown how these findings have theoretical and practical implications for our understanding of how the brain encodes and detects visual regularities and irregularities, respectively. We do not yet fully appreciate how the brain processes the various kinds of visual input that we experience, including those subtle visual irregularities. The work within this thesis represents just one small piece of this enormous puzzle and I hope to have convinced the reader that each small piece adds to the larger picture; understanding vision in the human brain.

# REFERENCES & APPENDICES

# REFERENCES

Acunzo, D. J., Mackenzie, G., van Rossum, M. C. W. (2012). Systematic biases in early ERP and ERF components as a result of high-pass filtering. *Journal of Neuroscience Methods, 209,* 212–218. https://dx.doi.org/10.1016/j.jneumeth.2012.06.011

Alho, K., Grimm, S., Mateo-León, S., Costa-Faidella, J., & Escera, C. (2012). Early processing of pitch in the human auditory system. *European Journal of Neuroscience, 36,* 2972–2978. https://dx.doi.org/10.1111/j.1460-9568.2012.08219.x

Alho, K., Woods, D.L., Algazi, A., & Näätänen, R. (1992). Intermodal selective attention. II. Effects of attentional load on processing of auditory and visual stimuli in central space. *Electroencephalography and Clinical Neurophysiology, 82,* 356–368. https://dx.doi.org/10.1016/0013-4694(92)90005-3

Althen, H., Grimm, S., & Escera, C. (2013). Simple and complex acoustic regularities are encoded at different levels of the auditory hierarchy. *European Journal of Neuroscience, 38,* 3448–3455. https://dx.doi.org/10.1111/ejn.12346

Amenedo, E., & Escera, C. (2000). The accuracy of sound duration representation in the human brain determines the accuracy of behavioural perception. *European Journal of Neuroscience, 12,* 2570–2574. https://dx.doi.org/10.1046/j.1460-9568.2000.00114.x

Amenedo, E., Pazo-Alvarez, P., & Cadaveira, F. (2007). Vertical asymmetries in pre-attentive detection of changes in motion direction. *International Journal of Psychophysiology, 64,* 184–189. https://dx.doi.org/10.1016/j.ijpsycho.2007.02.001

Anderson, N. H. (1972). Cross-task validation of function measurement. *Perception & Psychophysics, 12,* 389–395. https://dx.doi.org/10.3758/BF03205848

Astikainen, P., & Hietanen, J. K. (2009). Event-related potentials to task-irrelevant changes in facial expressions. *Behavioral and Brain Functions, 5*(30), 1–9. https://dx.doi.org/10.1186/1744-9081-5-30

Astikainen, P., Lillstrang, E., & Ruusuvirta, T. (2008). Visual mismatch negativity for changes in orientation: A sensory memory-dependent response. *European Journal of Neuroscience, 28,* 2319–2324. https://dx.doi.org/10.1111/j.1460-9568.2008.06510.x

Astikainen, P., Ruusuvirta, T., Wikgren, J., & Korhonen, T. (2004). The human brain processes visual changes that are not cued by attended auditory stimulation. *Neuroscience Letters, 368,* 231–234. https://dx.doi.org/10.1016/j.neulet.2004.07.025

Athanasopoulos, P., Dering, B., Wiggett, A., Kuipers, J., & Thierry, G. (2010). Perceptual shift in bilingualism: Brain potentials reveal plasticity in pre-attentive colour perception. *Cognition, 116,* 437–443. https://dx.doi.org/10.1016/j.cognition.2010.05.016

Attneave, F. (1954). Some informational aspects of visual perception. *Psychological Review, 61,* 183–193. https://dx.doi.org/10.1037/h0054663

Averbach, E., & Coriell, A. S. (1961). Short-term memory in vision. *Bell System Technical Journal, 40*, 309–328. http://dx.doi.org/10.1002/j.1538-7305.1961.tb03987.x

Baldeweg, T., Klugman, A., Gruzelier, J., & Hirsch, S. R. (2004). Mismatch negativity potentials and cognitive impairment in schizophrenia. *Schizophrenia Research, 69*, 203–217. https://dx.doi.org/10.1016/j.schres.2003.09.009

Baldeweg, T., Richardson, A., Watkins, S., Foale, C., & Gruzelier, J. (1999). Impaired auditory frequency discrimination in dyslexia detected with mismatch evoked potentials. *Annals of Neurology, 45*, 495–503. https://dx.doi.org/10.1002/1531-8249(199904)45:4<495::AID-ANA11>3.0.CO;2-M

Bastos, A. M., Usrey, W. M., Adams, R. A., Mangun, G. R., Fries, P., & Friston, K. J. (2012). Canonical microcircuits for predictive coding. *Neuron, 76*, 695–711. https://dx.doi.org/10.1016/j.neuron.2012.10.038

Berti, S. (2009). Position but not color deviants result in visual mismatch negativity in an active oddball task. *NeuroReport, 20*, 702–707. https://dx.doi.org/10.1097/WNR.0b013e32832a6e8d

Berti, S. (2011). The attentional blink demonstrates automatic deviance processing in vision. *NeuroReport, 22*, 664–667. https://dx.doi.org/10.1097/WNR.0b013e32834a8990

Berti, S., & Schröger, E. (2001). A comparison of auditory and visual distraction effects: Behavioral and event-related indices. *Cognitive Brain Research, 10*, 265–273. https://dx.doi.org/10.1016/S0926-6410(00)00044-6

Berti, S., & Schröger, E. (2004). Distraction effects in vision: Behavioral and event-related potential indices. *NeuroReport, 15*, 665–669. https://dx.doi.org/10.1097/01.wnr.0000116969.73984.bc

Berti, S., & Schröger, E. (2006). Visual distraction: A behavioral and event-related brain potential study in humans. *NeuroReport, 17*, 151–155. https://dx.doi.org/10.1097/01.wnr.0000195669.07467.e1

Berti, S., Roeber, U., & Schröger, E. (2004). Bottom-up influences on working memory: Behavioral and electrophysiological distraction varies with distractor strength. *Experimental Psychology, 51*, 249–257. https://dx.doi.org/10.1027/1618-3169.51.4.249

Bigdely-Shamlo, N., Mullen, T., Kothe, C., Su, K., & Robbins, K. A. (2015). The PREP pipeline: Standardized preprocessing for large-scale EEG analysis. *Frontiers in Neuroinformatics, 9*(16), 1–20. https://dx.doi.org/10.3389/fninf.2015.00016

Blasdel, G. G. (1992). Orientation selectivity, preference, and continuity in monkey striate cortex. *The Journal of Neuroscience, 12*, 3139–3161. https://dx.doi.org/10.1523/jneurosci.12-08-03139.1992

Bodnár, F., File, D., Sulykos, I., Kecskés-Kovács, K., & Czigler, I. (2017). Automatic change detection in vision: Adaptation, memory mismatch, or both? II: Oddball and adaptation effects on event-related potentials. *Attention, Perception, & Psychophysics, 79*, 2396–2411. https://dx.doi.org/10.3758/s13414-017-1402-x

Boll, S., & Berti, S. (2009). Distraction of task-relevant information processing by irrelevant changes in auditory, visual, and bimodal stimulus features: A behavioral and event-related potential study. *Psychophysiology, 46*, 645–654. https://dx.doi.org/10.1111/j.1469-8986.2009.00803.x

Böttcher-Gandor, C., & Ullsperger, P. (1992). Mismatch negativity in event-related potentials to auditory stimuli as a function of varying interstimulus interval. *Psychophysiology, 29*, 546–550. https://dx.doi.org/10.1111/j.1469-8986.1992.tb02028.x

Brainard, D. H. (1997). The psychophysics toolbox. *Spatial Vision, 10*, 433–436. Retrieved from http://bbs.bioguider.com/images/upfile/2006-4/200641014348.pdf

Bruce, V., Green, P. R., & Georgeson, M. A. (2003). *Visual perception: physiology, psychology, & ecology* (4th ed.). New York, NY, US: Psychology Press.

Bubic, A., Bendixen, A., Schubotz, R. I., Jacobsen, T., & Schröger, E. (2010). Differences in processing violations of sequential and feature regularities as revealed by visual event-related brain potentials. *Brain Research, 1317*, 192–202. https://dx.doi.org/10.1016/j.brainres.2009.12.072

Bubic, A., von Cramon, D. Y., Jacobsen, T., Schröger, E., & Schubotz, R. I. (2009). Violation of expectation: Neural correlates reflect bases of prediction. *Journal of Cognitive Neuroscience, 21*, 155–168. https://dx.doi.org/10.1162/jocn.2009.21013

Bubrovszky, M., & Thomas, P. (2011). Useful or not? How schizophrenic patients process the relevance of a visual stimulus. *Journal of Behavioral and Brain Science, 1*, 111–114. https://dx.doi.org/10.4236/jbbs.2011.13015

Burbeck, C. A., & Regan, D. (1983). Independence of orientation and size in spatial discriminations. *Journal of the Optical Society of America, 73*, 1691–1694. https://dx.doi.org/10.1364/JOSA.73.001691

Burr, D. C. (1980). Sensitivity to spatial phase. *Vision Research, 20*, 391–396. https://dx.doi.org/10.1016/0042-6989(80)90029-2

Butler, P. D., Schechter, I., Zemon, V., Schwartz, S. G., Greenstein, V. C., Gordon, J., ... Javitt, D. C. (2001). Dysfunction of early-stage visual processing in schizophrenia. *American Journal of Psychiatry, 158*, 1126–1133. https://dx.doi.org/10.1176/appi.ajp.158.7.1126

Butler, P. D., Zemon, V., Schechter, I., Saperstein, A. M., Hoptman, M. J., Lim, K. O., ... Javitt, D. C. (2005). Early-stage visual processing and cortical amplification deficits in schizophrenia. *Archives of General Psychiatry, 62*, 495–504. https://dx.doi.org/10.1001/archpsyc.62.5.495

Butler, R. A. (1968). Effect of changes in stimulus frequency and intensity on habituation of the human vertex potential. *Journal of the Acoustical Society of America, 44*, 945–950. https://dx.doi.org/10.1121/1.1911233

Caelli, T., & Bevan, P. (1982). Visual sensitivity to two-dimensional spatial phase. *Journal of the Optical Society of America, 72*, 1375–1381. https://dx.doi.org/doi:10.1364/JOSA.72.001375

Cammann, R. (1990). Is there a mismatch negativity (MMN) in visual modality? *Behavioral and Brain Sciences, 13,* 234–235. https://dx.doi.org/10.1017/S0140525X00078420

Carretié, L., Tapia, M., Mercado, F., Albert, J., López-Martín, S., & de la Serna, J. M. (2004). Voltage-based versus factor score-based source localization analyses of electrophysiological brain activity: A comparison. *Brain Topography, 17*, 109–115. https://dx.doi.org/10.1007/s10548-004-1008-1

Chambers, C. (2019). What's next for registered reports? *Nature, 573*, 187–189. https://dx.doi.org/10.1038/d41586-019-02674-6

Chang, Y., Xu, J., Shi, N., Pang, X., Zhang, B., & Cai, Z. (2011). Dysfunction of preattentive visual information processing among patients with major depressive disorder. *Biological Psychiatry, 69,* 742–747. https://dx.doi.org/10.1016/j.biopsych.2010.12.024

Chang, Y., Xu, J., Shi, N., Zhang, B., & Zhao, L. (2010). Dysfunction of processing task-irrelevant emotional faces in major depressive disorder patients revealed by expression-related visual MMN. *Neuroscience Letters, 472*, 33–37. https://dx.doi.org/10.1016/j.neulet.2010.01.050

Chaumon, M., Bishop, D. V. M., & Busch, N. A. (2015). A practical guide to the selection of independent components of the electroencephalogram for artifact correction. *Journal of Neuroscience Methods, 250*, 47–63. https://dx.doi.org/10.1016/j.jneumeth.2015.02.025

Chen, Y., Huang, X., Luo, Y., Peng, C., & Liu, C. (2010). Differences in the neural basis of automatic auditory and visual time perception: ERP evidence from an across-modal delayed response oddball task. *Brain Research, 1325*, 100–111. https://dx.doi.org/https://doi.org/10.1016/j.brainres.2010.02.040

Clark, A. (2013). Whatever next? Predictive brains, situated agents, and the future of cognitive science. *Behavioral and Brain Sciences, 36*, 181–204. https://dx.doi.org/10.1017/S0140525X12000477

Clark, V. P., Fan, S., & Hillyard, S. A. (1995). Identification of early visual evoked potential generators by retinotopic and topographic analyses. *Human Brain Mapping, 2*, 170–187. https://dx.doi.org/10.1002/hbm.460020306

Cleary, K., Donkers, F., Evans, A., & Belger, A. (2013). Investigating developmental changes in sensory processing: Visual mismatch response in healthy children. *Frontiers in Human Neuroscience*, *7*(922), 1–13. https://dx.doi.org/10.3389/fnhum.2013.00922

Clifford, A., Holmes, A., Davies, I. R. L., & Franklin, A. (2010). Color categories affect pre-attentive color perception. *Biological Psychology, 85*, 275–282. https://dx.doi.org/10.1016/j.biopsycho.2010.07.014

Cohen, J. (1977). *Statistical power analysis for the behavioral sciences.* (Rev. ed.). New York: Academic Press.

Cooper, R. J., Todd, J., McGill, K., & Michie, P. T. (2006). Auditory sensory memory and the aging brain: A mismatch negativity study. *Neurobiology of Aging, 27*, 752–762. https://dx.doi.org/10.1016/j.neurobiolaging.2005.03.012

Cornella, M., Leung, S., Grimm, S., & Escera, C. (2012). Detection of simple and pattern regularity violations occurs at different levels of the auditory hierarchy. *PLoS One, 7*(8), 1–8. https://dx.doi.org/10.1371/journal.pone.0043604

Cotman, C. W., & Monaghan, D. T. (1988). Excitatory amino acid neurotransmission: NMDA receptors and hebb-type synaptic plasticity. *Annual Review of Neuroscience, 11*, 61–80. https://dx.doi.org/10.1146/annurev.ne.11.030188.000425

Cowan, N., Winkler, I., Teder, W., & Näätänen, R. (1993). Memory prerequisites of mismatch negativity in the auditory event-related potential (ERP). *Journal of Experimental Psychology: Learning, Memory and Cognition, 19*, 909–921. https://dx.doi.org/10.1037/0278-7393.19.4.909

Csibra, G., & Czigler, I. (1991). Event-related potentials to irrelevant deviant motion of visual shapes. *International Journal of Psychophysiology, 11*, 155–159. https://dx.doi.org/10.1016/0167-8760(91)90007-K

Csukly, G., Stefanics, G., Komlósi, S., Czigler, I., & Czobor, P. (2013). Emotion-related visual mismatch responses in schizophrenia: Impairments and correlations with emotion recognition. *PLoS One, 8*(10), 1–11. https://dx.doi.org/10.1371/journal.pone.0075444

Czigler, I., & Csibra, G. (1990). Event-related potentials in a visual discrimination task: Negative waves related to detection and attention. *Psychophysiology, 27*, 669–676. https://dx.doi.org/10.1111/j.1469-8986.1990.tb03191.x

Czigler, I., & Csibra, G. (1992). Event-related potentials and the identification of deviant visual stimuli. *Psychophysiology, 29*, 471–485. https://dx.doi.org/10.1111/j.1469-8986.1992.tb01722.x

Czigler, I., & Pató, L. (2009). Unnoticed regularity violation elicits change-related brain activity. *Biological Psychology, 80*, 339–347. https://dx.doi.org/10.1016/j.biopsycho.2008.12.001

Czigler, I., & Sulykos, I. (2010). Visual mismatch negativity to irrelevant changes is sensitive to task-relevant changes. *Neuropsychologia, 48*, 1277–1282. https://dx.doi.org/10.1016/j.neuropsychologia.2009.12.029

Czigler, I., Balazs, L., & Pató, L. G. (2004). Visual change detection: Event-related potentials are dependent on stimulus location in humans. *Neuroscience Letters, 364*, 149–153. https://dx.doi.org/10.1016/j.neulet.2004.04.048

Czigler, I., Balázs, L., & Winkler, I. (2002). Memory-based detection of task-irrelevant visual changes. *Psychophysiology, 39*, 869–873. https://dx.doi.org/10.1111/1469-8986.3960869

Czigler, I., Weisz, J., & Winkler, I. (2006). ERPs and deviance detection: Visual mismatch negativity to repeated visual stimuli. *Neuroscience Letters, 401*, 178–182. https://dx.doi.org/10.1016/j.neulet.2006.03.018

Daikhin, L., & Ahissar, M. (2012). Responses to deviants are modulated by sub-threshold variability of the standard. *Psychophysiology, 49*, 31–42. https://dx.doi.org/10.1111/j.1469-8986.2011.01274.x

Daugman, J. G. (1984). Spatial visual channels in the fourier plane. *Vision Research, 24*, 891–910. https://dx.doi.org/10.1016/0042-6989(84)90065-8

Daugman, J. G. (1985). Uncertainty relation for resolution in space, spatial frequency, and orientation optimized by two-dimensional visual cortical filters. *Journal of the Optical Society of America. A, Optics and image science, 2*, 1160–1169. https://dx.doi.org/10.1364/JOSAA.2.001160

De Valois, R. L., Albrecht, D. G., & Thorell, L. G. (1982). Spatial frequency selectivity of cells in macaque visual cortex. *Vision Research*, *22*, 545–559. https://dx.doi.org/10.1016/0042-6989(82)90113-4

Delorme, A., & Makeig, S. (2004). EEGLAB: An open source toolbox for analysis of single-trial EEG dynamics including independent component analysis. *Journal of Neuroscience Methods*, *134*, 9–21. https://dx.doi.org/10.1016/j.jneumeth.2003.10.009

Dien, J. (1998). Issues in the application of the average reference: Review, critiques, and recommendations. *Behavior Research Methods, Instruments, & Computers*, *30*, 34–43. https://dx.doi.org/10.3758/BF03209414

Dien, J. (2010). The ERP PCA toolkit: An open source program for advanced statistical analysis of event-related potential data. *Journal of Neuroscience Methods*, *187*, 138–145. https://dx.doi.org/10.1016/j.jneumeth.2009.12.009

Dien, J. (2012). Applying principal components analysis to event-related potentials: A tutorial. *Developmental Neuropsychology*, *37*, 497–517. https://dx.doi.org/10.1080/87565641.2012.697503

Dien, J., & Frishkoff, G. A. (2005). Principal components analysis of event-related potential datasets. In T. Handy (Eds.), *Event-related potentials: A methods handbook* (pp. 189–208). Cambridge, MA: MIT Press.

Dien, J., Beal, D. J., & Berg, P. (2005). Optimizing principal components analysis of event-related potentials: Matrix type, factor loading weighting, extraction, and rotations. *Clinical Neurophysiology, 116*, 1808–1825. https://dx.doi.org/10.1016/j.clinph.2004.11.025

Dien, J., Khoe, W., & Mangun, G. R. (2007). Evaluation of PCA and ICA of simulated ERPs: Promax versus Infomax rotations. *Human Brain Mapping, 28*, 742–763. https://dx.doi.org/10.1002/hbm.20304

Durant, S., Sulykos, I., & Czigler, I. (2017). Automatic detection of orientation variance. *Neuroscience Letters, 658*, 43–47. https://dx.doi.org/10.1016/j.neulet.2017.08.027

Durant, S., Sulykos, I., & Czigler, I. (2018). Automatic detection of the duration of visual static and dynamic stimuli. *Brain Research, 1686*, 34–41. https://dx.doi.org/10.1016/j.brainres.2018.02.015

Eaton, J. W., Bateman, D., Hauberg, S., & Wehbring, R. (2014). *GNU Octave version 3.8.1 manual: A high-level interactive language for numerical computations.* CreateSpace Independent Publishing Platform. Retreived from http://www.gnu.org/software/octave/doc/interpreter/

Engeland, C., Mahoney, C., Mohr, E., Ilivitsky, V., & Knott, V. (2002). Nicotine and sensory memory in Alzheimer's disease: An event-related potential study. *Brain and Cognition, 49*, 232–234. https://dx.doi.org/10.1006/brcg.2001.1474

EyeLink. SR Research Ltd. Ottawa, Ontario, Canada.

Farkas, K., Stefanics, G., Marosi, C., & Csukly, G. (2015). Elementary sensory deficits in schizophrenia indexed by impaired visual mismatch negativity. *Schizophrenia Research, 166,* 164–170. https://dx.doi.org/10.1016/j.schres.2015.05.011

Faul, F., Erdfelder, E., Buchner, A., & Lang, A. G. (2009). Statistical power analyses using G*Power 3.1: Tests for correlation and regression analyses. *Behavior Research Methods, 41,* 1149–1160. https://dx.doi.org/10.3758/BRM.41.4.1149

Faul, F., Erdfelder, E., Lang, A., & Buchner, A. (2007). G*Power 3: A flexible statistical power analysis program for the social, behavioral, and biomedical sciences. *Behavior Research Methods, 39,* 175–191. https://dx.doi.org/10.3758/bf03193146

Ferree, T. C., Luu, P., Russell, G. S., & Tucker, D. M. (2001). Scalp electrode impedance, infection risk, and EEG data quality. *Clinical Neurophysiology, 112,* 538–544. https://dx.doi.org/10.1016/S1388-2457(00)00533-2

Field, D. J., & Tolhurst, D. J. (1986). The structure and symmetry of simple-cell receptive-field profiles in the cat's visual cortex. *Proceedings of the Royal Society of London. Series B, Biological Sciences, 228,* 379–400. Retrieved from https://www.jstor.org/stable/36176

File, D., File, B., Bodnár, F., Sulykos, I., Kecskés-Kovács, K., & Czigler, I. (2017). Visual mismatch negativity (vMMN) for low- and high-level deviances: A control study. *Attention, Perception, & Psychophysics, 79,* 2153–2170. https://dx.doi.org/10.3758/s13414-017-1373-y

Fischer, C., Morlet, D., & Giard, M. H. (2000). Mismatch negativity and N100 in comatose patients. *Audiology and Neurotology, 5*, 192–197. https://dx.doi.org/10.1159/000013880

Fischer, C., Morlet, D., Bouchet, P., Luaute, J., Jourdan, C., & Salord, F. (1999). Mismatch negativity and late auditory evoked potentials in comatose patients. *Clinical Neurophysiology, 110*, 1601–1610. https://dx.doi.org/10.1016/S1388-2457(99)00131-5

Fisher, D. J., Scott, T. L., Shah, D. K., Prise, S., Thompson, M., & Knott, V. J. (2010). Light up and see: Enhancement of the visual mismatch negativity (vMMN) by nicotine. *Brain Research, 1313*, 162–171. https://dx.doi.org/10.1016/j.brainres.2009.12.002

Flynn, M., Liasis, A., Gardner, M., Boyd, S., & Towell, T. (2009). Can illusory deviant stimuli be used as attentional distractors to record vMMN in a passive three stimulus oddball paradigm? *Experimental Brain Research, 197*, 153–161. https://dx.doi.org/10.1007/s00221-009-1901-7

Fredericksen, R. E., Bex, P. J., & Verstraten, F. A. J. (1998). How big is a Gabor patch, and why should we care? *Journal of the Optical Society of America A: Optics and Image Science, and Vision, 15*(1), 1–12. https://dx.doi.org/10.1364/JOSAA.15.001959

Friedman, D., Cycowicz, Y. M., & Gaeta, H. (2001). The novelty P3: An event-related brain potential (ERP) sign of the brain's evaluation of novelty. *Neuroscience Biobehavioral Reviews, 25*, 355–373. https://dx.doi.org/10.1016/S0149-7634(01)00019-7

Friedman, T., Sehatpour, P., Dias, E., Perrin, M., & Javitt, D. C. (2012). Differential relationships of mismatch negativity and visual P1 deficits to premorbid characteristics and functional outcome in schizophrenia. *Biological Psychiatry, 71*, 521–529. https://dx.doi.org/10.1016/j.biopsych.2011.10.037

Friston, K. & Kiebel, S. (2009). Cortical circuits for perceptual inference. *Neural Networks, 22*, 1093–1104. https://dx.doi.org/10.1016/j.neunet.2009.07.023

Friston, K. (2003). Learning and inference in the brain. *Neural Networks, 16*, 1325–1352. https://dx.doi.org/10.1016/j.neunet.2003.06.005

Friston, K. (2005). A theory of cortical responses. *Philosophical Transactions of the Royal Society B: Biological Sciences, 360*, 815–836. https://dx.doi.org/10.1098/rstb.2005.1622

Friston, K. (2010). The free-energy principle: A unified brain theory? *Nature Reviews Neuroscience, 11*, 127–138. https://dx.doi.org/10.1038/nrn2787

Frost, J. D., Winkler, I., Provost, A., & Todd, J. (2016). Surprising sequential effects on MMN. *Biological Psychology, 116*, 47–56. https://dx.doi.org/10.1016/j.biopsycho.2015.10.005

Fu, S., Fan, S., & Chen, L. (2003). Event-related potentials reveal involuntary processing of orientation changes in the visual modality. *Psychophysiology, 40*, 770–775. https://dx.doi.org/10.1111/1469-8986.00077

Fujimura, T., & Okanoya, K. (2013). Event-related potentials elicited by pre-attentive emotional changes in temporal context. *PLoS ONE, 8*(5), 1–13. https://dx.doi.org/10.1371/journal.pone.0063703

Garrido, M. I., Friston, K. J., Kiebel, S. J., Stephan, K. E., Baldeweg, T., & Kilner, J. M. (2008). The functional anatomy of the MMN: A DCM study of the roving paradigm. *Neuroimage*, *42*, 936–944. https://dx.doi.org/10.1016/j.neuroimage.2008.05.018

Garrido, M. I., Kilner, J. M., Stephan, K. E., & Friston, K. J. (2009). The mismatch negativity: A review of underlying mechanisms. *Clinical Neurophysiology*, *120*, 453–463. https://dx.doi.org/10.1016/j.clinph.2008.11.029

Giard, M. H., Lavikainen, J., Reinikainen, K., Bertrand, O., Perrin, J., Pernier, J., & Näätänen, R. (1995). Separate representation of stimulus frequency, intensity, and duration in auditory sensory memory: An event-related potential and dipole-model analysis. *Journal of Cognitive Neuroscience*, *7*, 133–143. https://dx.doi.org/10.1162/jocn.1995.7.2.133

Giard, M. H., Perrin, F., Pernier, J., & Bouchet, P. (1990). Brain generators implicated in the processing of auditory stimulus deviance: A topographic event-related potential study. *Psychophysiology*, *27*, 627–640. https://dx.doi.org/10.1111/j.1469-8986.1990.tb03184.x

Graham, N. V. S. (1989). *Visual pattern analyzers*. New York: Oxford University Press.

Grimm, S., Bendixen, A., Deouell, L. Y., & Schröger, E. (2009). Distraction in a visual multi-deviant paradigm: Behavioral and event-related potential effects. *International Journal of Psychophysiology*, *72*, 260–266. https://dx.doi.org/10.1016/j.ijpsycho.2009.01.005

Grimm, S., Escera, C., Slabu, L. M., & Costa-Faidella, J. (2011). Electrophysiological evidence for the hierarchical organization of auditory change detection in the human brain. *Psychophysiology, 48*, 377–384. https://dx.doi.org/10.1111/j.1469-8986.2010.01073.x

Groppe, D. M., Makeig, S., & Kutas, M. (2009). Identifying reliable independent components via split-half comparisons. *NeuroImage, 45*, 1199–1211. https://dx.doi.org/10.1016/j.neuroimage.2008.12.038

Groppe, D. M., Urbach, T. P., & Kutas, M. (2011). Mass univariate analysis of event-related brain potentials/fields I: A critical tutorial review. *Psychophysiology, 48*, 1711–1725. https://dx.doi.org/10.1111/j.1469-8986.2011.01273.x

He, J., Hu, Y., Pakarinen, S., Li, B., & Zhou, Z. (2014). Different effects of alcohol on automatic detection of colour, location and time change: A mismatch negativity study. *Journal of Psychopharmacology, 28*, 1109–1114. https://dx.doi.org/10.1177/0269881114548294

Hedge, C., Stothart, G., Jones, J. T., Frías, P. R., Magee, K. L., & Brooks, J. C. W. (2015). A frontal attention mechanism in the visual mismatch negativity. *Behavioural Brain Research, 293*, 173–181. https://dx.doi.org/10.1016/j.bbr.2015.07.022

Heslenfeld, D. J. (2003). Visual mismatch negativity. In J. Polich (Eds.), *Detection of change: Event-related potential and fMRI findings* (pp. 41–59). Dordrecht, The Netherlands: Kluwer.

Hesse, P. N., Schmitt, C., Klingenhoefer, S., & Bremmer, F. (2017). Preattentive processing of numerical visual information. *Frontiers in Human Neuroscience, 11*(70), 1–14. https://dx.doi.org/10.3389/fnhum.2017.00070

Hillyard, S. A., & Münte, T. F. (1984). Selective attention to color and location: An analysis with event-related brain potentials. *Perception and Psychophysics, 36*, 185–198. https://dx.doi.org/10.3758/BF03202679

Hohwy, J. (2012). Attention and conscious perception in the hypothesis testing brain. *Frontiers in Psychology, 3*(96), 1–14. https://dx.doi.org/10.3389/fpsyg.2012.00096

Hohwy, J. (2013). *The Predictive Mind.* Oxford: Oxford University Press.

Horimoto, R., Inagaki, M., Yano, T., Sata, Y., & Kaga, M. (2002). Mismatch negativity of the color modality during a selective attention task to auditory stimuli in children with mental retardation. *Brain and Development, 24*, 703–709. https://dx.doi.org/10.1016/S0387-7604(02)00086-4

Horn, J. L. (1965). A rationale and test for the number of factors in factor analysis. *Psychometrika, 30*, 179–185. Retrieved from https://link.springer.com/article/10.1007/BF02289447

Horváth, J., Czigler, I., Jacobsen, T., Maess, B., Schröger, E., & Winkler, I. (2008). MMN or no MMN: No magnitude of deviance effect on the MMN amplitude. *Psychophysiology, 45*, 60–69. https://dx.doi.org/10.1111/j.1469-8986.2007.00599.x

Hosák, L., Kremláček, J., Kuba, M., Libiger, J., & Čížek, J. (2008). Mismatch negativity in methamphetamine dependence: A pilot study. *Acta Neurobiologiae Experimentalis, 68*, 97–102. Retrieved from https://ane.pl/home

Huang, Y., & Rao, R. P. N. (2011). Predictive coding. *Wiley Interdisciplinary Reviews: Cognitive Science, 2*, 580–593. https://dx.doi.org/10.1002/wcs.142

Iijima, M., Osawa, M., Nageishi, Y., Ushijima, R., & Iwata, M. (1996). Visual mismatch negativity (MMN) in aging. In C. Ogura, Y. Koga, & M. Shimokochi (Eds.), *Recent advances in event-related brain potentials research* (pp. 804–809). Amsterdam, The Netherlands: Elsevier.

Jack, B. N., Roeber, U., & O'Shea, R. P. (2015). We make predictions about eye of origin of visual input: Visual mismatch negativity from binocular rivalry. *Journal of Vision, 15*(13), 1–19. https://dx.doi.org/10.1167/15.13.9

Jack, B. N., Widmann, A., O'Shea, R. P., Schröger, E., & Roeber, U. (2017). Brain activity from stimuli that are not perceived: Visual mismatch negativity during binocular rivalry suppression. *Psychophysiology, 54*, 755–763. https://dx.doi.org/10.1111/psyp.12831

James, W. (1890). *The principles of psychology*. New York: Henry Holt and Company.

Javitt, D. C., Spencer, K. M., Thaker, G. K., Winterer, G., & Hajós, M. (2008). Neurophysiological biomarkers for drug development in schizophrenia. *Nature Reviews Drug Discovery, 7*, 68–83. https://dx.doi.org/10.1038/nrd2463

Javitt, D. C., Steinschneider, M., Schroeder, C. E., & Arezzo, J. C. (1996). Role of cortical N-methyl-D-aspartate receptors in auditory sensory memory and mismatch negativity generation: Implications for schizophrenia. *Proceedings of the National Academy of Sciences of the United States of America*, *93*, 11962–11967. https://dx.doi.org/10.1073/pnas.93.21.11962

Jeffreys, H. (1961). *Theory of probability (3rd Ed.).* Oxford, UK: Oxford University Press.

Kappenman, E. S., & Luck, S. J. (2010). The effects of electrode impedance on data quality and statistical significance in ERP recordings. *Psychophysiology*, *47*, 888–904. https://dx.doi.org/10.1111/j.1469-8986.2010.01009.x

Kayser, J., & Tenke, C. E. (2010). In search of the Rosetta Stone for scalp EEG: Converging on reference-free techniques. *Clinical Neurophysiology*, *121*, 1973–1975. https://dx.doi.org/10.1016/j.clinph.2010.04.030

Kecskés-Kovács, K., Sulykos, I., & Czigler, I. (2013a). Visual mismatch negativity is sensitive to symmetry as a perceptual category. *European Journal of Neuroscience*, *37*, 662–667. https://dx.doi.org/10.1111/ejn.12061

Kecskés-Kovács, K., Sulykos, I., & Czigler, I. (2013b). Is it a face of a woman or a man? Visual mismatch negativity is sensitive to gender category. *Frontiers in Human Neuroscience*, *7*(532), 1–11. https://dx.doi.org/10.3389/fnhum.2013.00532

Kekoni, J., Hämäläinen, H., Saarinen, M., Gröhn, J., Reinikainen, K., Lehtokoski, A., & Näätänen, R. (1997). Rate effect and mismatch responses in the somatosensory system: ERP-recordings in humans. *Biological Psychology, 46*, 125–142. https://dx.doi.org/10.1016/S0301-0511(97)05249-6

Kenemans, J. L., Hebly, W., van den Heuvel, E., & Grent-'T-Jong, T. (2010). Moderate alcohol disrupts a mechanism for detection of rare events in human visual cortex. *Journal of Psychopharmacology, 24*, 839–845. https://dx.doi.org/10.1177/0269881108098868

Kenemans, J. L., Jong, T. G., & Verbaten, M. N. (2003). Detection of visual change: Mismatch or rareness? *NeuroReport, 14*, 1239–1242. https://dx.doi.org/10.1097/01.wnr.0000081871.45938.c4

Khodanovich, M. Y., Esipenko, E. A., Svetlik, M. V., & Krutenkova, E. P. (2010). A visual analog of mismatch negativity when stimuli differ in duration. *Neuroscience and Behavioral Physiology*, *40*, 653–661. https://dx.doi.org/10.1007/s11055-010-9308-2

Kimura, M. (2018, in press). Visual mismatch negativity and representational momentum: Their possible involvement in the same automatic prediction. *Biological Psychology*. https://dx.doi.org/10.1016/j.biopsycho.2018.10.015

Kimura, M., & Takeda, Y. (2013). Task difficulty affects the predictive process indexed by visual mismatch negativity. *Frontiers in Human Neuroscience*, *7*(267), 1–13. https://dx.doi.org/10.3389/fnhum.2013.00267

Kimura, M., & Takeda, Y. (2014). Voluntary action modulates the brain response to rule-violating events indexed by visual mismatch negativity. *Neuropsychologia, 65*, 63–73. https://dx.doi.org/10.1016/j.neuropsychologia.2014.10.017

Kimura, M., & Takeda, Y. (2015). Automatic prediction regarding the next state of a visual object: Electrophysiological indicators of prediction match and mismatch. *Brain Research, 1626*, 31–44. https://dx.doi.org/10.1016/j.brainres.2015.01.013

Kimura, M., Katayama, J., & Murohashi, H. (2005). Positive difference in ERPs reflects independent processing of visual changes. *Psychophysiology, 42*, 369–379. https://dx.doi.org/10.1111/j.1469-8986.2005.00297.x

Kimura, M., Katayama, J., & Murohashi, H. (2006a). An ERP study of visual change detection: Effects of magnitude of spatial frequency changes on the change-related posterior positivity. *International Journal of Psychophysiology, 62*, 14–23. https://dx.doi.org/10.1016/j.ijpsycho.2005.11.005

Kimura, M., Katayama, J., & Murohashi, H. (2006b). Independent processing of visual stimulus changes in ventral and dorsal stream features indexed by an early positive difference in event-related brain potentials. *International Journal of Psychophysiology, 59*, 141–150. https://dx.doi.org/10.1016/j.ijpsycho.2005.03.023

Kimura, M., Katayama, J., & Murohashi, H. (2006c). Probability-independent and -dependent ERPs reflecting visual change detection. *Psychophysiology, 43*, 180–189. https://dx.doi.org/10.1111/j.1469-8986.2006.00388.x

Kimura, M., Katayama, J., & Murohashi, H. (2008). Attention switching function of memory-comparison-based change detection system in the visual modality. *International Journal of Psychophysiology, 67*, 101–113. https://dx.doi.org/10.1016/j.ijpsycho.2007.10.009

Kimura, M., Katayama, J., Ohira, H., & Schröger, E. (2009). Visual mismatch negativity: New evidence from the equiprobable paradigm. *Psychophysiology, 46*, 402–409. https://dx.doi.org/10.1111/j.1469-8986.2008.00767.x

Kimura, M., Widmann, A., & Schröger, E. (2010a). Human visual system automatically represents large-scale sequential regularities. *Brain Research, 1317*, 165–179. https://dx.doi.org/10.1016/j.brainres.2009.12.076

Kimura, M., Widmann, A., & Schröger, E. (2010b). Top-down attention affects sequential regularity representation in the human visual system. *International Journal of Psychophysiology, 77*, 126–134. https://dx.doi.org/10.1016/j.ijpsycho.2010.05.003

Kleiner, M. (2013). *Introduction to Psychtoolbox-3.* Retrieved from https://github.com/Psychtoolbox-3/Psychtoolbox-3/blob/master/Psychtoolbox/PsychDocumentation/PTBTutorial-ECVP2013.pdf

Kok, A. (2001). On the utility of P3 amplitude as a measure of processing capacity. *Psychophysiology, 38*, 557–577. https://dx.doi.org/10.1017/S0048577201990559

Kolb, H., Fernandez, E., & Nelson, R. (1997, December 7). *Facts and figures concerning the human retina*. Retrieved from https://web.archive.org/web/19970227120913/http://www.insight.med.utah.edu/Webvision/facts.html.

Kolb, H., Fernandez, E., & Nelson, R. (2018, December 04). *WEBVISION: The Organization of the Retina and Visual System*. Retrieved from at: http:// www.webvision.med.utah.edu.

Kovarski, K., Latinus, M., Charpentier, J., Cléry, H., Roux, S., Houy-Durand, E., ... Gomot, M. (2017). Facial expression related vMMN: Disentangling emotional from neutral change detection. *Frontiers in Human Neuroscience, 11*(18), 1–13. https://dx.doi.org/10.3389/fnhum.2017.00018

Krauel, K., Schott, P., Sojka, B., Pause, B. M., & Ferstl, R. (1999). Is there a mismatch negativity analogue in the olfactory event-related potential? *Journal of Psychophysiology, 13*, 49–55. https://dx.doi.org/10.1027//0269-8803.13.1.49

Kreegipuu, K., Kuldkepp, N., Sibolt, O., Toom, M., Allik, J., & Näätänen, R. (2013). vMMN for schematic faces: Automatic detection of change in emotional expression. *Frontiers in Human Neuroscience, 7*(714), 1–11. https://dx.doi.org/10.3389/fnhum.2013.00714

Kremláček, J., Kreegipuu, K., Tales, A., Astikainen, P., Põldver, N., Näätänen, R., & Stefanics, G. (2016). Visual mismatch negativity (vMMN): A review and meta-analysis of studies in psychiatric and neurological disorders. *Cortex, 80*, 76–112. https://dx.doi.org/10.1016/j.cortex.2016.03.017

Kremláček, J., Kuba, M., Kubová, Z., & Langrová, J. (2006). Visual mismatch negativity elicited by magnocellular system activation. *Vision Research, 46*, 485–490. https://dx.doi.org/10.1016/j.visres.2005.10.001

Kujala, T., Tervaniemi, M., & Schröger, E. (2007). The mismatch negativity in cognitive and clinical neuroscience: Theoretical and methodological considerations. *Biological Psychology, 74*(1), 1–19. https://dx.doi.org/10.1016/j.biopsycho.2006.06.001

Kuldkepp, N., Kreegipuu, K., Raidvee, A., Näätänen, R., & Allik, J. (2013). Unattended and attended visual change detection of motion as indexed by event-related potentials and its behavioral correlates. *Frontiers in Human Neuroscience, 7*, 476–485. https://dx.doi.org/10.3389/fnhum.2013.00476

Lee, M. D., & Wagenmakers, E.-J. (2013). *Bayesian cognitive modeling: A practical course*. Cambridge, U.K.: Cambridge University Press. https://dx.doi.org/doi:10.1017/CBO9781139087759

Lee, T. S., & Mumford, D. (2003). Hierarchical Bayesian inference in the visual cortex. *Journal of the Optical Society of America A, 20*, 1434–1448. https://dx.doi.org/10.1364/JOSAA.20.001434

Lepistö, T., Soininen, M., Čeponiene, R., Almqvist, F., Näätänen, R., & Aronen, E. T. (2004). Auditory event-related potential indices of increased distractibility in children with major depression. *Clinical Neurophysiology, 115*, 620–627. https://dx.doi.org/10.1016/j.clinph.2003.10.020

Leung, S., Cornella, M., Grimm, S., & Escera, C. (2012). Is fast auditory change detection feature-specific? An electrophysiological study in humans. *Psychophysiology, 49*, 933–942. https://dx.doi.org/10.1111/j.1469-8986.2012.01375.x

Leung, S., Greenwood, L., Michie, P., & Croft, R. (2015). *The role of stimulus train length in mismatch negativity (MMN) abnormalities in schizophrenia: A comparison of the 'roving' and 'oddball' MMN paradigms.* [Abstract]. Paper presented at the XII International Conference on Cognitive Neuroscience, Brisbane, QLD. Retrieved from https://www.frontiersin.org/events/XII_International_Conference_on_Cognitive_Neuroscience(ICON-XII)/1692

Li, X., Lu, Y., Sun, G., Gao, L., & Zhao, L. (2012). Visual mismatch negativity elicited by facial expressions: New evidence from the equiprobable paradigm. *Behavioral and Brain Functions, 8*, 7–7. https://dx.doi.org/10.1186/1744-9081-8-7

Lieder, F., Stephan, K. E., Daunizeau, J., Garrido, M. I., & Friston, K. J. (2013). A neurocomputational model of the mismatch negativity. *PLOS Computational* Biology, 9(11), 1–14. https://dx.doi.org/10.1371/journal.pcbi.1003288

Lopez-Calderon, J., & Luck, S. J. (2014). ERPLAB: An open-source toolbox for the analysis of event-related potentials. *Frontiers in Human Neuroscience, 8*(213), 1–14. https://dx.doi.org/10.3389/fnhum.2014.00213

Lorenzo-López, L., Amenedo, E., Pazo-Alvarez, P., & Cadaveira, F. (2004). Pre-attentive detection of motion direction changes in normal aging. *NeuroReport, 15*, 2633–2636. https://dx.doi.org/10.1097/00001756-200412030-00015

Luck, S. J. (2005). *An introduction to the event-related potential technique*. Cambridge, Massachusetts: The MIT Press.

Luck, S. J., Chelazzi, L., Hillyard, S. A., & Desimone, R. (1997). Neural mechanisms of spatial selective attention in areas V1, V2, and V4 of macaque visual cortex. *Journal of Neurophysiology, 77*, 24–42. https://dx.doi.org/10.1152/jn.1997.77.1.24

lv, J., Zhao, L., Gong, J., Chen, C., & Miao, D. (2010). Event-related potential based evidence of cognitive dysfunction in patients during the first episode of depression using a novelty oddball task. *Psychiatry Research, 182*, 58–66. https://dx.doi.org/10.1016/ j.pscychresns.2010.02.005

Maekawa, T., Goto, Y., Kinukawa, N., Taniwaki, T., Kanba, S., & Tobimatsu, S. (2005). Functional characterization of mismatch negativity to a visual stimulus. *Clinical Neurophysiology, 116*, 2392–2402. https://dx.doi.org/10.1016/j.clinph.2005.07.006

Maekawa, T., Katsuki, S., Kishimoto, J., Onitsuka, T., Ogata, K., Yamasaki, T., … Kanba1, S. (2013). Altered visual information processing systems in bipolar disorder: Evidence from visual MMN and P3. *Frontiers in Human Neuroscience, 7*(403), 1–11. https://dx.doi.org/10.3389/fnhum.2013.00403

Maekawa, T., Tobimatsu, S., Ogata, K., Onitsuka, T., & Kanba, S. (2009). Preattentive visual change detection as reflected by the mismatch negativity (MMN): Evidence for a memory-based process. *Neuroscience Research, 65*, 107–112. https://dx.doi.org/10.1016/j.neures.2009.06.005

Makeig, S., Bell, A. J., Jung, T. P., & Sejnowski, T. J. (1996). Independent component analysis of electroencephalographic data. *Advances in Neural Information Processing Systems, 8*, 145–151. Retrieved from https://papers.nips.cc/paper/1091-independent-component-analysis-of-electroencephalographic-data.pdf

Male, A., Müller, D., Roeber, U., O'Shea, R. P., Schröger, E., & Widmann, A. (2018). *No visual mismatch negativity to well-controlled orientation deviants*. Paper presented at the MMN2018: 8th Mismatch Negativity conference "MMN from basic science to clinical applications", Helsinki.

Male, A., O'Shea, R. P., & Roeber, U. (2017). *Brain responses to unpredicted changes in the structure and clarity of unpredicted visual input: Visual mismatch negativity to orientation and contrast changes in upper and lower visual fields*. Paper presented at the 40th European Conference on Visual Perception (ECVP 2017), Berlin.

Male, A., Roeber, U., & O'Shea, R. (2016). An ERP study investigating memory-theory and predictive-coding of visual mismatch negativity (vMMN). Paper presented at the 2016 Australasian Cognitive Neuroscience Society (ACNS) Conference, Shoal Bay, NSW. Abstract published in F. Karayanidis, & J. Todd (Eds.), *2016 Australasian Cognitive Neuroscience Society (ACNS) Conference* (pp. 42). Shoal Bay, NSW: University of Newcastle.

Marčelja, S. (1980). Mathematical description of the responses of simple cortical cells. *Journal of Optical Society of America, 70*, 1297–1300. https://dx.doi.org/10.1364/JOSA.70.001297

Masland, R. H. (2017). Vision: Two speeds in the retina. *Current Biology, 27*, R303–R305. https://dx.doi.org/10.1016/j.cub.2017.02.056

MATLAB, 2015. The MathWorks, Inc., Natick, Massachusetts, United States.

May, P. J., & Tiitinen, H. (2009). Mismatch negativity (MMN), the deviance-elicited auditory deflection, explained. *Psychophysiology, 46*, 1–57. https://dx.doi.org/10.1111/j.1469-8986.2009.00856.x

Mazza, V., Turatto, M., & Sarlo, M. (2005). Rare stimuli or rare changes: What really matters for the brain? *NeuroReport, 16*, 1061–1064. https://dx.doi.org/10.1097/00001756-200507130-00006

Mo, L., Xu, G., Kay, P., & Tan, L. (2011). Electrophysiological evidence for the left-lateralized effect of language on preattentive categorical perception of color. *Proceedings of the National Academy of Sciences of the United States of America, 108*, 14026–14030. https://dx.doi.org/10.1073/pnas.1111860108

Mognon, A., Jovicich, J., Bruzzone, L., & Buiatti, M. (2011). ADJUST: An automatic EEG artifact detector based on the joint use of spatial and temporal features. *Psychophysiology, 48*, 229–240. https://dx.doi.org/10.1111/j.1469-8986.2010.01061.x

Müller, D., Roeber, U., Winkler, I., Trujillo-Barreto, N., Czigler, I., & Schröger, E. (2012). Impact of lower- vs. upper-hemifield presentation on automatic colour-deviance detection: A visual mismatch negativity study. *Brain Research, 1472*, 89–98. https://dx.doi.org/10.1016/j.brainres.2012.07.016

Müller, D., Widmann, A., & Schröger, E. (2013). Object-related regularities are processed automatically: Evidence from the visual mismatch negativity. *Frontiers in Human Neuroscience, 7*(259), 1–11. https://dx.doi.org/10.3389/fnhum.2013.00259

Müller, D., Winkler, I., Roeber, U., Schaffer, S., Czigler, I., & Schröger, E. (2010). Visual object representations can be formed outside the focus of voluntary attention: Evidence from event-related brain potentials. *Journal of Cognitive Neuroscience, 22*, 1179–1188. https://dx.doi.org/10.1162/jocn.2009.21271

Näätänen, R. (1990). The role of attention in auditory information processing as revealed by event-related potentials and other brain measures of cognitive function. *Behavioral and Brain Sciences, 13*, 201–233. https://dx.doi.org/10.1017/S0140525X00078407

Näätänen, R. (1992). *Event-related potentials and automatic information processing.* In R. Näätänen (Eds.), Attention and brain function (pp. 102–296.). Hillsdale, NJ: Lawrence Erlbaum Associates.

Näätänen, R., Astikainen, P., Ruusuvirta, T., & Huotilainen, M. (2010). Automatic auditory intelligence: An expression of the sensory–cognitive core of cognitive processes. *Brain Research Reviews, 64*, 123–136. https://dx.doi.org/10.1016/j.brainresrev.2010.03.001

Näätänen, R., Gaillard, A. W. K., & Mäntysalo, S. (1978). Early selective-attention effect on evoked potential reinterpreted. *Acta Psychologica, 42*, 313–329. https://dx.doi.org/10.1016/0001-6918(78)90006-9

Näätänen, R., Kujala, T., Escera, C., Baldeweg, T., Kreegipuu, K., Carlson, S., & Ponton, C. (2012). The mismatch negativity (MMN) - A unique window to disturbed central auditory processing in ageing and different clinical conditions. *Clinical Neurophysiology, 123*, 424–458. https://dx.doi.org/10.1016/j.clinph.2011.09.020

Näätänen, R., Paavilainen, P., & Reinikainen, K. (1989). Do event-related potentials to infrequent decrements in duration of auditory stimuli demonstrate a memory trace in man? *Neuroscience Letters, 107*, 347–352. https://dx.doi.org/10.1016/0304-3940(89)90844-6

Näätänen, R., Paavilainen, P., Rinne, T., & Alho, K. (2007). The mismatch negativity (MMN) in basic research of central auditory processing: A review. *Clinical Neurophysiology, 118*, 2544–2590. https://dx.doi.org/10.1016/j.clinph.2007.04.026

Näätänen, R., Pakarinen, S., Rinne, T., & Takegata, R. (2004). The mismatch negativity (MMN): Towards the optimal paradigm. *Clinical Neurophysiology, 115*, 140–144. https://dx.doi.org/10.1016/j.clinph.2003.04.001

Nelson, R. (2007). *Ganglion cell physiology by Ralph Nelson*. Retrieved from http://webvision.med.utah.edu/book/part-ii-anatomy-and-physiology-of-the-retina/ganglion-cell-physiology/

Neuhaus, A. H., Brandt, E. S. L., Goldberg, T. E., Bates, J. A, & Malhotra, A. K. (2013). Evidence for impaired visual prediction error in schizophrenia. *Schizophrenia Research, 147*, 326–330. https://dx.doi.org/10.1016/j.schres.2013.04.004

Novitski, N., Tervaniemi, M., Huotilainen, M., & Näätänen, R. (2004). Frequency discrimination at different frequency levels as indexed by electrophysiological and behavioral measures. *Cognitive Brain Research, 20*, 26–36. https://dx.doi.org/10.1016/j.cogbrainres.2003.12.011

Noyce, A., & Sekuler, R. (2014). Oddball distractors demand attention: Neural and behavioral responses to predictability in the flanker task. *Neuropsychologia*, *65*, 18–24. https://dx.doi.org/10.1016/j.neuropsychologia.2014.10.002

Nunez, P. L. (1990). Physical principles and neurophysiological mechanisms underlying event-related potentials. In J. W. Rohrbaugh, R. Parasuraman & J. R. Johnson (Eds.), *Event-related brain potentials: Basic issues and applications* (pp. 19–36). New York, NY: Oxford University Press.

Nunez, P. L. (2010). REST: A good idea but not the gold standard. *Clinical Neurophysiology*, *121*, 2177–2180. https://dx.doi.org/10.1016/j.clinph.2010.04.029

Nyman, G., Alho, K., Laurinen, P., Paavilainen, P., Radil, T., Reinikainen, K., Sams, M., & Näätänen, R. (1990). Mismatch negativity (MMN) for sequences of auditory and visual stimuli: Evidence for a mechanism specific to the auditory modality. *Electroencephalography and Clinical Neurophysiology, 77*, 436–444. doi:10.1016/0168-5597(90)90004-W

O'Shea, R. P. (2015). Refractoriness about adaptation. *Frontiers in Human Neuroscience, 9*(38), 1–3. https://dx.doi.org/10.3389/fnhum.2015.00038

O'Shea, R. P., Roeber, U., & Bach, M. (2010). Evoked potential: Vision. In E. B. Goldstein (Eds.), *Encyclopedia of Perception* (pp. 399–400). Thousand Oaks, California: Sage Publications, Inc.

Oostenveld, R., Fries, P., Maris, E., & Schoffelen, J. M. (2011). FieldTrip: Open source software for advanced analysis of MEG, EEG, and invasive electrophysiological data. *Computational Intelligence and Neuroscience, 2011*, 156869–156878. https://dx.doi.org/10.1155/2011/156869

Opitz, B., Rinne, T., Mecklinger, A., von Cramon, D. Y., & Schröger, E. (2002). Differential contribution of frontal and temporal cortices to auditory change detection: fMRI and ERP results. *NeuroImage, 15*, 167–174. https://dx.doi.org/10.1006/nimg.2001.0970

Paavilainen, P., Alho, K., Reinikainen, K., Sams, M., & Näätänen, R. (1991). Right hemisphere dominance of different mismatch negativities. *Electroencephalography and Clinical Neurophysiology, 78*, 466–479. https://dx.doi.org/10.1016/0013-4694(91)90064-B

Paavilainen, P., Simola, J., Jaramillo, M., Näätänen, R., & Winkler, I. (2001). Preattentive extraction of abstract feature conjunctions from auditory stimulation as reflected by the mismatch negativity (MMN). *Psychophysiology, 38*, 359–365. https://dx.doi.org/10.1111/1469-8986.3820359

Pakarinen, S., Lovio, R., Huotilainen, M., Alku, P., Näätänen, R., & Kujala, T. (2009). Fast multi-feature paradigm for recording several mismatch negativities (MMNs) to phonetic and acoustic changes in speech sounds. *Biological Psychology, 82*, 219–226. https://dx.doi.org/10.1016/j.biopsycho.2009.07.008

Pakarinen, S., Takegata, R., Rinne, T., Huotilainen, M., & Näätänen, R. (2007). Measurement of extensive auditory discrimination profiles using the mismatch negativity (MMN) of the auditory event-related potential (ERP). *Clinical Neurophysiology, 118,* 177–185. https://dx.doi.org/10.1016/j.clinph.2006.09.001

Patel, S. H., & Azzam, P. N., (2005). Characterization of N200 and P300: Selected studies of the event-related potential. *International Journal of Medical Sciences, 2,* 147–154. https://dx.doi.org/10.7150/ijms.2.147

Pazo-Álvarez, P., Amenedo, E., & Cadaveira, F. (2004b). Automatic detection of motion direction changes in the human brain. *European Journal of Neuroscience, 7,* 1978–1986. https://dx.doi.org/10.1111/j.1460-9568.2004.03273.x

Pazo-Álvarez, P., Amenedo, E., Lorenzo-López, L., & Cadaveira, F. (2004a). Effects of stimulus location on automatic detection of changes in motion direction in the human brain. *Neuroscience Letters, 371,* 111–116. https://dx.doi.org/10.1016/j.neulet.2004.08.073

Pazo-Álvarez, P., Cadaveira, F., & Amenedo, E. (2003). MMN in the visual modality: A review. *Biological Psychology, 63,* 199–236. https://dx.doi.org/10.1016/s0301-0511(03)00049-8

Pelli, D. G. (1997). The VideoToolbox software for visual psychophysics: Transforming numbers into movies. *Spatial Vision, 10,* 437–442. https://dx.doi.org/10.1163/156856897X00366

Perrin, F., Pernier, J., Bertnard, O., Giard, M. H., & Echallier, J. F. (1987). Mapping of scalp potentials by surface spline interpolation. *Electroencephalography and Clinical Neurophysiology, 66*, 75–81. https://dx.doi.org/10.1016/0013-4694(87)90141-6

Pesonen, H., Savić, A. M., Kujala, U. M., & Tarkka, I. M. (2017). Long-term physical activity modifies automatic visual processing. *International Journal of Sport and Exercise Psychology*, *2017*, 1–10. https://dx.doi.org/10.1080/1612197X.2017.1321031

Piotrowski, L. N., & Campbell, F. W. (1982). A demonstration of the visual importance and flexibility of spatial frequency amplitude and phase. *Perception, 11*, 337–346. https://dx.doi.org/doi:10.1068/p110337

Polich J. (2003). Overview of P3a and P3b. In J Polich (Eds.), *Detection of change: Event-related potential and fMRI findings* (pp. 83–98). Boston, MA: Kluwer.

Qian, X., Liu, Y., Xiao, B., Gao, L., Li, S., Dang, L., ... Zhao, L. (2014). The visual mismatch negativity (vMMN): Toward the optimal paradigm. *International Journal of Psychophysiology, 93*, 311–315. https://dx.doi.org/10.1016/j.ijpsycho.2014.06.004

Qin, Y., Zhan, Y., Wang, C., Zhang, J., Yao, L., Guo, X., … Hu, B. (2016). Classifying four-category visual objects using multiple ERP components in single-trial ERP. *Cognitive Neurodynamics, 10*, 275–285. https://dx.doi.org/10.1007/s11571-016-9378-0

Qiu, X., Yang, X., Qiao, Z., Wang, L., Ning, N., Shi, J., ... Yang, Y. (2011). Impairment in processing visual information at the preattentive stage in patients with a major depressive disorder: A visual mismatch negativity study. *Neuroscience Letters, 491*, 53–57. https://dx.doi.org/10.1016/j.neulet.2011.01.006

Raftery, A. E. (1995). Bayesian model selection in social research. In P. V. Marsden (Eds.), *Sociological methodology* (pp. 111–196). Cambridge, MA: Blackwell.

Rao, R. P. N. (1999). An optimal estimation approach to visual perception and learning. *Vision Research, 39*, 1963–1989. https://dx.doi.org/10.1016/S0042-6989(98)00279-X

Rao, R. P. N., & Ballard, D. H. (1999). Predictive coding in the visual cortex: A functional interpretation of some extra-classical receptive-field effects. *Nature Neuroscience, 2*, 79–89. https://dx.doi.org/10.1038/4580

Rao, R. P., & Ballard, D. H. (1997). Dynamic model of visual recognition predicts neural response properties in the visual cortex. *Neural Computation, 9*, 721–763. https://dx.doi.org/10.1162/neco.1997.9.4.721

Recasens, M., Grimm, S., Capilla, A., Nowak, R., & Escera, C. (2014). Two sequential processes of change detection in hierarchically ordered areas of the human auditory cortex. *Cerebral Cortex, 24*, 1047–3211. https://dx.doi.org/10.1093/cercor/bhs295

Rinne, T., Alho, K., Ilmoniemi, R. J., Virtanen, J., & Näätänen, R. (2000). Separate time behaviors of the temporal and frontal mismatch negativity sources. *Neuroimage, 12*, 14–19. https://dx.doi.org/10.1006/nimg.2000.0591

Ruhnau, P., Herrmann, B., & Schröger, E. (2012). Finding the right control: The mismatch negativity under investigation. *Clinical Neurophysiology, 123*, 507–512. https://dx.doi.org/10.1016/j.clinph.2011.07.035

Ruusuvirta, T., Huotilainen, M., Fellman, V., & Näätänen, R. (2009). Numerical discrimination in newborn infants as revealed by event-related potentials to tone sequences. *European Journal of Neuroscience, 30*, 1620–1624. https://dx.doi.org/10.1111/j.1460-9568.2009.06938.x

Sabri, M., Radnovich, A. J., Li, T. Q., & Kareken, D. A. (2005). Neural correlates of olfactory change detection. *NeuroImage, 25*, 969–974. https://dx.doi.org/10.1016/j.neuroimage.2004.12.033Sams, M., Paavilainen, P., Alho, K., & Näätänen, R. (1985). Auditory frequency discrimination and event-related potentials. *Electroencephalography and Clinical Neurophysiology/ Evoked Potentials*, 62, 437–448. https://dx.doi.org/10.1016/0168-5597(85)90054-1

Sagan, C. (1997). *Billions & billions: Thoughts on life & death at the brink of the millennium*. Toronto, Ontario: The Globe & Mail division of Bell Globemedia Publishing Inc.

Sakitt, B. (1976). Iconic memory. *Psychological Review, 83*, 257–276. http://dx.doi.org/10.1037/0033-295X.83.4.257

Sams, M., Alho, K., & Näätänen, R. (1993). Sequential effects on the ERP in discriminating to stimuli. *Biological Psychology, 17*, 41–58. https://dx.doi.org/10.1016/0301-0511(83)90065-0

Sams, M., Paavilainen, P., Alho, K., & Näätänen, R. (1985). Auditory frequency discrimination and event-related potentials. *Electroencephalography and Clinical Neurophysiology/ Evoked Potentials*, 62, 437–448. https://dx.doi.org/10.1016/0168-5597(85)90054-1

Schmitt, C., Klingenhoefer, S., & Bremmer, F. (2018). Preattentive and predictive processing of visual motion. *Scientific Reports*, *8*(12399), 1–12. https://dx.doi.org/10.1038/s41598-018-30832-9

Schröger, E. (1996). A neural mechanism for involuntary attention shifts to changes in auditory stimulation. *Journal of Cognitive Neuroscience, 8*, 527–539. https://dx.doi.org/10.1162/jocn.1996.8.6.527

Schröger, E., Marzecová, A., & SanMiguel, I. (2015). Attention and prediction in human audition: A lesson from cognitive psychophysiology. *European Journal of Neuroscience, 41*, 641–664. https://dx.doi.org/10.1111/ejn.12816

Shi, L. P., Wu, J., Sun, G., Dang, L. J., & Zhao, L. (2013). Visual mismatch negativity in the "optimal" multi-feature paradigm. *Journal of Integrative Neuroscience, 12*, 247–258. https://dx.doi.org/10.1142/S0219635213500179

Si, C., Ren, C., Wang, P., Bian, H., Wang, H., & Yan, Z. (2014). Impairment in preattentive processing among patients with hypertension revealed by visual mismatch negativity. *BioMed Research International, 2014*, 945121–945128. https://dx.doi.org/10.1155/2014/945121

Siok, W. T., Kay, P., Wang, W. S. Y., Chan, A. H. D., Chen, L., Luke, K., & Tan, L. H. (2009). Language regions of brain are operative in color perception. *Proceedings of the National Academy of Sciences, 106*, 8140–8145. https://dx.doi.org/10.1073/pnas.0903627106

Slabu, L. M., Escera, C., Grimm, S., & Costa-Faidella, J. (2010). Early change detection in humans as revealed by auditory brainstem and middle-latency evoked potentials. *European Journal of Neuroscience, 32*, 859–865. https://dx.doi.org/10.1111/j.1460-9568.2010.07324.x

Snyder, E., & Hillyard, S. A. (1976). Long-latency evoked potentials to irrelevant, deviant stimuli. *Behavioral Biology, 16*, 319–331. https://dx.doi.org/10.1016/S0091-6773(76)91447-4

Sperling, G. (1960). The information available in brief visual presentations. *Psychological Monographs: General and Applied, 74*(11), 1–29. http://dx.doi.org/10.1037/h0093759

Spratling, M. W. (2017). A review of predictive coding algorithms. *Brain and Cognition, 112*, 92–97. https://dx.doi.org/10.1016/j.bandc.2015.11.003

Squires, N. K., Squires, K. C., & Hillyard, S. A. (1975). Two varieties of long-latency positive waves evoked by unpredictable auditory stimuli in man. *Electroencephalography and Clinical Neurophysiology, 38*, 387–401. https://dx.doi.org/10.1016/0013-4694(75)90263-1

Srinivasan, M. V., Laughlin, S. B., & Dubs, A. (1982). Predictive coding: A fresh view of inhibition in the retina. *Proceedings of the Royal Society Series B: Biological Sciences, 216*, 427-459. https://dx.doi.org/10.1098/rspb.1982.0085

Stagg, C., Hindley, P., Tales, A., & Butler, S. (2004). Visual mismatch negativity: The detection of stimulus change. *NeuroReport, 15*, 659–663. https://dx.doi.org/10.1097/01.wnr.0000116966.73984.58

Stefanics, G., & Czigler, I. (2012). Automatic prediction error responses to hands with unexpected laterality: An electrophysiological study. *Neuroimage*, *63*, 253–261. https://dx.doi.org/10.1016/j.neuroimage.2012.06.068

Stefanics, G., Astikainen, P., & Czigler, I. (2015). Visual mismatch negativity (vMMN): A prediction error signal in the visual modality. *Frontiers in Human Neuroscience*, *8*(1074), 1–4. https://dx.doi.org/10.3389/fnhum.2014.01074

Stefanics, G., Csukly, G., Komlosi, S., Czobor, P., & Czigler, I. (2012). Processing of unattended facial emotions: A visual mismatch negativity study. *Neuroimage*, *59*, 3042–3049. https://dx.doi.org/10.1016/j.neuroimage.2011.10.041

Stefanics, G., Heinzle, J., Horváth, A. A., & Stephan, K. E. (2018). Visual mismatch and predictive coding: A computational single-trial ERP study. *The Journal of Neuroscience*, *38*, 4020–4030. https://dx.doi.org/10.1523/jneurosci.3365-17.2018

Stefanics, G., Kimura, M., & Czigler, I. (2011). Visual mismatch negativity reveals automatic detection of sequential regularity violation. *Frontiers in Human Neuroscience*, *5*(46), 1–9. https://dx.doi.org/10.3389/fnhum.2011.00046

Stefanics, G., Kremláček, J., & Czigler, I. (2014). Visual mismatch negativity: A predictive coding view. *Frontiers in Human Neuroscience, 8*(666), 1–19. https://dx.doi.org/10.3389/fnhum.2014.00666

Stevens, S. S. (1975). *Psychophysics: Introduction to its perceptual, neural, and social prospects*. New York: Wiley.

Stothart, G., & Kazanina, N. (2013). Oscillatory characteristics of the visual mismatch negativity: What evoked potentials aren't telling us. *Frontiers in Human Neuroscience, 7*(426), 1–9. https://dx.doi.org/10.3389/fnhum.2013.00426

Sulykos, I., & Czigler, I. (2011). One plus one is less than two: Visual features elicit non-additive mismatch-related brain activity. *Brain Research, 1398*, 64–71. https://dx.doi.org/10.1016/j.brainres.2011.05.009

Sulykos, I., & Czigler, I. (2014). Visual mismatch negativity is sensitive to illusory brightness changes. *Brain Research, 1561*, 48–59. https://dx.doi.org/10.1016/j.brainres.2014.03.008

Sulykos, I., Kecskés-Kovács, K., & Czigler, I. (2013). Mismatch negativity does not show evidence of memory reactivation in the visual modality. *Journal of Psychophysiology, 27*(1), 1–6. https://dx.doi.org/10.1027/0269-8803/a000085

Sulykos, I., Kecskés-Kovács, K., & Czigler, I. (2015). Asymmetric effect of automatic deviant detection: The effect of familiarity in visual mismatch negativity. *Brain Research, 1626*, 108–117. https://dx.doi.org/10.1016/j.brainres.2015.02.035

Susac, A., Heslenfeld, D. J., Huonker, R., & Supek, S. (2014). Magnetic source localization of early visual mismatch response. *Brain Topography, 27*, 648–651. https://dx.doi.org/10.1007/s10548-013-0340-8

Susac, A., Ilmoniemi, R. J., Pihko, E., & Supek, S. (2004). Neurodynamic studies on emotional and inverted faces in an oddball paradigm. *Brain Topography, 16*, 265–268. https://dx.doi.org/10.1023/B:BRAT.0000032863.39907.cb

Sysoeva, O. V., Lange, E. B., Sorokin, A. B., & Campbell, T. (2015). From pre-attentive processes to durable representation: An ERP index of visual distraction. *International Journal of Psychophysiology, 95*, 310–321. https://dx.doi.org/10.1016/j.ijpsycho.2014.12.007

Takács, E., Sulykos, I., Czigler, I., Barkaszi, I., & Balázs, L. (2013). Oblique effect in visual mismatch negativity. *Frontiers in Human Neuroscience, 7*, 591–594. https://dx.doi.org/10.3389/fnhum.2013.00591

Talbot, S. A., & Marshall, W. H. (1941). Physiological studies on neural mechanisms of visual localization and discrimination. *American Journal of Ophthalmology, 24*, 1255–1264. https://dx.doi.org/10.1016/S0002-9394(41)91363-6

Tales, A., & Butler, S. (2006). Visual mismatch negativity highlights abnormal preattentive visual processing in Alzheimer's disease. *NeuroReport, 17*, 887–890. https://dx.doi.org/10.1097/01.wnr.0000223383.42295.fa00001756-200606260-00008

Tales, A., Haworth, J., Wilcock, G., Newton, P., & Butler, S. (2008). Visual mismatch negativity highlights abnormal pre-attentive visual processing in mild cognitive impairment and Alzheimer's disease. *Neuropsychologia, 46*, 1224–1232. https://dx.doi.org/10.1016/j.neuropsychologia.2007.11.017

Tales, A., Newton, P., Troscianko, T., & Butler, S. (1999). Mismatch negativity in the visual modality. *NeuroReport, 10*, 3363–3367. Retrieved from https://www.ncbi.nlm.nih.gov/pubmed/9116228

Tales, A., Troscianko, T., Wilcock, G. K., Newton, P., & Butler, S. R. (2002). Age-related changes in the preattentional detection of visual change. *NeuroReport, 13*, 969–972. Retrieved from https://www.ncbi.nlm.nih.gov/pubmed/9116228

Tanner, D., Morgan-Short, K., & Luck, S. J. (2015). How inappropriate high-pass filters can produce artifactual effects and incorrect conclusions in ERP studies of language and cognition. *Psychophysiology, 52*, 997–1009. https://dx.doi.org/10.1111/psyp.12437

Tervaniemi, M., Maury, S., & Näätänen, R. (1994). Neural representations of abstract stimulus features in the human brain as reflected by the mismatch negativity. *NeuroReport, 5*, 844–846. Retrieved from https://journals.lww.com/neuroreport/

Thierry, G., Athanasopoulos, P., Wiggett, A., Dering, B., & Kuipers, J. (2009). Unconscious effects of language-specific terminology on preattentive color perception. *Proceedings of the National Academy of Sciences of the United States of America, 106*, 4567–4570. https://dx.doi.org/10.1073/pnas.0811155106

Tiitinen, H., May, P., Reinikainen, K., & Näätänen, R. (1994). Attentive novelty detection in humans is governed by pre-attentive sensory memory. *Nature, 372,* 90–92. https://dx.doi.org/10.1038/372090a0

Todd, J., & Cornwell, R. (2018). The importance of precision to updating models of the sensory environment. *Biological Psychology, 139,* 8–16. https://dx.doi.org/10.1016/j.biopsycho.2018.09.012

Todd, J., Provost, A., & Cooper, G. (2011). Lasting first impressions: A conservative bias in automatic filters of the acoustic environment. *Neuropsychologia, 49,* 3399–3405. https://dx.doi.org/10.1016/j.neuropsychologia.2011.08.016

Troscianko, T., & Harris, J. (1988). Phase discrimination in chromatic compound gratings. *Vision Research, 28,* 1041–1049. https://dx.doi.org/doi:10.1016/0042-6989(88)90081-8

Tugin, S., Hernandez-Pavon, J. C., Ilmoniemi, R. J., & Nikulin, V. V. (2016). Visual deviant stimuli produce mismatch responses in the amplitude dynamics of neuronal oscillations. *Neuroimage, 142,* 645–655. https://dx.doi.org/10.1016/j.neuroimage.2016.07.024

Tzovara, A., Simonin, A., Oddo, M., Rossetti, A. O., & De Lucia, M. (2015). Neural detection of complex sound sequences in the absence of consciousness. *Brain, 138,* 1160–1166. https://dx.doi.org/10.1093/brain/awv041

Ulanovsky, N., Las, L., & Nelken, I. (2003). Processing of low-probability sounds by cortical neurons. *Nature Neuroscience, 6,* 391–398. https://dx.doi.org/10.1038/nn1032

Umbricht, D., Vyssotki, D., Latanov, A., Nitsch, R., & Lipp, H. P. (2005). Deviance-related electrophysiological activity in mice: Is there mismatch negativity in mice? *Clinical Neurophysiology, 116*, 353–363. https://dx.doi.org/10.1016/j.clinph.2004.08.015

Urakawa, T., Inui, K., Yamashiro, K., & Kakigi, R. (2010). Cortical dynamics of the visual change detection process. *Psychophysiology, 47,* 905–912. https://dx.doi.org/10.1111/j.1469-8986.2010.00987.x

Urban, A., Kremláček, J., Masopust, J., & Libiger, J. (2008). Visual mismatch negativity among patients with schizophrenia. *Schizophrenia Research, 102,* 320–328. https://dx.doi.org/10.1016/j.schres.2008.03.014

van Rhijn, M., Roeber, U., & O'Shea, R. P. (2013). Can eye of origin serve as a deviant? Visual mismatch negativity from binocular rivalry. *Frontiers in Human Neuroscience*, 7(190) 1–10. https://dx.doi.org/10.3389/fnhum.2013.00190

Verhagen, J., & Wagenmakers, E. J. (2014). Bayesian tests to quantify the result of a replication attempt. *Journal of Experimental Psychology. General, 143*, 1457–1475. https://dx.doi.org/10.1037/a0036731

Wang, S., Li, W., Lv, B., Chen, X., Liu, Y., & Jiang, Z. (2016). ERP comparison study of face gender and expression processing in unattended condition. *Neuroscience Letters, 618*, 39–44. https://dx.doi.org/10.1016/j.neulet.2016.02.039

Webster, M. A., De Valois, K. K., & Switkes, E. (1990). Orientation and spatial frequency discrimination for luminance and chromatic gratings. *Journal of the Optical Society of America A, 7*, 1034-1049. https://dx.doi.org/doi:10.1364/JOSAA.7.001034

Wei, D., & Gillon-Dowens, M. (2018). Written-word concreteness effects in non-attend conditions: Evidence from mismatch responses and cortical oscillations. *Frontiers in Psychology, 9*(2455), 1–13. https://dx.doi.org/10.3389/fpsyg.2018.02455

Wei, J., Chan, T., & Luo, Y. (2002). A modified oddball paradigm "cross-modal delayed response" and the research on mismatch negativity. *Brain Research Bulletin*, 57, 221–230. https://dx.doi.org/10.1016/S0361-9230(01)00742-0

Westheimer, G. (1954). Mechanism of saccadic eye movements. *AMA Archives of Ophthalmology, 27*, 710–724. https://dx.doi.org/10.1001/archopht.1954.00920050716006

Widmann, A, Schröger, E, & Maess, B. (2015). Digital filter design for electrophysiological data – A practical approach. *Journal of Neuroscience Methods*, *250*, 34–46. https://dx.doi.org/10.1016/j.jneumeth.2014.08.002

Winkler, I. (2007). Interpreting the mismatch negativity. *Journal of Psychophysiology, 21*, 147–163. https://dx.doi.org/10.1027/0269-8803.21.34.147

Winkler, I., & Cowan, N. (2005). From sensory to long-term memory: Evidence from auditory memory reactivation studies. *Experimental Psychology, 52*, 3–20. https://dx.doi.org/10.1027/1618-3169.52.1.3

Winkler, I., & Czigler, I. (2012). Evidence from auditory and visual event-related potential (ERP) studies of deviance detection (MMN and vMMN) linking predictive coding theories and perceptual object representations. *International Journal of Psychophysiology, 83*, 132–143. https://dx.doi.org/10.1016/j.ijpsycho.2011.10.001

Winkler, I., Czigler, I., Sussman, E., Horváth, J., & Balázs, L. (2005). Preattentive binding of auditory and visual stimulus features. *Journal of Cognitive Neuroscience, 17*, 320–339. https://dx.doi.org/10.1162/0898929053124866

Winkler, I., Debener, S., Muller, K., & Tangermann, M. (2015). On the influence of high-pass filtering on ICA-based artifact reduction in EEG-ERP. *Proceedings of the Annual International Conference of the IEEE Engineering in Medicine and Biology Society*, 4101–4105, https://dx.doi.org/10.1109/EMBC.2015.7319296

Winkler, I., Reinikainen, K., & Näätänen, R. (1993). Event-related brain potentials reflect traces of the echoic memory in humans. *Perception & Psychophysics, 53*, 443–449. https://dx.doi.org/10.3758/BF03206788

Woods, D. L. (1990). Selective auditory attention: Complex processes and complex ERP generators. *Behavioral and Brain Sciences, 13*, 260–261. https://dx.doi.org/10.1017/S0140525X00078705

Woods, D. L., Alho, K., & Algazi, A. (1992). Intermodal selective attention. I. Effects on event-related potentials to lateralized auditory and visual stimuli. *Electroencephalography and Clinical Neurophysiology, 82*, 341–355. https://dx.doi.org/10.1016/0013-4694(92)90004-2

Yan, T., Feng, Y., Liu, T., Wang, L., Mu, N., Dong, X., ... Zhao, L. (2017). Theta oscillations related to orientation recognition in unattended condition: A vMMN study. *Frontiers in Behavioral Neuroscience, 11*(166), 1–8. https://dx.doi.org/10.3389/fnbeh.2017.00166

Yang, X., Yu, Y., Chen, L., Sun, H., Qiao, Z., Qiu, X., . . . Yang, Y. (2016). Gender differences in pre-attentive change detection for visual but not auditory stimuli. *Clinical Neurophysiology*, *127*, 431–441. https://dx.doi.org/10.1016/j.clinph.2015.05.013

Yu, M., Mo, C., Zeng, T., Zhao, S., & Mo, L. (2017). Short-term trained lexical categories affect preattentive shape perception: Evidence from vMMN. *Psychophysiology*, *54*, 462–468. https://dx.doi.org/10.1111/psyp.12797

Zhao, L., & Li, J. (2006). Visual mismatch negativity elicited by facial expressions under non-attentional condition. *Neuroscience Letters*, *410*, 126–131. https://dx.doi.org/10.1016/j.neulet.2006.09.081

Zhong, W., Li, Y., Li, P., Xu, G., & Mo, L. (2015). Short-term trained lexical categories produce preattentive categorical perception of color: Evidence from ERPs. *Psychophysiology*, *52*, 98–106. https://dx.doi.org/10.1111/psyp.12294

Zhou, K., Mo, L., Kay, P., Veronica, P. Y. K., Tiffany, N. M. I., & Tan, L. H. (2010). Newly trained lexical categories produce lateralized categorical perception of color. *Proceedings of the National Academy of Sciences of the United States of America*, *107*, 9974–9978. https://dx.doi.org/10.1073/pnas.1005669107

# APPENDICES

Appendix A, C, and D show the principal components identified in the PCA(s) for experiment(s) in which some components did not satisfy the criteria as a component of interest. It may be interesting to perform exploratory analyses of these components. However, this is beyond the scope of the current thesis.

# Appendix A

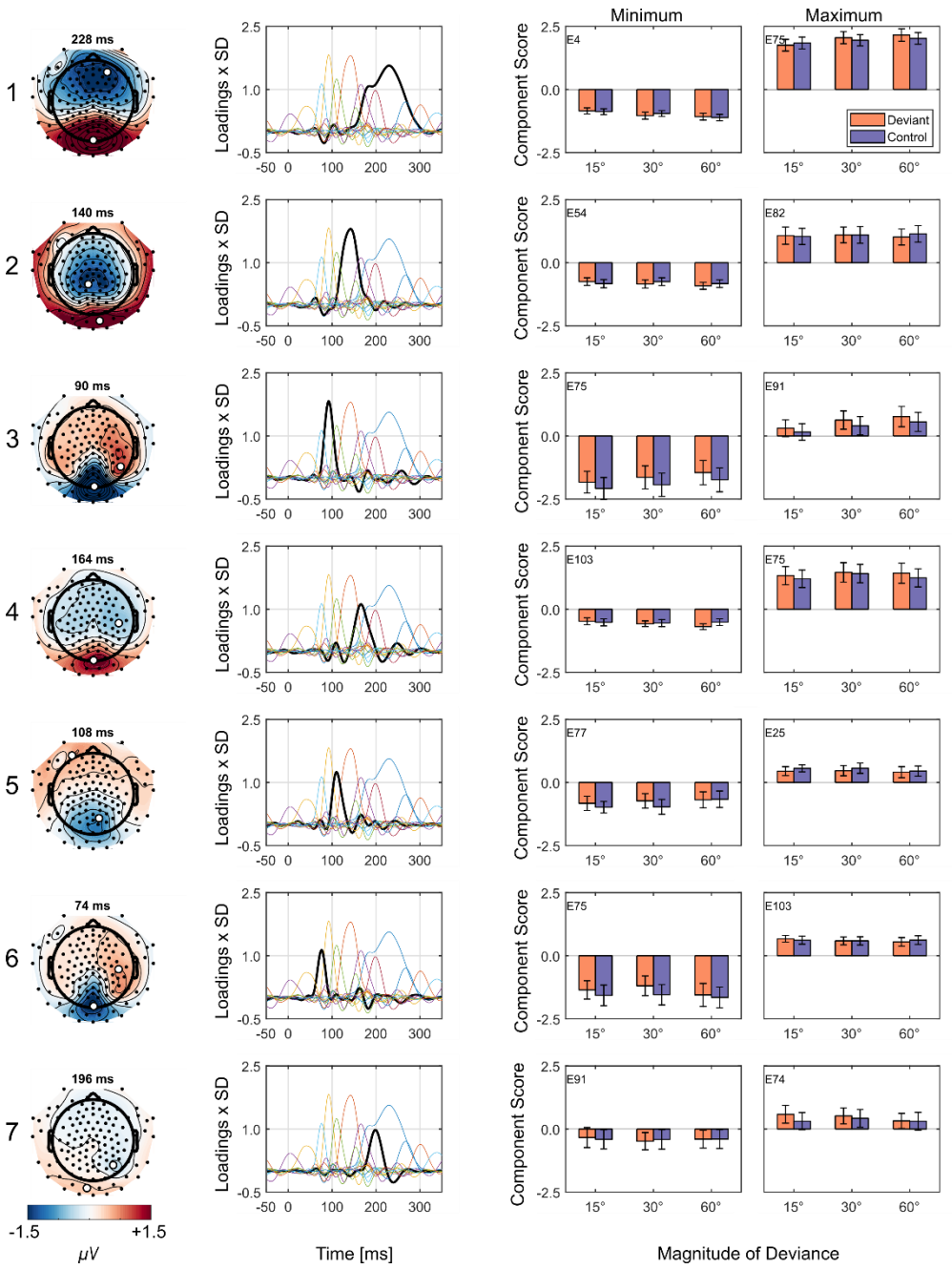


*Figure S1* Principal components 1-7 in Chapter 3. From left to right, we show: the component number, topographical maps (combined activity from deviant and standard trials at peak latency), component loadings (a component's contribution as a thick black line to the overall evoked activity relative to all other components as thin lines of different colours), component score for minimum, and component score for maximum. The last two, the bar graphs, show means for each deviant (orange) and control (purple) in each magnitude of deviance condition (15°, 30°, and 60°), ±1 standard-error bars, and electrode numbers. We show the location of these electrodes on the topographical maps by white disks.

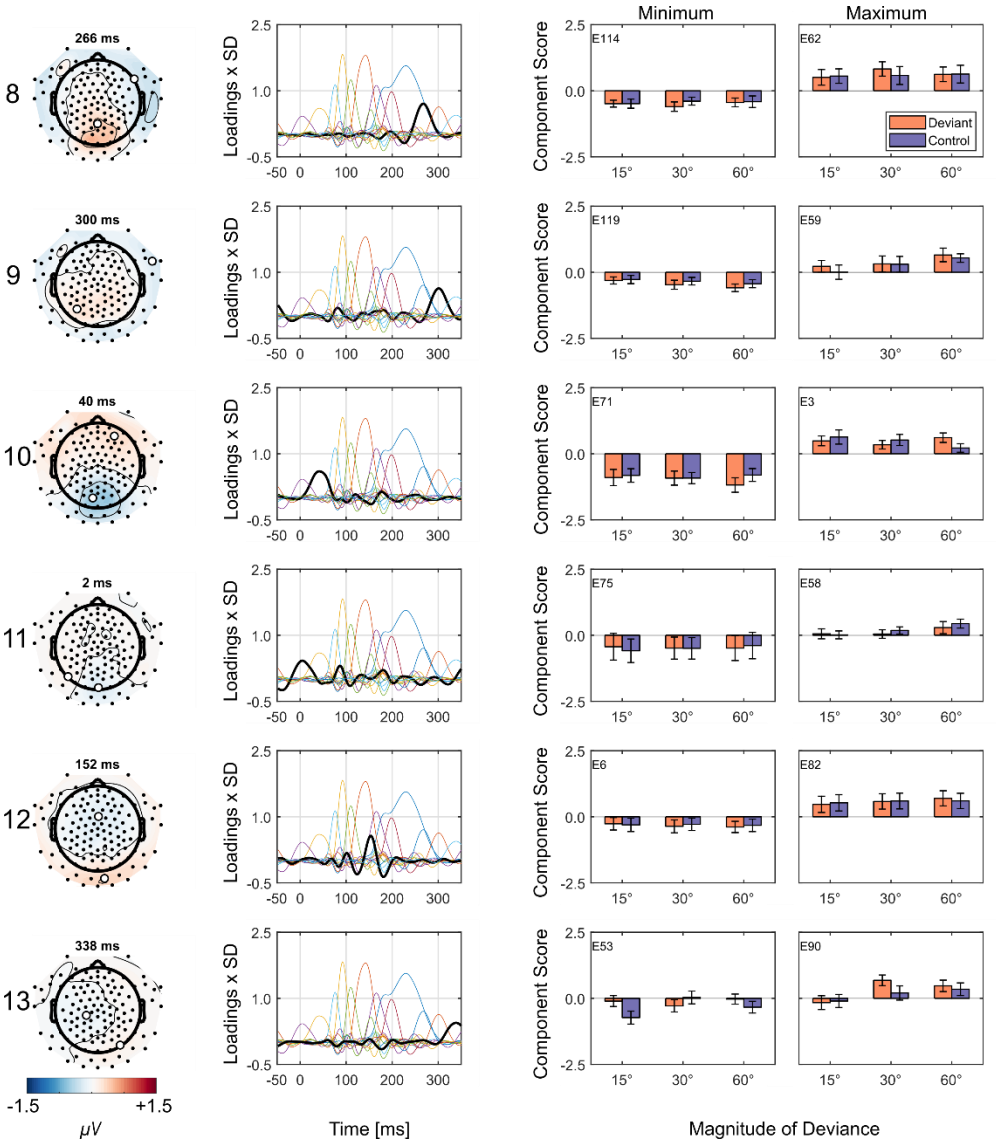


*Figure S2* Principal components 8-13 in Chapter 3. From left to right, we show: the component number, topographical maps (combined activity from deviant and standard trials at peak latency), component loadings (a component's contribution as a thick black line to the overall evoked activity relative to all other components as thin lines of different colours), component score for minimum, and component score for maximum. The last two, the bar graphs, show means for each deviant (orange) and control (purple) in each magnitude of deviance condition (15°, 30°, and 60°), ±1 standard-error bars, and electrode numbers. We show the location of these electrodes on the topographical maps by white disks.

# Appendix B

Table S1 *ANOVAs for N1 and P1 Components revealed in Principal Component Analysis (PCA) of Deviant and Control Trials in Chapter 3*

| Factor | *df* | *F*-value | *p* | $\eta^2$ | ε |
|---|---|---|---|---|---|
| N1 | | | | | |
| Region | 2, 40 | 1.261 | .293 | .059 | .928 |
| Magnitude of deviance | 2, 40 | 1.769 | .190 | .081 | .844 |
| Deviance | 1, 20 | 1.546 | .228 | .072 | |
| Region × Magnitude of deviance | 4, 80 | 1.040 | .376 | .049 | .661* |
| Region × Deviance | 2, 40 | 2.327 | .134 | .104 | .644* |
| Magnitude of deviance × Deviance | 2, 40 | 1.276 | .290 | .060 | .993 |
| Region × Magnitude of deviance × Deviance | 4, 80 | 0.712 | .504 | .034 | .529* |
| P1 | | | | | |
| Left parieto-occipital | | | | | |
| Magnitude of deviance | 2, 40 | 30.081 | < .001 | .601 | .722* |
| Deviance | 1, 20 | 9.836 | .005 | .330 | |
| Magnitude of deviance × Deviance | 2, 40 | 0.604 | .537 | .029 | .908 |
| Midline parieto-occipital | | | | | |
| Magnitude of deviance | 2, 40 | 17.667 | < .001 | .469 | .672* |
| Deviance | 1, 20 | 14.065 | .001 | .413 | |
| Magnitude of deviance × Deviance | 2, 40 | 0.029 | .970 | .001 | .975 |
| Right parieto-occipital | | | | | |
| Magnitude of deviance | 2, 40 | 17.294 | < .001 | .464 | .686* |
| Deviance | 1, 20 | 16.966 | < .001 | .459 | |
| Magnitude of deviance × Deviance | 2, 40 | 0.510 | .597 | .025 | .957 |

*Note*. Three-way repeated ANOVA was computed with factors Region (left vs. midline vs. right), Magnitude of deviance (small vs. medium vs. large), and Deviance (deviant vs. control) for the N1. Due to the differences in P1 amplitudes evidence by Figure 3.3 and 3.5, we performed the three, two-way ANOVAs at each parieto-occipital region (left, midline, and right) with factors Magnitude of deviance (small vs. medium vs. large) and Deviance (deviant vs. control) for the P1. We correct degrees of freedom using Greenhouse-Geisser (ε) for all factors or interactions with more than two levels. Eta squared ($\eta^2$) denotes effect size.

# Appendix C

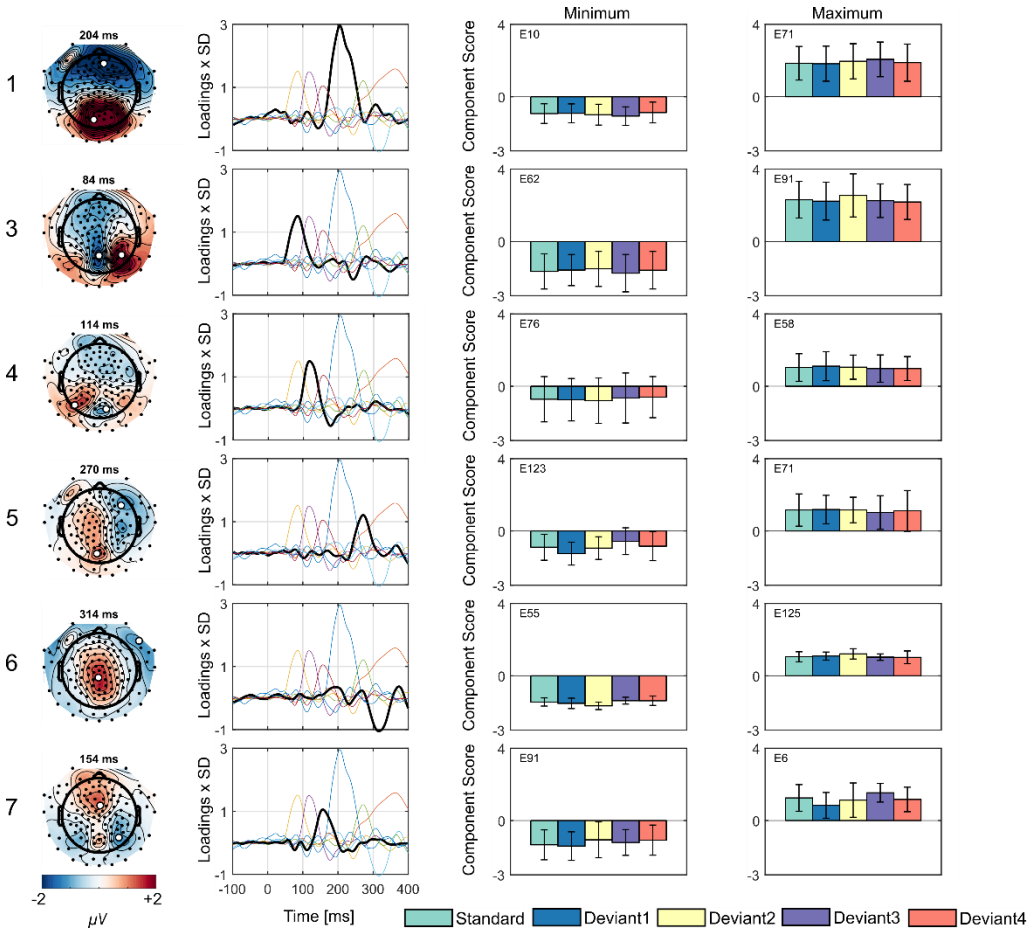


*Figure S3* All principal components with a single peak between 70 and 350 ms from follow-up testing in Experiment 1 ($N$ = 4) in Chapter 4. Stimuli are gratings. From left to right, we show: the component number, topographical maps (combined activity from deviant and standard trials at peak latency), component loadings (a component's contribution as a thick black line to the overall evoked activity relative to all other components as thin lines of different colours), component score for minimum, and component score for maximum. The last two, the bar graphs, show means for each deviant and standard conditions, ±1 standard-error bars, and electrode numbers. We show the location of these electrodes on the topographical maps by white disks.

# Appendix D

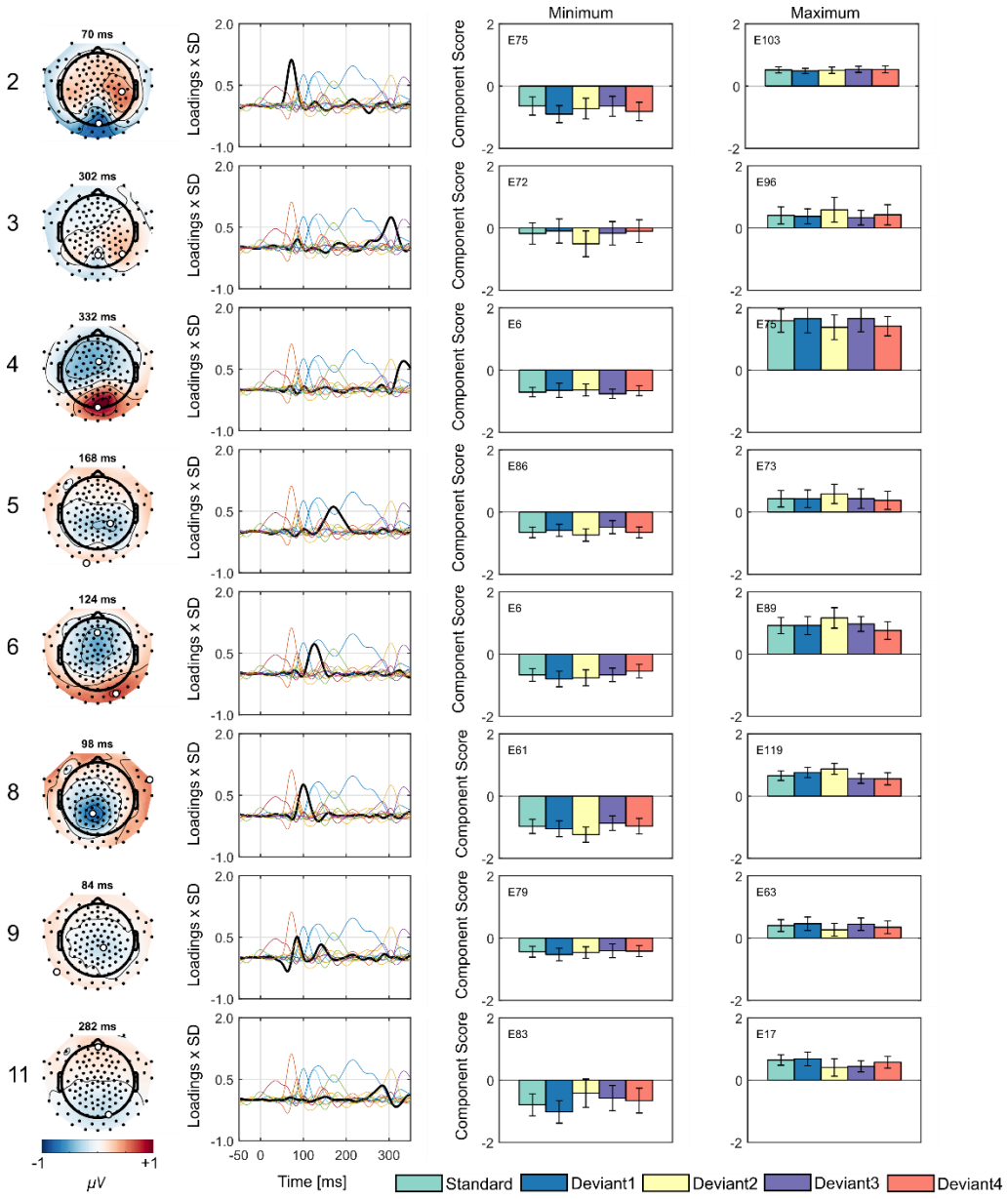


*Figure S4* All principal components with a single peak between 70 and 350 ms from Experiment 2 ($N$ = 20) in Chapter 4. Stimuli are Gabor patches. From left to right, we show: the component number, topographical maps (combined activity from deviant and standard trials at peak latency), component loadings (a component's contribution as a thick black line to the overall evoked activity relative to all other components as thin lines of different colours), component score for minimum, and component score for maximum. The last two, the bar graphs, show means for each deviant and standard conditions, ±1 standard-error bars, and electrode numbers. We show the location of these electrodes on the topographical maps by white disks.

# Appendix E

We performed a categorical magnitude estimation pilot to ensure equal perceptual differences between orientation and contrast deviant and standard stimuli in Chapter 5.

Gabor patches had a spatial frequency of 1.6 cycles per degree of visual angle (cpd), a phase of one-quarter of a cycle, and a standard deviation of the Gaussian of 1° of visual angle. The visible part of the Gabor patch was approximately 4°. There was a white central fixation cross. The length of each bar of the fixation cross was .60° of visual angle; the width was .03° of visual angle.

For orientation blocks, the Michelson contrast of the Gabor patch was always .35. The orientation of the Gabor patch varied randomly and equally among 7°, 17°, 27°, 37°, 47°, 57°, 67°, 77°, and 87°. For contrast blocks, the orientation of the Gabor patch was always 47° clockwise from vertical (0°). Michelson contrast of the Gabor patch varied randomly and equally among .1, .14, .2, .25, .35, .45, .6, .75, and .95. Stimuli appeared for 100 ms in the CVF or LVF (stimulus edge was .5° from the centre of the fixation cross).

At the beginning of each block, participants saw an anchor stimulus (also a Gabor patch) with which they were to compare each new stimulus. The Michelson contrast of the anchor was .35 for contrast blocks. The orientation of the anchor was 47° from vertical (0°) for orientation blocks. There were eight

blocks per feature. Each block contained 54 trials, six per value of a feature. We tested two naïve observers and AGM. Figure S1 shows the results.

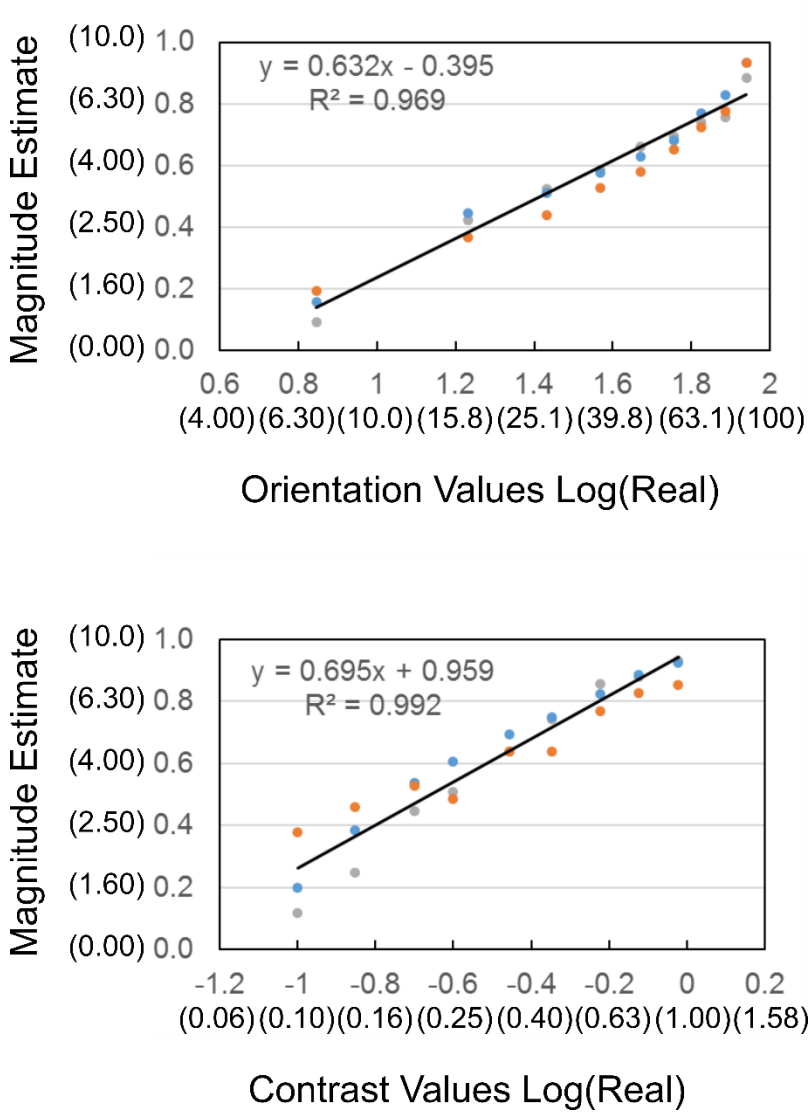


*Figure S5* Mean magnitude estimates for orientation (top) and contrast (bottom) in Chapter 5. Values in grey are logarithms. Values in parentheses are antilogarithms values. Antilogarithmic values for orientation are in degrees and antilogarithmic values for contrast are in Michelson. The black lines show the linear relationships from all three volunteers (grey, blue, and orange). Combined results from stimuli presented with their nearest edges 0.5° from fixation in the lower visual field (LVF) and central visual field (CVF). We illustrate exponents in each plot (rounded to three decimal places).

With the exponents from Figure S5, we found that the difference in magnitude estimates between 1° and 34° (33° orientation difference) was 3.34 units. We used this difference to calculate equally different deviant and standard

Michelson (M) contrast values for our contrast stimuli. The deviant was .393 M. Due to a coding error; the standard was .846 M instead of .845 M. Given the size of the difference in contrast, the six contrast values were equally different from one another by one third of the deviant and standard difference (.151 M) in our equiprobable control. These were .242, .393, .544, .695, .846, and .997 M. Similarly, the orientation values for our equiprobable control were 84°, 95°, 106°, 117°, 128°, and 139°.

# Appendix F

Table S2 *ANOVAs for Hit Rate (%) and Reaction Time (ms) in Chapter 5*

| **Condition** | ***F*-value** | ***p*** | **$\eta^2$** | **$BF_{Incl}$** |
|---|---|---|---|---|
| Hit Rate (%) | | | | |
| Feature | 0.285 | .002 | .472 | 16675.325 |
| Visual field | 13.426 | .601 | .019 | 0.098 |
| Block type | 0.818 | .380 | .052 | 0.152 |
| Feature × Visual field | 0.028 | .869 | .002 | 0.097 |
| Feature × Block type | 0.303 | .590 | .020 | 0.156 |
| Visual field × Block type | 0.144 | .710 | .009 | 0.035 |
| Feature × Visual field × Block type | 0.672 | .425 | .043 | 0.005 |
| Reaction Time | | | | |
| Feature | 0.022 | .885 | .001 | 0.131 |
| Visual field | 8.933 | .009 | .373 | 17494.162 |
| Block type | 2.309 | .149 | .133 | 0.142 |
| Feature × Visual field | 0.739 | .404 | .047 | 0.094 |
| Feature × Block type | 0.042 | .841 | .003 | 0.041 |
| Visual field × Block type | 0.007 | .933 | .000 | 0.148 |
| Feature × Visual field × Block type | 0.376 | .549 | .024 | 0.005 |

*Note*. Three-way 2×2×2 repeated ANOVAs were computed with factors Feature (orientation vs. contrast), Visual field (CVF vs. LVF), and Block type (oddball vs. control).

# Appendix G

## Statistical tests for Experiment 1's Bar-Edge condition

Table S3 *Replication ($BF_{r0}$) directed ($BF_{-0}$), and non-directed ($BF_{10}$) Bayesian t-tests of mean amplitudes (µV) between 100 and 150 ms*

| | Original results | | Replication results | | | | | | |
|---|---|---|---|---|---|---|---|---|---|
| **Contrast** | **Electrode** | ***t* (11)** | **Electrode** | **µV** | ***t* (23)** | ***p*** | ***BF*$_{r0}$** | ***BF*$_{-0}$** | ***BF*$_{10}$** |
| Dev vs. Sta | | | | | | | | | |
| | PO7 | −8.11 | P7 | −0.09 | −0.418 | .340 | 0.0005 | 0.304 | 0.232 |
| | PO7 | −8.11 | O1 | −0.08 | −0.283 | .390 | 0.0004 | 0.270 | 0.223 |
| | PO8 | −9.04 | O2 | −0.49 | −1.687 | .053 | 0.004 | 1.381 | 0.735 |
| | PO8 | −9.04 | P8 | −0.26 | −0.904 | .188 | 0.0005 | 0.498 | 0.310 |
| Con vs. Sta | | | | | | | | | |
| | PO7 | −5.38 | P7 | −0.32 | −1.120 | .137 | 0.020 | 0.640 | 0.376 |
| | PO7 | −5.38 | O1 | −0.42 | −1.128 | .135 | 0.021 | 0.647 | 0.379 |
| | PO8 | −8.99 | O2 | −0.66 | −1.882 | .036 | 0.006 | 1.864 | 0.223 |
| | PO8 | −8.99 | P8 | −0.08 | −0.294 | .385 | 0.0002 | 0.272 | 0.974 |

Table S4 *Replication ($BF_{r0}$), directed ($BF_{-0}$), and non-directed ($BF_{10}$) Bayesian t-tests of mean amplitudes (µV) between 200 and 250 ms*

| | Original results | | Replication results | | | | | | |
|---|---|---|---|---|---|---|---|---|---|
| **Contrast** | **Electrode** | ***t* (11)** | **Electrode** | **µV** | ***t* (23)** | ***p*** | ***BF*$_{r0}$** | ***BF*$_{-0}$** | ***BF*$_{10}$** |
| Dev vs. Sta | | | | | | | | | |
| | T5 | −5.88 | P7 | −0.19 | −0.486 | .315 | 0.003 | 0.324 | 0.239 |
| | T6 | −5.54 | P8 | −0.67 | −1.741 | .047 | 0.080 | 1.498 | 0.793 |
| Dev vs. Con | | | | | | | | | |
| | T5 | −4.83 | P7 | 0.99 | 3.027 | .997 | 0.003 | 0.063 | 7.454 |
| | T6 | −6.17 | P8 | 0.79 | 2.324 | .985 | 0.0005 | 0.074 | 1.992 |
| Con vs. Sta | | | | | | | | | |
| | T5 | −3.00 | P7 | −1.17 | −3.044 | .003 | 24.223 | 15.361 | 7.712 |
| | T6 | −2.90 | P8 | −1.46 | −4.489 | <.001 | 898.319 | 342.992 | 171.522 |

*Note.* Electrodes T5 and T6 (used by Kimura et al., 2009) are the same as P7 and P8, respectively.

**Reanalysis of Experiment 1's Bar-Edge condition**

To check whether our failure to replicate the results of Kimura et al. (2009) was because our pre-processing of the EEG data differed from theirs, we used their pre-processing steps for our data. That is, we low-pass filtered the data using a Hamming-windowed finite impulse response (FIR) filter with a cut-off frequency of 30 Hz (order 166). Kimura et al. used a 30 Hz cut-off value (window type and order were not reported). We segmented the data, using the 100-ms pre-stimulus time-window for baseline correction. Before averaging the data for each stimulus type, we rejected any epochs in which amplitudes exceeded ± 100 μV at any electrode (including bipolarized horizontal and vertical EOG channels). We removed the first three stimuli in each sequence, the first and second stimulus following a target, and any epoch containing a response (e.g., false alarms).

Overall, we retained fewer standard (M = 417, SD = 18), deviant (M = 164, SD = 9), and control (M = 149, SD = 6) trials in the bar-edge condition than what we did in our principal analysis. To optimize comparability, in Figure S6, we show the ERPs and difference waves using similar display parameters (e.g., colour) as used by Kimura et al. Compared with our principal analysis of the data, we found substantially larger effects of adaptation, with greater negativities within the vMMN time-window (200−250 ms) in the deviant-minus-standard difference waves (see also Table S6). This is mirrored by the larger control vs. standard comparisons in Table S6. However, there was no evidence of a genuine vMMN. Statistics for the replicated analysis of adaptation related differences in the 100−150 ms time window are also reported in the Table S5. We did not

replicate the large adaptation effects Kimura et al. reported. We conclude that differences in our analysis pipeline are not responsible for our failure to replicate Kimura et al.'s findings.

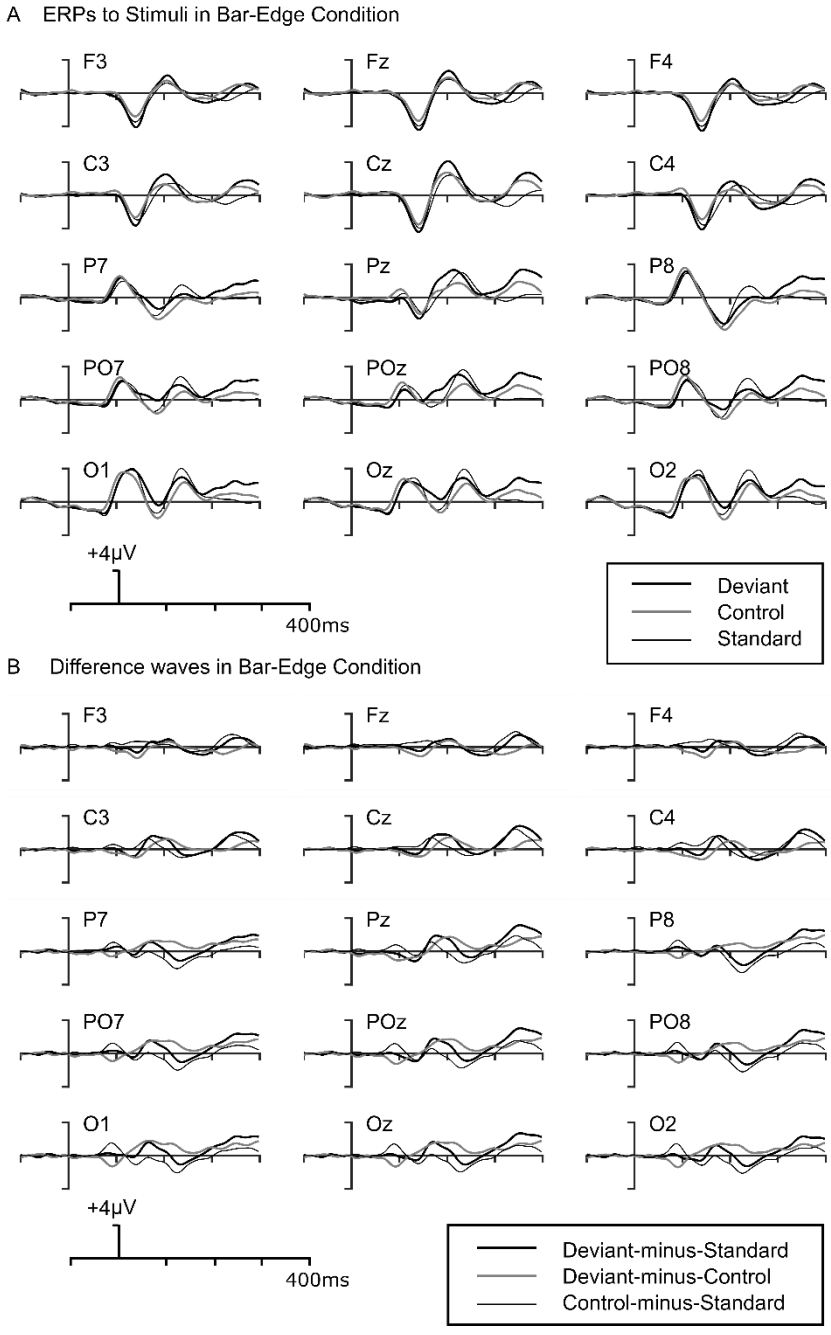


*Figure S6* ERPs from Experiment 1 Chapter 6 data. Data are pre-processed with Kimura et al.'s (2009) pre-processing parameters. Data are displayed similar to Kimura et al. Data at PO7, PO8, POz, and Oz are interpolated for illustrative purposes.

Table S5 *Replication ($BF_{r0}$) and directed ($BF_{-0}$) Bayesian t-tests of mean amplitudes (µV) between 100 and 150 ms*

| | Original results | | Replication results | | | | | |
|---|---|---|---|---|---|---|---|---|
| **Contrast** | **Electrode** | ***t* (11)** | **Electrode** | **µV** | ***t* (23)** | ***p*** | ***BF*$_{r0}$** | ***BF*$_{-0}$** |
| Dev vs. Sta | | | | | | | | |
| | PO7 | −8.11 | P7 | 0.05 | 0.211 | .583 | 0.00018 | 0.184 |
| | PO7 | −8.11 | PO7 | −0.11 | −0.423 | .338 | 0.00034 | 0.273 |
| | PO7 | −8.11 | O1 | 0.05 | 0.186 | .573 | 0.00019 | 0.188 |
| | PO8 | −9.04 | O2 | −0.41 | −1.467 | .078 | 0.00201 | 1.006 |
| | PO8 | −9.04 | PO8 | −0.43 | −1.628 | .059 | 0.00210 | 1.042 |
| | PO8 | −9.04 | P8 | −0.15 | −0.480 | .318 | 0.00022 | 0.322 |
| Con vs. Sta | | | | | | | | |
| | PO7 | −5.38 | P7 | −0.05 | −0.147 | .442 | 0.00328 | 0.241 |
| | PO7 | −5.38 | PO7 | −0.10 | −0.323 | .375 | 0.00328 | 0.265 |
| | PO7 | −5.38 | O1 | −0.23 | −0.585 | .282 | 0.00678 | 0.356 |
| | PO8 | −8.99 | O2 | −0.50 | −1.455 | .080 | 0.00198 | 0.990 |
| | PO7 | −8.99 | PO8 | −0.17 | −0.639 | .265 | 0.00029 | 0.347 |
| | PO8 | −8.99 | P8 | 0.04 | 0.164 | .564 | 0.00008 | 0.191 |

Table S6 *Replication ($BF_{r0}$) and directed ($BF_{-0}$) Bayesian t-tests of mean amplitudes (µV) between 200 and 250 ms*

| | Original results | | Replication results | | | | | |
|---|---|---|---|---|---|---|---|---|
| **Contrast** | **Electrode** | ***t* (11)** | **Electrode** | **µV** | ***t* (23)** | ***p*** | ***BF*$_{r0}$** | ***BF*$_{-0}$** |
| Dev vs. Sta | | | | | | | | |
| | T5 | −5.88 | P7 | −0.70 | −1.451 | .080 | 0.02726 | 0.985 |
| | T6 | −5.54 | P8 | −1.31 | −2.570 | .009 | 0.85853 | 6.113 |
| Dev vs. Con | | | | | | | | |
| | T5 | −4.83 | P7 | 0.95 | 2.351 | .986 | 0.00197 | 0.073 |
| | T6 | −6.17 | P8 | 0.78 | 1.819 | .959 | 0.00048 | 0.085 |
| Con vs. Sta | | | | | | | | |
| | T5 | −3.00 | P7 | −1.66 | −3.480 | .001 | 73.54386 | 37.870 |
| | T6 | −2.90 | P8 | −2.09 | −5.257 | <.001 | 5207.266 | 1907.174 |

*Note.* Electrodes T5 and T6 (used by Kimura et al., 2009) are the same as P7 and P8, respectively.